

Strategic Environmental Research & Development Program

Contract: DACA72-99-C-0011

September 1, 2004

Final Report

SERDP Pollution Prevention Project 1137

Non-Destructive Testing of Corrosion Under Coatings

Program Manager

John D. Weir, P.E.

Northrop Grumman Corporation

Spectral Nondestructive Principal Investigator

Dr. Don DiMarzio

Northrop Grumman Corporation

Electrochemical Measurements Principal Investigator

Dr. Hugh S. Isaacs

Brookhaven National Laboratory Upton, NY

Integrated Systems

Northrop Grumman Corp

600 Grumman Road West

Bethpage, New York 11714-3582

M/S A01-26

Bethpage, NY 11714

Report Documentation Page			Form Approved OMB No. 0704-0188		
Public reporting burden for the collection of information is estimated to average 1 hour per response, including the time for reviewing instructions, searching existing data sources, gathering and maintaining the data needed, and completing and reviewing the collection of information. Send comments regarding this burden estimate or any other aspect of this collection of information, including suggestions for reducing this burden, to Washington Headquarters Services, Directorate for Information Operations and Reports, 1215 Jefferson Davis Highway, Suite 1204, Arlington VA 22202-4302. Respondents should be aware that notwithstanding any other provision of law, no person shall be subject to a penalty for failing to comply with a collection of information if it does not display a currently valid OMB control number.					
1. REPORT DATE 1 SEP 2004		2. REPORT TYPE Final		3. DATES COVERED -	
4. TITLE AND SUBTITLE Non-Destructive Testing of Corrosion Under Coatings			5a. CONTRACT NUMBER		
			5b. GRANT NUMBER		
			5c. PROGRAM ELEMENT NUMBER		
6. AUTHOR(S) John D. Weir, Dr. Don DiMarzio			5d. PROJECT NUMBER PP 1137		
			5e. TASK NUMBER		
			5f. WORK UNIT NUMBER		
7. PERFORMING ORGANIZATION NAME(S) AND ADDRESS(ES) Northrop Grumman Corporation 600 Grumman Road West Bethpage, New York 11714-3582			8. PERFORMING ORGANIZATION REPORT NUMBER		
9. SPONSORING/MONITORING AGENCY NAME(S) AND ADDRESS(ES) Strategic Environmental Research & Development Program 901 N Stuart Street, Suite 303 Arlington, VA 22203			10. SPONSOR/MONITOR'S ACRONYM(S) SERDP		
			11. SPONSOR/MONITOR'S REPORT NUMBER(S)		
12. DISTRIBUTION/AVAILABILITY STATEMENT Approved for public release, distribution unlimited					
13. SUPPLEMENTARY NOTES The original document contains color images.					
14. ABSTRACT					
15. SUBJECT TERMS					
16. SECURITY CLASSIFICATION OF:			17. LIMITATION OF ABSTRACT SAR	18. NUMBER OF PAGES 247	19a. NAME OF RESPONSIBLE PERSON
a. REPORT unclassified	b. ABSTRACT unclassified	c. THIS PAGE unclassified			

Nondestructive Testing of Corrosion Under Coatings

Strategic Environmental Research & Development Program

Project Number: 1137

Final Report September 1, 2004

By

**John Weir, Don Di Marzio, Steve Chu
Northrop Grumman Corporation**

**Hugh S. Isaacs, Gordana D. Adzic
Brookhaven National Laboratory**

**Doug Hansen
Perkin Elmer Corporation**

FOREWORD

This Final Report for 2004 incorporates and summarizes the work completed in the previous annual reports issued to date. Note: An extension to the existing contract for testing non-chromated primer required the updating of this document. This additional work was completed and the results were incorporated into this report. Supporting data in Appendix 7 was also added to show method of calculating potential environmental savings, as well as potential cost saving. The contract is considered completed.

This report was prepared under contract to the Department of Defense Strategic Environmental Research and Development Program (SERDP). The publication of this report does not indicate endorsement by the Department of Defense, nor should the contents be construed as reflecting the official policy or position of the Department of Defense. Reference herein to any specific commercial product, process, or service by trade name, trademark, manufacturer, or otherwise, does not necessarily constitute or imply its endorsement, recommendation, or favoring by the Department of Defense.

THIS PAGE INTENTIONALLY LEFT BLANK

CONTENTS

Section	Page
EXECUTIVE SUMMARY	1
INTRODUCTION AND OVERVIEW	3
Technical Background	4
Spectral Nondestructive Evaluation (SNDE)	4
SNDE – Wide Area Spectral Imaging	5
SNDE/WASI Project Accomplishments	6
Sample Preparation	6
Paint Systems	9
Multiview Multispectral Camera System	10
Multispectral Amber IR Camera System	11
Alternative IR Imaging Systems	15
SNDE/WASI Discussion of Results	18
Experimentation	20
Sample Preparation	20
SNDE	20
Results and Discussion	21
SNE	21
Baseline Measurements	22
Corrosion Modeling	23
DHR of Corroded Coupons	24
Free Standing Paint Films	25
SNDE Sensitivity Study	26

CONTENTS (contd)

Section	Page
SNDE – Wide Area Spectral Imaging	30
WASI Project Accomplishments	30
Sample Preparation	30
Paint Systems	32
System Description and IR Imager Results.....	32
Corrosion Detection Filter Development.....	33
Specimen Indicating Corrosion Detection Limits	35
Laboratory and Field Detection of Corrosion in Real Aircraft Parts	37
Crack and Pit Detection	40
Polarization Results	43
Wide Area Imaging Discussion	43
IR Camera Configurations	46
Multi-Spectral Infrared Images.....	50
IR Imaging of E-2C Access Panel	50
Detail Imaging of E-2C Hawkeye Panels	50
Discussion of Detail Imaging of Fastener Heads.....	51
Multi-Spectral Images of Fatigue Cracks	52
Pit Detection through Paint.....	54
Image Processing and Frame Averaging.....	55
Grayscale Histograms	56
Crack Detection Study	56
Illumination Power Study	57
Imaging Through Highly Scattering Coatings	58
Imaging Through Coatings of Various Thickness	59

CONTENTS (contd)

Section	Page
Liquid Nitrogen Cooled Filter Study	68
Polarization Study of Dark Gray Paint on Aluminum	69
Bearcat Aircraft Corrosion Survey	73
Patent Pending Status.....	75
Business Trips, Presentations and Papers	76
Indigo Transition Trip – January 2002	76
Navy Corrosion Work Shop – August 2002	76
ESTCP/SERDP Partners in Environmental Technology – December 2002.....	76
NADEP, Jacksonville, FL Trip – November 2002	76
Northrop Grumman Corporation Saint Augustine, FL Trip – November 2002.....	77
SERDP Field Demonstrations and Meetings	78
Redstone Arsenal, Huntsville, AL, July 8–10, 2003.....	78
Boeing, Oklahoma City, OK, August 5–7, 2003.....	78
Summary of Surveyed Aircraft and Lessons Learned	78
Transition of Technology Activities for IR Camera.....	79
Investigation of an IR Detection System Utilizing Black Body Self-Illumination To Observe Structures and Defects Under Coatings	80
Electrochemical Impedance Spectroscopy	89
Scanning Volta Potential Measurements	89
Electrochemical Results.....	91
EIS	91
Scanning Volta Potentials Measurement	91
Electrochemical Impedance Spectrometry	94
Scanning Volta Potential Measurements	109

CONTENTS (contd)

Section	Page
Electrochemical Project Accomplishments BHL 2000	111
Summary	111
Sample Preparation	111
Localized Impedance Spectroscopy	111
Kelvin Probe Measurements	115
Volta Potential Measurements in Ionized Air	118
Electrochemical Plans for 2001	118
BNL Progress Summary for Year 2001	119
Volta Potential Measurements Year 2001	119
Experimental	119
Results	120
Identification of Corrosion by Infrared Microspectroscopy (IMS) for Year 2001	124
Experimental	124
Results	124
IMS Investigation of AA 2024	124
IMS Investigation of Different Alloys	125
Conclusions	132
BNL Progress Summary Year 2002	133
Sample Standards Year 2002	133
Infrared Microspectroscopy (IMS)	134
Experimental Year 2002	134
Results Year 2002	134
Impedance Spectroscopy	137
Experimental Year 2002	137

CONTENTS (contd)

Section	Page
Results Year 2002	138
Scanning Impedance Probes Year 2002	143
Experimental	144
Results	144
IMS Conclusions Year 2002.....	144
Conclusions and Future Work	145
SNDE	145
Impedance Measurements.....	145
Scanning Volta Potentials Measurements	145
Environmental and Business Case	146
Investment for Military and Commercial Aircraft.....	146
Aircraft Industry Cost Savings.....	146
Aircraft Industry Environmental Benefit/Savings	147
References.....	147
 Appendices	
A1 SUCCESS STORY	A1-1
A2 CARC IMAGES REPORT	A2-1
A3 REDSTONE ARSENAL IR DEMONSTRATION	A3-1
A4 B-52 FUEL TANK COATING.....	A4-1
A5 ESTCP PROPOSAL	A5-1
A6 JSF (F-35) PRIMER & TOPCOAT FEASIBILITY EVALUATION FOR THE DETECTION OF CORROSION UNDER COATINGS.....	A6-1
A7 POLLUTION SAVINGS CALCULATIONS & BUSINESS CASE	A7-1

THIS PAGE INTENTIONALLY LEFT BLANK

ILLUSTRATIONS

Fig.		Page
1	Integrating sphere system used to measure directional hemispherical reflectance.....	5
2	WASI Technique.....	6
3a	Alodine (chromate conversion) coated 2024 bare aluminum alloy coupon (2-in. x 2-in. center square scribed and exposed)	7
3b	Sulfuric acid anodized 2024 bare aluminum alloy coupon (2-in. x 2-in. center square scribed and exposed to salt fog)	7
3c	Alodine (chromate conversion) coated 2024 clad aluminum alloy coupon (2-in. x 2-in. center square scribed and exposed to salt fog)	7
3d	Sulfuric acid anodized 2024 clad aluminum alloy coupon (2-in. x 2-in. center square scribed and exposed to salt fog)	7
4	Photograph of a naturally corroded 12-in. x12-in. 2024 clad aluminum panel	8
5	Micrograph of an EDM simulated crack propagating from a hole in an aluminum bar	8
6	Micrograph of an aircraft fastener head in an aluminum part	8
7	Reflectance of Hentzen paint system on a partially corroded aluminum coupon. Significant reflectance difference seen in the 3.6 to 5.4 μm range between corroded and uncorroded areas	9
8	Unpainted partially corroded aluminum coupon	10
9	Four band Multiview image of an unpainted half-corroded coupon. Band 1: 2.1-2.3 μm , Band 2: 4.5-4.7 μm , Band 3: 3.5-4.0 μm , Band 4: 3.2-3.5 μm	10
10	Multiview band 1 image of a painted partially corroded coupon	11
11	Amber IR image of 3.7 mil thick primer and topcoat on half-corroded aluminum coupon.....	12
12	Comparison of an unpainted pre-corroded aluminum panel with an IR image of the sample panel coated with 3.7 mil of military spec paint.....	12
13	Comparison of a visible image of an unpainted corroded aluminum panel, and an IR image of the same panel with a 3.7 mil of military spec primer and topcoat	13
14	Comparison of a visible image of corroded panel with IR images of painted panels.....	13
15	Comparison of a visible image of a pre-corroded anodized aluminum coupon with IR images of painted versions.....	14

ILLUSTRATIONS (CONTD)

Fig.		Page
16	Comparison of a visible image of a pre-corroded Alodined aluminum coupon with IR images of painted versions	14
17	Comparison of the IR images of unpainted coupons with IR images of the coupons with approximately 5.6 mil of E2-C paint	15
18	Comparison of visible image of corroded aluminum panel with FLIR PtSi imaged of the same panel with 8.3 mil of primer and topcoat.....	16
19	Comparison of a visible image of an unpainted panel with an unfiltered Merlin InSb IR image of the same panel coated with 8.3 mil of paint	17
20	Comparison of a visible image of an unpainted panel with an unfiltered Merlin InSb IR image of the same panel coated with 8.3 mil of paint	17
21	Comparison of a visible image of an Alodined coupon with an unfiltered Merlin InSb IR image of the same coupon coated with 6 mil of paint.....	17
22	Comparison of the Merlin IR images of unpainted coupons with IR images of the coupons with approximately 5.6 mil of E2-C paint.....	18
23	DHR of 2024 and 7075 bare and clad aluminum 3" X 6" coupon, coated with CCC.....	21
24	DHR of as prepared sulfuric acid anodized 2024 and 7075 bare and clad aluminum coupons	21
25	Comparison of as prepared coated 2024 bare aluminum with salt fog corroded 2024 aluminum	22
26	Scanning electron micrograph of a salt fog corroded bare aluminum coupon. Oxide is primarily Al_2O_3	22
27	Reflectance of Al_2O_3 oxide on 3" X 6" aluminum coupon. (Corroded aluminum coupon included for comparison)	23
28	Measured and Modeled "Corroded" aluminum substrate. 45 mg Al_2O_3 powder on 3" x 6" aluminum coupon	24
29	DHR of salt fog exposed, CCC Al 2024.....	25
30	DHR of salt fog exposed SAA coated Al 7075	25
31	Long-term salt fog exposed heavily corroded CCC and SAA coupons.....	25
32	Directional hemispherical transmittance of topcoats and sealants	26
33	Transmittance of a series of camouflage gray	26
34	Reflectance of camouflage topcoat on uncorroded aluminum.....	27
35	Reflectance of camouflage topcoat on corroded aluminum.....	27

ILLUSTRATIONS (CONTD)

Fig.		Page
36	Comparison of measured and modeled reflectance of camouflage paint on un-corroded aluminum	28
37	Comparison of measured and modeled reflectance of camouflage topcoat on corroded substrate	28
38	Comparison of directly measured corroded substrate reflectance and the reflectance derived from DHR measurement of 1.4 mil camouflage painted substrate.....	29
39	Spectral ratio of reflectance of painted un-corroded substrate to the reflectance of a painted corroded substrate	29
40	2024 aluminum coupon exposed to salt fog. Visual image of corrosion before painting	31
41	Visual micrograph of a 0.250" fatigue crack propagating from a hole in a 2025 aluminum bar	31
42	Visual micrograph of a 0.001" diameter pit EDM machined into a 2024 aluminum bar.....	31
43	Indigo Merlin Mid IR imager for wide area spectral imaging through coatings a) 25 mm lens, b) 4x magnification lens.....	32
44	IR Illumination systems. a) quartz system, b) resistive reflector.....	33
45	Portable hand held wide area imaging system.....	33
46	Paint transmission window from 3.8 to 5.6 μ m	34
47	IR transmission curve of the medium band spectral filter	34
48	IR image of an unpainted corroded 2024 aluminum coupon. The corrosion products and pits are apparent.....	35
49	Visual image of 3.0 mil primer and topcoat on un-corroded 2024 aluminum coupon	35
50	Visual image of 3.0 mil primer and topcoat on corroded 2024 aluminum coupon	36
51	3 mil coating on corroded aluminum. The narrow strip on the left is unpainted.....	36
52	6 mil coating on corroded aluminum. The narrow strip on the left is unpainted.....	36
53	9 mil coating on corroded aluminum	36
54	12 mil coating on corroded aluminum	36
55	3 mil Dark Camo Grey topcoat on corroded aluminum. The narrow strip on the left is unpainted	37
56	3 mil Dark Camo Grey with Low IR primer on corroded aluminum. The narrow strip on the left is unpainted.....	37
57	Comparison of visible and IR image of an E2-C access panel. a) visible image of paint surface only, b) IR image through the paint to metal surface underneath	37

ILLUSTRATIONS (CONTD)

Fig.		Page
58	A visual (a) photo and an IR image (b) of corroded fasteners under paint in a Joint STARS 707 wing section.....	38
59	A visible image (a) of an unpainted fastener head, an IR image (b) of the same fastener covered with 3 mil primer and topcoat	38
60	Additional IR images of metal surface conditions through paint on aircraft parts.....	39
61	Outdoor imaging of painted test coupon: a) in shade, b) in sun with heating (summer).....	39
62	Outdoor imaging of painted wing section fastener corrosion: a) in shade, b) in sun after heating (summer).....	40
63	Successively smaller length fatigue cracks imaged under 3.5 mil primer and topcoat using a 25 mm IR lens.....	40
64	0.120" fatigue crack in 2024 aluminum bar imaged through 3.5 mil primer and topcoat	41
65	0.060" fatigue crack in 2024 aluminum bar imaged through 3.5 mil primer and topcoat	41
66	0.030" fatigue crack in 2024 aluminum bar imaged through 3.5 mil primer and topcoat	41
67	0.060" fatigue crack corroded, painted, and imaged with the IR system.....	42
68	EDM simulated pits in 2024 aluminum imaged through 3.5 mil primer and topcoat	42
69	Comparison of opposite polarizations on camera optics for IR imaging of 4 mil black paint on anodized aluminum coupon, a) polarizer parallel to plane of incidence, b) polarizer perpendicular to plane of incidence	43
70	IR camera mounted on a tripod.....	47
71	Portable IR System with Battery Pack	48
72	Portable System.....	48
73	Corrosion on an unpainted panel on the left and the same corrosion under 6 mils (.006') of paint once the panel was painted.....	49
74	Corrosion on the surface of an unpainted panel on the left and the same corrosion under 8 mils (.008') of paint once the panel was painted	49
75	Effect of IR signal clarity as a function of wavelength. The optimum wavelength in this study turns out to be 4.82 micrometers.....	50
76	Photographs of the overall panels as taken from an E-2C	
77	Details of an E2C Panel in various locations around fastener holes plus a hidden ink stamp part number and an inspection stamp marking.....	51
78	Hi-Lok® fastener head under visible light and under IR looking though 4 mils (.004") of paint	51

ILLUSTRATIONS (CONTD)

Fig.		Page
79	Detection limits of a fatigue crack produced in the laboratory by an MTS Fatigue Machine	53
80	0.060-in. crack under 3 mils (0.003in.) of paint	53
81	0.030" crack under 3 mils (.003") of paint	54
82	Corroded crack produced in the lab by placing the 2024-T3 bare, aluminum specimen in salt water for a number of days.....	54
83	Different size pits under 3 mils of paint using the IR camera system	55
84	Effect of averaging four pictures or frames and making a composite photograph	55
85	Grayscale Histograms	56
86	Crack detection as a function of paint thickness using 1X IR macro lens.....	57
87	Differences in grayscale level, but not gross differences	57
88	Effect of increasing the IR energy and the increase of clarity of the IR imaging as the energy increases	58
89	IR image that does not penetrate to the substrate	59
90a	Visible image of corroded sample C1	59
90b	Visible image of the corroded sample C1 with 2.5 mil Gloss White	60
90c	IR image of the corroded sample C1 with 2.5 mil Gloss White	60
90d	Visible image of corroded sample C2.....	60
90e	Visible image of the corroded sample C2 with 3.5 mil Gloss White	61
90f	IR image of corroded sample C2 with 3.5 mil Gloss White	61
90g	Visible image of corroded sample C3.....	61
90h	Visible image of corroded sample C3 with 5.6 mil Gloss White	62
90i	IR image of corroded sample C3 with 5.6 mil Gloss White	62
90j	Visible image of corroded sample C4.....	62
90k	Visible image of corroded sample C4 with 8.2 mil Gloss White	63
90l	IR image of corroded sample C4 with 8.2 mil Gloss White	63
90m	Grayscale variations drip significantly with increase paint thickness	64
90n	Visible image of corroded sample C5.....	64
90o	Visible image of sample C5 with 2.5 mil Camouflage Gray	65
90p	IR image of sample C5 with 2.5 mil Camouflage Gray	65
90q	Visible image of corroded sample C6.....	65
90r	Visible image of C6 with 4.6 mil Camouflage Gray	66
90s	IR Image of C6 with 4.6 mil Camouflage Gray	66

ILLUSTRATIONS (CONTD)

Fig.		Page
90t	Visible image of corroded sample C7.....	66
90u	Visible image of C7 with 7.3 mil Camouflage Gray	67
90v	IR image of C7 with 7.3 mil Camouflage Gray	67
90w	Visible image of C9	67
90x	Visible image of C9 with 2.5 mil Camouflage Gray and low IR primer	68
90y	IR image of C9 with 2.5 mil Camouflage Gray and low IR primer	68
91	LN2 cooled filter system image showing corrosion under 4 mil of paint.....	69
92	Uncooled filter produces images better than the cooled filter	69
93	Painted fastener heads under IR illumination	70
94	Effect of polarization on dark gray paint on aluminum	70
95	Fastener head corrosion and no presence of cadmium plating	71
96	Corrosion under green primer on actual Joint STARS stringer.....	71
97	Joint STARS aircraft in hangar during maintenance	72
98	Area on top of painted wing surface	72
99	Corrosion is indicated by dark areas around fasteners. Lines of sealant can be seen in all photographs.....	73
100	Grumman Bearcat Field Demonstration	74
101	Operator viewing welded duct from Bearcat in real time	74
102	Welded duct from Bearcat	74
103	LLDR camera with potential for SERDP Program modification for transition phototype	75
104a	Graphite painted panel at 89F, RT-calibration	80
104b	Graphite painted panel at 90F, 84F hot-calibration	81
104c	Graphite with Cu fiber painted panel at 90F, 84F hot-calibration.....	81
104d	Graphite with Cu fiber painted panel at 74F, 84F hot-calibration.....	81
104e	Graphite with Cu weave, painted panel at 91F, RT-calibration	82
104f	Graphite with Cu weave, painted panel at 87F, RT-calibration	82
104g	Graphite with Cu weave, painted panel at 82F, RT-calibration	82
104h	Graphite, painted panel at 90F, RT-calibration	83
104i	Graphite, painted panel at 86F, RT-calibration	83
104j	Graphite, painted panel at 82F, RT-calibration	83
104k	Graphite, painted panel at 78F, RT-calibration	84
104l	Graphite, painted and primed panel: Visible image.....	84
104m	Graphite with Cu weave, painted and primed panel: Visible image.....	84

ILLUSTRATIONS (CONTD)

Fig.		Page
104n	Aluminum C2 : Visible image	85
104o	Aluminum C2 1x mag. at 77F, IR Reflectance image	85
104p	Aluminum C2 1x mag. at 75F, IR Reflectance image	85
104q	Aluminum C2 1x mag. At 84F, RT-calibration	86
104r	Aluminum C2 1x mag. At 78F, RT-calibration	86
104s	Aluminum C2 1x mag. At 72F, RT-calibration	86
104t	Aluminum C9 (low IR primer) IR Reflectance Image.....	87
104u	Aluminum C9 (low IR primer) at 96F, 78F hot-calibration.....	87
104v	Aluminum C9 (low IR primer) at 86F, 78F hot-calibration.....	87
104w	Aluminum C9 (low IR primer) at 79F, 78F hot-calibration.....	88
104x	Aluminum C9 (low IR primer), Visible Image	88
105	Schematic of electrochemical cell for localized impedance measurement.....	92
106	Schematic of the Volta potential measurements in ionized air.....	93
107	Impedance spectra on scribed SAA prepared Al2024, exposed to salt fog for 0, 3, 7 and 14 days, measured in borate solution pH 8.4	95
108	Impedance spectra on SAA prepared Al2024, exposed to salt fog for 0, 3, 7 and 14 days, measured in borate solution pH 8.4	96
109	Impedance spectra for scribed and prepared surface on SAA prepared Al2024, exposed to salt fog for 14 days, measured in borate solution pH 8.4	97
110	Impedance spectra in borate solution pH 8.4, 0.1M Na ₂ SO ₄ and 0.1M NaCl on SAA prepared Al2024, exposed to salt fog for 7 days	99
111	Impedance spectra in borate solution pH 8.4, 0.1M Na ₂ SO ₄ and 0.1M NaCl on scribed SAA prepared Al2024, exposed to salt fog for 7 days.....	100
112	Impedance spectra for scribed and prepared surface on scribed SAA prepared Al2024, exposed to salt fog for 14 days, measured in 0.1M NaCl.....	101
113	Impedance spectra on SAA prepared Al2024, exposed to salt fog for 0, 7 and 14 days, measured in 0.1M Na ₂ SO ₄	102
114	Impedance spectra on scribed SAA prepared Al2024C, exposed to salt fog for 0, 7 and 14 days, measured in 0.1M Na ₂ SO ₄	103
115	Impedance spectra for SAA prepared Al7075, Al 7075C and Al 2024, exposed to salt fog for 7 days, measured in 0.1M NaCl	105
116	Impedance spectra unexposed Al2024C with surface treatment SAA, DEOX and CCC, measured in 0.1M Na ₂ SO ₄	106

ILLUSTRATIONS (CONTD)

Fig.		Page
117	Impedance spectra on unexposed Al2024 and Al2024C, each with surface treatment SAA and CCC, measured in 0.1M Na ₂ SO ₄	107
118	Impedance spectra on scribed Al 2024C prepared with SAA and CCC, exposed to salt fog for 14 days, measured in a two electrode cell in 0.1M Na ₂ SO ₄	108
119	Scans showing Volta potential variations over a multi-metal sample	109
120	Volta potential measurements in ionized air for a simulated coating defect	110
121	Wet (0.1M Na ₂ SO ₄) and dry impedance measurements of painted Al (#6 prime 2.4 mil #655 ghost gray 36375); (a) Bode plot; (b) Nyquist plot	112
122	Changes in wet impedance measurements with time.....	113
123	Dry impedance measurements of scratched, clad AA2024 painted after corrosion	114
124	Dry impedance measurements of AA2024 painted after corrosion	115
125	Dry impedance measurements of AA2024 painted after corrosion	116
126	Volta potential measurements over corroded and painted AA2024	117
127	Volta potential measurements over corroded and painted AA2024	117
128	Volta potential measurements in ionized air over a scratched and partly corroded clad AA2024 sample.....	118
129	Volta potential measurements of corroded clad Al alloy AA2024.....	121
130	Volta potential measurements of Al alloy AA2024 covered with four different thickness of itrocellulose paint	122
131	SKP Volta potential measurements of corroded clad Al alloy AA2024 covered with several layers of paint	123
132	Detection of corrosion under 3.6 mil paint layer using three different scanning techniques	124
133	IMS of corroded sulfuric acid anodized AA 2024.....	125
134	IMS of painted AA2024 scribed before corrosion.....	126
135	IMS of AA 7075 anodized in sulfuric acid after crevice corrosion under masking	128
136	Video images of the corrosion in 1M NaCl Agar gel: (a) Al alloy AA2024; (b) Al alloy AA7075.....	129
137	IMS on the corroded Al alloys AA2024 and AA7075. Video images of the samples after 12 weeks corrosion in gel	130
138	IMS on Al alloy AA7075 (shown in Fig. 9b) after 12 weeks of corrosion in gel	131
139	XRD patterns for AL alloys AA2024 and AA7075 corroded in 1M NaCl gel and for the corresponding non corroded alloys.....	132

ILLUSTRATIONS (CONTD)

Fig.		Page
140	Effect of paint thickness on reflectance of painted non-corroded Al alloys 2024-T3	135
141	Reflectance spectral ratio of painted non-corroded/corroded Al 2024- T3 samples	136
142	Reflectance spectral ratio vs. paint thickness for different paint systems	137
143	Impedance measurement of Mylar layers with a dry copper disk	139
144	Impedance measurements of Insignia White paint on Al alloys 2024-T3 with dry copper disk	140
145	Impedance measurements of Insignia White paint on corroded and non-corroded Al alloys 2024-T3 with wet stainless steel hemisphere probe.....	141
146	Impedance measurements of Dark Camouflage paint on corroded and non-corroded Al alloys 2024-T3 with wet stainless steel hemisphere probe.....	142
147	Impedance measurements of Low IR paint on corroded and non-corroded Al alloys 2024-T3 with wet stainless steel hemisphere probe	143
148	Scanning impedance probe measurements on painted Al alloy 2024.....	144

THIS PAGE INTENTIONALLY LEFT BLANK

ACRONYMS

BNL	Brookhaven National Laboratory
CCC	Chemical Conversion Coating
CTC	Concurrent Technologies Corporation
DEOX	Deoxidized
DHR	Directional Hemispherical Reflectance
ECS	Environmental Control System
EDM	Electro Discharge Maching
EDS	Energy Dispersive X-ray Spectroscopy
EDX	Energy Depressive X-ray
EIS	Electromechanical Impedance Spectroscopy
ESTCP	Environmental Security Technology Certification Program
FLIR	Forward Looking Infrared
FTIR	Fourier Transform Infra Red
IMS	Infrared Microspectroscopy
IPR	Interim Progress Review
IR	Infrared
ITAR	International Traffic and Arms Regulations
LLDR	Lightweight Laser Designator Rangefinder(from Indigo, see their website)
LN2	Liquid Nitrogen
MCT	Mercury Cadmium telluride
MPK	Methyl Propyl Ketone
NADEP	Naval Depot
NDI	Non-Destructive Inspection
NEAT	Noise Equivalent Delta Temperature
OML	Outer Mold Line

ACRONYMS (CONTD)

PVDC	Polyvinylidene Dichloride
RT	Room Temperature
SAA	Sulfuric Acid Anodize
SDLM	Standard Depot Level Maintenance
SERDP	Strategic Environmental Research & Development
SKP	Scanning Kelvin Probe
SNDE	Spectral Nondestructive Evaluation
VOC	Volatile Organic Compounds
WASI	Wide Area Spectral Imaging
XRD	X-ray Diffraction

EXECUTIVE SUMMARY

Project awarded “Pollution Prevention Project of the Year” for 2003
--

Surface corrosion on aluminum aircraft skins, near joints and around fasteners is often an indicator of buried structural corrosion and cracking. Aircraft paints are routinely removed to reveal the presence of corrosion on the surface of metal structures, and the aircraft is subsequently repainted. This process can be very expensive, time consuming, and results in the generation of air pollution and process waste. A method is needed to detect the early onset of corrosion on metal substrates covered by protective coatings so that aircraft paints do not have to be stripped without cause. By employing nondestructive techniques to inspect the aircraft exterior structure without removing coatings, the amount of stripping and reapplication of coatings that occurs at the military rework facilities can be substantially reduced.

The objective of this SERDP Project 1137 was to develop nondestructive inspection techniques to locate hidden corrosion on aircraft surfaces without requiring removal of the coating. Several techniques have been identified that can achieve this: imaging of the surface using spectral nondestructive evaluation (SNDE) and wide area spectral imaging (WASI), and scanning reference electrode measurement techniques using instrumentation such as the Scanning Kelvin Probe (SKP).

This report describes progress made for years 1999 through 2004 for Corrosion *Detection and Standards Development*. Four principal techniques were investigated: spectral nondestructive evaluation (SNDE), wide area spectral imaging (WASI), electrochemical impedance spectroscopy (EIS) and a scanning probe in a conducting gas (SPG).

The results of the spectral imaging work indicate that this technique can be used to detect small quantities of corrosion under most conventional coating systems. It has been shown that adequate transmittance is obtained with standard epoxy primers, as well as Koroflex (MIL-P-85582, MIL-P-23377, and TT-P-2760). These coatings are typically applied to a thickness range of 0.6 to 0.9 mils. In addition, this technique can “see through” up to 10 mils of a standard, polyurethane topcoat (MIL-PRF-85285). Two areas of difficulty were encountered during this phase of the program. The data indicates that the aluminum oxide peak does not image well through the sprayable polysulfide primer (MIL-S-81733) or Low IR primer.

Electrochemical measurements have been made of a range of samples with different surface preparation, coatings before and after exposure to corrosion environments. Two techniques were investigated EIS and SGP to measure Volta or work function difference. A probe was developed to make the EIS measurements on localized areas of coated and uncoated samples. The measurements have shown that scratches in chromate conversion coatings and sulfuric acid anodized aluminum alloys can be detected. SGP measurements have demonstrated that the results obtained with uncoated metals are in good agreement with conventional work function measurements using a Kelvin probe. The SGP method was found to be very sensitive of defects in organic coatings.

After much investigation, it was found that the spectral imaging methods both in the Infrared (IR) Reflectance Mode and the Black Body Mode demonstrated a level of maturity warranting field trials. Both inspection processes are patent pending in accordance with the SERDP Contract No. DACCA72-99-C-0011.

The SERDP Pollution Prevention Project 1137, Non-Destructive Testing of Corrosion Under Coatings has successfully investigated a number of specific techniques that showed significant promise to reliably detect corrosion under coatings to warrant a recommendation to perform a comprehensive ESTCP Demonstration and Validation Program. Specifically these methods developed under this SERDP Project include, the infrared (IR) reflectance mode and the method known as the black body mode. The IR reflectance mode works by illuminating the surface with IR energy, which passes directly through the coating in the 3 to 5 micron region. The IR energy then reflects off the metallic surface under the coating and back through the coating to an IR camera, which detects corrosion by contrasting the corrosion as darker, as the corrosion is a lower reflecting surface from the higher reflecting surface or lighter non-corroded surfaces. The black body mode detects corrosion by the metallic surface emitting IR radiation, as a black body radiation with the corrosion showing up in the IR as a lighter structure, while the non-corroded surface shows up as a darker surface with emitting surface being the reciprocal of the reflectance. Basically, the warm surface of the structure or part being observed provides the IR illumination, which is filtered in the black body mode by the coating itself, prior to being detected by the camera. The advantage of the black body method is that the IR radiation only has to pass through the coating once and that special IR illumination handling equipment is not required in this mode.

Both these modes are capable of producing high fidelity images of corrosion and other structural defects under coatings that can be used to make real time decisions regarding whether or not the outer mode line (OML) removal of the organic coatings from an existing aircraft structure is required to repair existing corrosion or other structural defects beneath the coating. It is anticipated that significant amounts of pollution will be saved either by extending the time between organic coating removal and/or by enabling the use of newly developed and implemented extended life topcoats. Other pollution reductions are anticipated, once the IR Reflectance/Black Body system has been established as a common tool to inspect critical fittings, hardware such as fasteners, landing gear, fuel tank areas, seat rails, and other internal aircraft structures. Note. Extended life topcoats have been implemented in the field on the C-17 and the F-15 weapon platforms with no validated means to economically inspect for corrosion and other structural defects under the coatings.

Once demonstrated and validated, this newly developed and patent pending technology could be used to save a significant amount of pollution by eliminating unnecessary and costly steps to remove organic coatings that would otherwise be acceptable for continued use. The pollution saved would include the pollution generated from the use of organic paint removers, surface preparation chemicals, and pollution generated from the application of new replacement paints, which includes volatile organic compounds, carcinogenic chromates, and

toxic solid waste sludge that needs to be specially processed and land filled causing long term environmental liability concerns.

Pollution savings can be projected for both military and commercial aircraft based on extending the life of the exterior Outer Mold Line (OML) coatings. For projection purposes, extending the life from a 5-year cycle to a 10-year cycle would result in savings of an estimated 48,000 lbs of volatile organic compounds (VOC) per year and 8,000 lb of toxic chromate per year for military operations, as well as an estimated 280,000 lbs of VOC per year and 62,000 lb of toxic chromates per year for commercial aircraft operation. The number of aircraft used for this calculation (see Appendix 7, pages A7-1 and A7-2) is conservatively low, so actual savings could be higher. It also must be understood that long life coatings currently used are gaining field time and that the actual extension period could be less than 10 years, in which case pollution and cost saving need to be prorated for a more accurate projection.

In regards to the business case, cost savings resulting from the elimination of a 5-year cost removal cycle and going to a 10-year cycle would be significant. These cost savings can be projected and are \$40M for military aircraft and \$159M per year for commercial aircraft.

Factors negatively influencing these projections include the use of low IR primers and specialty coatings filled with fillers that impede IR radiation. This is the case with a number of military aircraft. However, it must be understood that standard military aircraft coatings such as MIL-PRF-23377 TYI, MIL-PRF-85582 TYI, MIL-PRF-85285 TYI, and TT-P-2760 TYI are transparent to IR radiation in the 3 to 5 micron range and work well, with respect to the IR reflectance system investigated. Commercial aircraft normally do not employ IR and specialty thick coatings, so pollution saving projecting should not be influenced by these specialty coatings.

Special Note: Certain items in this document may contain ITAR sensitive material or be controlled by ITAR. A review of this document should be made by the applicable government agency before public release.

INTRODUCTION AND OVERVIEW

Aircraft rework typically involves the stripping and reapplication of coatings applied to protect the outer mold line (OML) of aircraft structure. Recent advances in coating technology are leading to the development of coatings that will last beyond standard depot level maintenance (SDLM) cycles for military aircraft. It is currently feasible to apply corrosion inhibiting primers that provide excellent adhesion properties and are not intended to be routinely stripped. In addition, it is anticipated that the next generation of cleanable, durable topcoats may remain on the air vehicle for extended periods (10+ years). In the past, stripping of the coatings provided a means to visually inspect the condition of the substrate. As we move toward application of more permanent coatings, it is imperative that alternate inspection techniques be developed which can verify the integrity of the coating system and substrate without relying on coating removal.

Over the years, a variety of nondestructive detection methods have been evaluated for detecting corrosion with varying degrees of success. One of the limitations of these previous techniques is their inability to detect relatively small concentrations of corrosion products at the metal/paint interface. Ultrasonic, thermography, and eddy current techniques are useful for crack detection, however, these methods tend to concentrate on detecting significant amounts of bulk corrosion and defects in structural members. This SERDP project addresses the use of technologies and techniques that can be used for detecting changes in the coating system and very small amounts of corrosion under the coatings.

The objective of this SERDP project is to develop nondestructive inspection techniques to locate hidden corrosion on aircraft surfaces without requiring removal of the coating. Several techniques have been identified that can achieve this: imaging of the surface using spectral nondestructive evaluation (SNDE) and wide area spectral imaging (WASI), and scanning reference electrode measurement techniques using instrumentation such as the Scanning Kelvin Probe (SKP).

For the SNDE portion of the program, the bulk of the early effort concentrated on:

- Establishing baseline spectral properties relevant to corroded aluminum aero-structures;
- Gauging quantitative spectral measurement through modeling of corrosion and salt fog exposure for variety of surface treated aluminum coupons;
- Spectral evaluation of coated panels plus conduct an analysis of the corrosion signature sensitivity.

For the two electrochemical measurement techniques early efforts concentrated on:

- Development of the impedance measurements probes
- Development of measurement techniques optimized for field detection of corrosion underneath a paint

- Performing Volta potential measurement using conventional Kelvin probe methods and with conducting gases and baseline against measurements obtained using the Kelvin Probe.

The following sections describe these novel inspection techniques for detecting corrosion under a paint film and the progress made toward meeting the objectives of this program.

TECHNICAL BACKGROUND

Corrosion can occur at a variety of locations on an aircraft. These include joints, fasteners, and repairs, as well as skin surfaces exposed to harsh environments (i.e., sea spray). A variety of aircraft at Northrop Grumman's facility in St. Augustine, Florida were examined, included the E-2C and the EA-6B, which are primarily carrier-based aircraft and are consequently exposed to sea spray and salt fog. Corrosion was found to concentrate around joints, fasteners, and in areas where water could accumulate. Extensive corrosion causes obvious blistering to the paint, but incipient corrosion could not be detected visually.

A variety of nondestructive detection methods have been evaluated in the past for detecting corrosion with varying degrees of success. One of the problems encountered with these previous techniques is their inability to detect relatively small concentrations of corrosion products at the metal/paint interface. Ultrasonics, thermography, and eddy current techniques are useful for crack detection; however, these methods tend to concentrate on detecting significant amounts of bulk corrosion and defects in structural members. This program addresses the use of technologies and techniques that can be used for detecting changes in the coating system and very small amounts of corrosion under the coatings. The following paragraphs describe the emerging inspection techniques for detecting corrosion under a paint film that will be evaluated in this program.

The following paragraphs provide background information and descriptions for each of the nondestructive corrosion detection and measurement techniques evaluated by this program.

SPECTRAL NONDESTRUCTIVE EVALUATION

SDNE uses directional hemispherical reflectance (DHR) to determine the spectral properties of surfaces. As shown in Figure 1, a collimated IR beam in the range of 1.8 to 15.4 μm is directed near normal to the surface, and then the reflected light, both specular and diffuse, is measured in an integrating sphere. Reflectance is plotted as a function of wavelength or wavenumber. It is important to collect the diffuse component of the reflected light since the reflectance signal from any corrosion at the metal surface will be significantly scattered by the overlying paint layer.

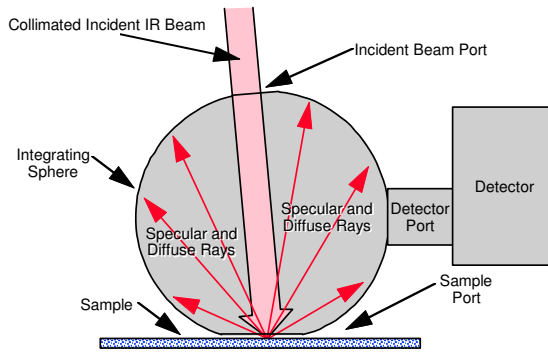


Figure 1 Integrating sphere system used to measure directional hemispherical reflectance.

The SNDE technique depends on the generation of a database for the spectral signatures of corroded surfaces. Baseline reflectance measurements for clean, uncoated aluminum alloys are compared to measurements made on corroded panels in order to identify and quantify corrosion byproduct signatures. Similarly, the reflectance through typical aircraft coatings must be measured and characterized. Using this database and appropriate analysis techniques should enable identification of corrosion on painted aircraft structure.

Spectral Nondestructive Evaluation – Wide Area Spectral Imaging

One way to detect corrosion products at the paint/metal interface is to use an optical reflectance probe to detect changes in reflectance as a result of corrosion. Spectral reflectance signatures may be used to detect the presence of various chemical species, including corrosion products. A light beam must be able to pass through the paint, reflect off the metal surface, and pass back out through the paint coating. This concept is referred to as Spectral Nondestructive Evaluation (SNDE). Paints are normally designed with pigment sizes tailored so that they are opaque in the optical region of the spectrum (0.4 to 0.8 μm), so they preclude using optical techniques in the visible to “see” through the coating to the metal. However, the scattering power of pigments is diminished as the probe wavelength becomes longer. For many paints, a spectral window opens in the near and mid infrared spectral regions.

We have first concentrated our efforts in SNDE in the area of spectral imaging. A natural application of the SNDE concept is to employ the use of IR focal plane technology coupled to spectral filters to image the reflectance of large areas of an aircraft’s structure simultaneously. We refer to this as wide area spectral imaging (WASI). Sensitive high-resolution IR focal plane cameras are already used to obtain thermal images for use in thermography. For WASI, however, we will use these IR cameras to image reflectance variations over a painted aluminum surface as a function of wavelength. We will be using our experience in hyperspectral imaging systems for remote sensing to develop an “up close” version for NDE. From the spectral database of paints and corrosion of metal surfaces developed for SNDE, we selected band pass filters whose wavelengths correspond to the paint spectral windows and to paint opaque regions. Figure 2 shows a schematic of the WASI technique. We

will use spectral imaging systems specially designed and built by Northrop Grumman for remote sensing applications, as well as commercial systems. These systems include Northrop Grumman's Multiview and commercial IR cameras. Multiview is a complete imaging system, including an IR focal plane divided into four quadrants, each with its own narrow bandpass spectral filter. Images are collected at four wavelengths simultaneously, and with a suitable choice of bandpass filters, a corrosion map of the aircraft surface is automatically generated. Commercial cameras can also be used with IR filters to obtain a multispectral image. These systems were incorporated in a hand-held camera, which produces images that can be quickly downloaded to a computer for analysis.

A WASI hand-held camera system can be used to look at broad areas of an aircraft fuselage, and with a change of lens, it can be converted into a low power magnifying system to get a detailed assessment of corrosion.

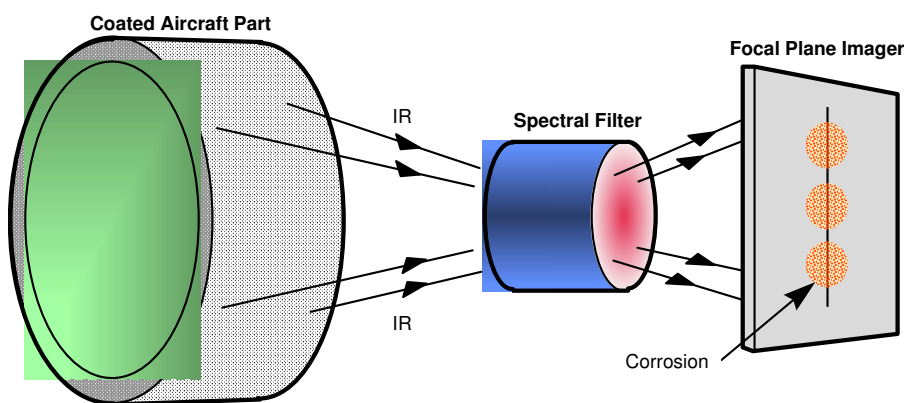


Figure 2 WASI Technique

SNDE/WASI Project Accomplishments

Sample Preparation – Typical aircraft structural aluminum consists mainly of 2024 and 7075 alloys. This material is used either clad with an outer layer of pure aluminum, or with a bare surface. The clad layer is there to provide extra resistance to corrosion. A large number of 3" x 6" and 4" x 6" coupons of the 2024 and 7075 bare and clad aluminum were made to be pre-corroded and coated with a variety of aircraft paint systems. After the coupons were cut from sheet stock, they were surface treated either with an Alodine chromate conversion coating or anodized in sulfuric acid. These surface treatments provide the critical corrosion protection to the underlying aluminum. These coupons were then scribed to expose the underlying aluminum, and exposed to either humidity or salt fog to accelerate corrosion.

Figure 3 shows visual image photographs of a set of salt fog exposed coupons. The samples were masked, and the scribed center square sections were placed in a salt fog chamber to accelerate corrosion. As can be seen in Figure 3, various amounts of corrosion are present in these samples. The corrosion exists only as a superficial thin film on the surface.

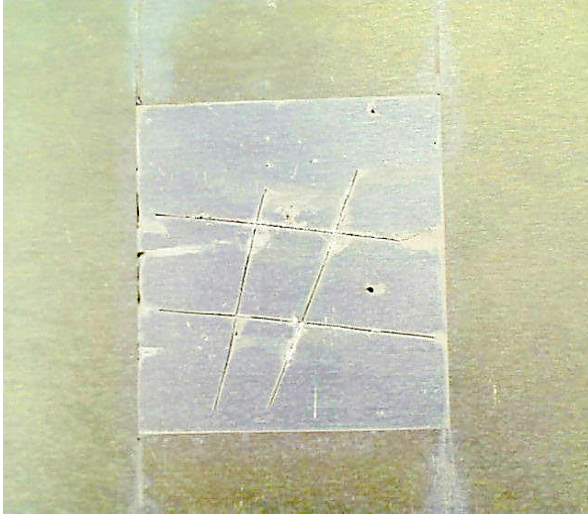


Figure 3a Alodine (chromate conversion) coated 2024 bare aluminum alloy coupon (2-in. x 2-in. center square scribed and exposed).

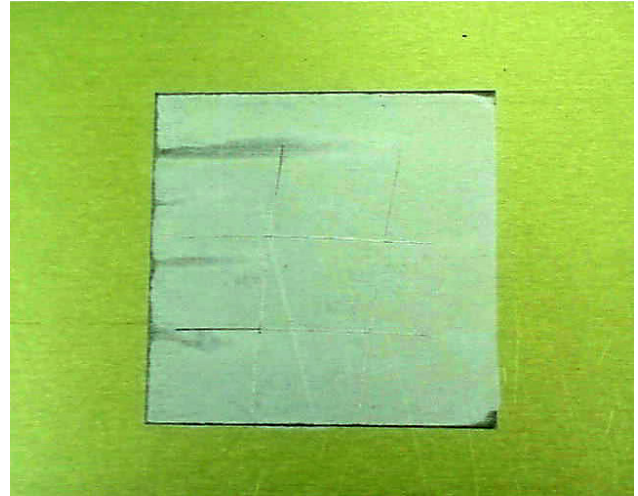


Figure 3b Sulfuric acid anodized 2024 bare aluminum alloy coupon (2-in. x 2-in. center square scribed and exposed to salt fog).

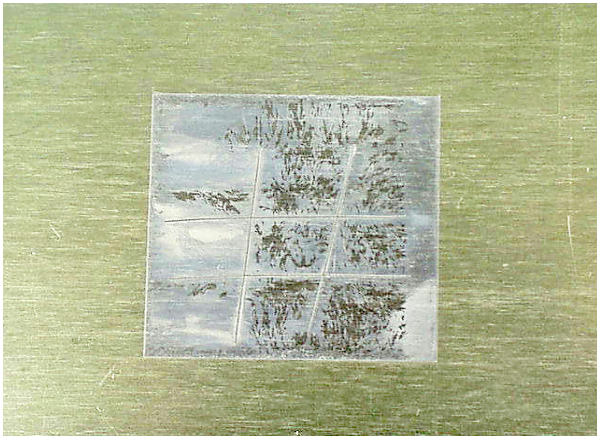


Figure 3c Alodine (chromate conversion) coated 2024 clad aluminum alloy coupon (2-in. x 2-in. center square scribed and exposed to salt fog).

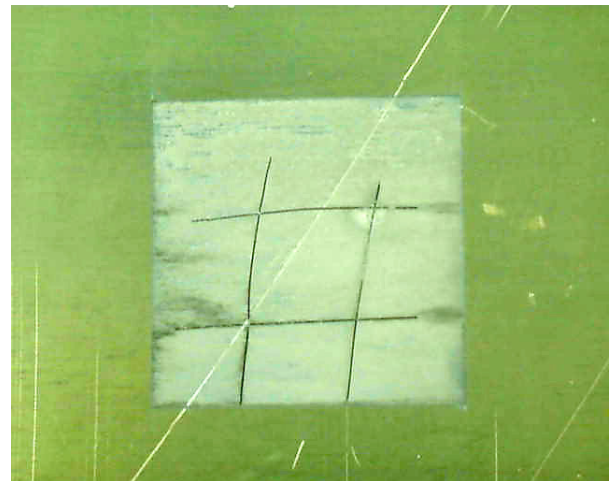


Figure 3d Sulfuric acid anodized 2024 clad aluminum alloy coupon (2-in. x 2-in. center square scribed and exposed to salt fog).

Other corrosion samples were prepared via a combination of accelerated and natural corrosion. Figure 4 shows a photo of a 12-in. x 12-in. pre-corroded clad 2024 aluminum panel.



Figure 4 Photograph of a naturally corroded 12-in. x12-in. 2024 clad aluminum panel.

In addition to corrosion specimens, we fabricated a number of simulated crack and surface morphology samples to determine the extent to which the WASI technique can see details on the metal surface. Figure 5 shows an example of a simulated notch or crack machined into a hole in an aluminum bar via electro discharge machining (EDM). Figure 6 shows a photograph of a fastener in an aluminum part. These parts were later coated for imaging under the applied coatings.

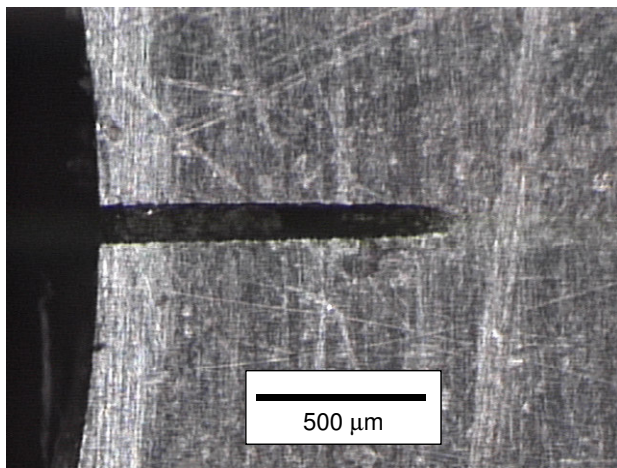


Figure 5 Micrograph of an EDM simulated crack propagating from a hole in an aluminum bar.

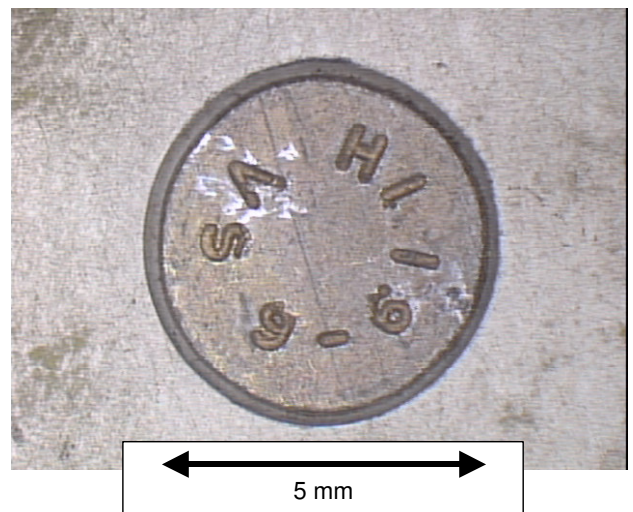


Figure 6 Micrograph of an aircraft fastener head in an aluminum part.

Paint Systems – For painting the coupons and parts, a quick drying topcoat was initially chosen for convenience. A Hentzen military specification topcoat (MIL-PRF-85285) was used along with a military specification primer (MIL-PRF-23377TYICLC) as a first test of the imaging capability of the IR cameras. Figure 7 shows the spectral reflectance of a Hentzen coated aluminum coupon.

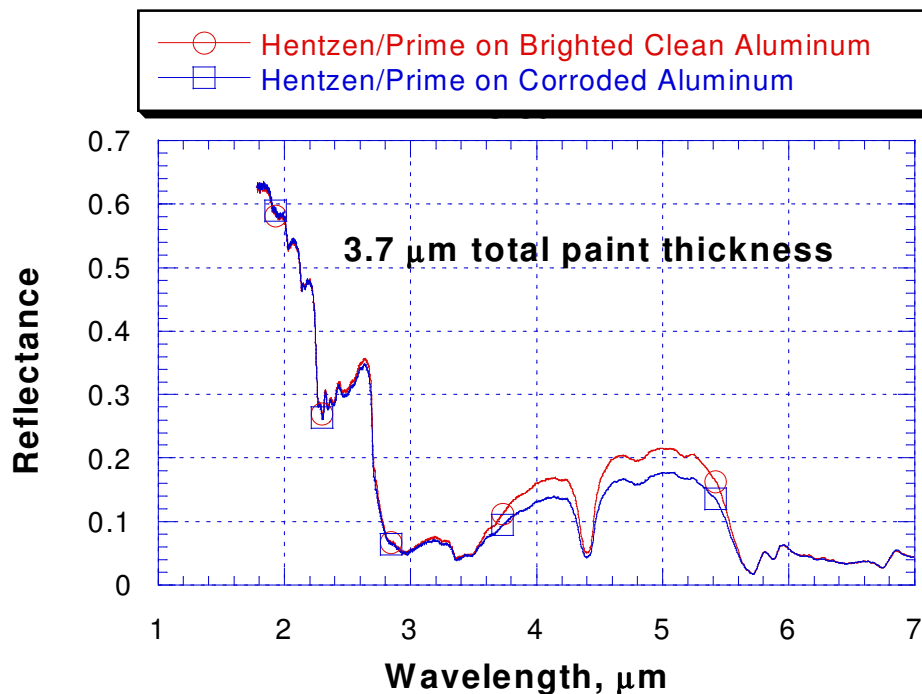


Figure 7 Reflectance of Hentzen paint system on a partially corroded aluminum coupon. Significant reflectance difference seen in the 3.6 to 5.4 μm range between corroded and uncorroded areas

The Hentzen topcoat shows a spectral transmittance window in a region similar to the other mil spec paints investigated previously. In addition to the Hentzen system, we also looked at coating systems such as those used for the Northrop Grumman E-2C Hawkeye airborne early warning aircraft. The spectral characteristics of these paints were previously reported.

Multiview Multispectral Camera System

Work on wide area imaging began with Multiview. Multiview has a 256 x 256 MCT detector divided into four quadrants. Each quadrant has its own band pass filter so that a four band spectral image is obtained. Figure 8 shows a photograph of a 4" x 6" aluminum coupon. The left hand side is corroded, and the right hand side is clean aluminum. Figure 9 shows a four band image of this unpainted coupon. The four bands all show contrast between the corroded and un-corroded areas, but the four quadrants have reduced the resolution of the image (128 x 128 pixels). Figure 10 shows a painted version of the same coupon in the 4.5 to 4.7 μm band. This coupon was painted with 0.8 mil of MIL-PRF-23377 primer and 2.9 mils Hentzen gloss white topcoat. The painted surface appeared smooth with no visible indication of the corrosion underneath. Some contrast can be seen between the corroded and un-corroded sides, but the resolution is poor. The initial limitations shown by the present configuration of the Multiview system led us to put it aside temporarily, and use a simple camera configuration to evaluate the WASI concept.

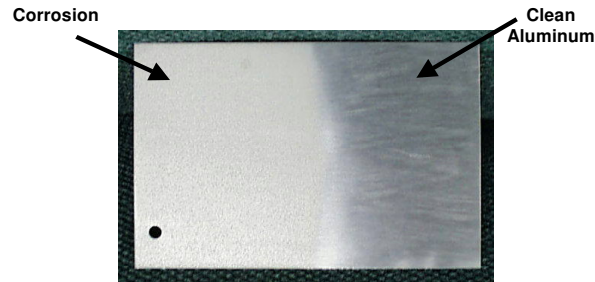


Figure 8 Unpainted partially corroded aluminum coupon.

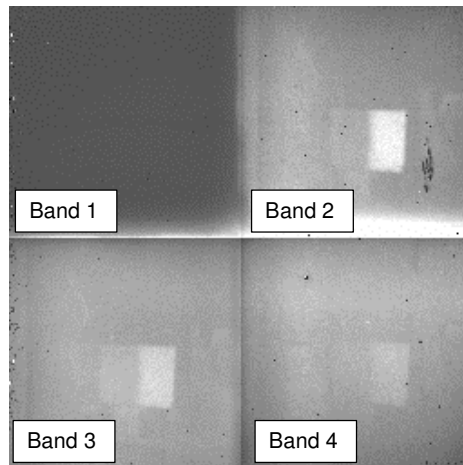


Figure 9 Four band Multiview image of an unpainted half-corroded coupon.
Band 1: 2.1-2.3 μm , Band 2: 4.5-4.7 μm , Band 3: 3.5-4.0 μm , Band 4: 3.2-3.5 μm .

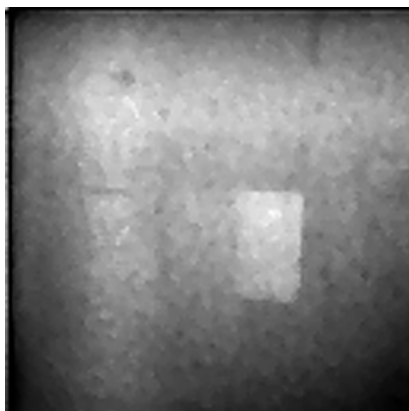


Figure 10 Multiview band 1 image of a painted partially corroded coupon.

Multispectral Amber IR Camera System

It was decided to shift emphasis away from the Multiview camera to the Amber camera system as a test bed for the WASI concept. The Amber camera has a 256 x 256 pixel InSb focal plane array sensitive in the 3 to 5 μm range. It has a nominal $\text{Ne}\Delta\text{T}$ (contrast sensitivity) of 20 mK. It is a liquid nitrogen cooled system with a cooled filter wheel to give it multispectral selectivity. It is equipped with a 50 mm germanium IR compatible lens. Image data is displayed in real time on a monitor, and it can be saved to a videotape or in 12 bit or TIFF digital format.

The internally cooled filter wheel has a number of IR filters that are compatible with the ranges needed for IR spectral imaging through paint. Specifically, we chose the 4.6 μm band pass filter to coincide with the paint transmission window shown in Figure 7. A hotplate illuminator was used for these first trials of the Amber system. Figure 10 shows an IR image of the coupon shown in Figure 8 painted with a total thickness of 3.7 mil primer and topcoat. Contrast can definitely be seen between the corroded and uncorroded sides. Apart from brightness and contrast adjustments, no image processing was applied to this image.

In order to obtain more detailed corrosion images underneath paint, 12" x 12" pre-corroded panels were fabricated with a random distribution of a thin layer of corrosion on the surface. They were then painted with primer and topcoat to a thickness of 3.7 mil. Figure 12 shows a comparison between a visible photo of an unpainted corroded region of the panel, and an IR image in the 4.6 μm band of the same area of the painted panel. As before the sample was illuminated with a simple hotplate. The corrosion pattern can be seen in significant detail in the IR image. This also includes buffing scratches in the un-corroded aluminum surface. The buffing was done to help the paint adhere to the untreated surface. It must be noted that none of the corrosion products could be visibly detected from the smooth painted surface.

Subsequent improvements were made in panel illumination. A large calibrated black body panel was employed as the illumination system. To achieve the maximum IR light output of the black body illuminator in the wavelength range of the paint transmission window, the black body was set to 617 F. Figure 13 shows an improved image comparison between a painted and unpainted panel. Direct blackbody imaging was used to illuminate the panel. Not only is corrosion shown in the IR image, but detailed abrasion scratches in the un-corroded areas are seen as well.

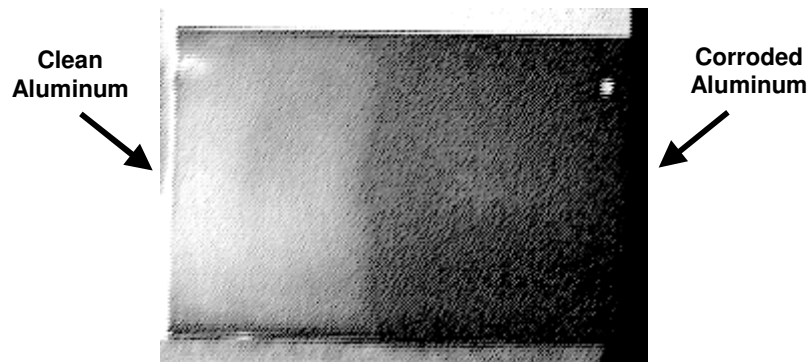


Figure 11 Amber IR image of 3.7 mil thick primer and topcoat on half-corroded aluminum coupon.

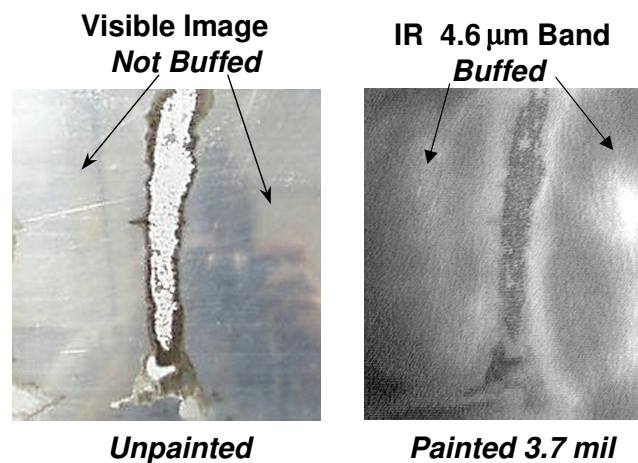


Figure 12 Comparison of an unpainted pre-corroded aluminum panel with an IR image of the sample panel coated with 3.7 mil of military spec paint.

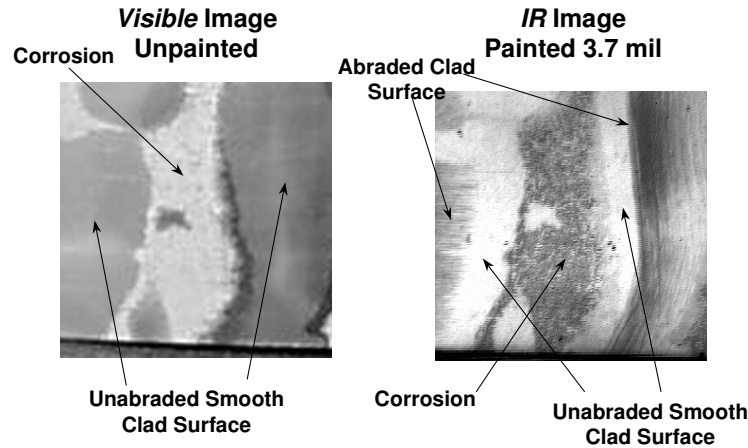


Figure 13 Comparison of a visible image of an unpainted corroded aluminum panel, and an IR image of the same panel with a 3.7 mil of military spec primer and topcoat. Both corrosion and scratches are detected.

Using this Amber camera and illumination combination, a paint thickness study was performed. A pre-corroded aluminum panel was painted with successive layers of primer and topcoat to thickness over 9 mil. Figure 14 shows a comparison of an unpainted panel with a series of successively thicker paint coatings. Again, direct blackbody reflective imaging was used to illuminate the panel. Corrosion features, using the IR camera setup described previously, can be seen through 8.8 mil of primer and topcoat.

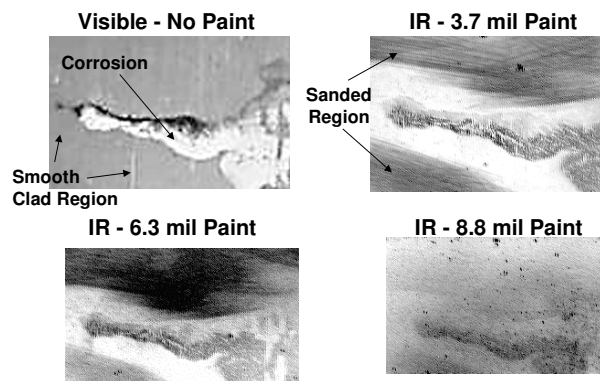


Figure 14 Comparison of a visible image of corroded panel with IR images of painted panels.

After achieving impressive results with pre-corroded clad aluminum panels, we began to look at pre-corroded Alodined and anodized pre-corroded coupons. This presented a more realistic situation as these pretreatments are used for corrosion protection before painting on aircraft. Figure 15 shows a comparison of a visible image of a pre-corroded anodized aluminum coupon with an IR image with no paint, 3mil, and 6 mil of paint. There is strong contrast in the $4.6\ \mu\text{m}$ spectral band between corrosion and the anodized surface, even though they are both made up of aluminum oxide. Like the previous test panels, the corrosion including the scribe lines can be clearly seen above 6 mil of primer and topcoat. Figure 16 shows the same comparison with an Alodined chromate conversion coated pre-corroded aluminum coupon. The Alodined surface also shows strong IR image contrast with the corroded area, and more than 6 mil of paint can be seen through.

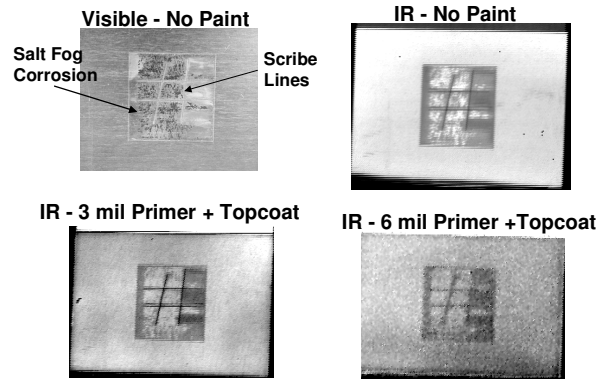


Figure 15 Comparison of a visible image of a pre-corroded anodized aluminum coupon with IR images of painted versions.

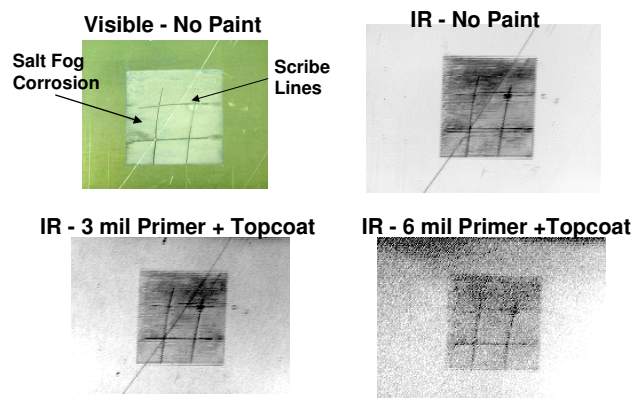


Figure 16 Comparison of a visible image of a pre-corroded Alodined aluminum coupon with IR images of painted versions.

The MIL-PRF-23377TYICLC, primer and Hentzen MIL-PRF-85285TYI, topcoats are typical of military specification paints. They have similar IR transmission windows in the 3 to 5 μm band. There are specialty coatings, however that may be more difficult to see through. One of these is a Koroflex urethane primer sealer used on Northrop Grumman's E-2C Hawkeye early warning aircraft. Pre-corroded aluminum coupons, like those shown in Figures 15 and 16, were coated with 0.9 mil of MIL-PRF-23377 primer, 2.1 mil of Koroflex primer, and 2.6 mil of milspec gloss gray topcoat, (total thickness of 5.6 mil). Figure 17 shows a comparison of the IR images of two unpainted coupons with the IR images after coating with the E-2C paint scheme.

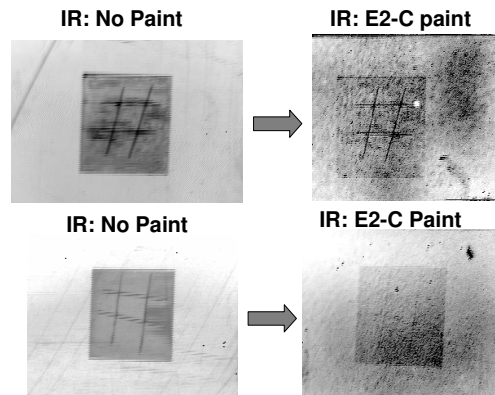


Figure 17 Comparison of the IR images of unpainted coupons with IR images of the coupons with approximately 5.6 mil of E-2C paint.

The results from the Amber IR camera test bed were very encouraging. Not only does WASI detect corrosion through as much as 9 mil of paint, but it can also see detailed surface morphology such as scratches. The clarity of the images is due to the relatively long wavelength of light used to probe through the paint. Pigments, which impart the light blocking abilities to paints, are designed to scatter light in the visible light spectrum. The eye is sensitive to light from 0.4 to 0.8 μm . Pigment sizes of a few tenths of a micron are optimum for scattering light in this range. The paint transmission window, however, is in the area of 4.7 μm , which is an order of magnitude larger wavelength than the visible spectrum. The scattering power of these pigments is dramatically reduced for Mid IR light. The net effect is that the coating is equivalent to a “tinted clear coat” in the mid IR range, where a clear image of the substrate can be seen, but the reflected light is partially absorbed by the coating.

This reduced light scattering in the Mid IR permits an imaging method that not only reveals broad corrosion signatures, but detailed surface morphology such as cracks as well. The SNDE/WASI method has the potential to be an IR equivalent of the visual inspection of a depainted aircraft surface. Anything that can be visually seen (or with the aid of magnification) on a depainted aircraft surface can now be seen with the IR technique without paint stripping.

Alternative IR Imaging Systems

Rather than return to the Multiview system, it was decided to evaluate commercial off-the-shelf IR cameras that had the potential to be adapted to the WASI application. FLIR Systems manufactures a variety of IR imaging systems. Two Forward Looking Infrared (FLIR) products were evaluated; a platinum silicide (PtSi) focal plane system, and a high performance Indium Antimonide (InSb) camera. Both these system were internally cooled (no LN_2) and were hand-held. Except from broad band internal filters, these system were not filtered for the paint transmission window. Although InSb cameras have ideal sensitivity in the Mid IR region, we looked at this PtSi camera because it was easy to use and images could be stored digitally. Figure 18 shows a

comparison of a visible image of an unpainted corroded aluminum panel with a FLIR PtSi IR camera image of the same panel painted with 8.3 mil of primer and topcoat. Although this systems response falls off between 4.6 and 5 μm , a good image is still obtained even without narrow band filtering. Diffuse lighting, rather than a direct reflective image of the black body panel, was used. Like the Amber system described previously, this is a 256 x 256 focal plane, so the image has sufficient detail.

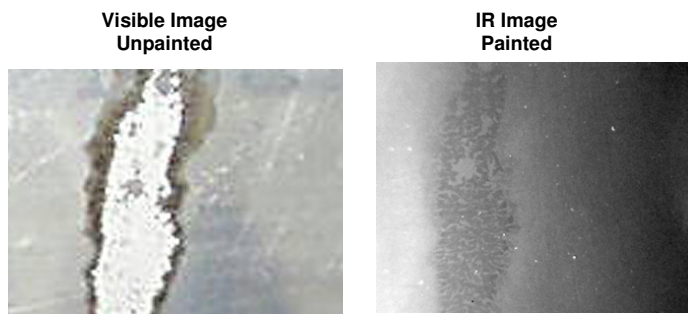


Figure 18 Comparison of visible image of corroded aluminum panel with FLIR PtSi imaged of the same panel with 8.3 mil of primer and topcoat.

The FLIR InSb camera performed better than the PtSi, but it did not have digital imaging capability. Images were recorded live on videotape, but are not reported in this report. Although the FLIR InSb camera had better image contrast, it did not to have the flexibility needed for a field demo of the WASI concept.

The next vendor evaluated was Indigo Systems. They have a variety of fully digital high sensitivity cameras from near to mid to far IR. We evaluated the MerlinTM Mid IR system equipped with an internally cooled InSb focal plane. The focal plane was larger than the other systems tested with dimension of 320 x 256. Figure 18 shows a comparison of a visible image of a corroded aluminum panel with the MerlinTM IR image. Diffuse lighting from the blackbody illuminator was used. Even through 8.3 mil of paint, a large amount of the corrosion detail is still visible. This is considerably better than the original Amber camera for thick paint coatings shown in Figure 14 for similar panels. Figures 19 and 20 show another example of the MerlinTM camera's ability to see through thick coatings. These images were taken unfiltered throughout the whole 3 to 5 μm range. Referring to Figure 6, this means that these images had a significant contribution from the 3 to 4 μm band where the paint is mostly opaque and the reflected image is mostly from the paint surface. The transparent image between 4 and 5 μm is superimposed on the opaque image, thus reducing image contrast of the metal surface beneath the coating. With suitable multiband spectral filtering, image contrast can be improved with better paint penetrating power. Figure 21 shows a comparison of a visible unpainted clad aluminum alodined coupon with the same coupon painted with 6 mil of primer and topcoated imaged with the MerlinTM system.

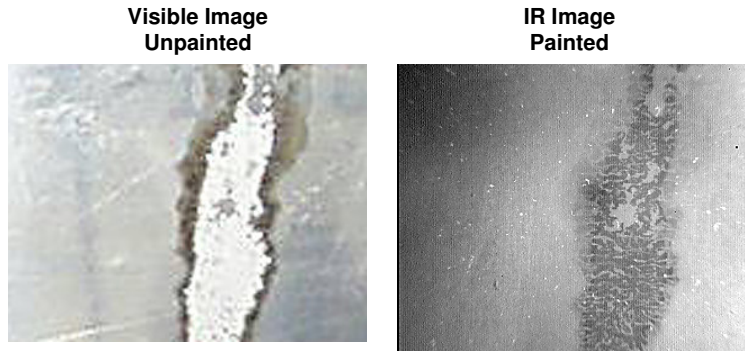


Figure 19 Comparison of a visible image of an unpainted panel with an unfiltered Merlin InSb IR image of the same panel coated with 8.3 mil of paint.

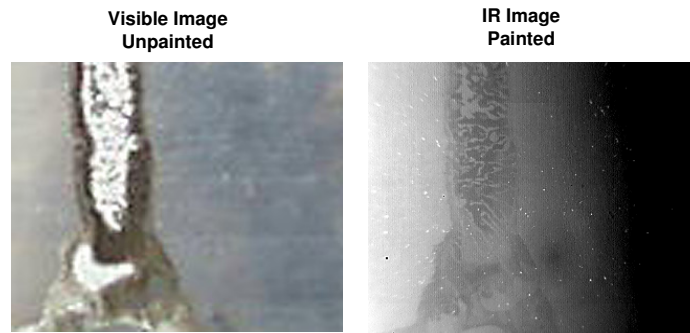


Figure 20 Comparison of a visible image of an unpainted panel with an unfiltered Merlin InSb IR image of the same panel coated with 8.3 mil of paint.

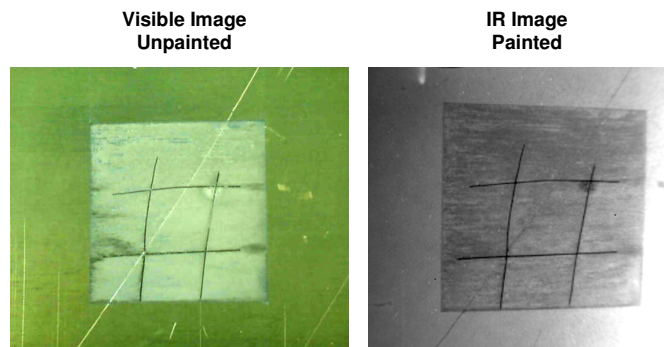


Figure 21 Comparison of a visible image of an Alodined coupon with an unfiltered Merlin InSb IR image of the same coupon coated with 6 mil of paint.

Figure 22 shows images of corrosion underneath 6 mil of E-2C paint system. This is a considerable and significant improvement over images obtained with the previous IR camera systems.

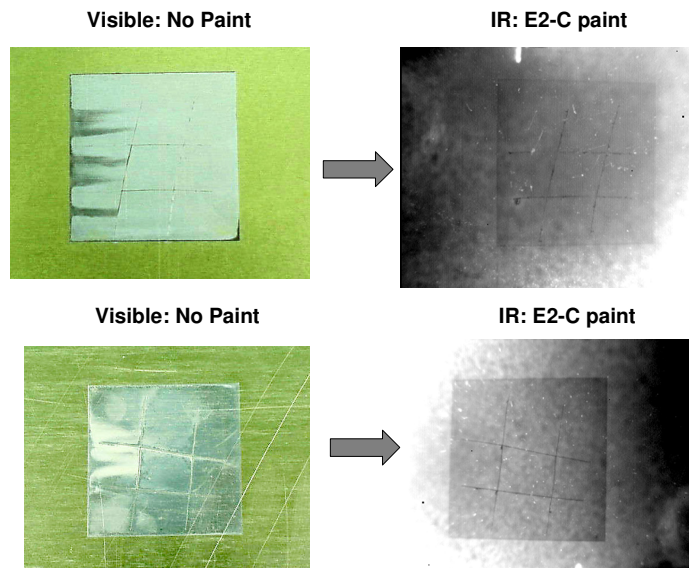


Figure 22 Comparison of the Merlin™ IR images of unpainted coupons with IR images of the coupons with approximately 5.6 mil of E-2C paint.

Detailed images of corrosion and scribe lines can be seen with the Merlin system through the particularly light absorbing paint of the E-2C aircraft.

SNDE/WASI Discussion of Results

We have successfully demonstrated the feasibility of using IR wide area spectral imaging to see through real aircraft coatings to the underlying metal surface. Not only were corrosion products visible, but surface morphology such as scratches and potentially cracks are visible. This was achieved with a relatively simple multispectral IR camera and suitable IR illumination. At this point work has started on seeing cracks and general metal surface morphology through paints, and the results are reported later in this report (Fig. 63–67). In addition, more paint systems were evaluated including milspec low IR and commercial aircraft paints. A commercial InSb camera system was purchased using Northrop Grumman funds and adapted to the WASI application using multispectral filters. The Merlin™ camera system employed multiple lens to permit up-close and magnified imaging of corrosion detail and surface cracks.

An InSb camera system, such as the Amber or Indigo Merlin™ system used here, is the most sensitive for bring out small contrast differences between areas of deferent reflectance. Of the systems used here, the Merlin has the best $\text{Ne}\Delta T$ (~18 mK). This is a measure of the cameras ability to see small differences in reflectance. This is important for small reflectance differences on the metal surface, or for thick paint layers. The Amber test bed system first used here has a nominal sensitivity close to that of the Merlin™, but was suffering from age related heat leaks which reduced its performance. Calculations indicated that an optimized system should be able to extract images form the metal surface of a coupon coated with conventional paints up to thicknesses of 13 to

14 mil. The MerlinTM system is self cooled (no LN₂), and it is compact enough to be hand-held or tripod mounted and can be run off of batteries.

The InSb focal plane is sensitive from 3 to 5 μm , but most paints are transparent in the 4 to 5 μm range. The 3 to 4 μm contribution will add an unwanted image of the top surface “glare” of the paint, thus obscuring the image coming from below the paint. This is why it was considered necessary to use filters to block unwanted spectral bands from reducing image contrast. For the MerlinTM system, simple band pass filters will be used behind the lens (warm filter) to achieve this goal. The image obtained in the 3 to 4 μm range will not be discarded, however. It was used to determine if anything in the 4 to 5 μm image is actually coming from the paint surface. This could include dirt and chipped paint. A multispectral subtraction was performed in order to “clean up” the paint-transparent 4 to 5 μm image. Optimized filters such as polarizing filters (Figures 93 and 94) were tested.

In the 4 to 5 μm wavelength band used for imaging, all the panel and coupon surfaces, including visibly diffuse Alodined and anodized coupons, appear mirror-like. This is due to the longer wavelength of light not being scattered by the grainy surface of the coupons. Thus, the imaging problem is equivalent to detecting defects in a tinted (absorbing) mirror. The choice of illumination is important in such situations. Wien’s Law states that a black body needs to be at a temperature of 617°F to get a maximum photon output at 4.6 μm . This is readily achievable by conventional black body sources used for radiometric applications. Anything hotter than this (such as a light bulb) can be used assuming the IR is not being filtered out. For the Amber test bed IR imager, a direct reflective image of the uniform black body panel was used to detect defects in the metal surface of the painted coupons. A nonuniformity of the black body panel may show up in the coupon image depending on the depth of focus from the black body to the coupon. For a more efficient camera, like the MerlinTM, better images were obtained using only lower power diffuse light from the black body. This means that the coupon surface remains illuminated at any angle of viewing, which is a definite advantage. This also simplifies the illumination geometry. A simple illuminator can be attached to the camera, or a separate lamp on a stand can be used to light up the surface to be inspected.

One of the keys to the success of this technique is the extraordinary sensitivity to small differences in reflectance that can be seen by the modern Mid IR cameras such as the MerlinTM. The inherent sensitivity of the focal plane is one of the keys to the success of this technique is the extraordinary sensitivity to small differences in reflectance that can be seen by the modern Mid IR cameras. Focal plane images may be stored digitally as 12 bit or better. This means that many more (4096) shades of gray can be discerned in these images than for the conventional 8-bit image (256), and much smaller contrast differences can be measured. These small differences are brought out by adjusting both brightness and contrast on the camera controls. However, because of local differences in contrast in an image, one set of image adjustments that highlight one feature in one area of the picture may obscure other features. An automatic contrast enhancement scheme will have to be devised to compensate for different degrees of contrast in different areas of the image.

Finally, polarization was evaluated as a potential method for enhancing contrast sensitivity. By using polarized IR illumination, the reflected light from the paint surface can be minimized and the underlying metal image can be improved as a result.

EXPERIMENTATION

Sample Preparation

The test specimens used for the validation of the measurement techniques were manufactured in the Northrop Grumman Material & Process Laboratory. The specimens were prepared using aluminum alloys that are most typically found on the aircraft outer mold line (OML); specifically, 2024-T3 Bare (Al 2024), 2024-T3 Clad (Al 2024C), 7075-T6 Bare (Al 7075) and 7075-T6 Clad (Al7075C). Surface Preparations included both chemical conversion coating (CCC), applied per MIL-C-5541 and sulfuric acid anodize (SAA), applied per MIL-A-8625 Type II. The bottom half of the specimens (4" x 6") were scribed down to the base metal to provide an area that would be more susceptible to corrosion upon exposure to the salt spray or humidity. Different exposure durations were used to induce varying degrees of substrate corrosion. The salt spray exposure proceeded for 3, 7, 10 and 14 days. The humidity exposure proceeded for 3 days, 7 days, 10 days, 2 weeks, 4 weeks and 6 weeks. These specimens were used to baseline and quantify the various changes that occur in the substrate due to the varying levels of corrosion. Both untreated and unexposed SAA and CCC specimens were prepared to provide a baseline for untreated aluminum, unexposed CCC, and unexposed SAA.

Coupon samples of the coating schemes currently applied to F-14, E-2C, EA-6B, and F-5 were prepared to represent the "as applied" coatings. These included MIL-PRF-85582 Type II, TT-P-2760, MIL-S-81733, MIL-C-85285 (Fed-STD-595 color nos. 16440, 36375, 36320, 35237). To simulate the barrier provided by these coatings, free-standing paint films were prepared using MIL-PRF-85582, TT-P-2760, MIL-C-85285, and MIL-S-81733 over the range of 1 to 10 mils. Using the IR imaging technique, the directional hemispherical reflectance of the free-standing films was determined. The films were then placed over the pre-corroded specimens to the appropriate coating stack-up.

Field hardware for the first phase of the component evaluation was obtained from Northrop Grumman's St. Augustine site. Scrap E-2C access doors were selected for this portion of the study. The access doors have a complex curvature and have rivet holes located around the outer edges. The surface preparation used in the manufacture of the doors is SAA. Fasteners made of a more noble metal such as steel were installed.

SNDE

In order to determine the sensitivity of SNDE to such factors as the amount of corrosion present, the type of aluminum surface treatment, and the type and amount of paint coating present, we decided to measure these

aspects separately. Unpainted aluminum coupons with surface treatments were corroded and their spectral reflectance measured. Corrosion was modeled using an alumina powder contamination technique. Likewise, free standing paint films were fabricated and their transmittance and reflectance were measured as a function of type and thickness. Finally, the films were applied to the corroded substrates to determine how much corrosion can be seen through a variety of coating thicknesses.

RESULTS AND DISCUSSION

SNDE

The DHRs of a variety of surface treated aluminum coupons were measured in order to generate a spectral database of substrate reflectance. This will tell us how much change in reflectance we can expect from a certain amount of corrosion present. Once this has been established, a first cut at corrosion sensitivity will be determined using free-standing paint films covering corroded coupons.

Baseline Measurements –Figures 23 and 24 show the DHR of a number of as-prepared (un-corroded) representative 3” X 6” aluminum coupons. Two aluminum alloys, 2024 and 7075, were used in both bare and clad form. The 2024 alloy exhibits more corrosion resistance than does 7075 alloy. Clad coupons in general have better resistance than unclad coupons. In addition, two types of surface coatings were used, sulfuric acid anodized (SAA) and Alodine 1200 chromated conversion coating (CCC). The SAA coupons are expected to show more corrosion resistance than those prepared with CCC.

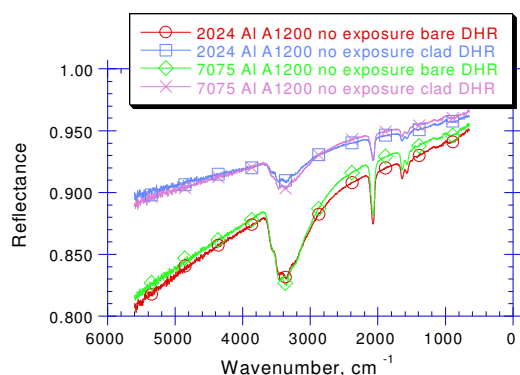


Figure 23 DHR of 2024 and 7075 bare and clad aluminum 3” X 6” coupon, coated with CCC.

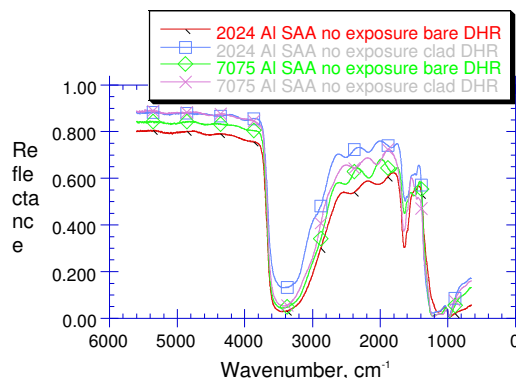


Figure 24 DHR of as prepared sulfuric acid anodized 2024 and 7075 bare and clad aluminum coupons.

Figure 23 shows higher reflectance for the CCC clad coupon compared to the unclad. This indicates that there is some transparency in the CCC. This is also true for the SAA coated coupons shown in Figure 24. In

both cases, the reflectance difference is relatively small. The corrosion products will have to make their way through the coating to the primer for the SNDE technique to be able to “see” any significant corrosion.

Figure 25 shows a comparison of the two as prepared surfaces (SAA and CCC, with the DHR of a bare salt fog corroded 2024 aluminum coupon. The corrosion products, shown in the scanning electron microscope (SEM) image in Figure 26, appear as a white patina on the surface. Analyzed by electron microprobe (EDAX), the corrosion products are essentially aluminum oxide (Al_2O_3) with excess oxygen and some trace amounts of sodium, magnesium, and chlorine from the salt fog. There is a similarity in all three reflectance spectrums. This is especially so in the 3400 cm^{-1} region. This is the absorption band from hydroxyl groups, which are found bound to oxides. As the oxide layer increases due to weathering, this hydroxyl absorption increases.

It is no surprise that is hydroxyl absorption is also found in the SAA and CCC, as these also tend to bind hydroxyl groups.

Accelerated weathering was performed in both humidity and salt fog chambers. “X”s were scribed into the surface of each coupon to promote corrosion. Samples were initially weathered for 3 to 14 days. In addition, large regions of coated aluminum coupons were extensively weathered to approximate an aluminum sheet with a significant amount of corrosion damage.

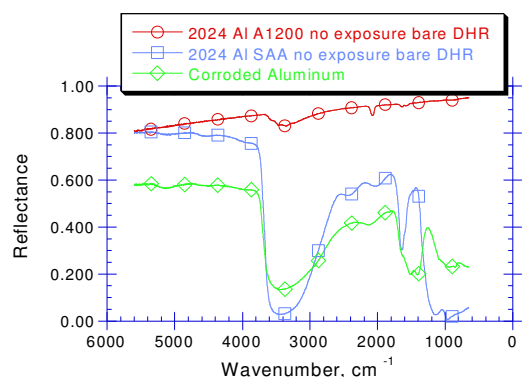
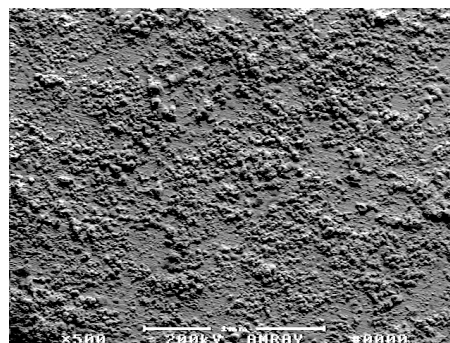


Figure 25 Comparison of as prepared coated 2024 bare aluminum with salt fog corroded 2024 aluminum.



Magnification 500x

Figure 26 Scanning electron micrograph of a salt fog corroded bare aluminum coupon. Oxide is primarily Al_2O_3 .

Corrosion Modeling – An alumina contamination study on aluminum alloy sheets was performed to quantify the amount of corrosion present using spectral reflectance techniques. Accelerated corrosion, induced by exposure to salt spray, is essentially a layer of Al_2O_3 (alumina) on the surface. This can be approximated by sprinkling successive amounts of Al_2O_3 powder on an aluminum surface and measuring the DHR. The series of spectra are used to model the DHR of a corroded aluminum sample. By measuring the reflectance, an approximation can be made as to the amount of corrosion present. Depending on the sensitivity and signal-to-noise found in the SNDE technique, this can be used to obtain a quantitative determination of the amount of corrosion present.

Figure 27 shows a series of DHR spectra of a bare aluminum (uncoated) coupon covered with Al_2O_3 powder. The powder was from Aldrich with a nominal grain size of 1 micrometer. As the amount of Al_2O_3 coverage increases, the DHR approaches that of an “infinitely” thick Al_2O_3 layer in the spectral region below 4000 cm^{-1} . Above 4000 cm^{-1} , the reflectance of the thick powder layer is higher than the thinner layers which indicated some degree of multiple reflection is at work. A theory of optical reflectance and transmission of particulate and diffusive surfaces known as Kubelka-Munk (KB) is frequently used to model such systems. KB theory will be discussed further in connection to modeling the optical properties of paint layers later, but for the Al_2O_3 contamination study a simpler area fraction model will be used.

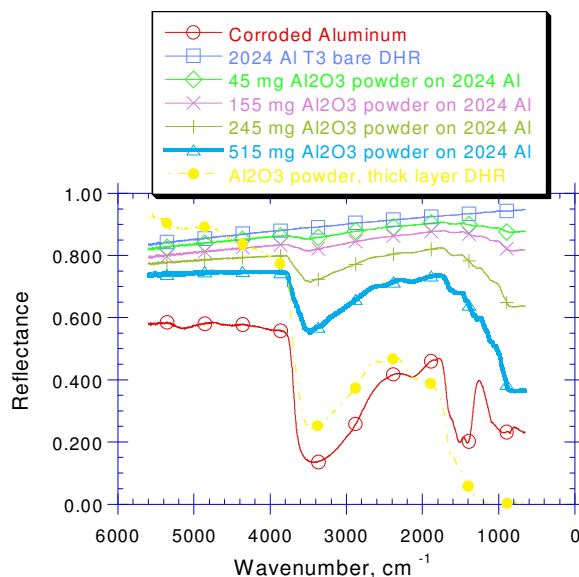


**Figure 27 Reflectance of Al_2O_3 oxide on 3" X 6" aluminum coupon.
(Corroded aluminum coupon included for comparison)**

The reflectance, R_t , of a particulate (Al_2O_3) contaminated surface (aluminum) is given by (Equation A:

(Equation A)

$$R_t = R_p + (R_s - R_p)e^{(-ad)}$$

where R_p is the reflectance of an optically thick (“infinite”) layer of Al_2O_3 powder, R_s is the reflectance of the substrate (aluminum), a is a scattering factor, and d is the average oxide thickness. This area fraction model works well for a large variety of particulate contaminants and substrates.

Figure 28 shows a comparison of the area fraction model with the measured reflectance of the Al_2O_3 contaminated surface. The model uses the end point spectra (bare aluminum and thick Al_2O_3 DHR) as well as a scattering factor derived from the measured spectral shown in Figure . There is reasonable agreement between the modeled and measured spectra. For larger amounts of Al_2O_3 (thicker oxide), there is some deviation above 4000 cm^{-1} due to multiple reflectance effects. Of course, real world corrosion differs from this idealized model, but we can still get an idea of the magnitude of corrosion present by the total reflectance as presented in Equation A, above.

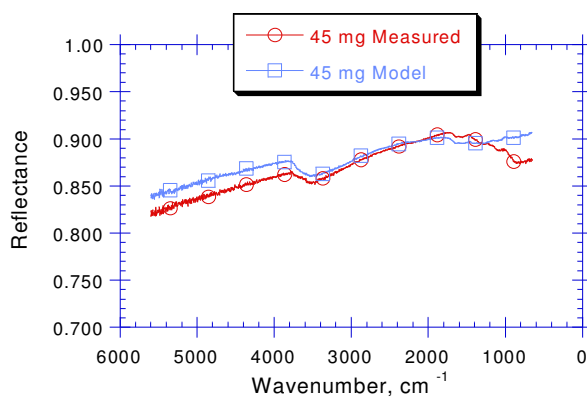


Figure 28 Measured and Modeled “Corroded” aluminum substrate. 45 mg Al_2O_3 powder on 3” X 6” aluminum coupon.

DHR of Corroded Coupons – The DHR system used to implement the SNDE technique has an incident IR beam diameter of approximately 0.5”; hence, a five-spot-average reflectance was measured from the scribed coupons. The DHR was measured over the center of the scribe “X”, as well as over the four legs of the “X”, in order to maximize the amount of corrosion that may be detected. Initial measurements indicated that the corrosion measured correlated with the type of aluminum, coating, and weathering. The most susceptible combination to corrosion was salt fog weathered Al 7075, and the least susceptible was humidity exposed, Al 2024C. However, in all cases for the maximum exposures made, the amount of corrosion generated was not large and the change in reflectance was not great. Figure 29 shows the reflectance’s of a series of salt fog exposed, CCC Al 7075 coupons. There is a general trend to a growing hydroxyl absorption band, as is expected from a growing oxide layer. It should be pointed out again these measurements consist mostly of reflectance from nominally un-corroded regions with no scribe and a relatively narrow region of corrosion where the scribe is present. Figure 30 shows representative DHR measurements of salt fog exposed SAA coated bare coupons. There is some reduction in reflectance reflecting a growing amount of oxide, but not much. These coupons were subsequently returned to the environmental chambers for further weathering.

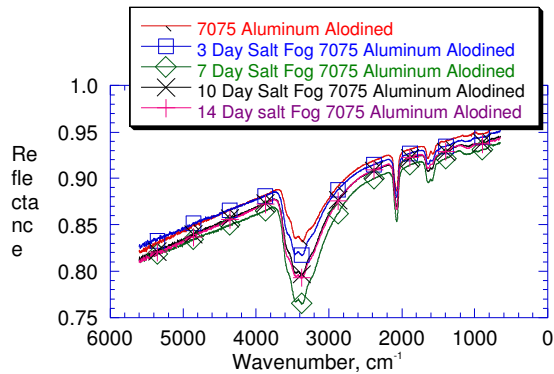


Figure 29 DHR of salt fog exposed, CCC Al 2024

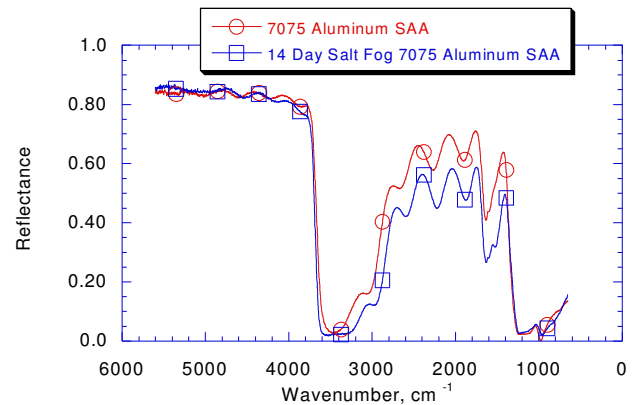


Figure 30 DHR of salt fog exposed SAA coated Al 7075.

Because the most extensive corrosion was caused by salt fog exposure, we made a series of coated coupons to expose a 2" X 2" square center. These coupons were given a strong salt fog treatment. Figure 31 shows the reflectance of these coupons. Like the salt fog exposed 2024 uncoated coupon described before, these samples show a strong corrosion signature. Electron microprobe results show the presence primarily of Al_2O_3 with some trace amounts salt.

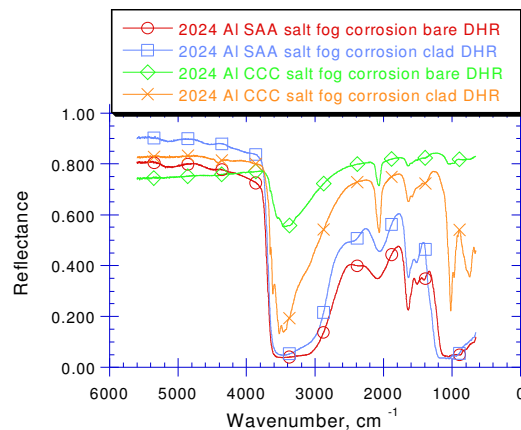


Figure 31 Long-term salt fog exposed heavily corroded CCC and SAA coupons.

Free Standing Paint Films – In order to relate the reflectance of painted corroded aluminum to the corrosion at the metal/paint interface, free standing paint films of a variety of types and thickness' were applied to a characterized corroded surface. In order to get quantitative results that can be modeled; the reflectance and transmittance of these films by themselves were first measured. These quantities, along with the reflectance of the corroded aluminum substrate (coupon), are used to predict the reflectance of the painted coupon.

Figure 32 shows the directional hemispherical reflectance (DHT) of a series of freestanding topcoats and sealants used on aircraft such as the Northrop Grumman EA-6B and E-2C. DHT measures the amount of the

transmitted light including the diffuse scattered component. The thickness shown reflects actual application thickness' on painted airframes. The camouflage gray and gloss gray topcoats exhibit a high degree of transmissivity in the 2200 cm^{-1} region. This is the “window” where we hope to see through to the aluminum substrate. The Koroflex urethane primer sealer, which is used on some aircraft, also has a transmissive window in the same region, but at a significantly lower value. The polysulfide sealer transmits about 5% in this region and is essentially opaque for our applications.

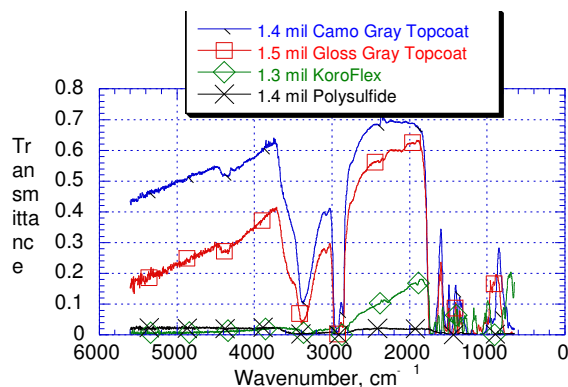


Figure 32 Directional hemispherical transmittance of topcoats and sealants.

Figure 33 shows the DHT of a series of thickness for the camouflage gray topcoat. This topcoat is transmissive up to a thickness of approximately 10 mil. These results also hold for the gloss gray topcoat. In addition to the DHTs, the DHRs of the freestanding coatings was measured with no backing (no substrate). This also included the reflectance of an “infinitely” thick layer (where the DHT is effectively zero). These measurements were necessary as inputs for the model to be described below.

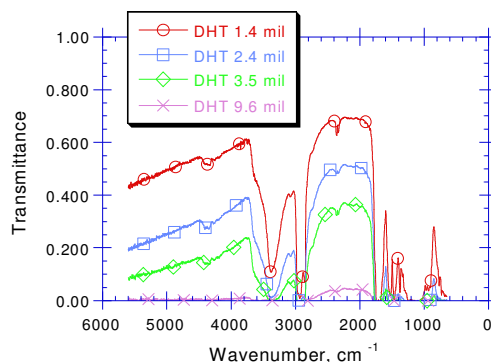


Figure 33 Transmittance of a series of camouflage gray

SNDE Sensitivity Study – For the initial sensitivity study, the long-term salt fog exposed aluminum plate describe above was used as the substrate. This represented an amount of corrosion that could eventually lead to structural damage, but not so much that it would cause visibly obvious blistering to the paint layer covering it. Initial work was done with the free-standing camouflage topcoat. Figures 34 and 35 show the DHR for a series

of camouflage topcoat films of various thicknesses over uncorroded and corroded aluminum substrates, respectively. The prominent reflectance peak around 2200 cm^{-1} is the result of the substrate reflecting the IR light through the transmissive window of the paint. This is clearly seen from both the uncorroded and corroded substrates. Clearly, the signature of corrosion in the substrate is folding into the overall reflectance of paint on substrate combination.

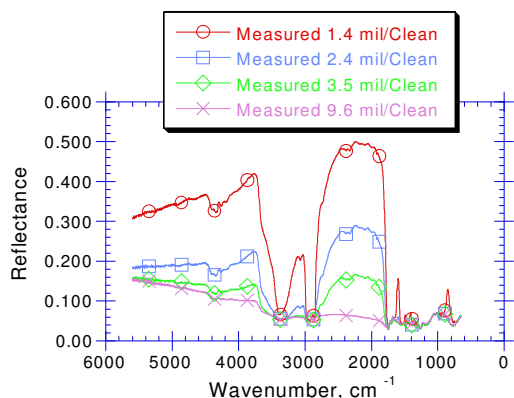


Figure 34 Reflectance of camouflage topcoat on uncorroded aluminum.

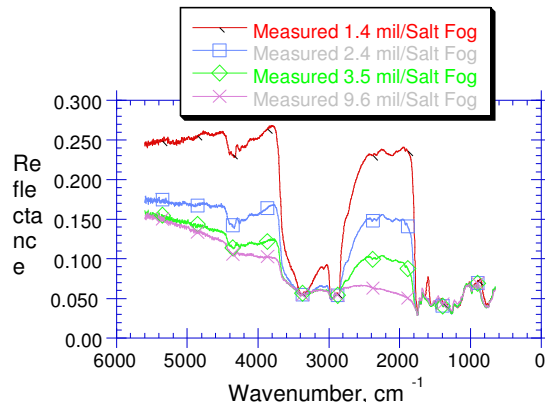


Figure 35 Reflectance of camouflage topcoat on corroded aluminum.

Reflectances of painted surfaces have been traditionally modeled using a diffusive two beam propagation model. The solution to this model was first found by Kubelka and Munk (KB). The KB model describes the transmission and reflectance of a completely diffusive (lambertian) scattering layer. This layer may also have an opaque but diffusely scattering substrate underneath. This approach has been taken in the past to analyze paintings. Here, the art conservator is interested to see the original charcoal drawing on the canvas surface. Known as infrared reflectography, near IR (up to 2 micrometer) images of a painting are taken. The paint layers, which are opaque in the visible, become partially transparent in the IR, and the underlying drawing is revealed.

One of the problems inherent in the KB model is the assumption of a totally diffusive surface. This implies that there is not an abrupt smooth boundary between the air and the paint surface with a corresponding change in index of refraction. This is clearly not the case for aircraft paints. Paint consists of an organic binder and a light scattering pigment, and the binder by itself has an index of refraction in the area of $n = 1.5$. The sudden change from air ($n = 1.0$) to the binder will cause a portion of incident light to be reflected at this boundary, independent of the diffusely scattering pigment. This effect is not included in the KB model. Multiple-reflection from this boundary and a specular (non-diffuse) reflection from the paint/substrate interface are also not included. Attempts to use the KB model to simulate transmittance and reflectance from freestanding paint films, as well as paint films on substrates were not particularly successful. Current efforts are investigating a simple to use alternate paint film model that will predict coating transmittances as a function of type and thickness.

For the prediction of DHR of painted substrates, a simple model based on multiple reflectance's and empirically measured paint transmittances and reflectance's was successfully used. The total reflectance, R_t , of a paint layer is given by (Equation B):

$$(Equation\ B) \quad R_t = R_f + T_f^2 R_s / (1 - R_f R_s)$$

where R_f is the reflectance of the free standing paint film, T_f is the reflectance of the free standing paint film, and R_s is the reflectance of the substrate. This model applies directly to the sensitivity experiments described in this section. However, a question arises as to the validity of the model when applied to a painted substrate where the coating has an intimate contact with the substrate precluding multiple reflections from this boundary. Calculations indicate that for the paint system and substrates considered here, the differences should be relatively small and will not have an adverse impact on the SNDE technique.

Figures 36 and 37 show a measured and simulated DHR for a 1.4 mil thick camouflage coating on a clean aluminum substrate and a corroded substrate, respectively. Considering the approximations made in the measurement of the DHT of this film, the agreement between the measured and modeled curves is remarkably good. Good agreement between the modeled and measured spectra is also made with the other paints, as well.

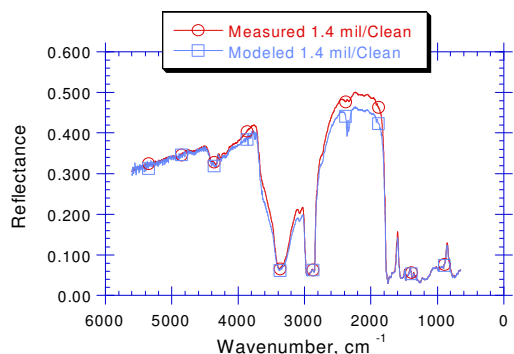


Figure 36 Comparison of measured and modeled reflectance of camouflage paint on un-corroded aluminum.

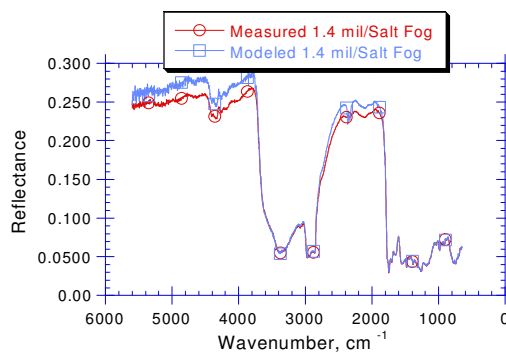


Figure 37 Comparison of measured and modeled reflectance of camouflage topcoat on corroded substrate.

Equation B can be inverted to give the substrate reflectance as a function of the measured DHR of the painted surface. This is shown Figure 38. Except for regions where the paint film is opaque, there is good agreement between the derived substrate reflectance and the actual substrate reflectance measured without a paint coating. The signature of corrosion on the substrate can be clearly seen. However, this analysis can be performed only if there is sufficient transmission of IR light through the coating to provide the needed signal to noise ratio. A better (and simpler) data analysis technique is to ratio the reflectance of a painted uncorroded substrate to the reflectance of a painted corroded substrate. Figure 39 shows this ratio for a series of thicknesses of camouflage topcoat. We can see the signature of corrosion even up to a thickness of 10 mil.

For the ratio technique, the reflectance spectra are normalized at the spectral regions where the paint is opaque (1100 cm^{-1}). This eliminates variations due to topcoat weathering and fouling. In addition, signature variation due to different topcoat thickness may be separated from the effects of substrate corrosion. However, a separate thickness measurement may have to be made in order to eliminate this variable.

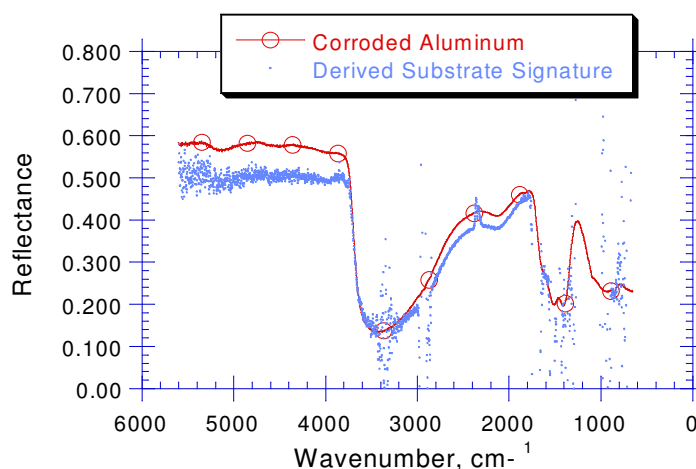


Figure 38 Comparison of directly measured corroded substrate reflectance and the reflectance derived from DHR measurement of 1.4 mil camouflage painted substrate.

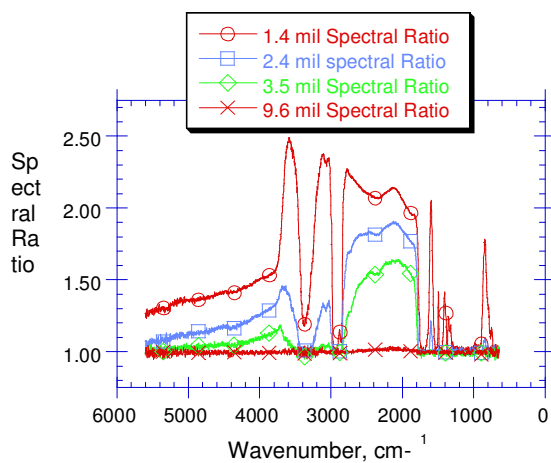


Figure 39 Spectral ratio of reflectance of painted un-corroded substrate to the reflectance of a painted corroded substrate.

Spectral Nondestructive Evaluation – Wide Area Spectral Imaging

One way to detect corrosion products at the paint/metal interface is to use an optical reflectance probe to detect changes in reflectance as a result of corrosion. Spectral reflectance signatures may be used to detect the presence of various chemical species, including corrosion products. A light beam must be able to pass through the paint, reflect off the metal surface, and pass back out through the paint coating. We have referred to this concept as Spectral Nondestructive Evaluation (SNDE). Paints are normally designed with pigment sizes tailored so that they are opaque in the optical region of the spectrum (0.4 to 0.8 μm), so they preclude using optical techniques in the visible to “see” through the coating to the metal. However, the scattering power of pigments is diminished as the probe wavelength becomes longer. For many paints, a spectral window opens in the near and mid infrared spectral regions.

Northrop Grumman continued its efforts in SNDE in the area of spectral imaging. A natural application of the SNDE concept is to employ the use of IR focal plane technology coupled to spectral filters to image the reflectance of large areas of an aircraft’s structure simultaneously. As previously discussed, we refer to this as wide area spectral imaging (WASI). Sensitive high-resolution IR focal plane cameras are already used to obtain thermal images for use in thermography. For WASI, however, we used these IR cameras to image reflectance variations over a painted aluminum surface as a function of wavelength. We used our experience in hyperspectral imaging systems for remote sensing to develop an “up close” version for NDE. From the spectral database of paints and corrosion of metal surfaces developed for SNDE, we chose band pass filters whose wavelengths correspond to the paint spectral windows and to paint opaque regions.

WASI Project Accomplishments

Sample Preparation – As previously discussed, typical aircraft structural aluminum consists mainly of 2024 and 7075 alloy. This alloy material is used either clad with an outer layer of pure aluminum, or with a bare surface. The clad layer is there to provide extra resistance to corrosion. To complement the corrosion standards that were made previously, another batch of coupons were made that represented lower levels of corrosion and also allowed for multiple paint thickness on each coupon to test for depth penetration. Coupons of the 2024-T3 bare aluminum (3-in. x 6-in.) were made to be pre-corroded and coated with a variety of aircraft paint systems. All coupons were solvent wiped with methyl-propyl-ketone (MPK) plus 5% by Volume Z-6040, prior to finishing, Ref. Patent No’s 6,248,403 and 6,096,700. These panels were exposed to 2 weeks salt fog prior to finishing.

Figure 40 shows two examples of visual photographs of unpainted salt fog exposed coupons. The whole coupon was exposed. In addition to superficial corrosion, there is pitting also in the aluminum surface. This is in contrast to the lighter surface corrosion in the original set of standards.

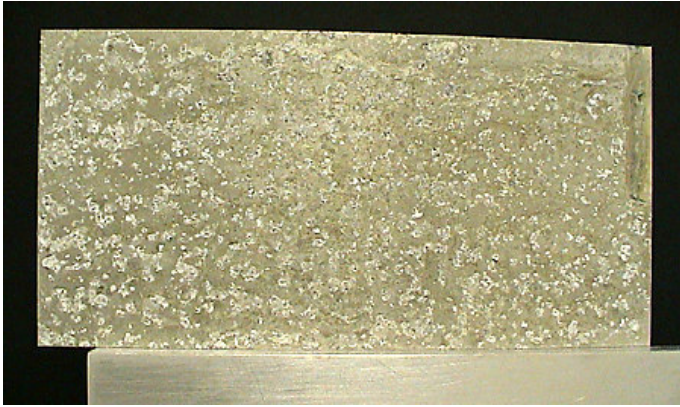


Figure 40 2024 aluminum coupon exposed to salt fog. Visual image of corrosion before painting.

In addition to these new aluminum skin corrosion specimens, we fabricated a number of simulated crack and pit coupons to determine the extent to which the WASI technique can see details on the metal surface. Figure 41

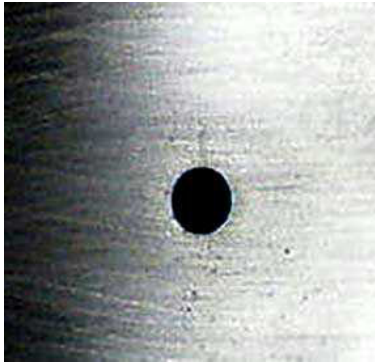


Figure 41 Visual micrograph of a 0.250" fatigue crack propagating from a hole in a 2025 aluminum bar.

shows an example of a real fatigue crack in a 2024 aluminum bar. A hole was drilled into the bar and a small notch was made in it's interior. The bar was subjected to cyclic fatigue so that a crack of a given length was generated. The hole was then drilled out only leaving the crack. Crack length standards from 0.250" to below 0.030" were generated. These cracks were extremely difficult to see optically under normal illumination.

Electrical discharge machined holes were made in 2024 aluminum to simulate pits of various depths and diameters. Diameters ranged from 0.001" to 0.008" and depths from 0.001" to 0.008" inch. Figure 42 shows a visual image of a 0.001" diameter EDM pit in the center of an aluminum coupon.

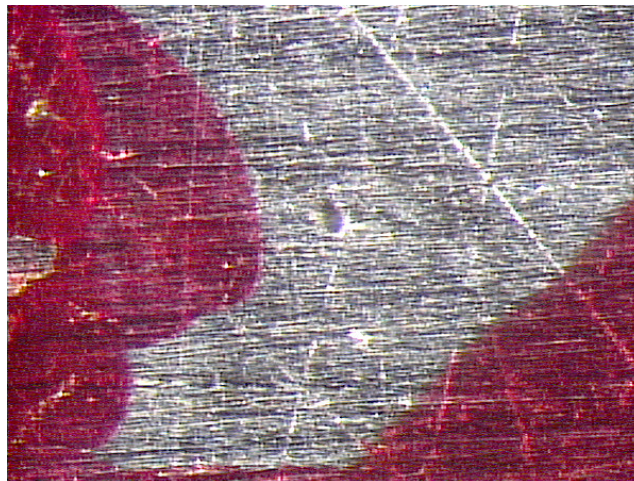


Figure 42 Visual micrograph of a 0.001" diameter pit EDM machined into a 2024 aluminum bar.

Paint Systems – For painting the coupons and parts, we used primarily MIL-PRF-23377TY1CLC Plus MIL-PRF-85285TY1 Insignia White Fed-STD-595 17925, Dark Camouflage, and Low IR primer MIL-PRF-23377TYIICLC. We also continued to use coating systems such as those used for the Northrop Grumman E-2C Hawkeye airborne early warning aircraft.

System Description and IR Imager Results – As mentioned previously, an Indigo Merlin™ Mid IR camera was purchased for the system demonstration. Figure 43 shows the camera mounted on a tripod.

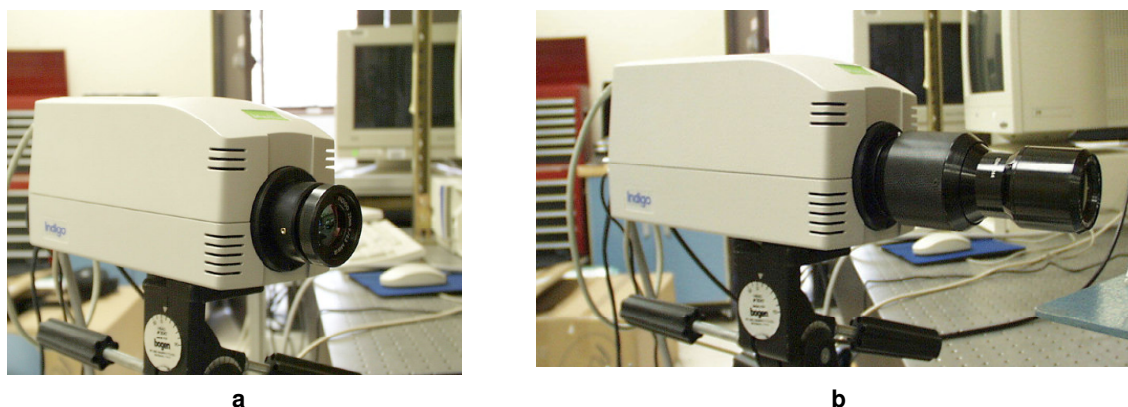
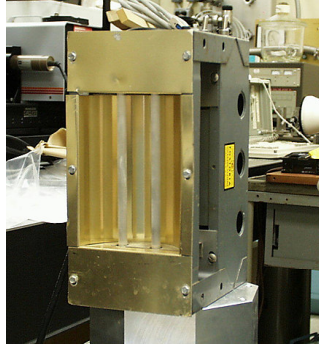


Figure 43 Indigo Merlin™ Mid IR imager for wide area spectral imaging through coatings
a) 25 mm lens, b) 4x magnification lens

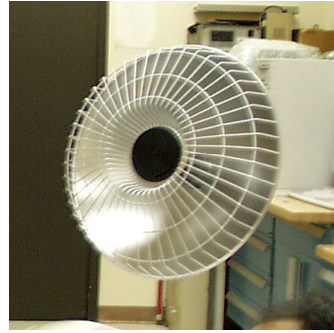
This system uses a 320 x 256 InSb focal plane array. The focal plane is cooled by an internal Sterling refrigerator. Cool-down time is approximately 20 minutes, prior to use. Interchangeable IR lenses are available including 50, 25, 13 mm as well as a 1X and 4x macro lens system. A full set of camera controls is included in a control pad on the top of the camera. Brightness and contrast can be adjusted manually or can be set to automatic. Output is via BNC or S-Video, or 14 bit digital images. Power is 24VDC (from a 110VAC converter).

Illumination is provided by a variety of heat sources. Figure 44 shows two that have been used so far. Figure 44a shows a quartz IR lamp with a back reflector. Figure 44b shows a resistive coil heater with a parabolic reflector. Both systems work well but the parabolic illuminator minimized image reflection with a stronger diffuse component is more efficient, and it takes less power.

This system was made portable by attaching the camera to a hand held shoulder rest and attaching a compact digital video camera to its side. See Figure 45. The S-video output of the Merlin is fed into the input of the video camera to obtain a live digital record on tape. Power is provided by a pack of rechargeable nickel metal hydride batteries with an operating life of 3 hours. Figure 45 shows the portable system in operation on aircraft parts in the lab.



a



b

Figure 44 IR Illumination systems. a) quartz system, b) resistive reflector.

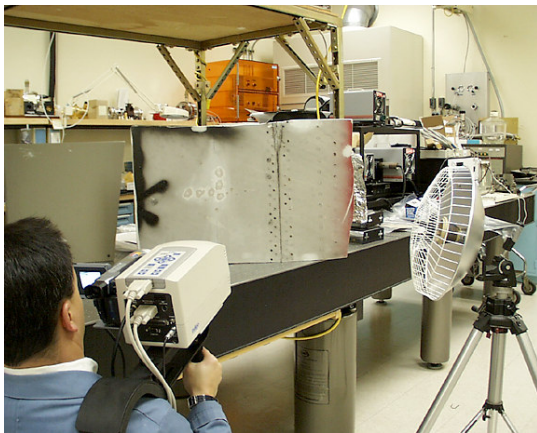


Figure 45 Portable hand held wide area imaging system.

Corrosion Detection Filter Development

Figure 46 shows a typical paint spectral window. The commercial MerlinTM camera, as well as other Mid IR systems, is designed to image light in the 3 to 5 μm spectral transmission window in the atmosphere. For paint

transmission however, we need to eliminate reflectance contributions from spectral regions where the paint is opaque. For the paint system in Figure 46, this is in the 3.0 to 3.8 μm range. The current MerlinTM camera cuts off at 5 μm , whereas the paint is transmissive to 5.6 μm . There is an internal cold filter that can not be changed without a redesign of the camera. This will be discussed later. We have investigated the use of spectral band pass filters to improve image clarity and penetrate thicker paint films. Figure 47 shows the transmission spectrum of a filter we designed and manufactured to be used in the MerlinTM camera.

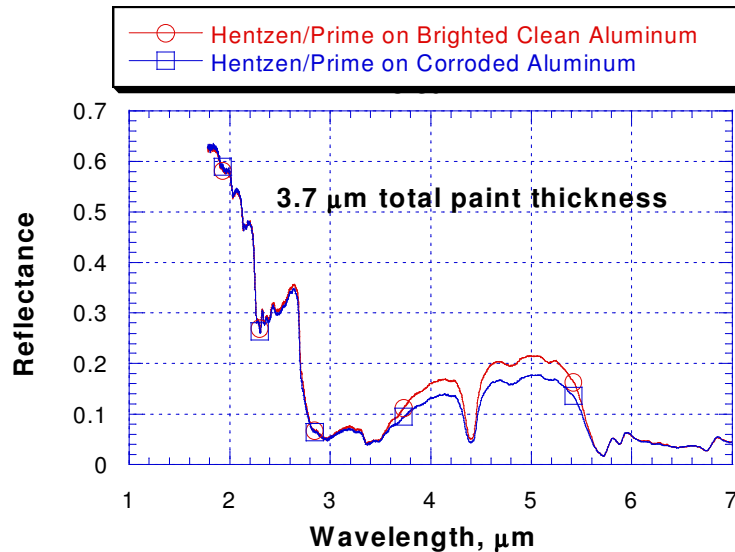


Figure 46 Paint transmission window from 3.8 to 5.6 μm .

By using this filter, we can exclude paint surface images from the 3 to 3.8 μm spectral range which would obscure the sub surface image.

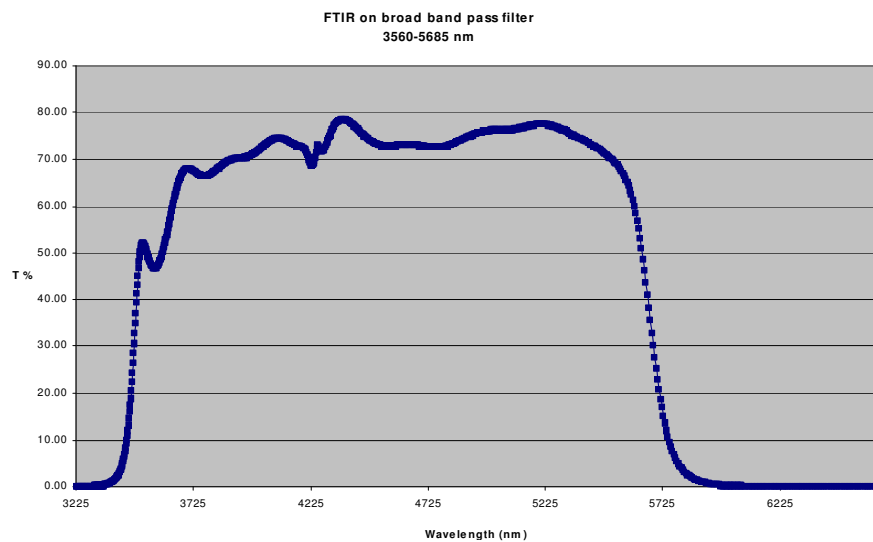
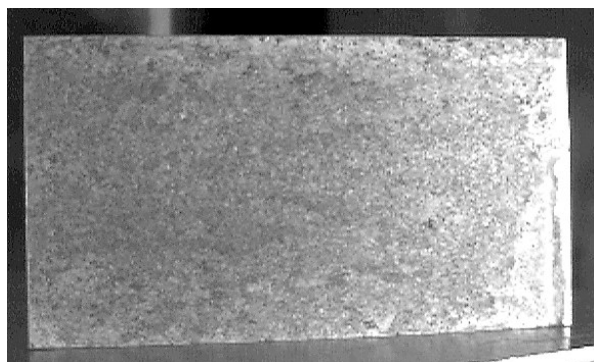


Figure 47 IR transmission curve of the medium band spectral filter.

Previous experience with narrow band filters resulted in large flux losses and reduced signal to noise resulting in degrading images. Surprisingly, there was not much difference between a filtered and non-filtered image using the broad band filter with the same internal non-uniformity correction. The non-uniformity correction is necessary in order to optimize the camera's performance for a given illumination range. Typically a two point correction is done for this purpose. For normal camera operations this involves using a room temperature black body as the low temperature point, and an elevated temperature black body at the high temperature point (typically 10 degrees Centigrade above room temperature). Studies have begun on modifying the two point non-uniformity correction procedure to account for higher "apparent temperature" imaging when IR lamps illuminate the object of interest.

Specimen Indicating Corrosion Detection Limits

The corrosion coupons shown previously in Figure 40 were coated with various thicknesses of paint and IR images taken. Figure 48 shows an IR image of the corrosion and pits on an unpainted coupon.



**Figure 48 IR image of an unpainted corroded 2024 aluminum coupon.
The corrosion products and pits are apparent.**

Figure 49 shows a visual image of an un-corroded coupon coated with 3.0 mil primer and topcoat. Figure 50 shows a corroded coupon with a total of 3.0 mil primer and topcoat. Due to coupon roughness, some of the surface morphology comes through the paint. These coupons were imaged in the IR with multiple coats of primer and topcoat.

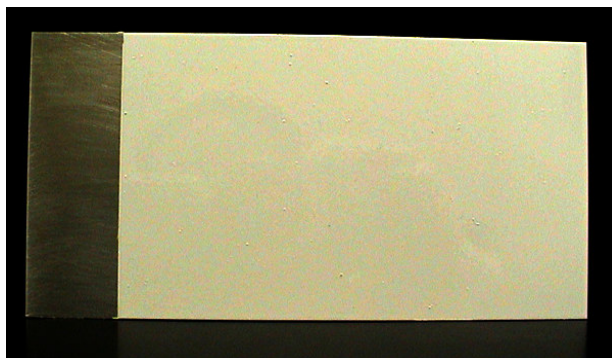


Figure 49 Visual image of 3.0 mil primer and topcoat on un-corroded 2024 aluminum coupon.

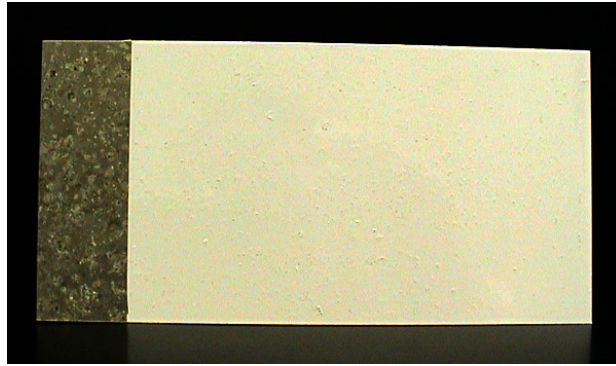


Figure 50 Visual image of 3.0 mil primer and topcoat on corroded 2024 aluminum coupon.

Figure 51 shows the baseline IR image of 3 mil coating on a corroded coupon. The corrosion and pits are readily apparent as observed under IR illumination.

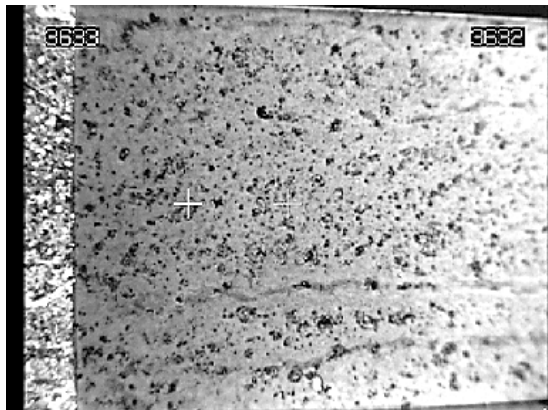


Figure 51 3 mil coating on corroded aluminum. The narrow strip on the left is unpainted

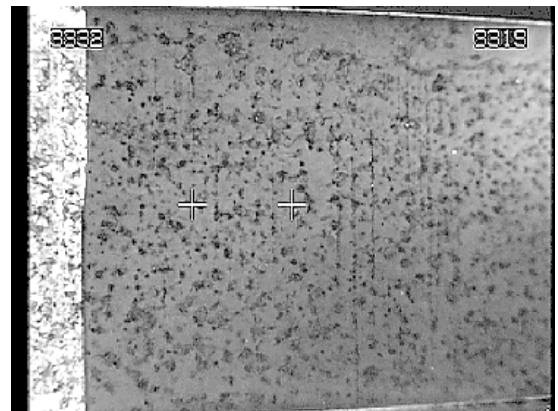


Figure 52 6 mil coating on corroded aluminum. The narrow strip on the left is unpainted

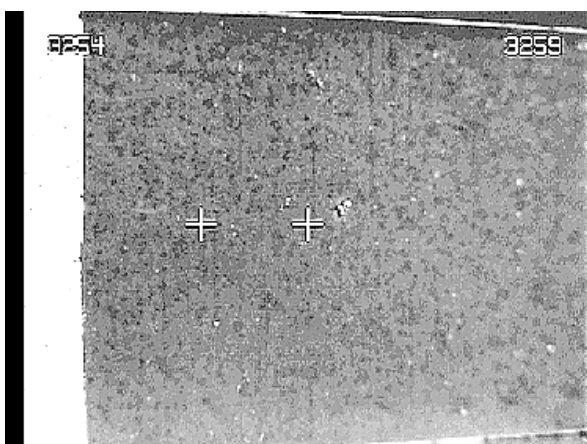


Figure 53 9 mil coating on corroded aluminum.

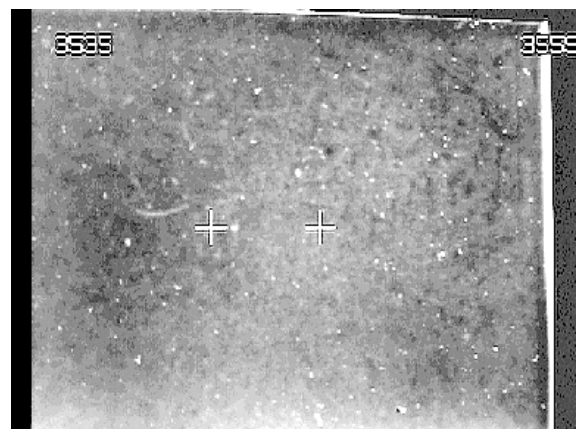


Figure 54 12 mil coating on corroded aluminum

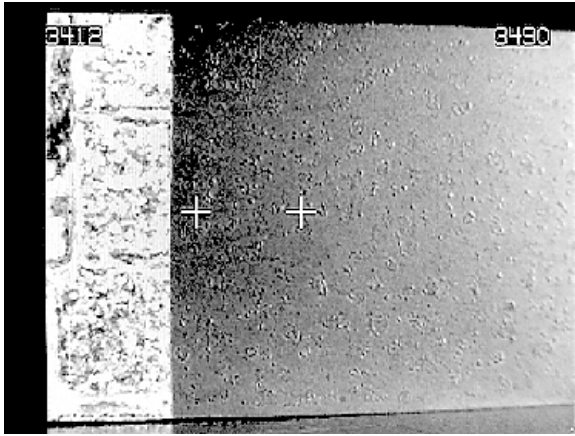


Figure 55 3 mil Dark Camo Grey topcoat on corroded aluminum. The narrow strip on the left is unpainted.

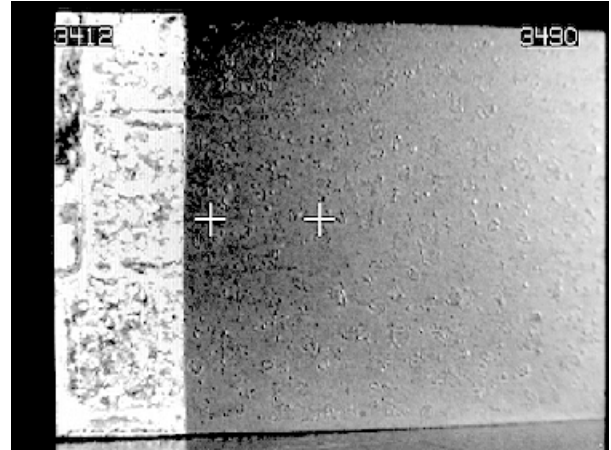
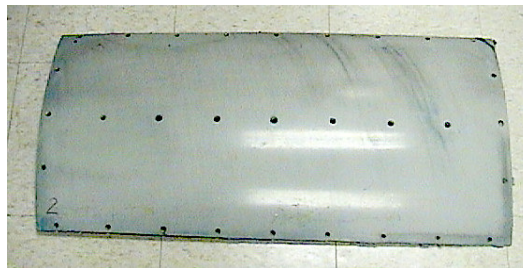


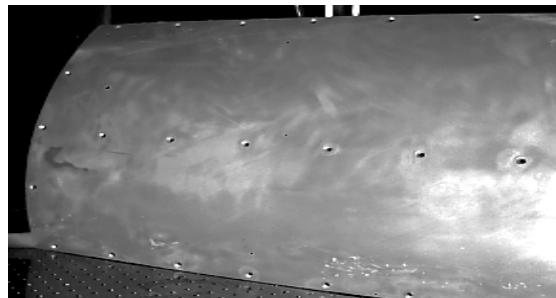
Figure 56 3 mil Dark Camo Grey with Low IR primer on corroded aluminum. The narrow strip on the left is unpainted.

Laboratory and Field Detection of Corrosion in Real Aircraft Parts

A variety of corroded and un-corroded painted real aircraft parts were imaged both in the lab and in the field in daylight. Parts came from a variety of Northrop Grumman aircraft, including the E-2C, EA-6B, F-14, and Joint STARS (707). Figure 57 shows an E-2C access panel imaged visually under normal illumination and with the IR camera system. The metal surface morphology come through quite clearly. This includes scratches, blemishes, and metal rework (corrosion removal) not visible from the painted surface.



a.



b.

**Figure 57 Comparison of visible and IR image of an E-2C access panel
a) visible image of paint surface only, b) IR image through the paint to metal surface underneath.**

Figure 58 shows a comparison of a visual image of a portion of a JSTARS 707 wing and an IR image revealing corrosion on the fastener heads under the paint. Dark fastener heads indicate cadmium plate missing.

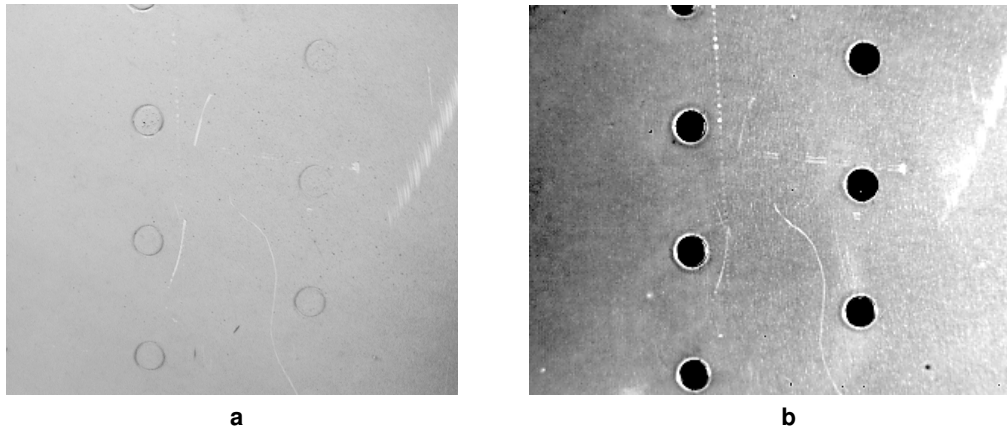


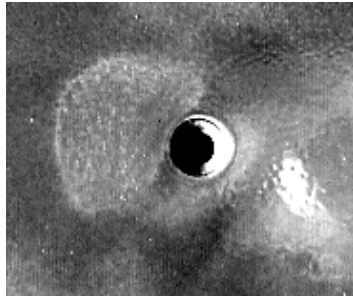
Figure 58 A visual (a) photo and an IR image (b) of corroded fasteners under paint in a Joint STARS 707 wing section.

Figure 59 shows a visual image on an unpainted fastener head next to an IR image of the same fastener covered with 3 mil of primer and topcoat. The fastener markings can be clearly seen through the coating.

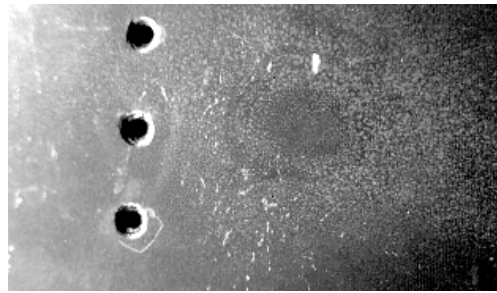


Figure 59 A visible image (a) of an unpainted fastener head, an IR image (b) of the same fastener covered with 3 mils of primer and topcoat.

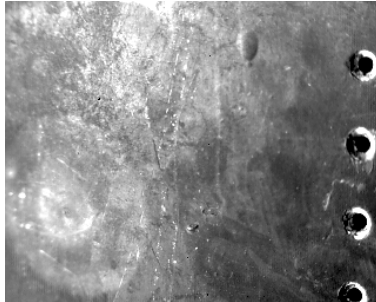
Figure 60 shows a collection of IR images of additional aircraft parts. Figures 61 and 62 shows IR images taken on a painted corroded coupon outdoor in daylight (cloudless day - summer). In Figure 61a, the first image is taken with indirect sunlight (shaded) with no artificial IR illumination. The corrosion pattern clearly comes through. The second image (Figure 61b) was taken with direct sunlight after the coupon was allowed to heat up. Although the corrosion image is still there, its contrast is reversed from the “cold” image. A similar situation



Metal Rework



Coating Porosity



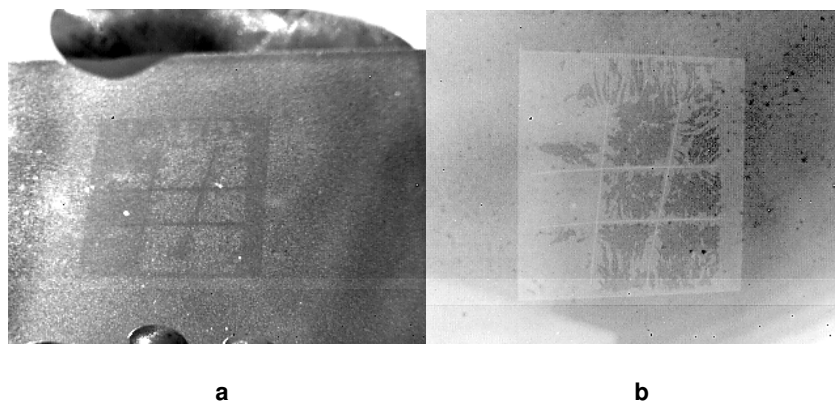
Metal Rework



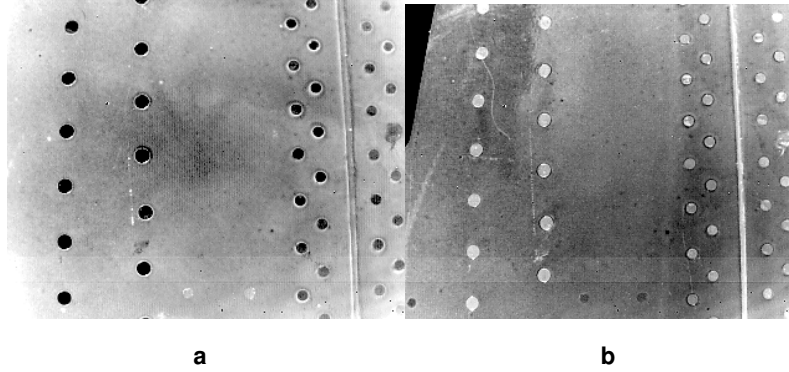
Painted Over Markings

Figure 60 Additional IR images of metal surface conditions through paint on aircraft parts.

holes for the Joint STARS 707 wing panel in Figure 62. The wide area IR imaging technique relies on differences in surface reflectance's using an external IR illumination source. This is essentially ordinary photography in the IR. However, as the part heats up in the sun, the part starts to radiate thermal energy on its own independent of external illumination. Since high emissivity regions (low reflectance) of the part will appear brighter when emitting IR radiation, there is a contrast reversal in the image. Essentially, the conditions have changed from IR reflectography to IR thermography. This is a complication that must be accounted for in any outdoor or flight line application of wide area imaging through paint.



**Figure 61 Outdoor imaging of painted test coupon
a) in shade, b) in sun with heating (summer).**



**Figure 62 Outdoor imaging of painted wing section fastener corrosion
a) in shade, b) in sun after heating (summer).**

Crack and Pit Detection

Due to the extraordinary detail and clarity of the IR images through the paint, it was decided to perform some studies on crack and pit detection, as well. Figure 63 shows a range of laboratory created fatigue crack lengths emanating from fastener holes in 2024 aluminum bar material.

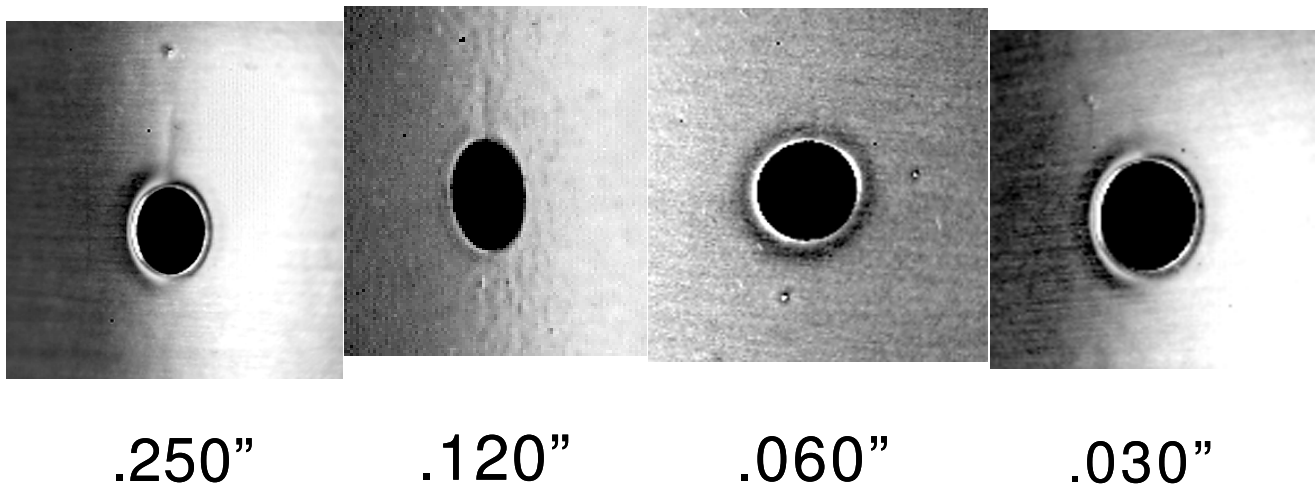


Figure 63 Successively smaller length fatigue cracks imaged under 3.5 mil primer and topcoat using a 25 mm IR lens.

Fatigue cracks could be detected down to 0.030\" in real time using the 25 mm lens. Better images could be obtained with 1x and 4x IR magnification lenses. See Figure 63. Figures 64 through 66 show wide area detailed images of fatigue cracks under paint.

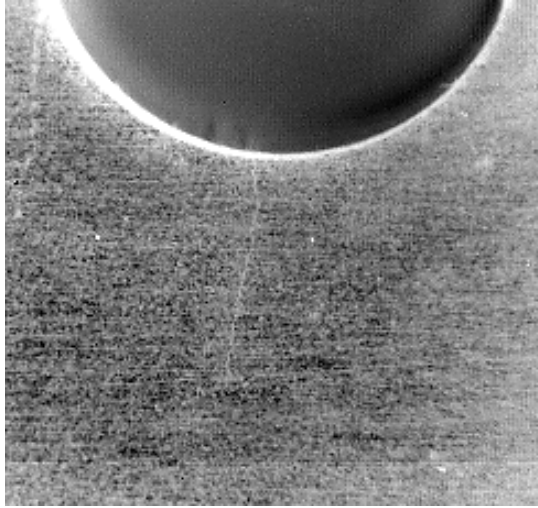


Figure 64 0.120" fatigue crack in 2024 aluminum bar imaged through 3.5 mil primer and topcoat.

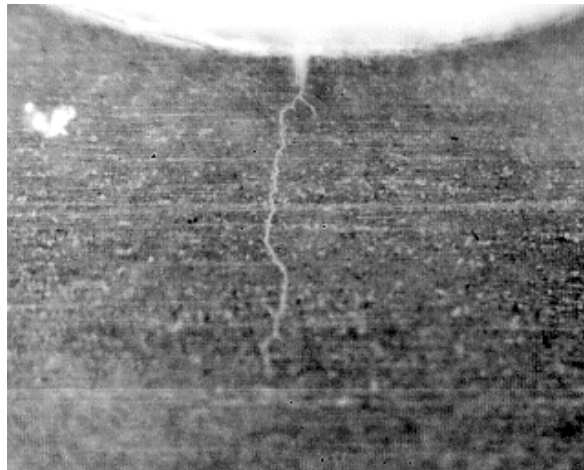


Figure 65 0.060" fatigue crack in 2024 aluminum bar imaged through 3.5 mil primer and topcoat.

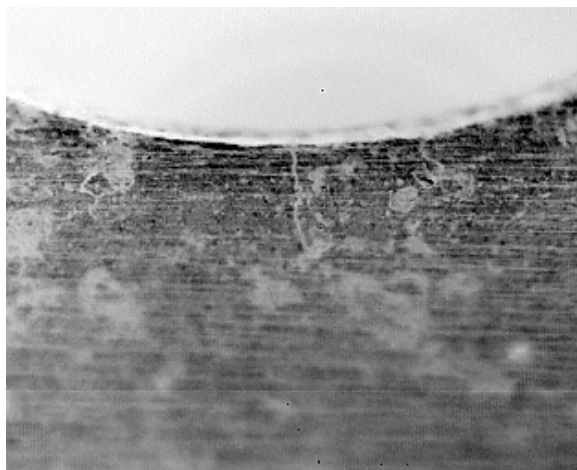


Figure 66 0.030" fatigue crack in 2024 aluminum bar imaged through 3.5 mil primer and topcoat.

In addition to clean fatigue cracks, we imaged corroded fatigue cracks as well. Figure 67 shows a drilled aluminum plate with a fatigue crack exposed to salt fog, corroded, and painted. The crack is still clearly visible through the paint.

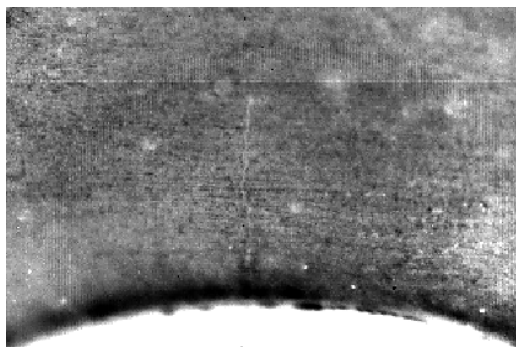
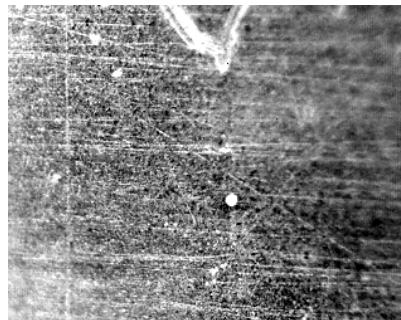


Figure 67 0.060" fatigue crack corroded, painted, and imaged with the IR system.

A series of electrical discharge machined (EDM) holes were drilled into aluminum bars and painted with milspec primer and topcoat (3.5 mil thick). These simulated pits were then imaged with the IR camera. Figure 68 shows a series of successively larger EDM pits imaged through the paint.



**1.3 mil diameter
1.2 mil depth**



**2.4 mil diameter
2.1 mil depth**



**4.4 mil diameter
4.1 mil depth**



**8.4 mil diameter
8.2 mil depth**

Figure 68 EDM simulated pits in 2024 aluminum imaged through 3.5 mil primer and topcoat.

Polarization Results

In preparation for investigating the use of IR polarization to minimize scatter from heavily pigmented and nonuniform coatings, we purchased a set of custom polarizers. Manufactured by Molelectron Detector, Inc., these are specialized wire grid polarizers designed to operate in the mid IR range (3 to 6 μm in this case) with a transmission efficiency of 70%. Some conventional polarizers can operate in this range, but attenuate the IR flux to unacceptably low levels. The polarizers were used separately and together to see the effects of a polarized light source and polarized camera optics. Initial results on thick and “difficult” coatings were encouraging. Figure 69 shows a comparison of different polarizations of back paint on an anodized aluminum coupon.

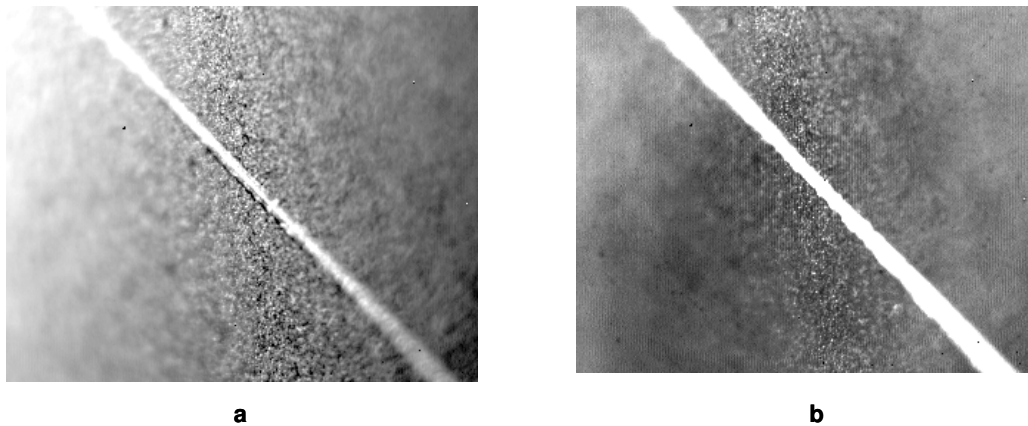


Figure 69 Comparison of opposite polarizations on camera optics for IR imaging of 4 mil black paint on anodized aluminum coupon, a) polarizer parallel to plane of incidence, b) polarizer perpendicular to plane of incidence. Diagonal line is a scribe to the metal surface (overexposed in this photo).

There is noticeably more detail from the aluminum undersurface visible in Figure 69a than from the smoother paint surface in Figure 69b. There is significantly greater penetration of the paint with the electric field direction perpendicular to the paint surface (parallel to plane of incidence) as expected from Brewster’s Law.

Wide Area Imaging Discussion

We have successfully demonstrated the use of multispectral wide area IR imaging to see through a variety of paints of various thicknesses to image both low level corrosion as well as crack, pits, and other surface morphology of the underlying metal substrate. A commercial high performance InSb IR camera was purchased, modified with filters, and used as the imaging system. Conventional mil spec paints were imaged through over 12 mils of paint. These results were obtained repeatably and reliably with a number of multiple trials. Surface morphology studies resulted in high fidelity images of cracks down to 0.030” and pits down to 0.001” diameter. Both 25 mm IR lenses as well as 1x and 4x IR magnifying lens were demonstrated to give excellent images. Improved IR illumination was obtained with low power resistive elements and parabolic reflectors. Real aircraft

parts were imaged, and a variety of surface features included rework and corrosion could be detected. The camera was made portable by combining it with a compact digital camcorder to record the IR images in real-time. The system was mounted on a shoulder rest and a battery pack was used for power. Additionally, images were taken outdoors. Although there were some problems encountered with reverse contrast due to heating, the system was still able to see through the coatings. The latest results with broadband filters show some improvement in imaging.

We worked to improve the system sensitivity. One major effort was in customizing the two point non-uniformity correction (NUC) algorithm to improve camera baseline performance at elevated IR illumination and to accommodate the IR filters. Normally, these cameras are calibrated with sources at or near room temperature. The apparent temperature of the objects image here, however, are much higher due to the external IR illumination. Maximum camera focal plane sensitivity much be achieved at these illumination temperature, which varies with illumination conditions.

The InSb focal plane in the Indigo Merlin™ camera has an internal “cold” window from 3.0 to 5.0 μm , but most paints are transparent in the 3.8 to 5.6 μm range. The 3.0 to 3.8 μm contribution will add an unwanted image of the top surface of the paint, thus partially obscuring the image coming from below the paint. This is why it may be necessary to use filters to block unwanted spectral bands from reducing image contrast. However, currently a significant amount of IR light from 5 to 5.6 μm going through the coating is not being imaged by the camera. We are currently collaborating with Indigo Cameras to explore the possibility of widening the spectral range of the internal cold window to capture this additional energy. This could potentially significantly increase the maximum thickness the camera is able to penetrate.

We continued to improve the hand held portability of the current camera system demo unit. This includes better weight balance, longer life batteries, and portable light weight illuminators. A series of field trials on aircraft were made at our facilities and will be described later in the report.

By using polarized IR illumination an/or polarized camera optics, reflected light from the paint surface can be minimized, and the underlying metal image can be improved. A pair of specialized wire grid polarizers were purchased and placed in the optical path of the camera and part. Initial results show some improvement in imaging of difficult coatings such as black, and specialty coatings (thermoplastics). Thermal emission from the polarizer resulting in back reflection of the camera optics can sometimes obscure the image, and solutions to this will be considered.

We conducted discussions with the Indigo company for custom modification of their cameras for optimized performance and for the manufacture of a ruggedized compact imaging system for field use. We have also generated interest in the Navy, Air Force, and Army in the wide area system.

During the first quarter of 2002, the Merlin™ mid range IR camera had to be sent back to the manufacturer for repairs. The camera was returned to Northrop Grumman by Indigo with a repaired remote control and a new

cable connector. After repair of the IR camera, Images were taken of an actual corroded J-STARS aircraft part that demonstrated field produced or naturally produced corrosion could be seen clearly under the production primer coating used. In June 2002, Indigo shipped us a loaner Merlin™ mid range liquid nitrogen cooled camera. Images could be captured directly via the computer where previously images needed to be captured first by the camcorder video system, prior to down loading into the computer. The non-uniform correction setting could not be changed from the factory defaults. So image improvement was limited. The liquid nitrogen cooled camera also had a different focal length than our Merlin™ mid range. Images of the previous SERDP Project samples were taken. The images were compared between the two Merlin™ cameras, however this might not have been a true one for one comparison due to the focal length differences in the cameras.

During July of 2002, we received the 1x and 4x microscope lens from Indigo. Images of Hi-Lok® fastener heads show great detail, but parameters may need to be optimized further due to depth of field issues at the higher magnifications. In addition we received Lab-View and Image Analysis software from National Instruments. This software was installed on the computer so that detailed image analysis can now be performed on future and existing stored IR images.

Cold filter trials using medium band spectral filters resulted in limited improvement in image quality and paint layer penetration. Ongoing work in polarization shows little effect in strain mapping, but some progress in scatter reduction depending on paint properties. Plans developed for limited probability of detection (POD) analysis including for both corrosion and cracks. Crack detection limits studies began using polarization techniques and studying the effects of illumination wavelengths. It was shown that wavelength as expected based on past work including transmission studies had a significant effect on the clarity of images produced in the IR.

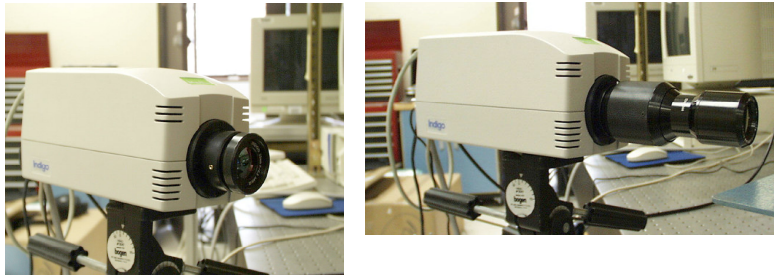
During this time period, progress has been made in the areas of portable systems integration and implementation of field corrosion survey demonstrations. These include hanger demonstrations on aircraft including 707's for J-STARS applications. An IR video was taken of a J-Stars wing skin outside the hanger while illuminated by Florida sunshine showing extensive corrosion and rework of corrosion around fasteners. This corrosion movie of the corrosion survey was played at the IPR that took place October 2002.

A number of other corrosion field surveys were conducted since October 2002 in order to better understand the potential problems associated transitioning the IR camera system into field operations. These corrosion surveys are detailed in the following section.

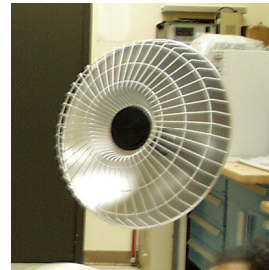
IR Camera Configurations

Different IR camera configurations were investigated in order to determine which configurations would lend themselves best for transition of the technology into field maintenance and inspection operations. Examples of investigated configurations are illustrated in Figure 70. Figure 70 shows the standard lens configuration and an extended lens used for close up operations such as the investigation of small cracks and corrosion pits in the aircraft structure. The extended lens magnification setup is on the order of up to 4X magnification. It must be noted that the extended length could be a problem depending on the location of the camera and the angle of IR source observation as they both relate to the location of the surface area that is in need of inspection. The third photograph in Figure 70 shows a low cost approach for an IR source. This source is basically constructed of a heater coil in the center of a parabolic mirror. The coil is controlled by a variable resistor to adjust the flow of current in the heater coil, which in turn controls the amount of wattage and hence amount of IR energy emitting from the coil. The heater coil emits IR energy that reflects off the parabolic mirror to the surface of the part being observed by the IR camera. This simple illumination source has been shown to be quite effective in both a laboratory environment, as well as in field operations. A battery pack has been assembled and installed to complete a portable imaging system prototype (see Figure 71). The system has in addition to the IR camera, a digital video camera that can be attached to the side of the IR camera. We are considering designing the next generation of this system with a lighter-weight IR camera and a built-in digital video recording mechanism. It is envisioned that ultimately a two-track digital recording system will be used to simultaneously record both visible and IR imaging for parts registration and identification. A split screen could be designed into the system for real time viewing during the corrosion survey of both the IR Image and the normal imaged produced by light illumination. The photographs in Figure 72 (identical to Figure 45) show the IR Camera and the Digital Video Camera. The purpose of the video camera was to record both the IR signal in video format and to record standard video visible images of the surfaces, as seen by normal vision.

IR Camera



Compact System – Hand-Held,
Real-Time Imaging; Internal Cooling;
Interchangeable Lenses Adaptable to
Multi-Spectral Imaging; 24 Vdc; Output
To VCR, Computer



*Simple Illumination
System*

Figure 70 IR camera mounted on a tripod.

In Figure 70, Photograph 1 illustrates the standard lens configuration and Photograph 2 shows the extended lens configuration used to magnify the image to 4X. Photograph 3 illustrates the simple and portable IR source illumination system.

Figure 71 shows how the addition of a battery pack can enhance the portability of both the IR and camcorder the camera system. This method may be useful if standard 110 single phase voltage is not available. Note: The battery belt drives the IR Camera only. The camcorder is already driven, as designed by its own battery and does not need an external power source of 110 voltage.

Figure 72 Photograph 1 shows the portable IR camera attached to a standard Sony camcorder by an aluminum bracket. As can be seen in all photographs, the camcorder and IR camera have been additionally mounted to a personnel adaptor, which acts as a shoulder mount that aids in holding the camera during the corrosion surveys. Photographs 2 and 3 show the operator surveying aircraft parts. Note the placement of the IR illumination system in Photograph 3 to enhance the IR reflected signal off the part. Photograph 4 shows a side view of the operator and the method for personnel shoulder support of the cameras.



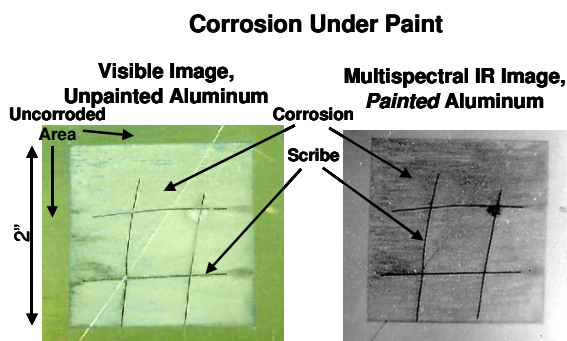
Figure 71 Portable IR System with Battery Pack

Portable System



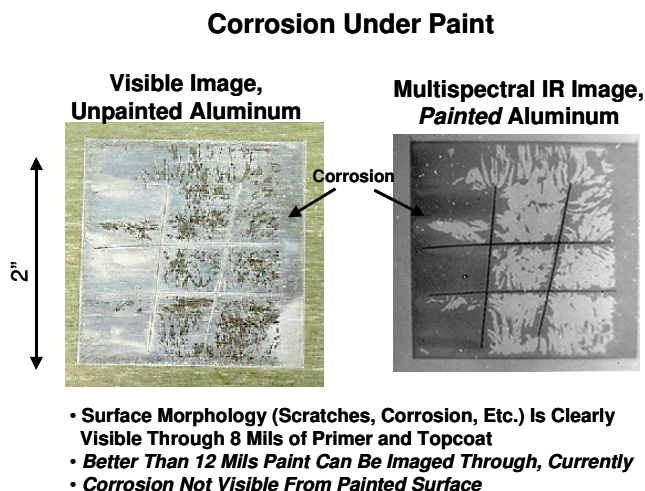
Figure 72 Portable System

Studies to detect corrosion and other defects under coatings as a function of thickness were on going during 2002. Figures 73 and 74 show what a panel looks like before painting/coating and after painting under IR illumination. Note: The painted panels were completely covered with paint and the corrosion was not visible except under IR imaging. Figure 73 shows high clarity under 6 mils of paint, while Figure 74 exhibits clarity under 8 mils of primer and top coating, when viewed in the IR.



- Surface Morphology (Scratches, Corrosion, Etc.) On Anodized Aircraft Aluminum Is Clearly Visible Through 6 Mils of Primer and Topcoat
- Corrosion Not Visible From Painted Surface

Figure 73 Corrosion on an unpainted panel on the left and the same corrosion under 6 mils (.006') of paint once the panel was painted.



- Surface Morphology (Scratches, Corrosion, Etc.) Is Clearly Visible Through 8 Mils of Primer and Topcoat
- Better Than 12 Mils Paint Can Be Imaged Through, Currently
- Corrosion Not Visible From Painted Surface

Figure 74 Corrosion on the surface of an unpainted panel on the left and the same corrosion under 8 mils (.008') of paint once the panel was painted.

These studies indicate that field produced corrosion should be detectable up to at least 8 mils of Mil-PRF-23377, epoxy primer and Mil-PFR-85582 TYI, polyurethane topcoat. This is important as many field aircraft have additional multiple coatings applied and in some cases far beyond specification requirements/limits.

Note: The original finish specifications limits generally max out at 3-4 mils of thickness except for specialty coatings.

Multi-Spectral Infrared Images

Figure 75 shows the effect of using different wavelengths of IR radiation on the clarity of the under coating corrosion image produced. As shown for this particular coating, the optimum wavelength was determined to be 4.84 micrometers and that the window of opportunity was between 3.4 micrometers and 5.3 micrometers. This study shows the importance of selecting the correct wave band for the application and in fact may also show the importance for the correct selection of an optimum wave band for coatings formulated with different fillers and pigment sizes.

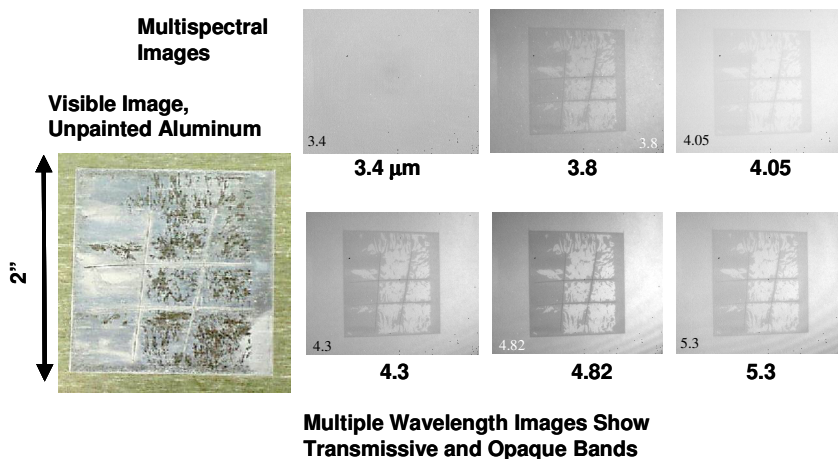


**Figure 75 Effect of IR signal clarity as a function of wavelength.
The optimum wavelength in this study turns out to be 4.82 micrometers.**

IR Imaging of E-2C Access Panel continued

An E-2C production access panel was examined for corrosion and other defects. A general part survey was made first, as shown in Figure 76. As can be seen in Figure 76 potentially defective and/or discrepant areas can be seen by demarcations. These areas are denoted by un-uniform color and outlines in the IR Image. This was initially thought to be all corrosion related, however, it was later determined that upon close microscopic examination of the actual organic coating porosity was the problem. This can be seen in the second photograph of Figure 77.

Detail Imaging of E-2C Hawkeye Panels continued

Figure 77 shows a more detailed and up close survey of the panel depicted by Figure 76. Metal rework can be seen in the first photograph. This rework is most likely the result of previous corrosion that was at least partially cleaned up by sanding or abrading. The second photograph illustrates what coating porosity looks like under IR. This is not a surface effect on the aluminum substrate and hence IR may also be a good tool to investigate coating quality as it relates to spray techniques and flow prior to setting up. The third photograph in Figure 77 shows another area where rework has taken place. The fourth and last photograph was an old part

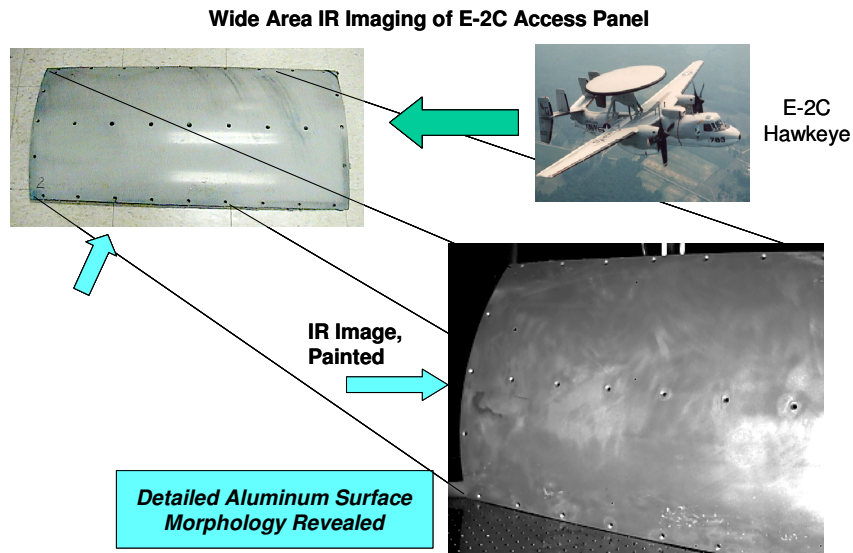


Figure 76 Photographs of the overall panels as taken from an E-2C. The first photo shows the painted panel; the second is a picture of an E-2C; the third photo shows the panel image taken under IR.

marking under the top coat. The assembly number and even the individual inspector's stamp can be clearly seen. This capability could well help in a future failure investigation. Normally this information is virtually impossible to obtain under a painted part by other economical means.

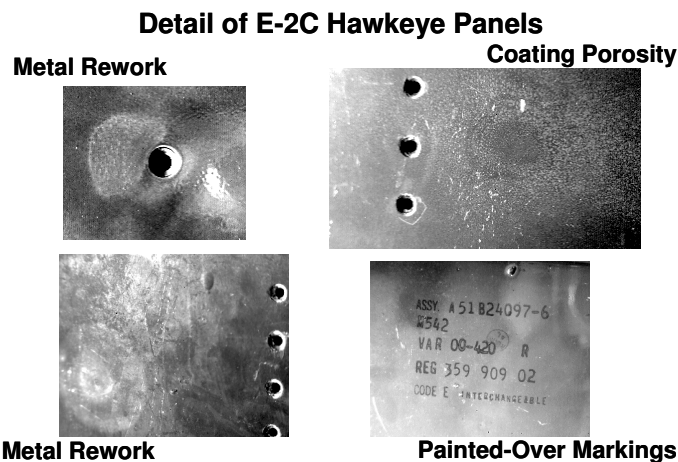


Figure 77 Details of an E2C Panel in various locations around fastener holes plus a hidden ink stamp part number and an inspection stamp marking.

Discussion of Detail Imaging of Fastener Heads continued

In the aerospace industry fasteners obviously play a key role in the structural integrity of aircraft structures and components. It sometimes becomes necessary to inspect certain critical fasteners for part numbers and manufacturers who have supplied these fasteners. In some cases, certain fasteners that were thought to be good initially were installed and are later found to be discrepant. The IR system can play a key roll in economically and environmentally inspecting these fasteners. Normally this type of inspection requires the removal of the

organic coating from the head of the fastener to read the part numbers and/or determine the manufacturer. This entails a significant amount of work in the form of labor (elbow grease) and the application of paint strippers and wipe solvents to the affected areas. After the inspection, if the fasteners are found to be good, the fastener has to be refinished around the adjacent area as well as on the head. This activity results in additional environmental pollution and potential worker exposure to toxic solvents, cancer causing chromated paints and additional VOC's.

Figure 78 shows a standard aircraft Hi-LoK® Part Number HL19-6 manufactured by Fairchild Industries, as indicated by the VS on the fastener head. As can be seen the IR Image, which was taken under 4 mils (.004") of paint clearly shows the applicable part number and manufacture designation.

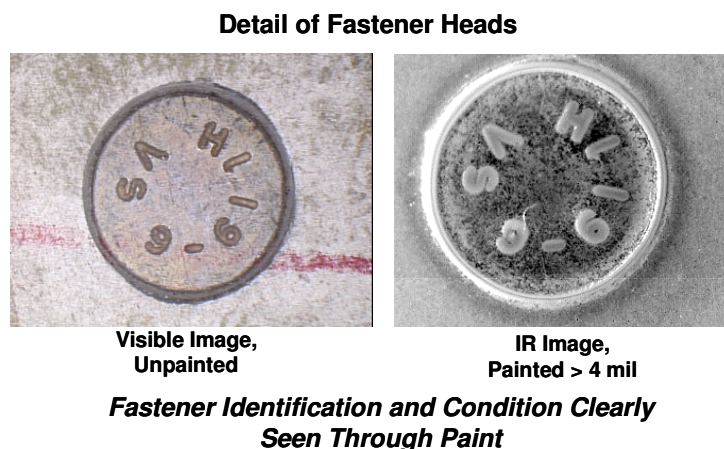


Figure 78 Hi-Lok® fastener head under visible light and under IR looking through 4 mils (.004") of paint. The part number can be clearly seen under the organic coating under IR illumination.

Multi-Spectral Images of Fatigue Cracks

Fatigue cracks emanating from fastener holes need to be inspected successfully in order to avoid the stripping of paint from the aircraft surfaces. Hence a study was conducted to establish detection limits. All the photographs in Figure 79 indicate a crack located at the top of the hole. The crack can be seen relatively clearly in the study up to approximately .060" to .030" in length. These cracks were not naturally produced under conditions in the field, which would generally produce both fatigue and corrosion in the crack as it travels down the part. Hence, the naturally produced crack would be more open in nature as the corrosion products would help to keep the crack more open and with a larger displacement perpendicular to the direction of the crack path. This type of crack would not snap shut when the load is released such as when the aircraft is on the ground. Therefore, it is anticipated that a naturally produced crack of a given length would be more easily detected than a laboratory produced crack. The detection limits of a lab produced crack appear to be approaching .030" in this study. Note: It is important to be able to detect a crack down to .030" as most standard one (1) over size repair fasteners require the drilling out a hole diameter to .030" on a side larger than the original diameter.

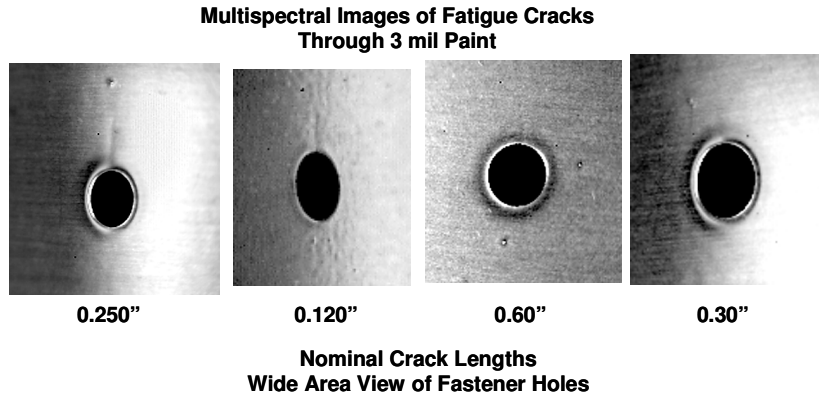


Figure 79 Detection limits of a fatigue crack produced in the laboratory by an MTS Fatigue Machine. Note crack varies from 0.250 in. to .030 in.

Figure 80 shows what a crack looks like under magnification on an aluminum anodized surface. This crack is hardly visible under a standard optical stereo microscope as is considered a tight crack that snaps back into place once the stress has been released from the fatigue machine.

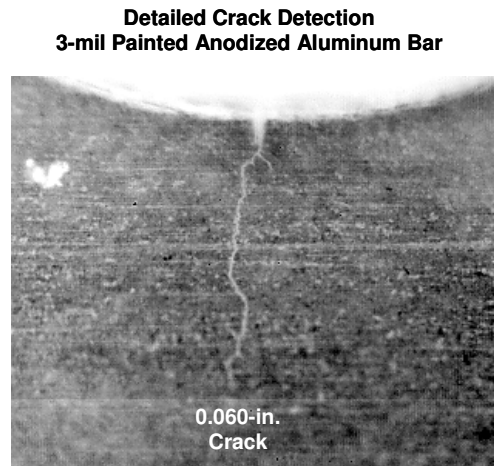


Figure 80 0.060-in. crack under 3 mils (0.003in.) of paint. The top of the figure is the circumference of the hole and the initial site of the crack.

Figure 81 shows that a .030" crack is close to the absolute detection limit. However, a further study is required to obtain a probability at (BOD) detection by an operator of the IR Image system. It is anticipated that a complete study will be required, prior to deployment of this IR system.

Figure 82 was an attempt to simulate a field produced crack that would most likely have corrosion present. Photograph No. 1 shows spotted/pitted corrosion on the surface with corrosion around the crack in visible light. Photograph No. 2 and No. 3 show the surface using a 25 mm lens and then magnification of the crack area by 4X. The crack can be seen, however, the demarcation lines between the crack and the surface are not as clean as in the case of Figures 80 and 81. Anodize may provide a clearer demarcation line between the crack and surface.

**Detailed Crack Detection
3-mil Painted Anodized Aluminum Bar**

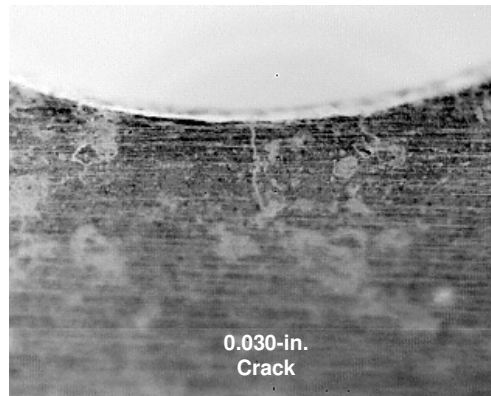


Figure 81 0.030" crack under 3 mils (.003") of paint. The top of the figure is the circumference of the hole and the initial site of the crack.

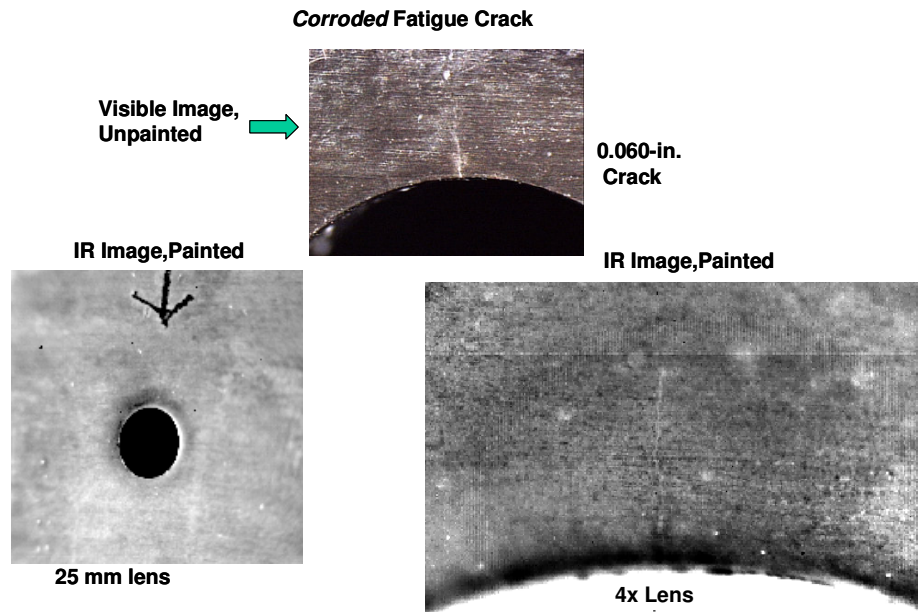


Figure 82 Corroded crack (photo No. 1) produced in the lab by placing the 2024-T3 bare, aluminum specimen in salt water for a number of days. This specimen although not totally realistic maybe more indicative of a more open crack. Photos No. 2 and No. 3 are of painted bare panels under IR illumination.

Pit Detection through Paint

Pit detection and understanding the limits of pit detection is critical to the detection of corrosion under coatings. Hence standards were produced by the aid of electro-chemical discharge machining. A standard set of pits was manufactured by using a tungsten wire of different diameters. The diameters selected were on the order

of 8.4 mils, 4.4 mils, 2.4 mils, and 1.3 mils. Figure 83 shows that you can see a pit under 3 mils of paint down to a diameter of 1.3 mils and a depth down to 1.2 mils.

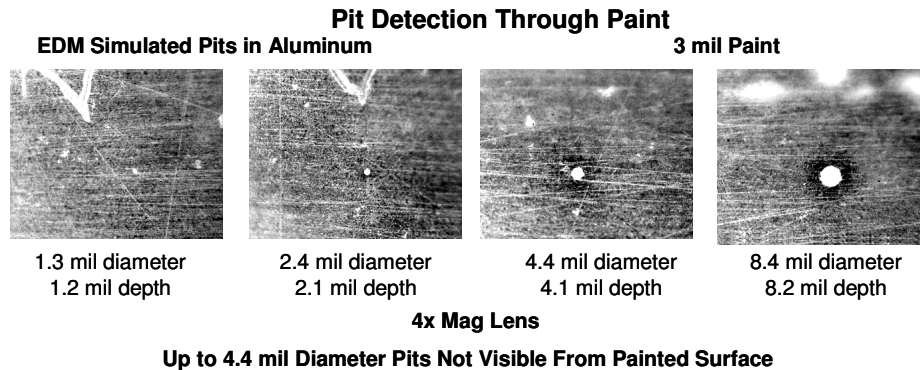


Figure 83 Different size pits under 3 mils of paint using the IR camera system. The detection limit is as low as 1.3 mils, which can be seen in the first photograph of the series. The pits are more easily seen as the diameter approximately doubles in each photograph to the right.

Image Processing and Frame Averaging

Frame averaging is one way to improve image quality. This can be accomplished by the appropriate computer software, as illustrated in Figure 84. Although camera quality plays a significant role in resolution, so can computer processing software and techniques such as frame averaging. Frame averaging involves taking rapid time average multiple frames. With the high speed InSb camera this is possible in one shot. Statistical noise reduction improves as \sqrt{N} where N is the number of frames to be averaged. This efficiently reduces the $Ne\Delta t$ and thus the minimal resolvable contrast. This results in better image sensitivity.

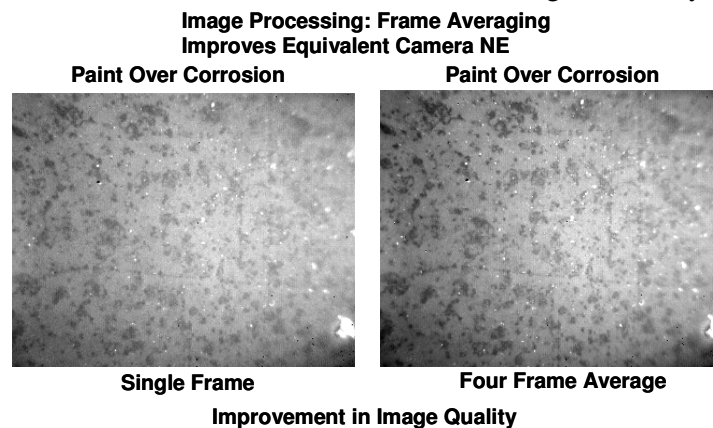
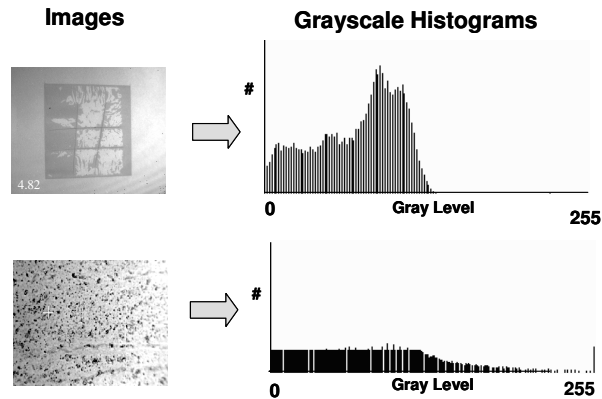


Figure 84 Effect of averaging four pictures or frames and making a composite photograph. The left hand photograph is an example of one photograph and the typical resolution. The photograph to the right shows what happens when four photographs are averaged together for improved resolution.

Grayscale Contrast Studies for Feature Resolution



•Resolution Improves with Broad Grayscale Distribution

Figure 85 Grayscale Histograms

Grayscale Histograms

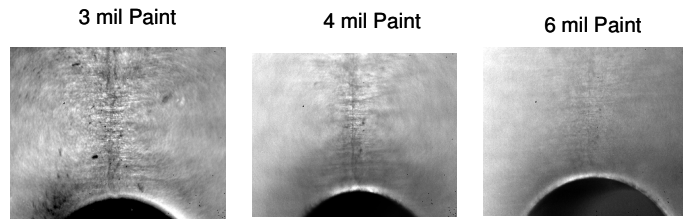
This is the qualitative analysis of the grayscale distribution in the IR images (Figure 85). Improved grayscale distribution is important for visual image contrast and minimum level of feature detect ability.

Crack Detection Study:

New 1X and 4X IR lens directly mounting on the Indigo camera produced images of cracks under 4 mils of paint, see Figure 86. However, the 1X lens apparently did not show the crack as well as the 4X lens. Figure 86 shows that performance was greatly restricted after the application of 6 mils of paint. Multi frame averaging may improve the detection limits and should be tried along with planned future activities. Figure 87 also shows grayscale scans of No Crack vs. Crack. The crack scan produced somewhat more pronounced differences in the grayscale level but not gross differences. This analysis shows minimal gray level difference for visual discrimination of crack and corrosion features (see Figure 87).

Crack Detection Study

Painted Fatigue Crack (0.250") Specimen
1X IR Macro Lens



- New 1X and 4X IR Lenses Obtained for Program
- Performance of Lenses not to Level of Previous Evaluation

Figure 86 Crack detection as a function of paint thickness using 1X IR macro lens.

Crack Detection Study

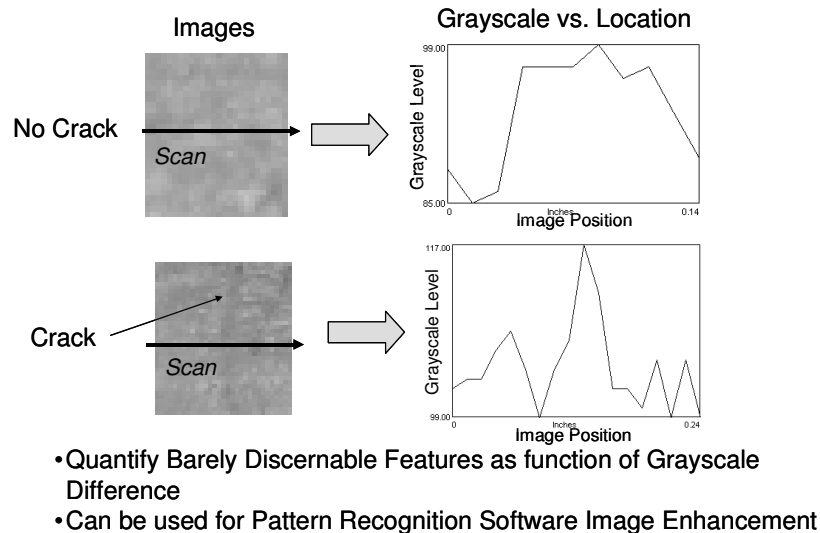
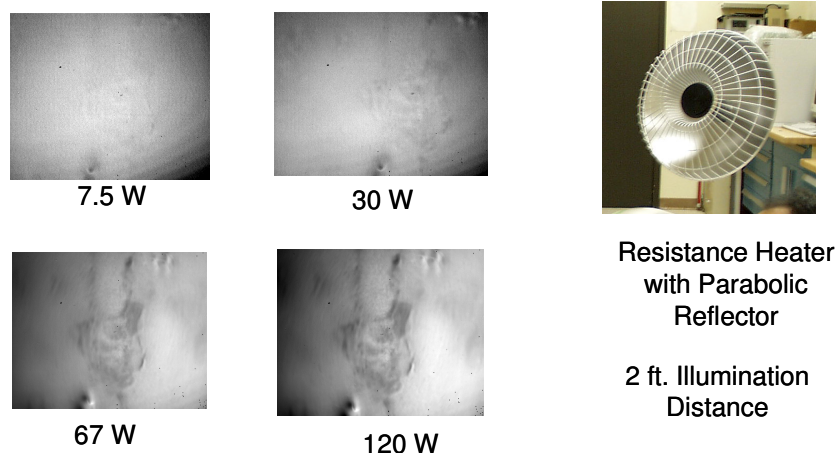


Figure 87 Differences in grayscale level, but not gross differences

Illumination Power Study

The correct illumination is another key to producing clear and detailed images. Figure 88 shows what happens to an image as the power is increased from 7.5 watts to 120 watts. As can be seen with increasing IR flux, the detail of the image improves. It would be expected that this image would improve until the focal plan becomes over saturated or the sterling cooler in the camera can no longer keep up with the imposed heating load from the reflected IR. Additional heating from the IR source will eventually heat the surface and the part to the point where black body radiation may interfere with the image processing capability of the focal plane. This black body mechanism could also be technically used to one's advantage, but is in need of more investigation.

Illumination Power Study



- IR Images of Corrosion Under Paint as a Function of Illuminator Power
- Increased IR Flux Improves Sensitivity

Figure 88 Effect of increasing the IR energy and the increase of clarity of the IR imaging as the energy increases.

See the figures of the Joint STARS wing taken in the IR. These IR photos were created in the hot sun in Florida. It appears to be the hot sections have been fully saturated, but that the corrosion prone areas are not radiating as much energy. This phenomenon warrants additional investigation as the implication is that IR reflectance is only one piece in the puzzle and that IR energy being emitted from a part or surface by the black body phenomenon could be used possibly for surfaces other than metal. This is different again from the thermography technique, which studies the impact of flash heat source and the decaying heat flux on a part. Again, thermography is similar to IR reflectance in that an external heat source is used or required. Using this black body technique for example, composite structures that are heated to a given temperature could be analyzed under the coating for structural integrity.

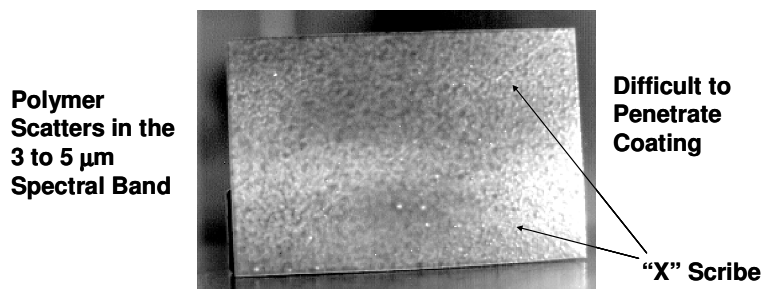
With increased part temperature, the part becomes its own radiator with a “one pass” optical path through the coating for the image. This is opposed to a “two pass” for externally illuminated parts. A “one coating pass” of the IR energy may allow for a much thicker coating or paint to be imaged through. This effort will be further investigated.

Imaging Through Highly Scattering Coatings

Liquid crystalline Polymer coatings present a problem for the penetration of the IR radiation, as the crystalline structure is on the order of the wavelength of the IR radiation (see Figure 89). This problem is not apparent with the standard organic resin systems used for standard military and commercial coatings. For one reason the resin systems of these coatings do not form crystalline structures. Another reason is that the pigmentation used in standard aircraft coating systems is significantly less than the order of the wavelength of the

IR radiation. Hence, the radiation is allowed to pass in and out though the bulk of most standard aircraft coatings without much interference from the pigmentation or the organic resin matrix, which is not crystallized.

Liquid Crystalline Polymer on Scribed Aluminum



IR Image
IR wavelength on the order of polymer crystalline domain size

Figure 89 IR image that does not penetrate to the substrate.

Imaging Through Coatings of Various Thickness

In order for the IR Camera system to be successful, the IR radiation must be able to penetrate standard military paint systems and provide a clear image to the operator. Coating of the IR signal is key to development of a useful inspection system. The better the IR system configuration, the thicker the paint or coating system can be penetrated. Hence a controlled test was performed to assess clarity of the Image produced from the IR signal as a function of thickness of primed and top coated panels with a given or standard amount of corrosion (Figure 90 a-y). To obtain a standard corroded panel all 2024-T3 panels were exposed to salt fog in accordance with the requirements of ASTM B117 for one week. A series of panels were coated with MIL-PRF-23377TYI CLC and MIL-PRF-85285TYI to obtain different and controlled paint thickness.



Figure 90a Visible image of corroded sample C1



Figure 90b Visible image of the corroded sample C1 with 2.5 mil Gloss White

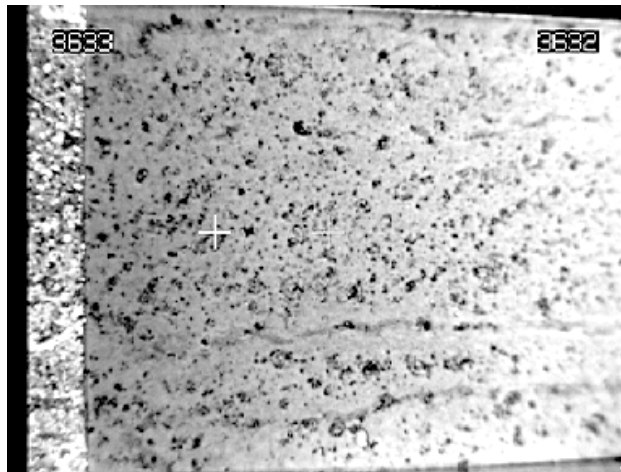


Figure 90c IR image of the corroded sample C1 with 2.5 mil Gloss White

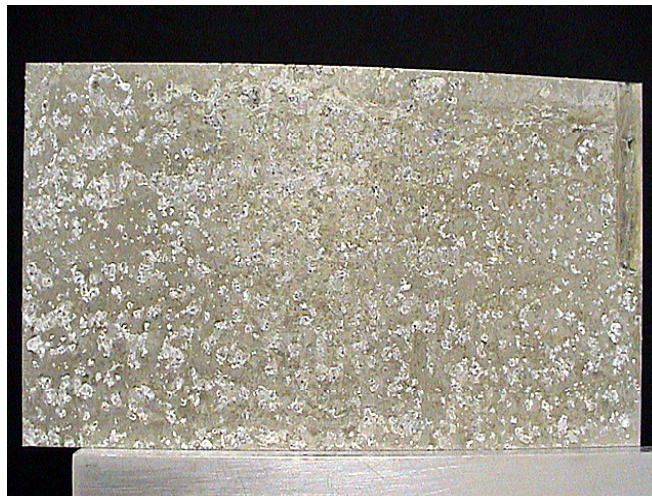


Figure 90d Visible image of corroded sample C2

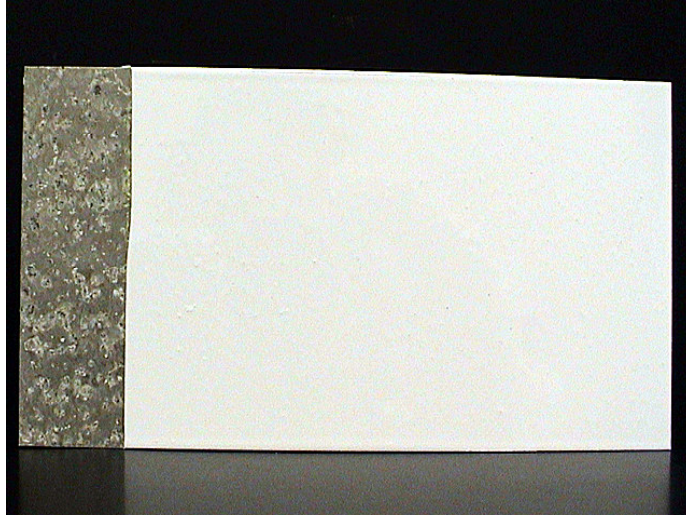


Figure 90e Visible image of the corroded sample C2 with 3.5 mil Gloss White

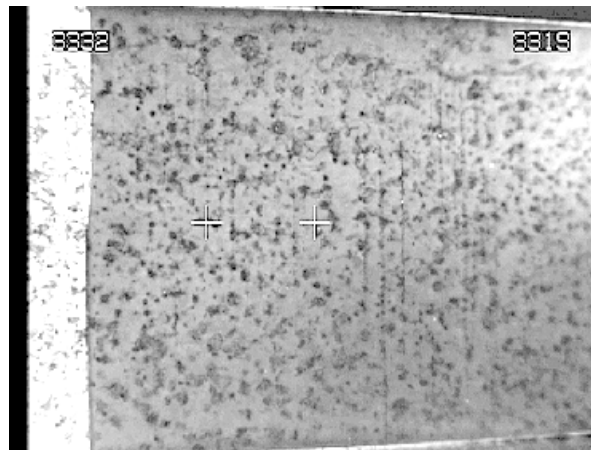


Figure 90f IR image of corroded sample C2 with 3.5 mil Gloss White

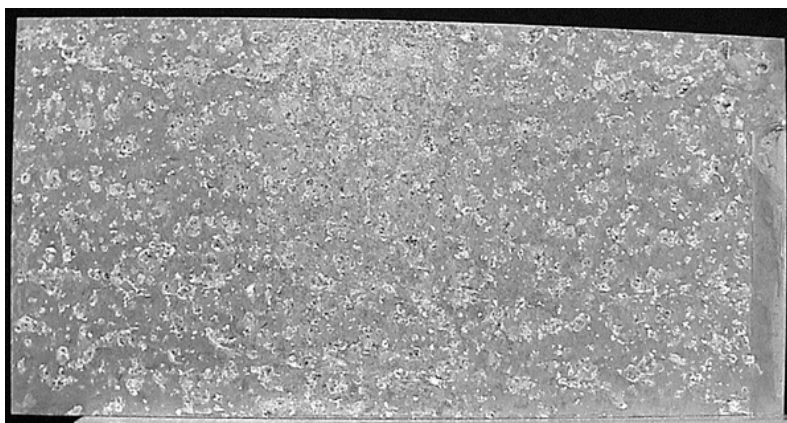


Figure90g Visible image of corroded sample C3

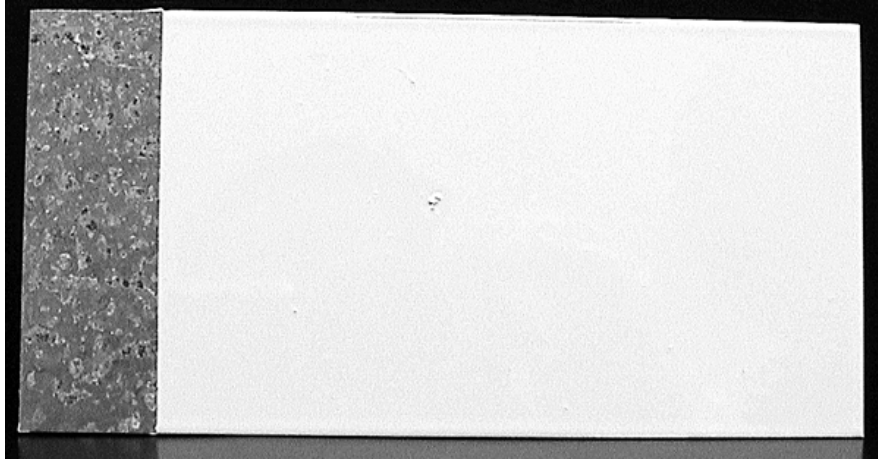


Figure 90h Visible image of corroded sample C3 with 5.6 mil Gloss White

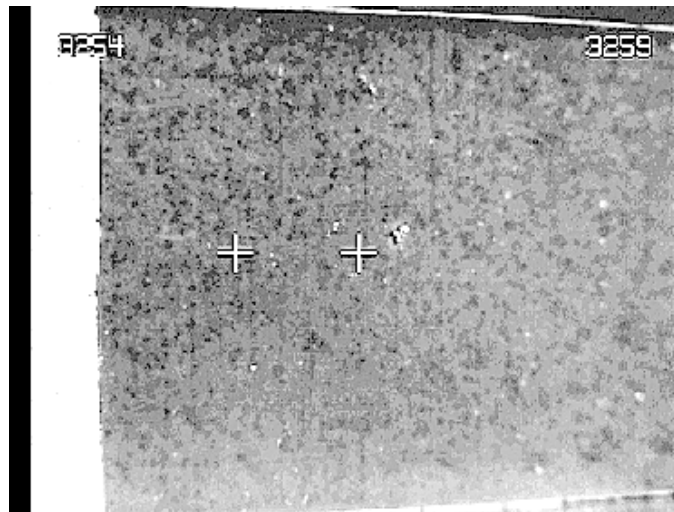


Figure 90i IR image of corroded sample C3 with 5.6 mil Gloss White

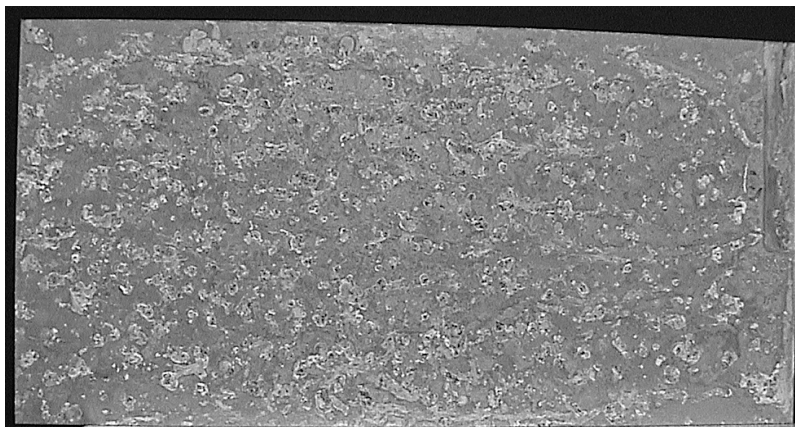


Figure 90j Visible image of corroded sample C4



Figure 90k Visible image of corroded sample C4 with 8.2 mil Gloss White

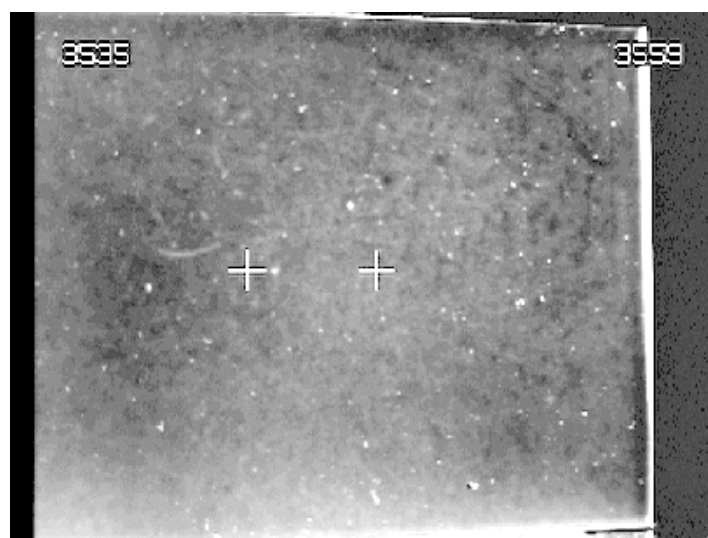
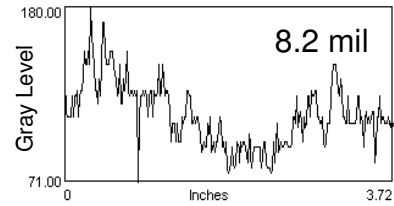
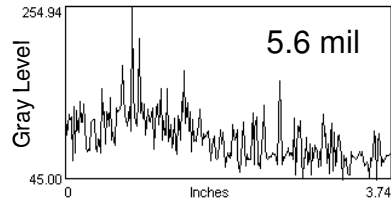
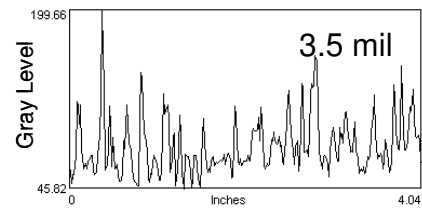
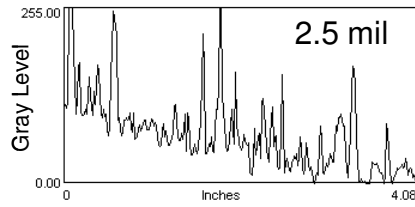


Figure 90l IR image of corroded sample C4 with 8.2 mil Gloss White

Grayscale Density Plots Gloss White



• RMS Grayscale Variation Determines Sensitivity

Figure 90m Grayscale variations drip significantly with increase paint thickness
Comparative Plots of samples C1, C2, C3, and C4. The plots indicate sensitivity decreases with increasing coating thickness. Hence, the thicker the coating the less fidelity in the images as expected.

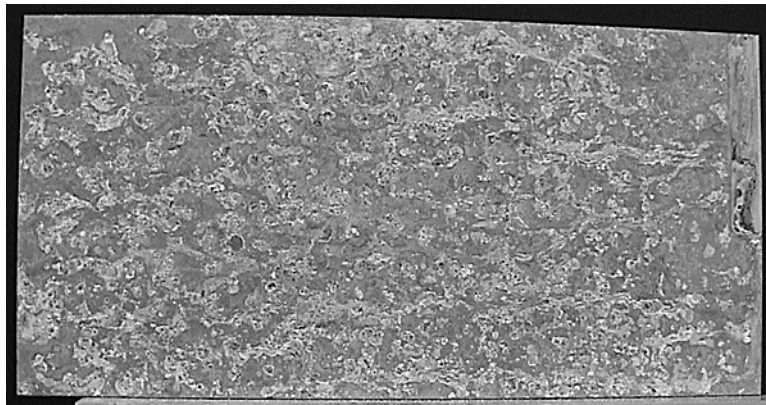


Figure 90n Visible image of corroded sample C5



Figure 90o Visible image of sample C5 with 2.5 mil Camouflage Gray

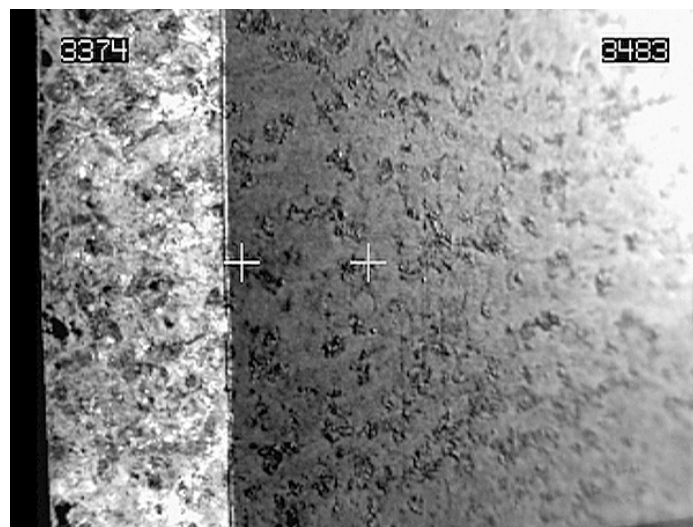


Figure 90p IR image of sample C5 with 2.5 mil Camouflage Gray



Figure 90q Visible image of corroded sample C6

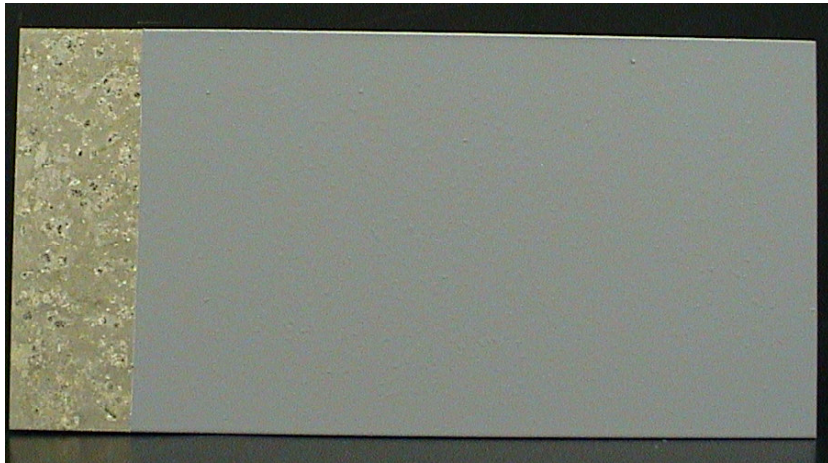


Figure 90r Visible image of C6 with 4.6 mil Camouflage Gray

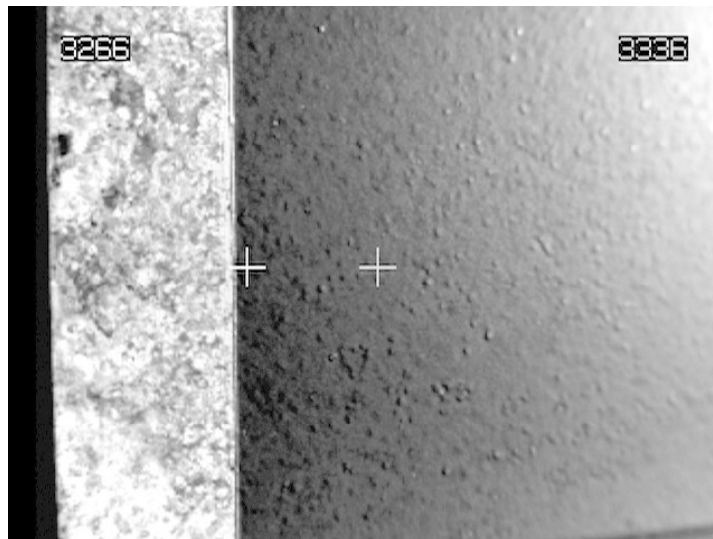


Figure 90s IR Image of C6 with 4.6 mil Camouflage Gray



Figure 90t Visible image of corroded sample C7

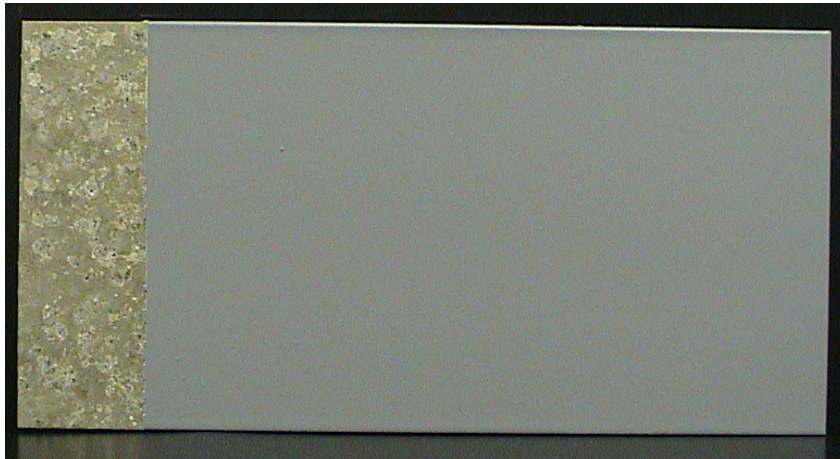


Figure 90u Visible image of C7 with 7.3 mil Camouflage Gray

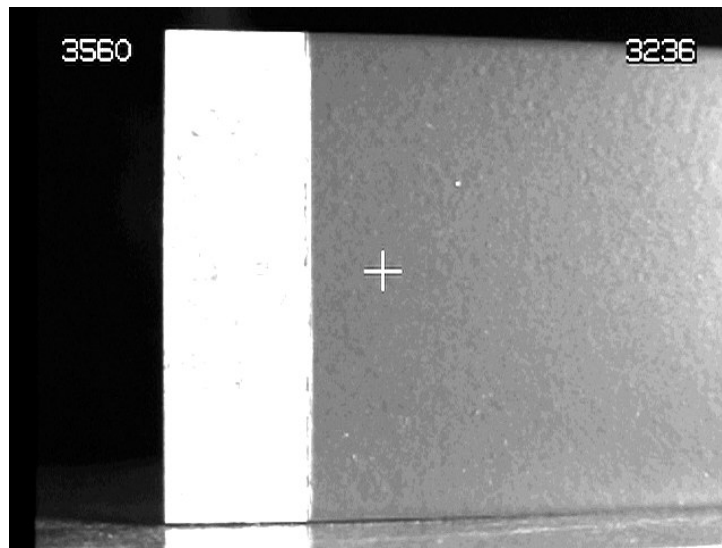


Figure 90v IR image of C7 with 7.3 mil Camouflage Gray

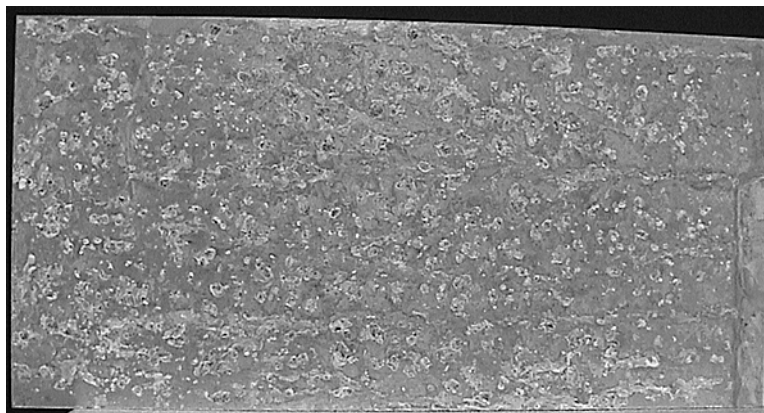


Figure 90w Visible image of C9

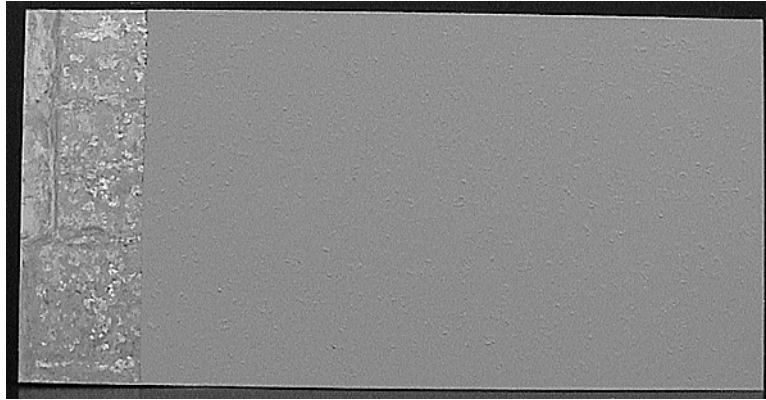


Figure 90x Visible image of C9 with 2.5 mil Camouflage Gray and low IR primer

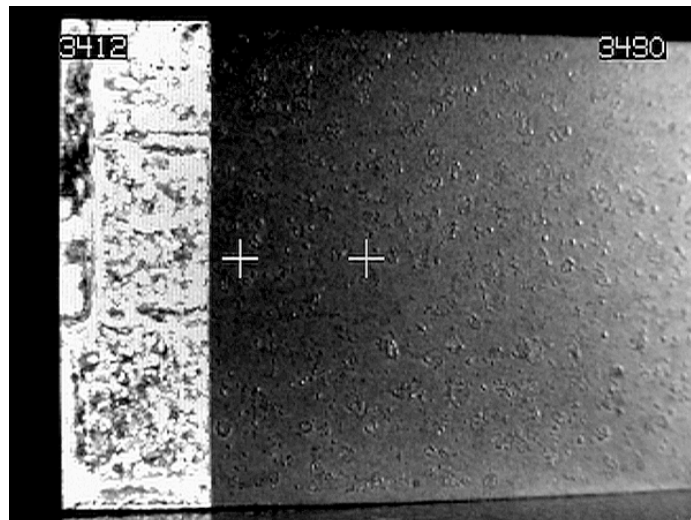


Figure 90y IR image of C9 with 2.5 mil Camouflage Gray and low IR primer

It is more difficult to see through this coating system because of the IR absorbing characteristics of this primer MiL-PRF-23377TYIICLC (see Figure 90 (y)).

Liquid Nitrogen Cooled Filter Study

Limited improvement was found for medium bandwidth filter for LN₂ cooled filter system. Figure 91 shows an image of corrosion pits under 4 mil (.004") of primer and topcoat. This camera was equipped with an LN₂ cooled internal filter with a bandwidth from 3.5 to 5.5 micrometers. This is designed to avoid the non-transmissive regions of the paint and to include the top end of the InSb detector sensitivity. Possibly due to a combination of flux reduction and camera performance variation, there was not a significant improvement in

image quality or depth of penetration as compared to the broadband filter camera. One explanation may be that there is not a significant benefit to going out beyond 5 micrometers in the conventional filter arrangement.

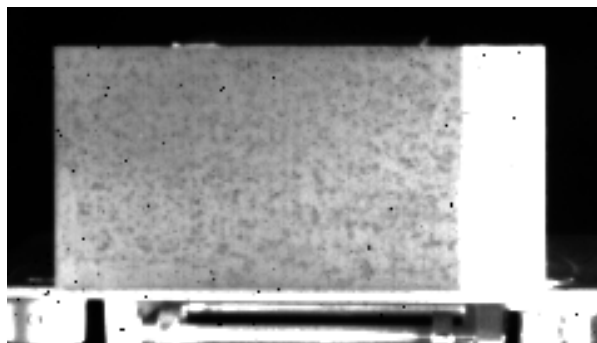
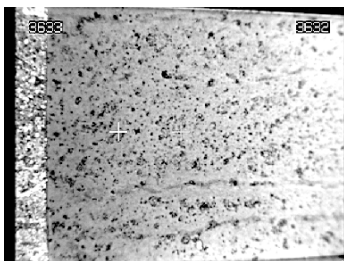


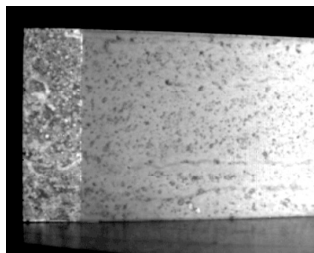
Figure 91 LN2 cooled filter system image showing corrosion under 4 mil of paint

Liquid Nitrogen Cooled Filter Study

Paint Over Corrosion



Uncooled Filter



Cooled 3.5 to 5.5 mm filter

- Attempt to Reduce Room Temperature Glow of Filter
- Obtained LN2 cooled Merlin from Indigo Systems
- Unable to Correct for Nonuniformity in Software
- Images not Improved – Need to Perform Uniformity Correction

Figure 92 Uncooled filter produces images better than the cooled filter

Polarization Study of Painted Fasteners

A comparison between polarized IR and non-polarized IR as made. The studies did not indicate better fidelity with polarized IR when examining painted fastener heads (see Figure 93).

Polarization Study of dark Gray Paint on Aluminum

Polarization work has progress with the analysis of different types of paints. Cross polarization studies did not show significant strain patterns. This was due to the weakly birefringent nature of the primers and topcoats. If these paints could be modified to exhibit birefringence, than this technique may work. Straight polarization initially suffers from the same room temperature thermal emission problem that the uncooled filter exhibited. We are attempting to ameliorate this problem with a newly purchased set of IR macro lenses (1X and 4X). This has

helped in the past to divert filter emission from the camera focal plane. We are also looking at IR lamp illumination pre-polarization.

Polarization Study

Painted Fasteners

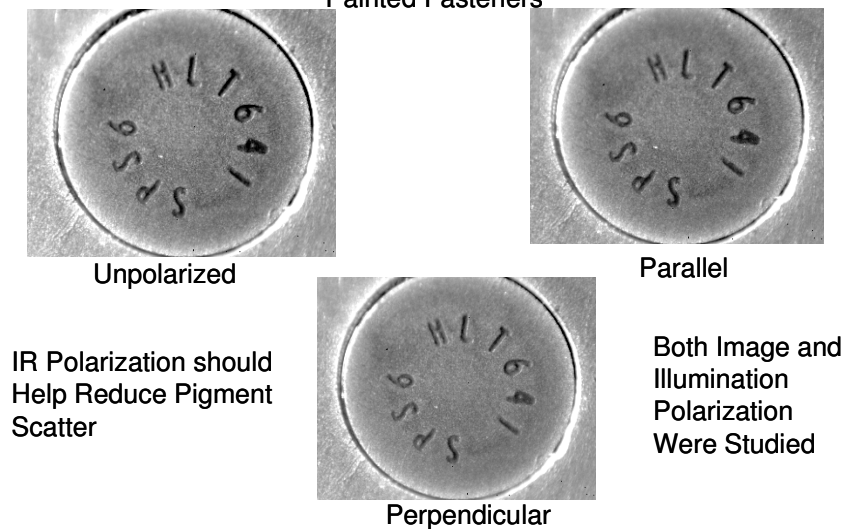
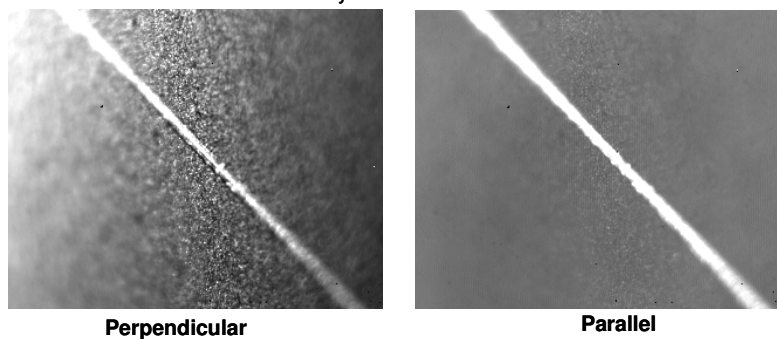


Figure 93 Painted fastener heads under IR illumination. Comparison between polarized and non-polarized illumination

Dark Gray Paint on Aluminum



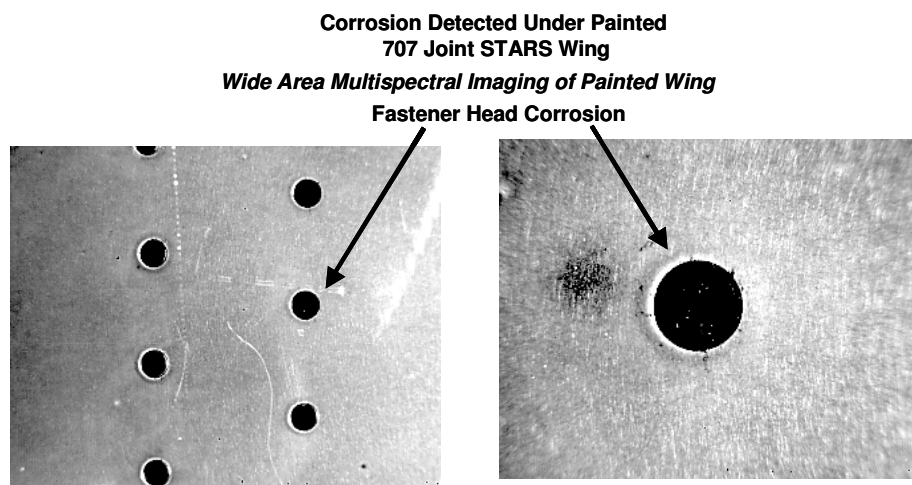
- Some Improvement Seen Depending on Paint Composition
- Uncolled Polarizers Used – Cooled May Reduce RT Glow
- Little Evidence of Strain birefringence in Coatings Studied

Figure 94 Effect of polarization on dark gray paint on aluminum. Perpendicular appears better than parallel polarization in this example.

Pigment scattering was already dramatically reduced by going to the mid IR camera. Polarization filters take out the remaining scattering.

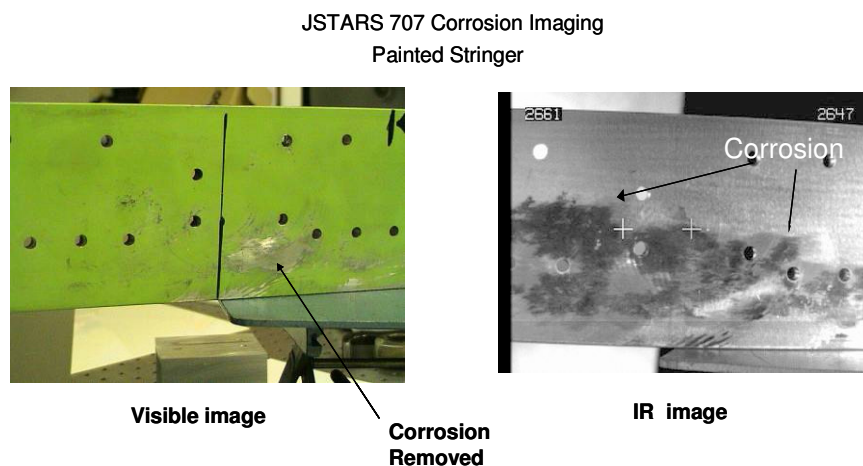
Corrosion and loss of cadmium plating can result in dissimilar metal corrosion. Photograph No. 1 (left side) of Figure 95 indicates all fasteners in view have loss the cadmium plating. The photograph No. 2 (right side)

indicated the starting of dissimilar metal corrosion around the fastener and at the 10 o'clock position. Early detection of this type of corrosion can save thousands in man-hours later and ultimately the possible loss of the wing skin.



Corrosion Not Visibly Detectable from Painted Surface

Figure 95 Fastener head corrosion and no presence of cadmium plating.



Extensive Corrosion Detected on Real Part that is not Apparent V
Figure 96 Corrosion under green primer on actual Joint STARS stringer

Joint STARS 707 Field Demonstration

- Facilities at Melbourne, FL
- JSTARS Program
- Refurbishes Old 707s
- IR Survey Made in Direct Sunlight
- 707 Shown Here was Rejected for Excess Corrosion



Figure 97 Joint STARS aircraft in hangar during maintenance

Joint STARS 707 Field Demonstration



Visible Images
of Painted Wing
Sections



Corrosion Not
Apparent in Many
Areas

Figure 98 Area on top of painted wing surface

Figure 98 shows some of the painted locations that were surveyed for corrosion under the coatings by the IR camera system. As can be seen in the above photographs very little corrosion can be observed on the painted surface, which is usually indicated by corrosion deposits and peeling paint. The photographs in Figure 99 on the show what the corroded metallic surface looks like below the surface of the paint.

It must be noted that this aircraft is no longer in service and was decommissioned due to corrosion around fasteners and other locations on the wing. Early detection could have saved this aircraft, which is now a complete loss to the Air Force inventory.

Joint STARS 707 Field Demonstration

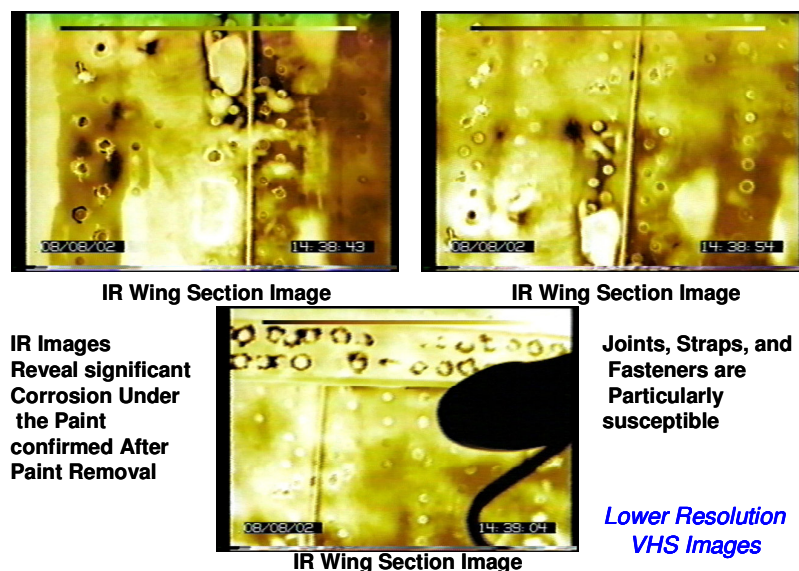


Figure 99 Corrosion is indicated by dark areas around fasteners. Lines of sealant can be seen in all photographs.

Bearcat Aircraft Corrosion Survey

A corrosion survey was conducted on a Grumman-produced WWII aircraft (see Figure 100). This aircraft was produced at the end of WWII and was approximately 50 years old plus is currently under restoration by a number of Grumman retirees in Bethpage, NY. Some of these individuals actually worked on the original Bearcat production aircraft. Much of the aircraft was in the unpainted or bare condition, but a number of components were being refinished and hence were used to test out the IR camera system. Some of these components included environmental ducts, which are shown in Figure 101. The figure shows Dr. Don DiMarzio on the right and John Weir examining the duct for corrosion in real time. The camcorder viewer is being used to observe the IR image of the aluminum duct surface for corrosion under the polyurethane coating. Figure 102 shows the duct up close on a work- bench with an up close shot of the duct in the IR. The IR image shows a darkened/abraded area and weld zones.

Other locations surveyed on the aircraft included the landing gear and the wing structure. Corrosion was observed in both locations. The engine cowls that had been painted were also observed and they had been cleaned of corrosion prior to the application of the primer. This was quite apparent as the sanding and abrasion around fasteners was witnessed under the paint in the real time IR Images taken.



Figure 100 Grumman Bearcat Field Demonstration

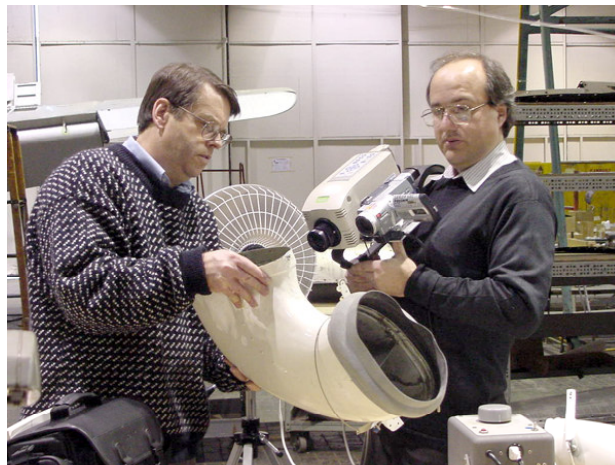


Figure 101 Operator viewing welded duct from Bearcat in real time



Aircraft Ductwork



IR Image Through Paint

Figure 102 Welded duct from Bearcat. Photograph No. 1 shows white paint and photograph No. 2 shows weld area and corrosion that was reworked/abraded under the painted surface

The photographs in Figure 102 show a typical Bearcat environmental control system (ESC) duct that has been welded in at least two locations, as shown by the lower photograph. As can be seen from the top figure, the duct has been painted and the coating is most likely a coating of primer, MIL-PRF-23377 TYI and a top coated with MIL-PRF-85285TYI Gloss Insignia White Color No.17925. The lower photograph shows the aluminum surface of the ECS duct, which has been most likely abraded, prior to painting. The abraded area is located in the center of the photograph and is a little darker than the surrounding area. These figures were snap shots taken digitally from a movie that was made during the real time corrosion survey. Note: Two movies were made. One of the movies was output from the IR camera feed into the camcorder and the other movie was just the standard illumination feed into the camcorder much the same way a home movie is made.

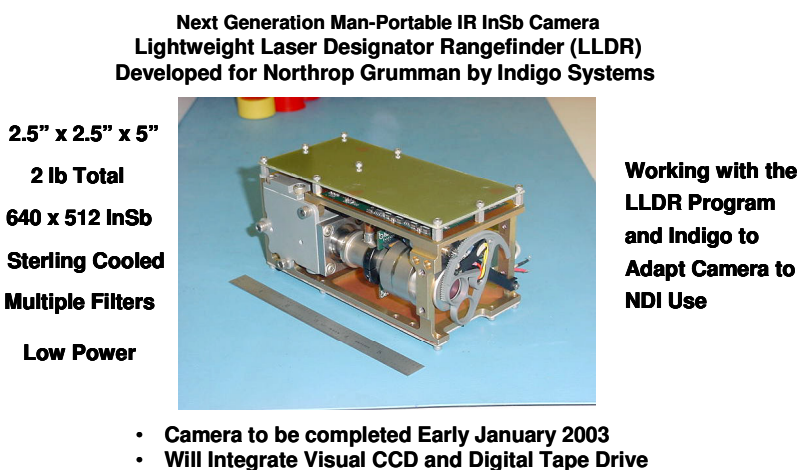


Figure 103 LLDR camera with potential for SERDP Program modification for transition phototype

The key to obtaining the smallest neaAt is to screen InSb focal planes prior to camera production. This gives the highest sensitivity to small contrast. Also low noise electronics is important for resolution.

Patent Pending Status

Northrop Grumman Corporation has filed for a Patent on the Detection System and Process to detect corrosion, cracks, and other detects under coatings. The patent was filed to protect Northrop Grumman Corporation interests and well as the interests of the government in accordance with the SERDP contract. The patent application was filed during August of 2002. The new patent policy and regulations have changed. The actual application will be posted on the public US patent website, prior to and in advance of the actual release of the patent. As of Dec 2002, the patent application has yet to be printed and posted by the government.

Business Trips, Presentations and Papers

Indigo Transition Trip -January 2002 – A trip was made to Indigo during the first quarter of the year by Don DiMarzio and John Weir. The purpose of the trip was to brief Indigo Management and the technical staff on the SERDP 1137 Project, as well as review potential desired improvements to the camera system that could enhance the project and the transition potential into field operations. Technical areas of discussion included focal plane manufacturing, temperature sensitivity, wavelength-windows, miniaturization of the camera body, and portability. It was noted by Indigo personnel that they were currently working on another camera system that was smaller and battery operated to make it portable in the field. This system has been previously described and designated as the LLDR camera system.

Navy Corrosion Work Shop- August 2002 – Approximately 175 DOD and Military Contractor personnel were briefed on the operation and advantages of the IR Camera system for the Detection of Corrosion Under Coatings. Since the audience was an audience dedicated to corrosion abatement and maintenance of field aircraft and systems, this Work Shop was an ideal form for explaining the advantages of such as system as every one was focused on corrosion issues. The Navy Personnel from the NADEP in Jacksonville, FL were particularly interested in the IR camera system as a means to test for corrosion and other structural defects under coatings.

IPR and Demonstration of IR Camera System October 2002 – The IPR was conducted during the last quarter of 2002. Progress was reported on all the advanced techniques and imaging methods investigated during the year as described in this report. Additionally, a Lab Bench demonstration of the camera system was conducted. This demonstration was presented to show how easy it is to detect corrosion and other structural defects under standard military and commercial aircraft coatings.

ESTCP/SERDP Partners in Environmental Technology - December 2002 – Both a poster and a technical talk were presented at this conference. Additionally a Lab Bench Demonstration of the IR Camera system was made at the Poster Session after the technical talk. Interest in this emerging technology was apparent by the many questions fielded after the talk and from the number of interested people who stopped by to see the poster and actual real time demonstration of the Non-Destructive testing process of the detection of corrosion under coatings. Various parts and specimens were shown during this demonstration.

NADEP, Jacksonville, FL-Trip –November 2002 – At the request of Jack Benfer, a trip was made to the Naval Air Station in Jacksonville, FL. Note: Jack is responsible for Materials Protection and Corrosion Science Technologies used at the NADEP. Jack expressed interest in the potential transitioning of the technology developed by Northrop Grumman Corporation under the SERDP contract during the Navy Corrosion Work Shop, which he attended. We visited Jacksonville and demonstrated the system to Jack and others out on the aircraft hanger floor. The demonstration took place on detail parts and in the fuel tank of a P3 Orion aircraft that was in for repair and overhaul. Little corrosion was found with just a few minor suspect areas. Actually, this was good news and maybe what was to be expected as the aircraft was having repairs and corrosion addressed at that time.

Some difficulty with getting into the fuel tank and having the correct illumination was apparent. Natural illumination had to be used in the fuel tank area as the IR source as previously described could not be easily adapted to extend into the inside of the fuel tank. This would indicate that a smaller IR source would be of interest for these types of applications.

The IR camera system was demonstrated in the lab as well. Test specimens as selected by Jack were investigated. These specimens included non-chromated primers and advanced system primers and topcoats. Filiform corrosion test specimens were observed for the first time under IR illumination. The filament structure was quite detailed and the extend of how the corrosion progressed under the coatings was clearly observed. A discrepant web that had been removed from a P3 was also observed under the IR reflectance.

Camcorder tapes were made of both the IR signal coming from the IR camera and visible light movies were made as well. The camcorder view screen was used to observe the IR signal in real time during the recording of said signal. The tapes are currently being analyzed and indexed so that IR and visible light snap shots can be viewed side by side. It is anticipated that these movies will be available during the first quarter of 2003.

Northrop Grumman Corporation Saint Augustine, FL-Trip- November 2002 – A trip was made to Saint Augustine, FL to Brief the IR Technical Presentation to Quality and Engineering personnel, as well as conduct a field demonstration on actual field aircraft. A number of actual aircraft were surveyed for corrosion during this trip. These aircraft included an E2C, an EA-6B, and F5 plus an EA-6B center section as well as an F5 center section. In general low IR MIL-PRF-23377TYII coatings were hard to penetrate while MiL-PRF-23377 TYI and MIL-PRF-85285TYI urethane top coats could be penetrated quite well as documented in the paint thickness study as previously described. In particular a few fasteners on the wing of an E2C had to have their identification checked to assure the correct installation was made. The camera was hand held and the fasteners were hard to focus on but it is anticipated that the reduction of data by freezing a frame that was focused in the movie will give enough time to read the fastener heads and determine the type and manufacture of fasteners used.

An F5 was surveyed for corrosion, however no corrosion was found. This was some what expected as the ship was reported to have been stored in the dessert and had not obviously been though a corrosive environment. On the other hand an EA-6B wing center section was surveyed and a significant amount of corrosion could be found on fittings and wing skin surfaces. Also, shot-peening marks could be clearly observed under the primed and top coated wing skin. Some corrosion was also observed in the shot peened area, as well. The survey was recorded in both the IR and visible light spectrums. It is anticipated that the data will be indexed between the visible and the IR as both recordings were taken in real time. During this survey and the other surveys conducted the need to index the movies has become obvious. It is an anticipated that a split screen will help solve this problem. Another obvious and possibly lower cost approach would be to index the aircraft with 3M Post-it® type markers. These markers could be placed in a predetermined grid, which is mapped on to the part of aircraft to

determine locations of the observed corrosion. This would be similar to marking a trail in the woods with trail blazes and these markers could be numbered and tell the individual how and where to conduct the survey.

SERDP Field Demonstrations and Meetings

Redstone Arsenal, Huntsville, AL, July 8-10, 2003 – Met with Steve Cargill (CTC) and Joe Pecina (CTC) and representatives of the U.S. Army NDI team, Walt Matulewicz (focal point). In addition to examining lab samples of CARD coatings, we used the IR camera system to examine helicopter parts. A talk on the detection of corrosion under paint was given to corrosion NDI personnel.

Boeing, Oklahoma City, OK, August 5-7, 2003 – Technical Interchange Meeting with the Fuel Tank Corrosion group. This includes representatives of Tinker AFB, industry, and academia. Fuel Tank Topcoat Peeling is a current problem under investigation. Presented findings from B-52 fuel tank liner parts that were examined using the IR camera system of imaging through the paint. Many attendees were interested in further field demos. Follow-on lab work indicated that corrosion could be detected under the B-52 fuel tank coating.

Summary of Surveyed Aircraft and Lessons Learned

To date the following aircraft or portions of the following Navy and Air Force aircraft have been surveyed:

- E-2C
- EA-6B
- E-8 Joint Stars (707) Wing
- P-3 Orion
- F-5 Aircraft
- F-5 Wing
- WWII Grumman Bear including Landing Gear.

These surveys were recorded in real time by the use of an IR Sony camcorder. Both the IR signals showing corrosion and other structural defects under the coatings and the normal illumination created by visible light was used to index the corrosion on the particular component or aircraft structure.

Work has started with the Merlin IR camera manufacturer to define the needs or develop a wish list for the transition the technology into the depot field operations. It was also determined during discussions with Indigo that a smaller compact battery operated IR camera was being developed for another customer and application.

However, it was determined during the discussion that this camera could possibly be modified and used to detect corrosion under coatings. Leveraging of this newer technology could possibly lower overall production costs for the next generation camera.

These surveys have been of value to establish the needed equipment modifications or improvements to enhance the process of detecting corrosion and structural defects under coatings. It can be noted by the author that the experience gained by each of these surveys has enhanced the knowledge with respect to obtaining more data in the real world with the IR camera system. In general, it was noted that particular areas seemed to have more corrosion and were more problematic than other areas. It is obvious that working with the aircraft depots and rework facilities will be most beneficial as many of the high corrosion areas should already be known and that a methodical plan for conducting a corrosion survey will save time with not having to survey areas that in general have little or no corrosion.

Transition of Technology Activities for IR Camera

Technology transition work in the last quarter has included meeting with Indigo representatives regarding a new improved IR camera known as the Phoenix™. A preliminary demonstration of the Phoenix™ camera indicated the camera was more sensitive to detecting corrosion plus could detect corrosion through thicker paint coatings. A quotation was requested and a ROM for a system including lens and real time images electronics would cost approximately \$130K to \$170K, depending on selected configuration and options available.

INVESTIGATION OF AN IR DETECTION SYSTEM UTILIZING BLACK BODY SELF-ILLUMINATION TO OBSERVE STRUCTURES AND DEFECTS UNDER COATINGS

Description of Process – It is understood that black body radiation is emitted from all matter above 0 degrees Kelvin. In particular, bodies at or near room temperature emit a significant amount of IR black body thermal radiation. It is known that many organic coating polymers exhibit significant IR transmission in certain wavelength bands. An object's own black body radiation can penetrate an organic coating covering the body and potentially reveal the object's surface condition under the coating. The radiation that transfers or transmits through the coating can be observed in a detector such as an IR camera. This IR camera will then produce images from the self-illuminated article that are capable of detecting corrosion, cracks, pits, and structures under the coating. The body or article to be inspected becomes illuminated by its own IR radiation which is a function of temperature of the body. The distinct advantage of the Black Body/Self Illumination Method is that the part is illuminated due to its own thermal emittance, and an independent IR illumination source is not needed. In some cases the objects emittance at room or ambient temperature is sufficient to allow imaging through the coating, while in other situations moderate heating of the article or part to be inspected is required. Object heating can be achieved naturally (sunlight), by a heat gun, thermal blankets, an IR heat lamp or by other means.

Another advantage of the Black Body Method is that the IR radiation only has to make one pass through the coating. This is compared to the IR reflectance technique, where IR radiation from an external illuminator must first penetrate the coating, reflect off the substrate (object) and pass through the coating again. An additional advantage of the Black Body Method is the reduction or elimination of the coating surface reflection. In the Reflectance Method, IR energy is reflected off the coating surface partially obscuring the image from the substrate underneath. **Special note:** This process/method is Patent Pending. Figures (a) through (x) are images produced by the Black Body Method (unless otherwise noted):

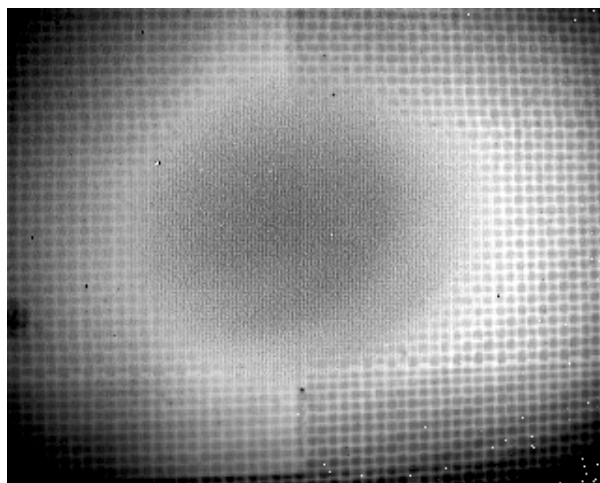


Figure 104a Graphite painted panel at 89F, RT-calibration

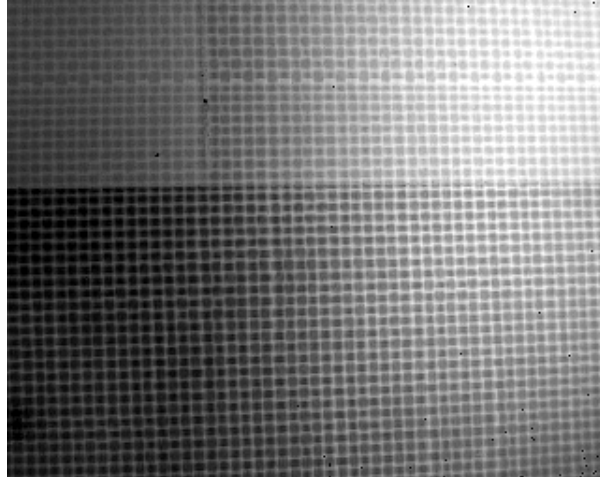


Figure 104b Graphite painted panel at 90F, 84F hot-calibration

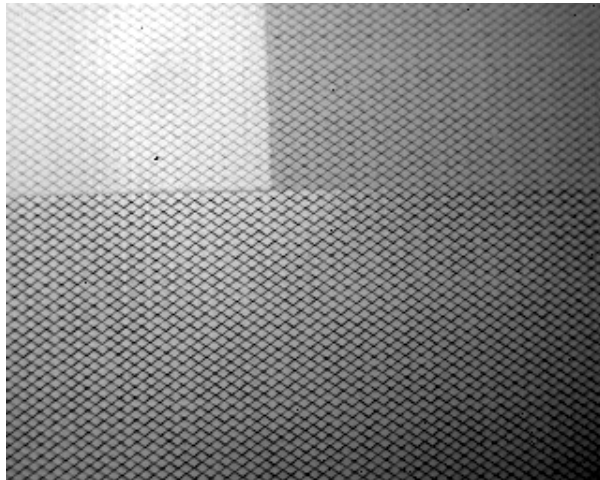


Figure 104c Graphite with Cu fiber painted panel at 90F, 84F hot-calibration

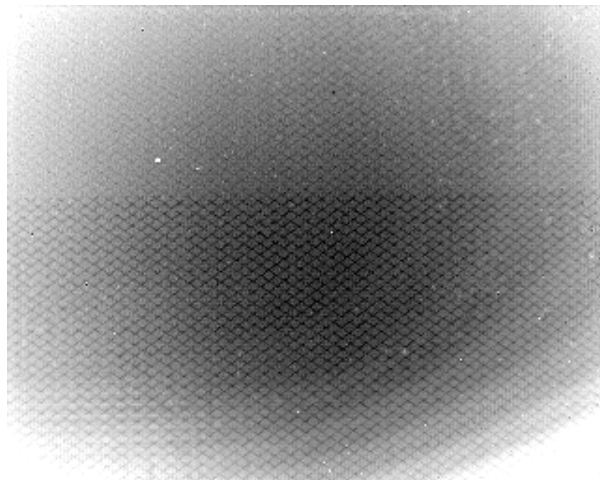


Figure 104d Graphite with Cu fiber painted panel at 74F, 84F hot-calibration

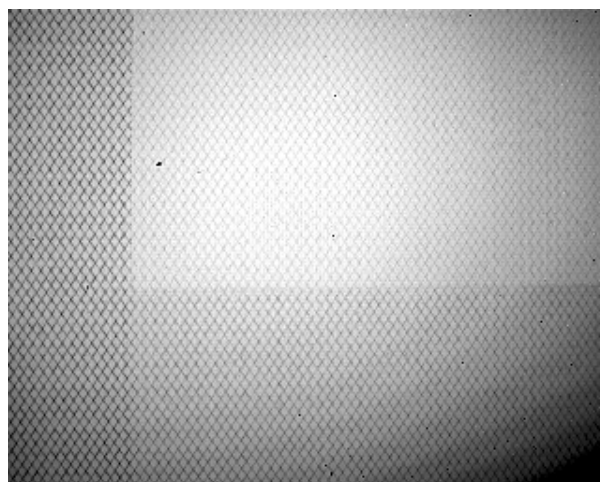


Figure 104e Graphite with Cu weave, painted panel at 91F, RT-calibration

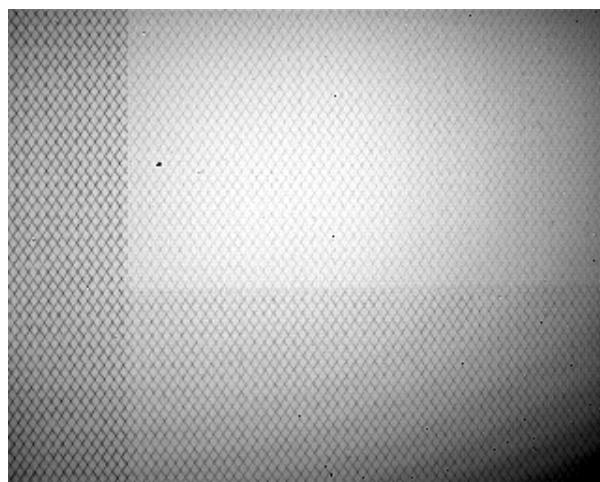


Figure 104f Graphite with Cu weave, painted panel at 87F, RT-calibration



Figure 104g Graphite with Cu weave, painted panel at 82F, RT-calibration

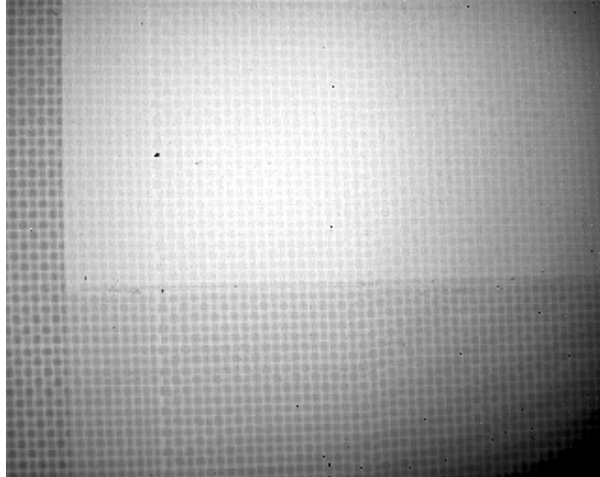


Figure 104h Graphite, painted panel at 90F, RT-calibration

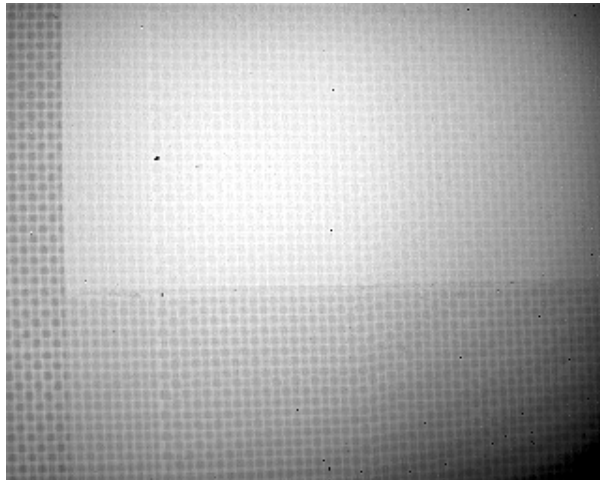


Figure 104i Graphite, painted panel at 86F, RT-calibration

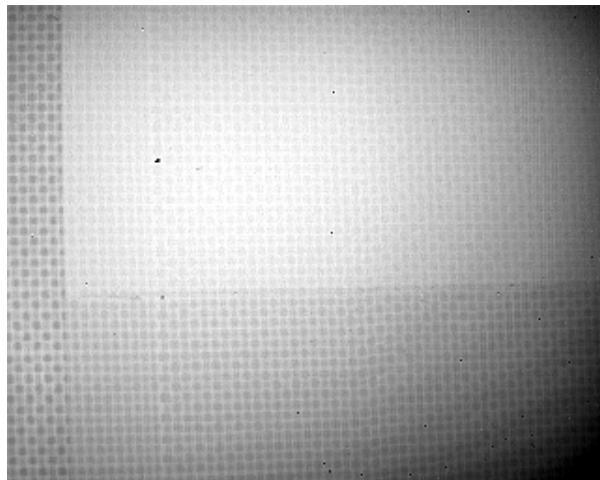


Figure 104j Graphite, painted panel at 82F, RT-calibration

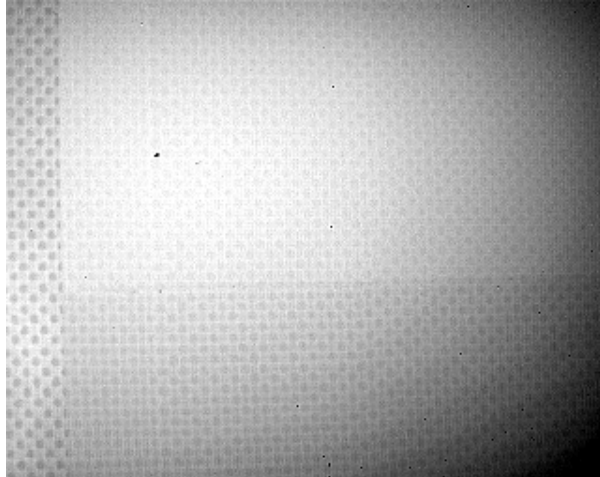


Figure 104k Graphite, painted panel at 78F, RT-calibration



Figure 104l Graphite, painted and primed panel: Visible image



Figure 104m Graphite with Cu weave, painted and primed panel: Visible image



Figure 104n Aluminum C2 : Visible image

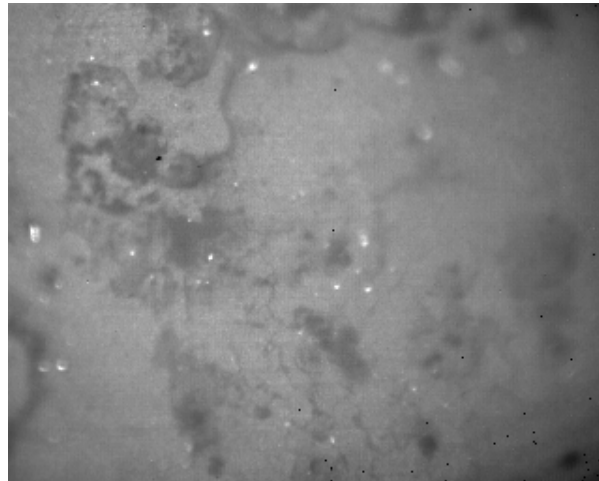


Figure 104o Aluminum C2 1x mag. at 77F, IR Reflectance image

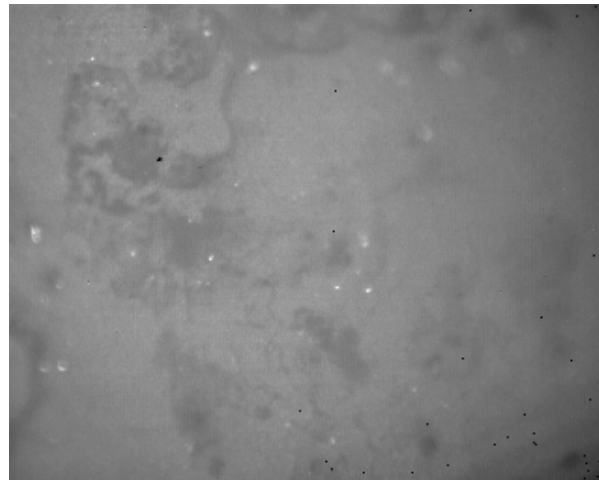


Figure 104p Aluminum C2 1x mag. at 75F, IR Reflectance image

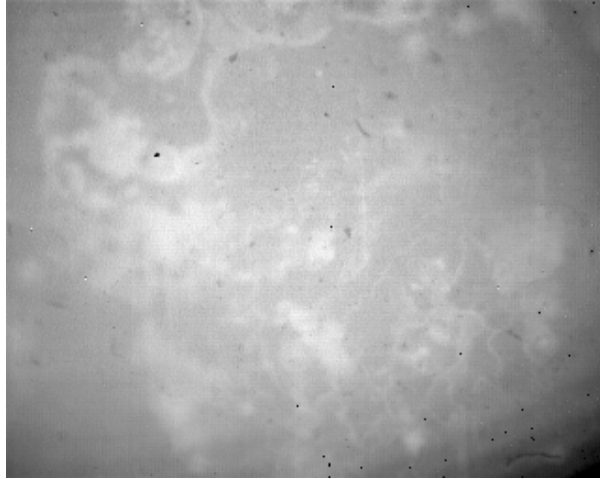


Figure 104q Aluminum C2 1x mag. At 84F, RT-calibration



Figure 104r Aluminum C2 1x mag. At 78F, RT-calibration



Figure 104s Aluminum C2 1x mag. At 72F, RT-calibration

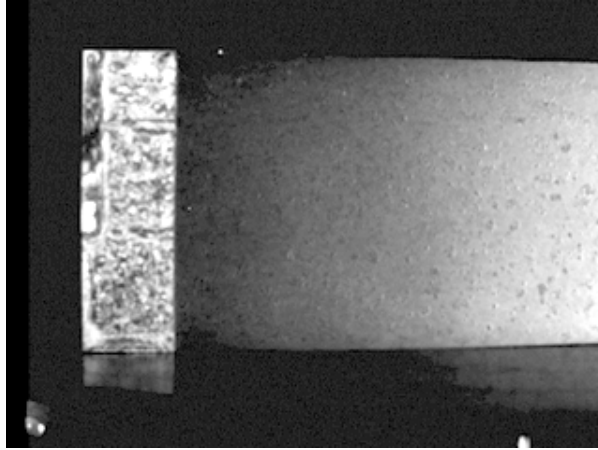


Figure 104t Aluminum C9 (low IR primer) IR Reflectance Image

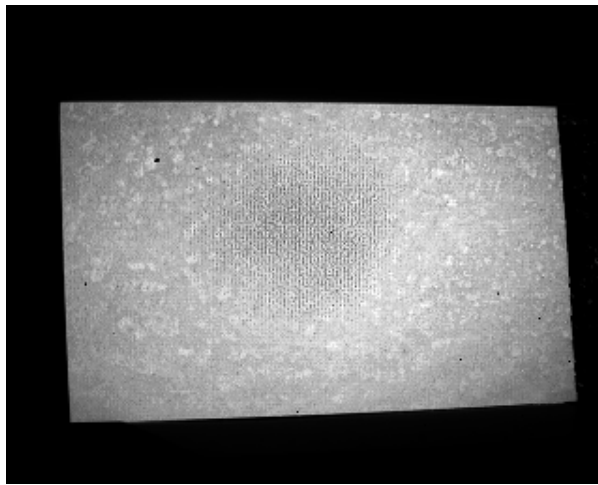


Figure 104u Aluminum C9 (low IR primer) at 96F, 78F hot-calibration

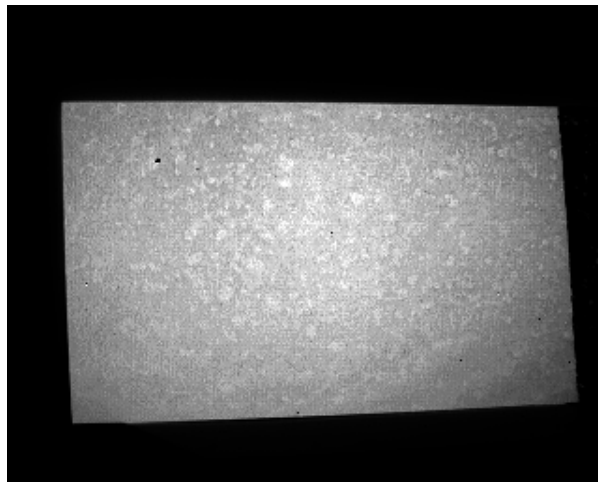


Figure 104v Aluminum C9 (low IR primer) at 86F, 78F hot-calibration

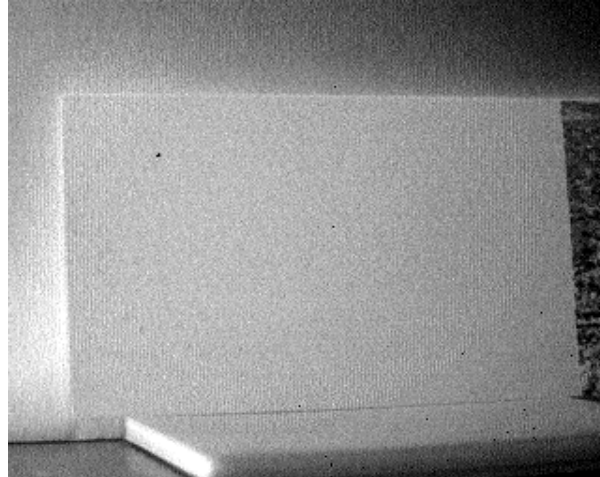


Figure 104w Aluminum C9 (low IR primer) at 79F, 78F hot-calibration



Figure 104x Aluminum C9 (low IR primer), Visible Image

ELECTROCHEMICAL IMPEDANCE SPECTROSCOPY

Electrochemical techniques for the detection and quantification of corrosion under paint films historically have involved AC impedance and DC measurements, requiring the immersion of the samples in an electrolyte. This program is studying an electrochemical measurement technique that requires no electrolyte (in liquid form), and therefore no direct contact with the sample.

The objective of this research is to determine the ability of EIS to make localized measurements that detect corrosion under coatings and to develop simplified techniques to perform field measurements. The apparatus used for the measurements being reported consisted of components designed to form an electrochemical cell using a conducting gas, which will potentially be used for corrosion measurements at aircraft surfaces.

SCANNING VOLTA POTENTIAL MEASUREMENTS

Recently the scanning Kelvin probe has been employed, highly successfully, as a non-contacting technique for the measurement of Volta potentials in studies of corrosion under coatings. The scanning Kelvin probe consists of a vibrating microelectrode close to a surface to produce a variable capacitance that induces an AC signal in the circuit directly connecting the probe and surface. Intrinsically, the method has a high impedance and necessitates both scanning close to the surface being studied, and care in shielding to reduce electrical noise. In contrast to the well-known Kelvin probe method, the direct (DC) measurements of the Volta or contact potential difference have been made in ionized air by Case and Parsons and Smith. In these studies, a radioactive α emitting source was used to ionize the air between the reference metal/gas electrode and a gas/solution interface or a second gas/metal electrode.

X-ray ionization of a gas is initiated by a primary x-ray absorption photoelectric process and is followed by ionization caused by ejected secondary electrons. Electron and fluorescent photon emission takes place in the gas around the site where the beam impinges on the metal and increases the ionization. Ionization by the electrons continues until they have lost their energy and attach to molecules. The process produces negative and positive charged gaseous molecules that combine and interact to form a range of products. Recombination of the ions and secondary electrons takes place rapidly as they diffuse from the path of the x-ray beam. The high concentration of charged species can be detected over distances of the order of a few 0.1 mm and depend on pressure and gas composition.

The present task is using the DC ionized-air technique to measure the Volta potential to with the view to locate corrosion under coatings. It is similar to a localized DC electrochemical measurement of the corrosion potential and hence may be able to locate corrosion sites. In order to obtain a conducting gas we have used high intensity synchrotron x-rays to produce a local ionized atmosphere adjacent to the metal surface under investigation. The technique has advantages over conventional Kelvin probe as it greatly simplifies the Volta

potential measurements. In particular, Volta measurements using ionized air are relatively insensitive to reference/sample distances. Thus, the need for complicated electronics to maintain a constant height above the surface is avoided. Additional advantages are relatively low impedance even with a small reference electrode, and the ability to carry out electrochemical (current versus voltage) polarization measurements of the metal/conducting-gas interface.

ELECTROCHEMICAL RESULTS

EIS

Samples with three surface conditions are being evaluated: defect free coatings, coatings with scribes, and these surfaces after exposure to corrosion conditions. Our goal is to detect and characterize the surfaces by using EIS technique. The EIS investigation in 1999 was conducted on the samples prepared as previously described in this section. EIS experiments were performed with the aim to simplify the measurements, to avoid immersion of the sample in liquid electrolyte and to shorten measuring time. Such technique was able to detect a big difference in impedance between the scribed and intact spots on the samples after different exposures to corrosive environment.

A special probe consisting of a reference and a counter electrode was designed for the impedance measurements. A copper disk was used as a counter electrode with an insulated embedded small silver disc in the middle, serving as a reference electrode. Filter paper placed between sample and a probe served as the electrolyte container. The copper disk acted as the second electrode in two electrode cell measurements. The working area of the surface whose impedance is measured is determined by the size of counter electrode and filter paper (3.14 cm²). A series of sponges were tried as alternatives to the filter paper but these were not as reliable as the filter paper and required recesses in the copper disk to hold the sponge.

Experiments were performed with non-aggressive borate solution pH 8.4, 0.1M Na₂SO₄ and with a more aggressive electrolyte, 0.1M NaCl. The measurements were made using a Solartron Electrochemical Interface Model 1287 in combination with Solartron Frequency Response Analyzer Model 1250. The amplitude of the modulating signal was 30 mV with the frequency in the region from 0.01 to 50 kHz Spectra are presented in the form of Bode plots and Nyquist plots for data at high frequencies. All results reported were obtained in the potentiostatic mode at the corrosion potential.

Scanning Volta Potentials Measurement

A multi-metal specimen was used to demonstrate the technique using x-rays. It consisted of the abraded edges of a series of metal sheets about 1 to 4 mm thick, pressed together in a holder. The metals were type 304 stainless steel, Al, Ni, Zr, Cu, Sn, and Fe. The specimen was abraded on SiC paper down to a 600 mesh. Care was taken to prevent cross contamination of adjacent metals during the final abrasion of the sheet cross sections.

A schematic of the measuring setup is shown in Figure 105. In this system, the beam is 45° to the sample. A stepper motor driven x-y-z stage with a minimum step size of 1 μm was used for positioning the sample. A reference electrode probe was positioned about 0.1 mm from the sample. Generally, the reference probes were

parylene coated, 0.25 mm diameter Pt-20% Ir alloy wires with exposed cross sections positioned 0.1 mm above the sample. Ag and Ni wire reference probes were also used with equal success.

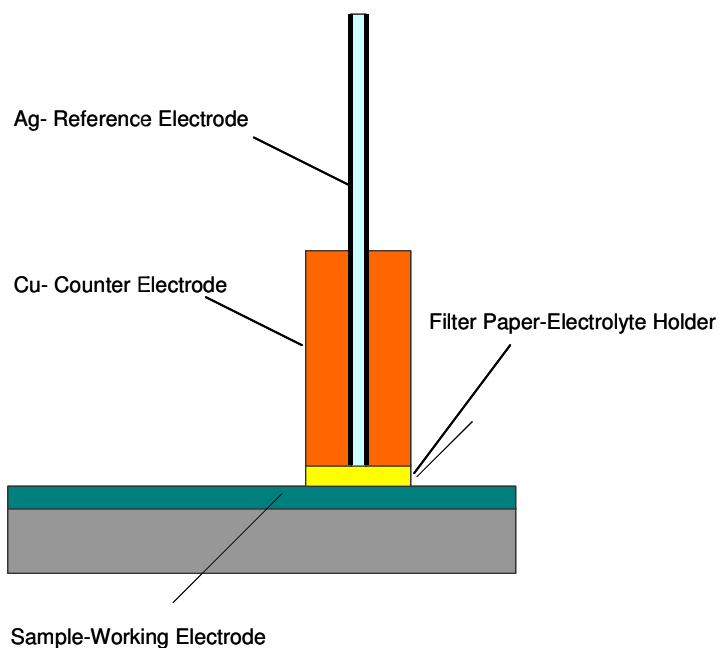


Figure 105 Schematic of electrochemical cell for localized impedance measurement

Volta potentials were also measured using an EG&G Scanning Kelvin Probe System 100E with a Ni scanning electrode having a tip diameter of 0.1 mm (see Figure 106). The measurements were made at Beamline X26A and X19 at the National Synchrotron Light Source. The X26A is designed for x-ray microprobe measurements using either monochromatic or polychromatic x-rays. The monochromatic beam has a photon flux of about 10^4 photons $s^{-1}\mu m^{-2}$ for an x-ray ring current of 200 mA. The beam was focused to a diameter of close to 25 μm . The diameter of the polychromatic beam was about 8 μm with a flux of about 10^8 photons $s^{-1}\mu m^{-2}$ having energies above 4 keV at a ring current of 200 mA. The measurements on X19 were at a fixed energy of usually 6090 eV and up to 1x2 mm in size although apertures collimating the beam have been used.

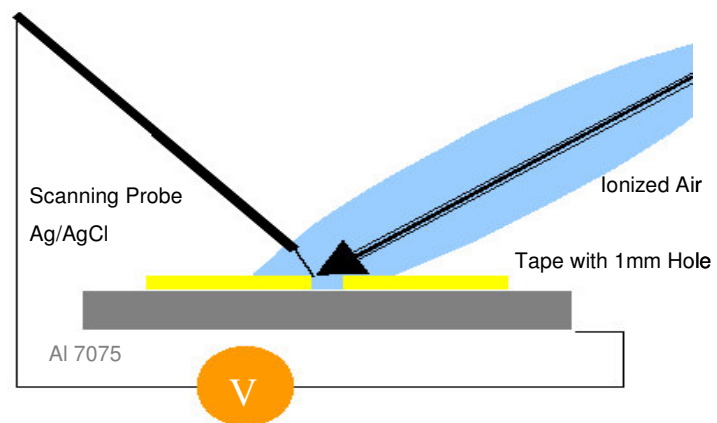


Figure 106 Schematic of the Volta potential measurements in ionized air

ELECTROCHEMICAL IMPEDANCE SPECTROMETRY

Figures 107 and 108 show the effect of exposure time on the impedance characteristics for the scribed and SAA prepared Al 2024 surface. The exposure was for 3, 7 and 14 days in a salt fog atmosphere. As a reference, spectra for unexposed samples are also shown. With the scribed surface, the differences in responses were clearly seen in the Bode plot of the phase angle, *theta*, versus the logarithm of the frequency. A distinct change in the phase angle occurs after the first 3 days at frequencies of 1 to 1000 Hz but little changes thereafter. Changes are also seen in Z , the impedance magnitude, which increased slightly at frequencies higher than 10 Hz. In contrast, for the unscribed surface in Figure , there was little change after 3 days but distinct changes occur after 7 and 14 days as evidenced by the phase angle and the increase in Z .

An alternative way of representing the results is the Nyquist plot giving the relation between the real (Z') and imaginary (Z'') components of the impedance. The curved portion of the plot after 14 days (Figure) at lower impedances is interpreted in terms of the passive film's properties. The linear section at the higher impedances is a function of the electrochemical kinetics and dissolution rate of the sample. The large curved, semicircular section for 14 days shows there is a marked increase in the resistance of the oxide film compared to the results for 7 days, where some resistance increase is apparent. No oxide resistance is apparent for the 3 day exposure.

In the low frequency region (at 0.01Hz), Z is characteristic of the corrosion resistance of the aluminum oxide barrier film. Mansfield and Kendig have shown that it is not possible to see the changes at these frequencies after short times of immersion. It should be pointed out that during the impedance measurements, areas were exposed to electrolyte for a relatively short period of time, approximately 2-3 hours. In addition, the borate solution is non-aggressive and would tend to help passivate the surface. The results show that the SAA surface on Al 2024 reacts in the salt fog and continually changes its electric characteristics. The changes suggest that in the salt fog some sealing of the SAA surface occurs, increasing the oxide resistance while decreasing capacitance. The exposed unprotected metal in the scribe changes rapidly at first also producing a small increase in impedance and suggestive an improved protective passive film. Figure compares impedances of the scribed and unscribed SAA Al2024 exposed for 14 days.

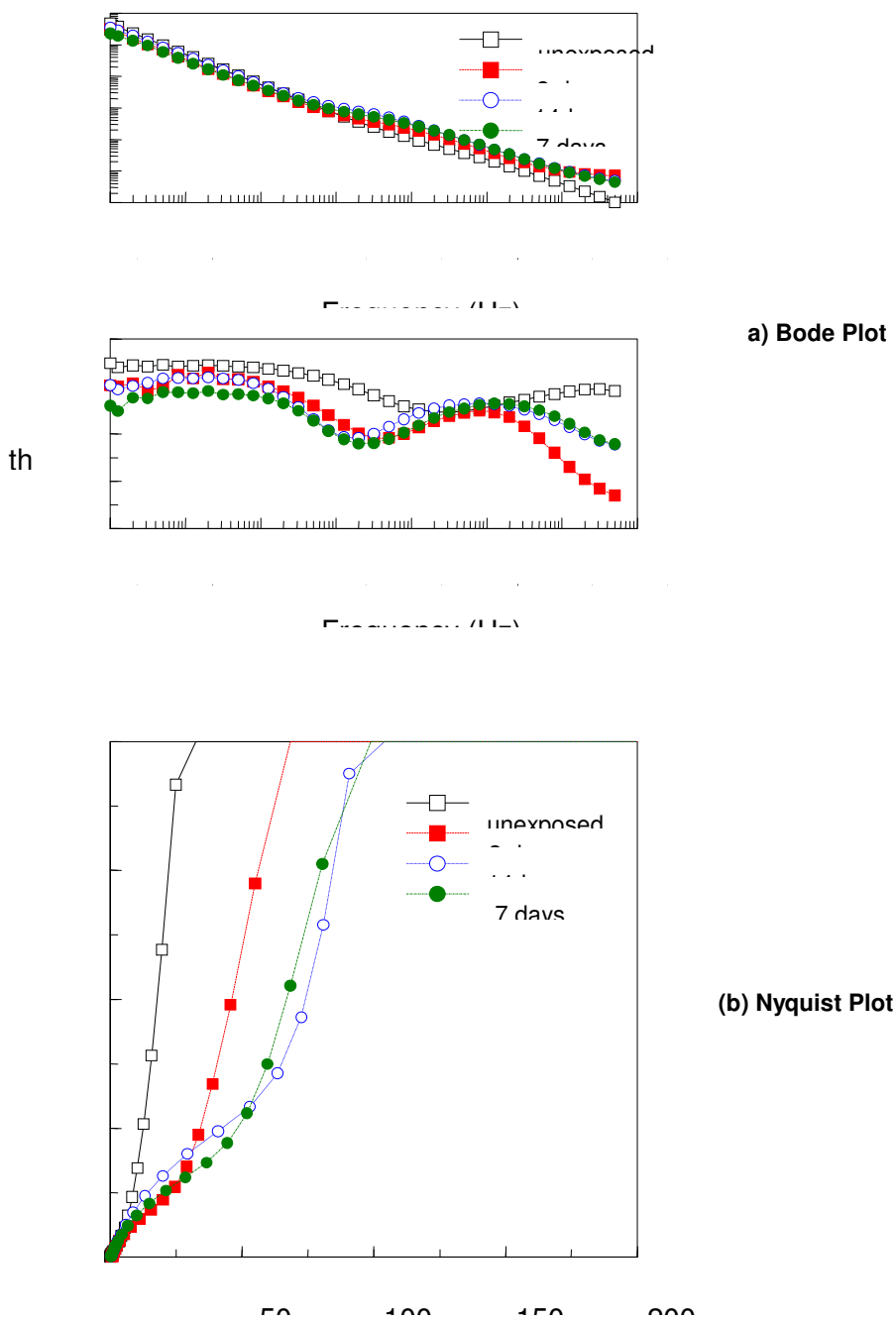
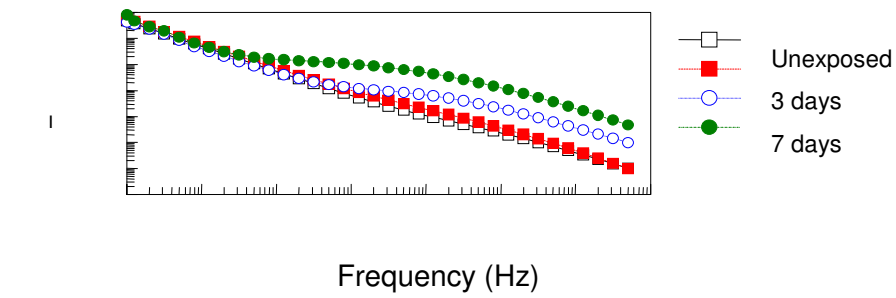
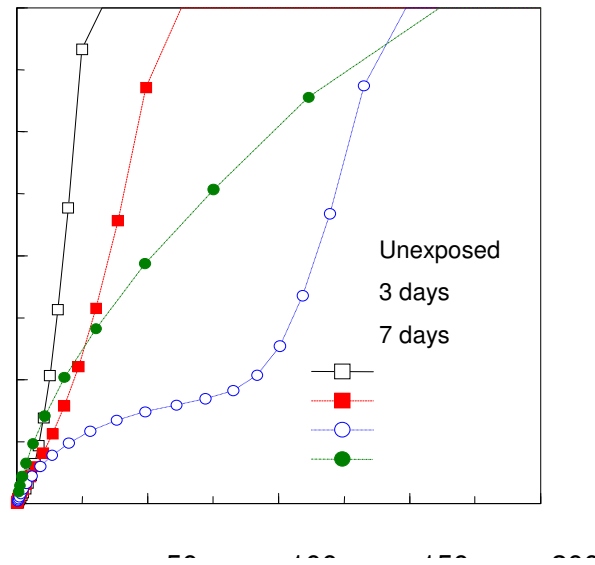
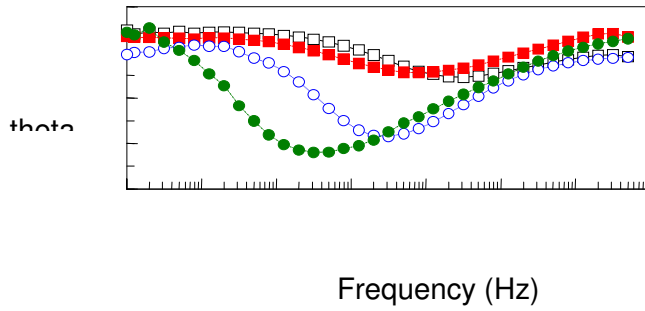


Figure 107 Impedance spectra on scribed SAA prepared Al 2024, exposed to salt fog for 0, 3, 7 and 14 days, measured in borate solution pH 8.4.



a) Bode Plot



(b) Nyquist Plot

Figure 108 Impedance spectra on SAA prepared Al2024, exposed to salt fog for 0, 3, 7 and 14 days, measured in borate solution pH 8.4.

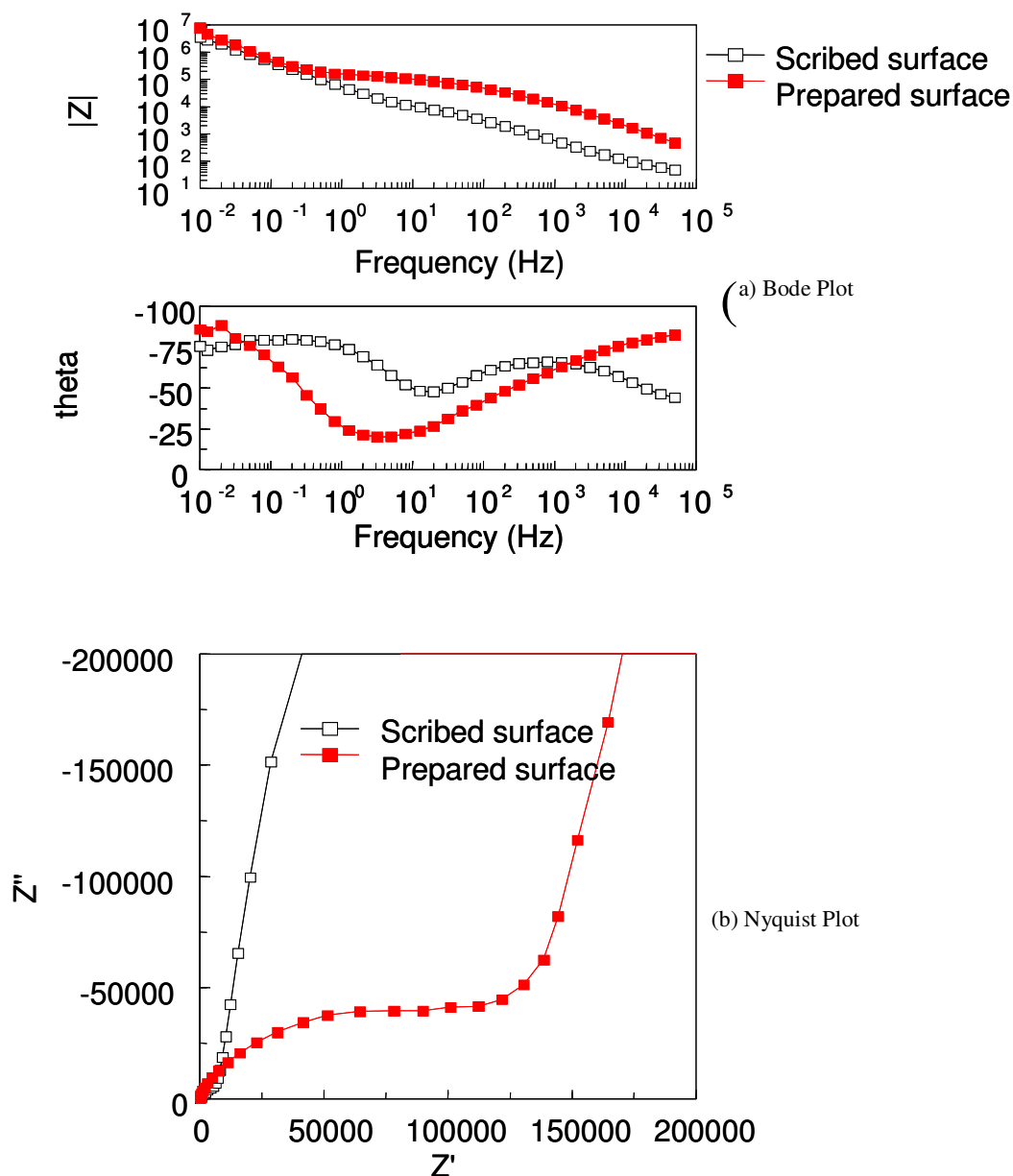


Figure 109 Impedance spectra for scribed and prepared surface on SAA prepared Al2024, exposed to salt fog for 14 days, measured in borate solution pH 8.4

The impedance in different electrolytes are shown in Figures 110 and 111 for the Al 2024B SAA surface after 7 days salt fog for scribed and unscribed surfaces respectively. Somewhat similar differences in the response were observed. The highest impedance was for the sulfate and lowest for the borate solutions. This behavior was counterintuitive because the lowest impedance would be expected for the most corrosive, chloride electrolyte.

The differences in the impedances with scribed and unscribed surfaces, shown in Figure 109, were again seen with the SAA on Al 2024C. Figure 112 presents impedance data for Al2024C, after exposure for 14 days in salt fog. The impedance measurements were made in 0.1M NaCl. The differences between the scribed and unscribed surfaces are again most obvious in the phase angle plots. The results, as before, indicate a sealing of the SAA during the exposure to salt fog.

A similar conclusion was reached for clad sample in 0.1M Na₂SO₄. Figure 113 shows the impedance at different times of exposure to salt fog. Again, the impedances increased with salt fog exposure, as did the results in Figure 108. There was a difference between that of SAA Al 2024 and the clad as continued exposure after 7 days did not lead to any further increases in impedance of the clad. However, the scribed clad (Figure 114) showed a different behavior following salt fog exposure. In contrast to the all the other results after salt fog exposure, its impedance decreased. The reasons for the decrease are not clear and need further investigation. The results, as seen in the Nyquist and impedance magnitude plots in Figure 114, indicate a decrease in the resistance of the passive oxide. This is expected since pure aluminum (representative of the clad) is less susceptible to corrosion in aqueous solutions than Al 2024. This is because the potential decreases on exposure, which also allows the passive film to decrease with time. However, the unscribed clad should also have shown similar behavior but did not. Aluminum alloys containing copper show potential increases with time. This leads to increase in passive film thickness. Unfortunately, when the potential increases still further, the pitting potential is reached and pitting corrosion takes place. This condition does not appear to have been reached after 14 days of salt fog exposure. Measurements after longer periods of salt fog exposure are planned to determine when the pitting is apparent on SAA and CCC surfaces.

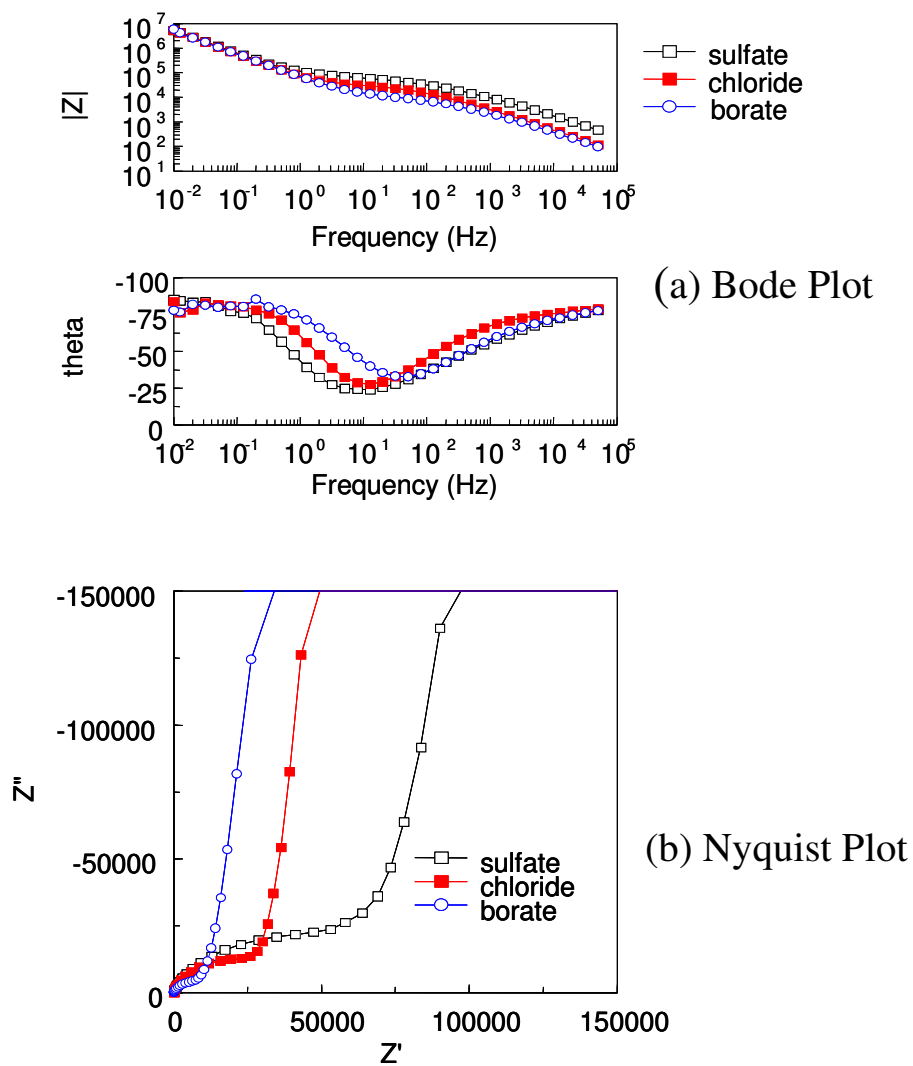
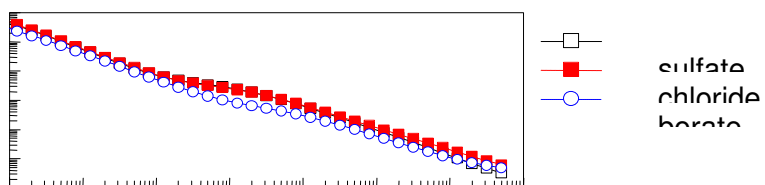
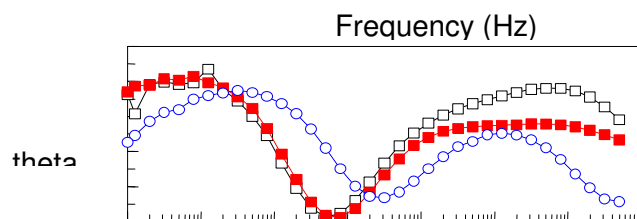


Figure 110 Impedance spectra in borate solution pH 8.4, 0.1M Na_2SO_4 and 0.1M NaCl on SAA prepared Al_2O_3 , exposed to salt fog for 7 days

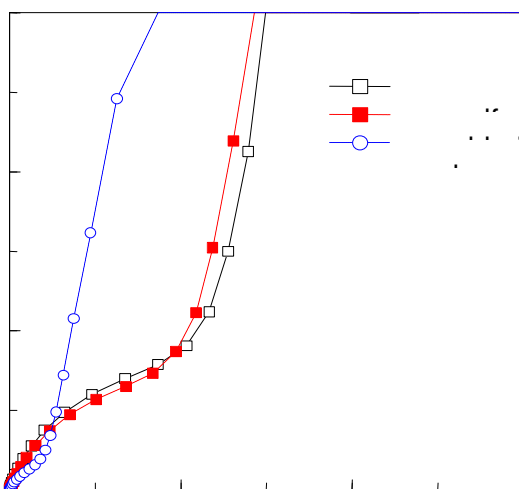
17



a) Bode Plot

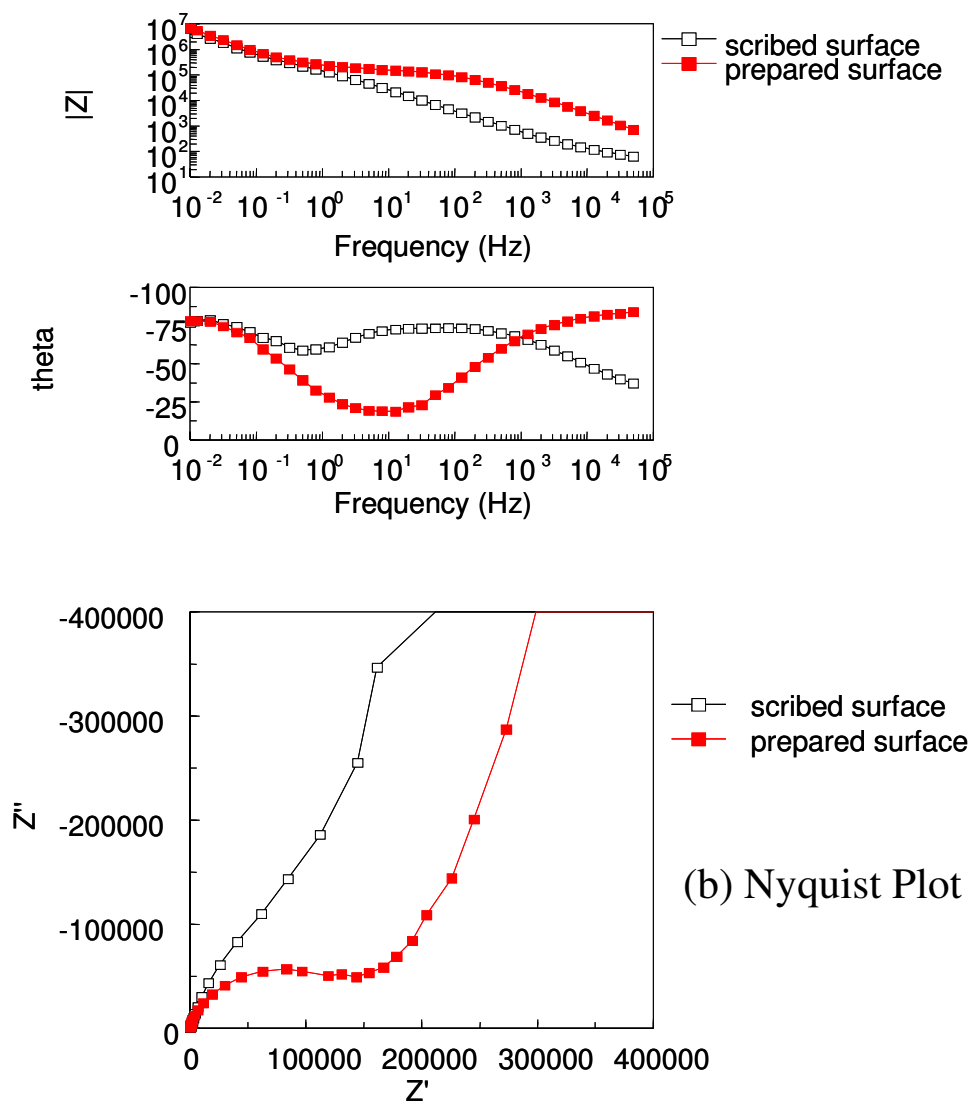


Frequency (Hz)



(b) Nyquist Plot

Figure 111 Impedance spectra in borate solution pH 8.4, 0.1M Na₂SO₄ and 0.1M NaCl on scribed SAA prepared Al2024, exposed to salt fog for 7 days.



(b) Nyquist Plot

Figure 112 Impedance spectra for scribed and prepared surface on scribed SAA prepared Al2024, exposed to salt fog for 14 days, measured in 0.1M NaCl

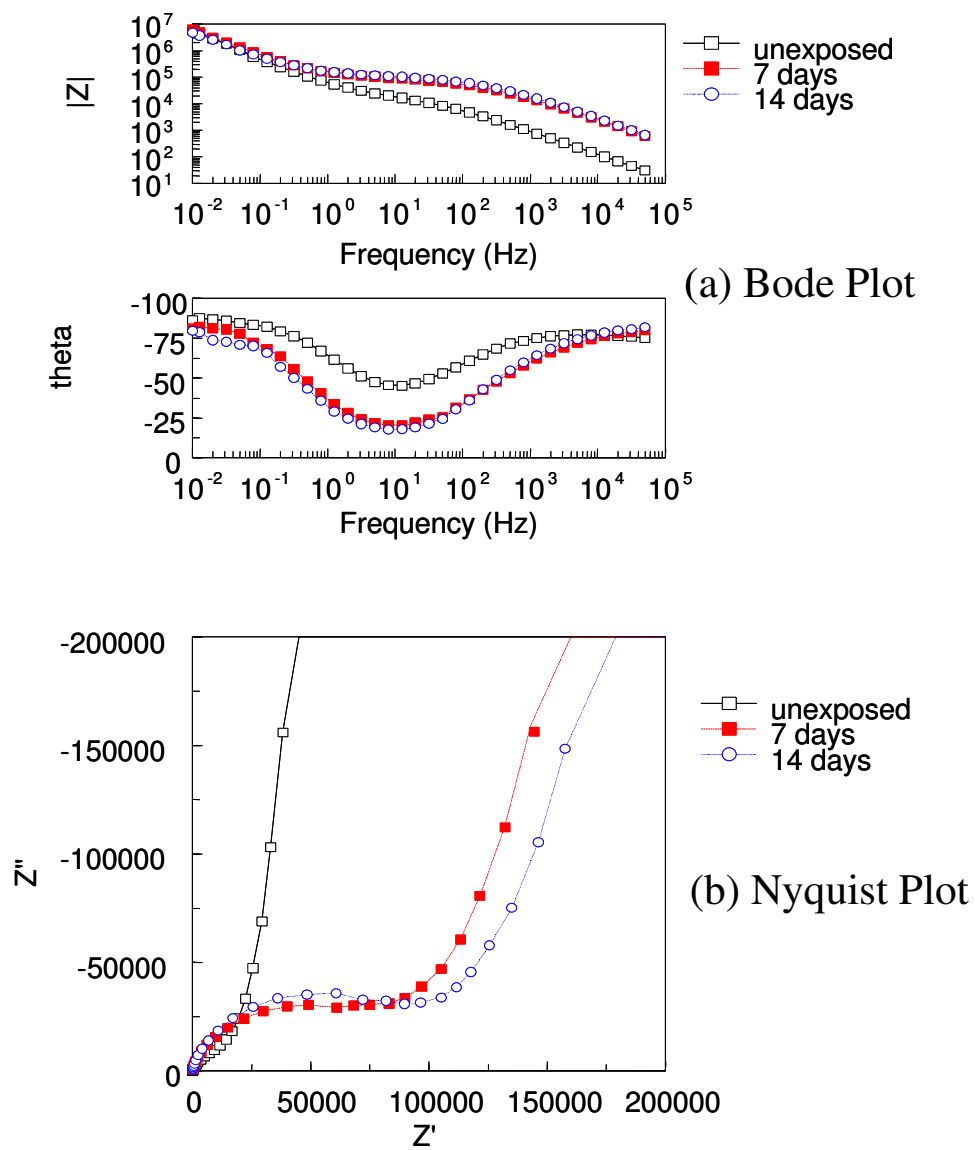


Figure 113 Impedance spectra on SAA prepared Al₂₀₂₄, exposed to salt fog for 0, 7 and 14 days, measured in 0.1M Na₂SO₄.

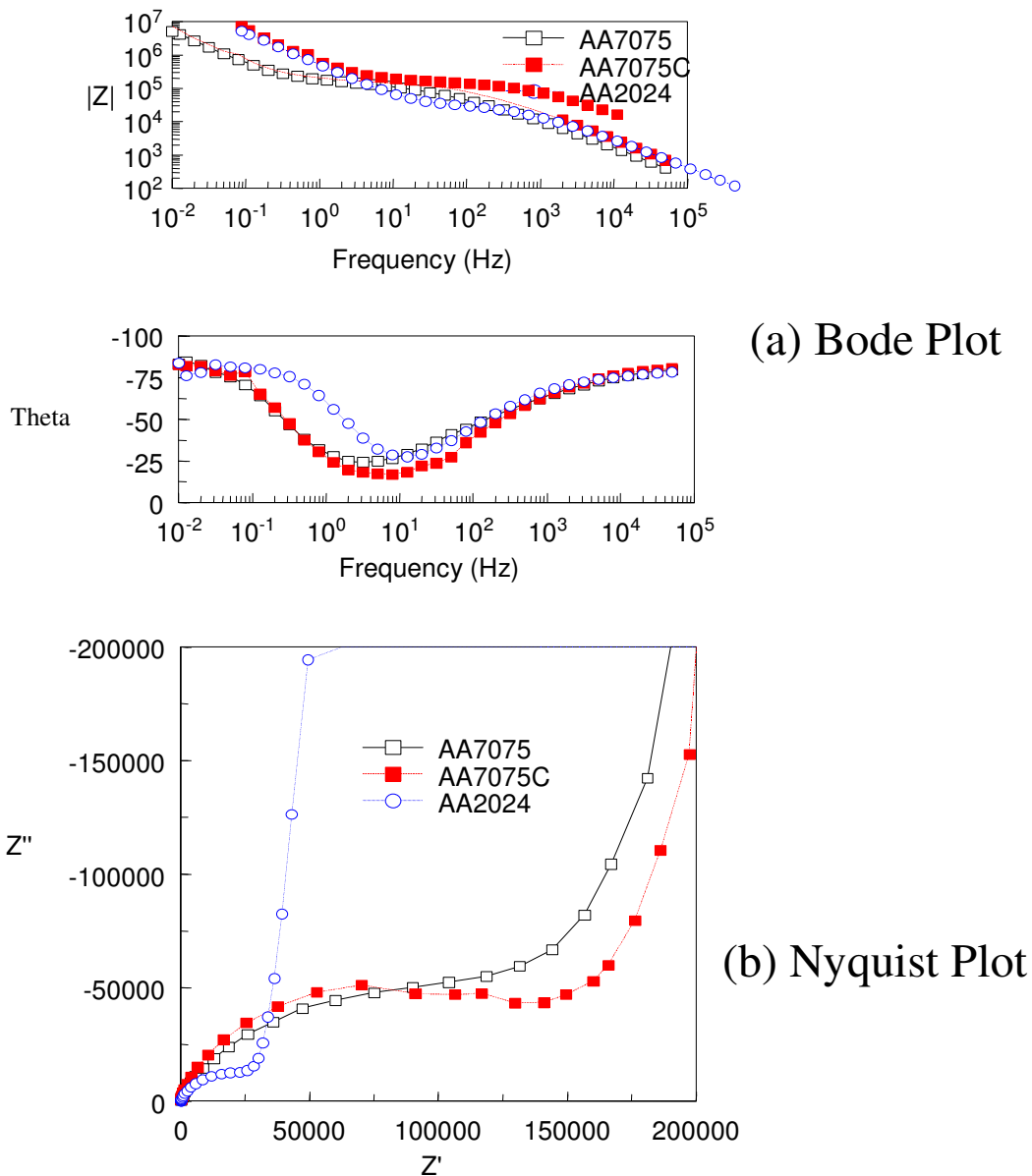


Figure 114 Impedance spectra on scribed SAA prepared Al2024C, exposed to salt fog for 0, 7 and 14 days, measured in 0.1M Na₂SO₄

The present study will covers a range of variables and a series of comparisons are required to establish a baseline for their effects on the impedance response. For example, the effect of different alloys and the effect of

surface treatments are being established and are reported here. Figure 115 shows a comparison of the impedance response of three alloys, Al 7075, the Al 7075C, and Al 2024. They had had a SAA treatment, and had been exposed 7 days to salt fog. Measurements were made in 0.1M NaCl on the prepared surface of these alloys. They show a small difference in the spectra for Al 7075 and its cladding different from that for Al 2024. The Al 2024 showed the lowest resistance above 0.5 Hz and as seen from both the Bode and Nyquist plots indicating a lower resistance and possibly a lower corrosion resistance of its anodic oxide.

The effect of different surface treatments is shown Figure 116, where a comparison is made between DEOX, SAA and CCC treatments. Bode Plots for unexposed alloys in 0.1M Na₂SO₄ show higher impedance for Al 2024C with SAA surface treatment. The spectra for deoxidized alloy and the alloy with a CCC, are almost identical.

Impedance spectra in 0.1M Na₂SO₄ for the unexposed, bare and clad Al2024 with different surface treatment are presented in Figure 117. These spectra show that, regarding corrosion resistance, the alloys with surface anodized in sulfuric acid (SAA) have superior behavior compared to the alloys with the CCC. Overall, the sample SAA Al 2024C has the highest impedance.

The superior performance is found for SAA Al2024, which were exposed to salt fog for 14 days, compared to the same sample with CCC. Impedance spectra for these samples were obtained in a two-electrode cell and they are shown in Figure 118 in 0.1M Na₂SO₄. This data also show that it is possible to obtain a difference in impedance behavior between two different samples in a two-electrode cell.

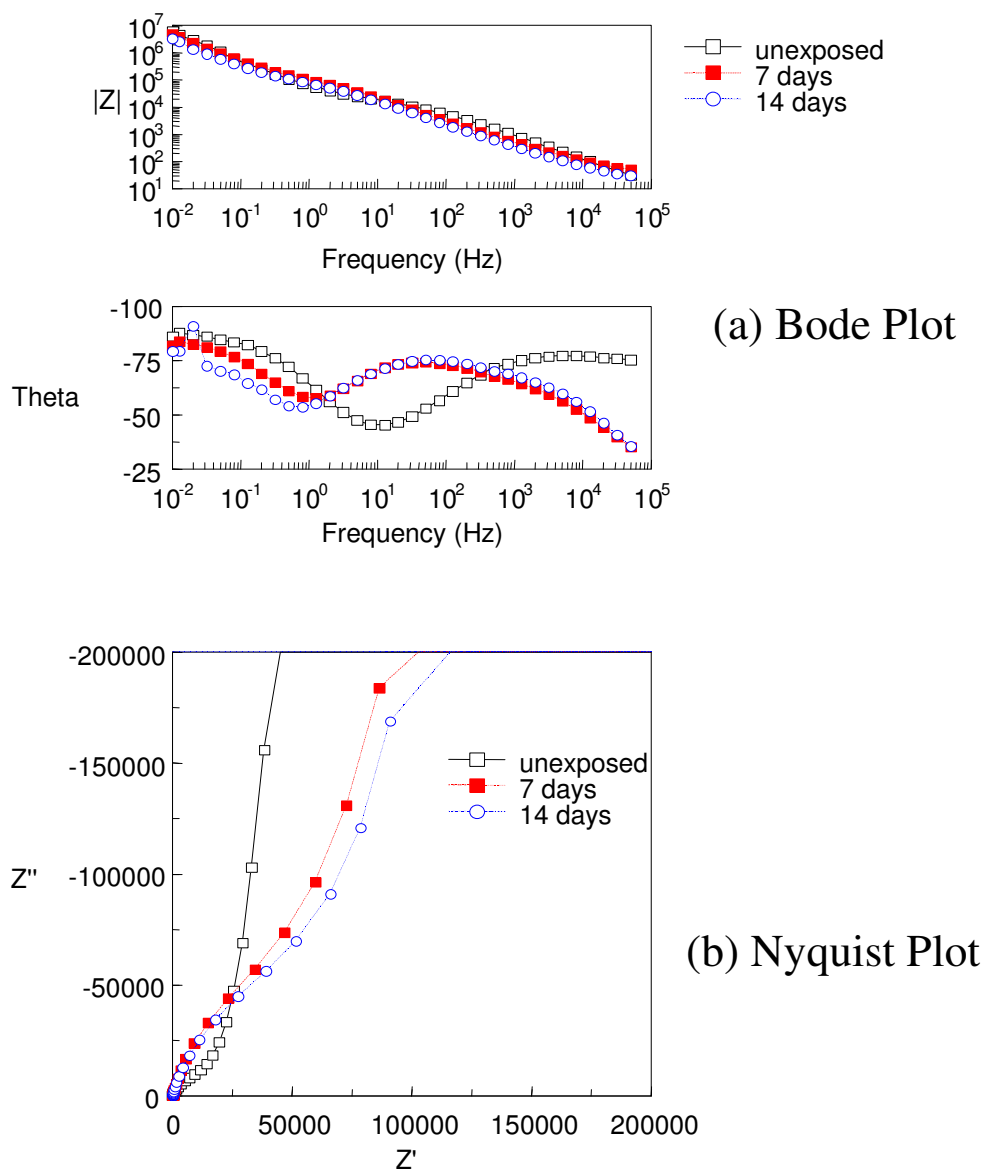
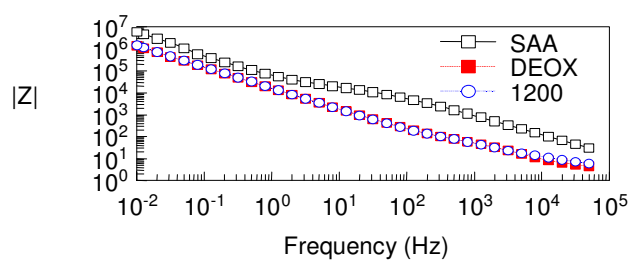
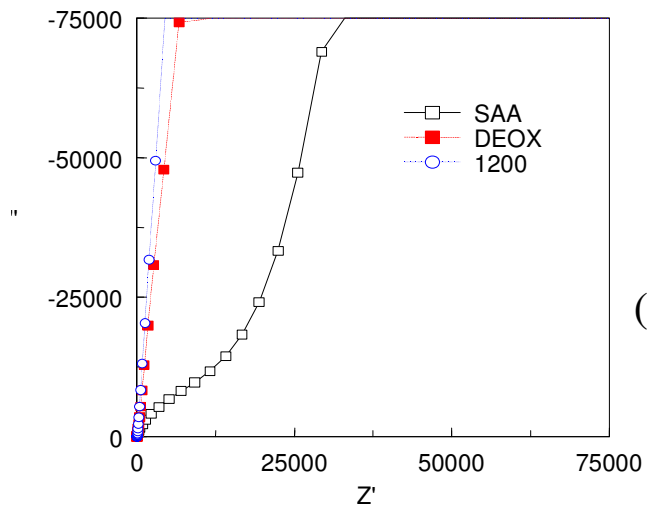
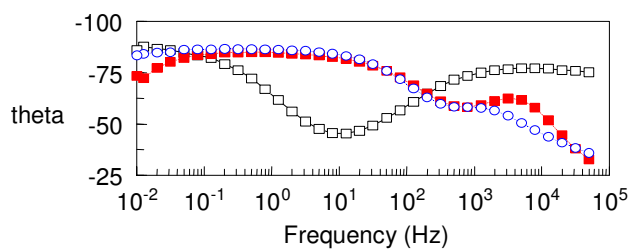


Figure 115 Impedance spectra for SAA prepared Al7075, Al 7075C and Al 2024, exposed to salt fog for 7 days, measured in 0.1M NaCl.



(a) Bode Plot



(b) Nyquist Plot

Figure 116 Impedance spectra unexposed Al2024C with surface treatment SAA, DEOX and CCC, measured in 0.1M Na₂SO₄.

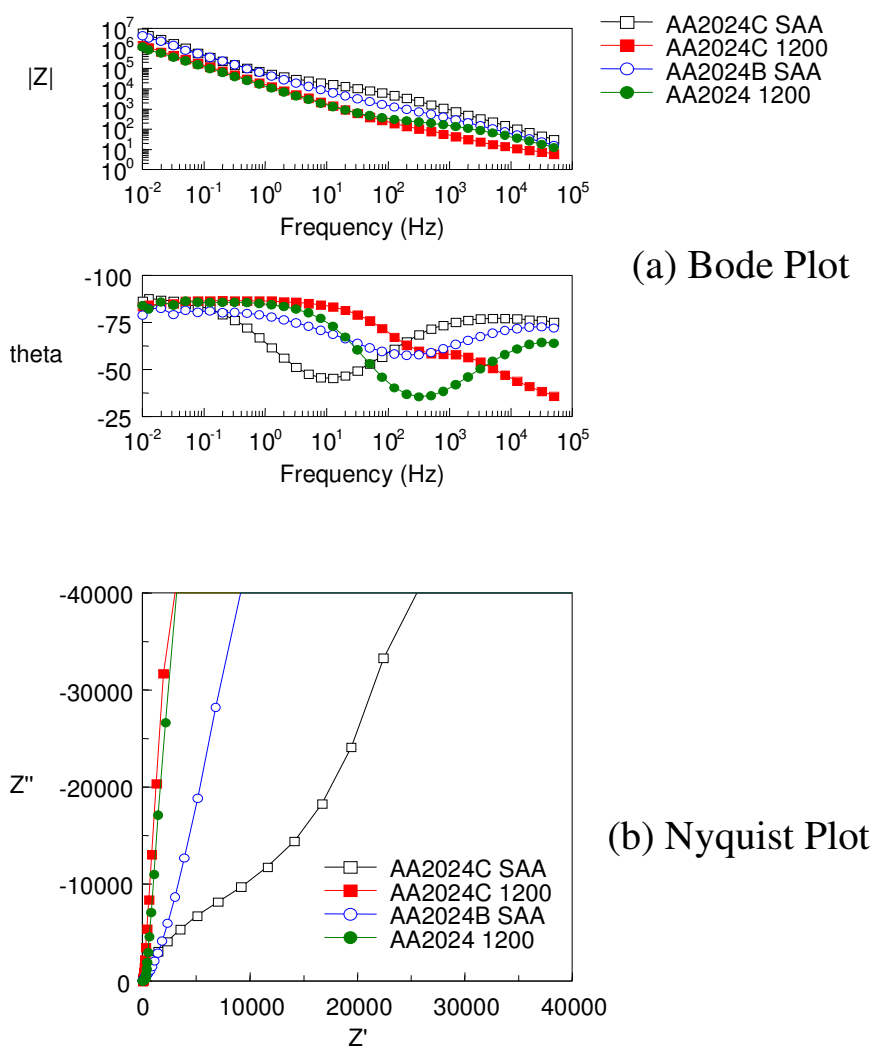
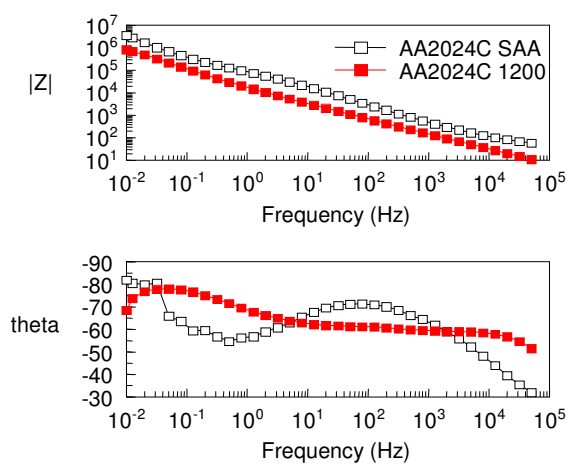
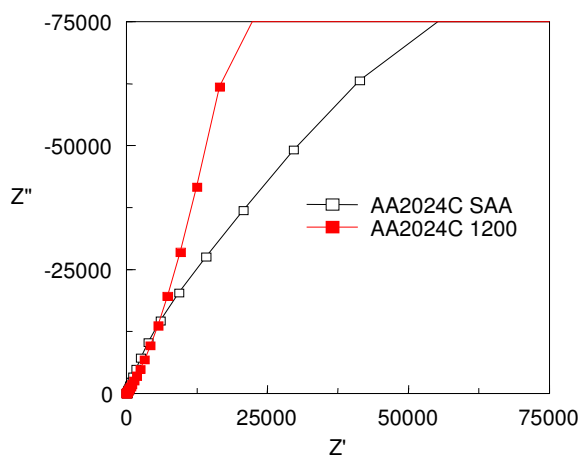


Figure 117 Impedance spectra on unexposed Al2024 and Al2024C, each with surface treatment SAA and CCC, measured in 0.1M Na₂SO₄.



(a) Bode Plot



(b) Nyquist Plot

Figure 118 Impedance spectra on scribed Al 2024C prepared with SAA and CCC, exposed to salt fog for 14 days, measured in a two electrode cell in 0.1M Na_2SO_4

Scanning Volta Potential Measurements

Figure 119 shows a Kelvin probe scan in air over the sample consisting of a series of metal referenced relative to the Ni metal and two measurements made of the Volta potentials for the same sample in the ionized air created by an x-ray beam with a monochromatic x-ray energy of 6.1 keV with a Pt-Ir probe. Measurements in ionized air with the beam impinging on the sample or passing above it and parallel to the surface gave similar results. Comparison of the three curves demonstrates there is a clear relation between the potential variations measured with the Kelvin probe and the direct Volta potential measurements in the ionized air. The potentials over each metal varied in accordance with its electron affinity and with its position in the galvanic series as has been noted previously by other investigators. The distinct shifts in potential between the Kelvin probe and ionized gas measurements, is due to a different reference potential. The effect of distance between probe and sample was to reduce the spatial resolution and to decrease the amplitude. However, even at a height of 1 mm where the decrease in amplitude was about 50% changes in potential could still be measured. This contrasts with the Kelvin probe where the probe height must be less than about 0.05 mm from the surface.

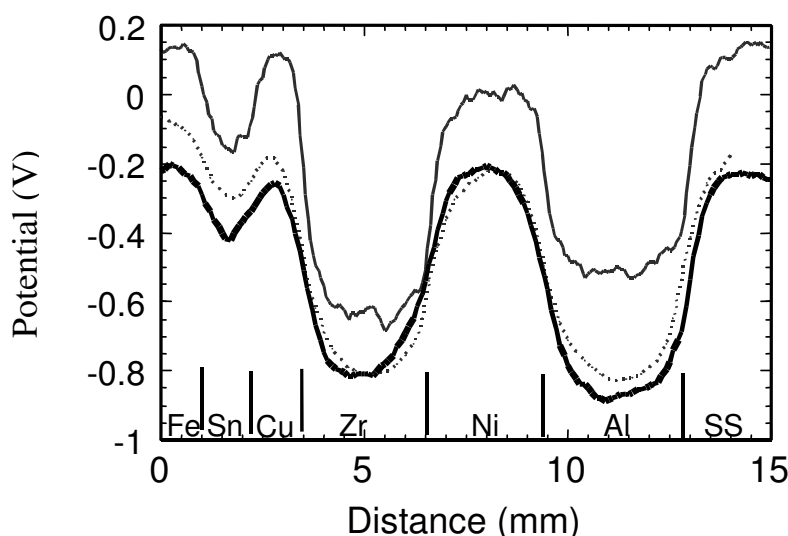


Figure 119 Scans showing Volta potential variations over a multi-metal sample. (A) Potential measured using Kelvin probe. (B) the beam impinging on the sample; (C) the beam passing over the surface.

Measurements were made on a sample of Al7075 covered with a polyester adhesive tape (3M Type 5) to simulate a painted surface. The metal has been prepared by abrasion down to 600# grade silicon carbide paper. The tape has a 1 mm diameter hole to simulate a defect in a coating. The reference electrode and x-ray beam was scanned across the center of the hole. Figure 120 shows the results for scans, without further treatment, and then after subjecting the sample to corrosion.

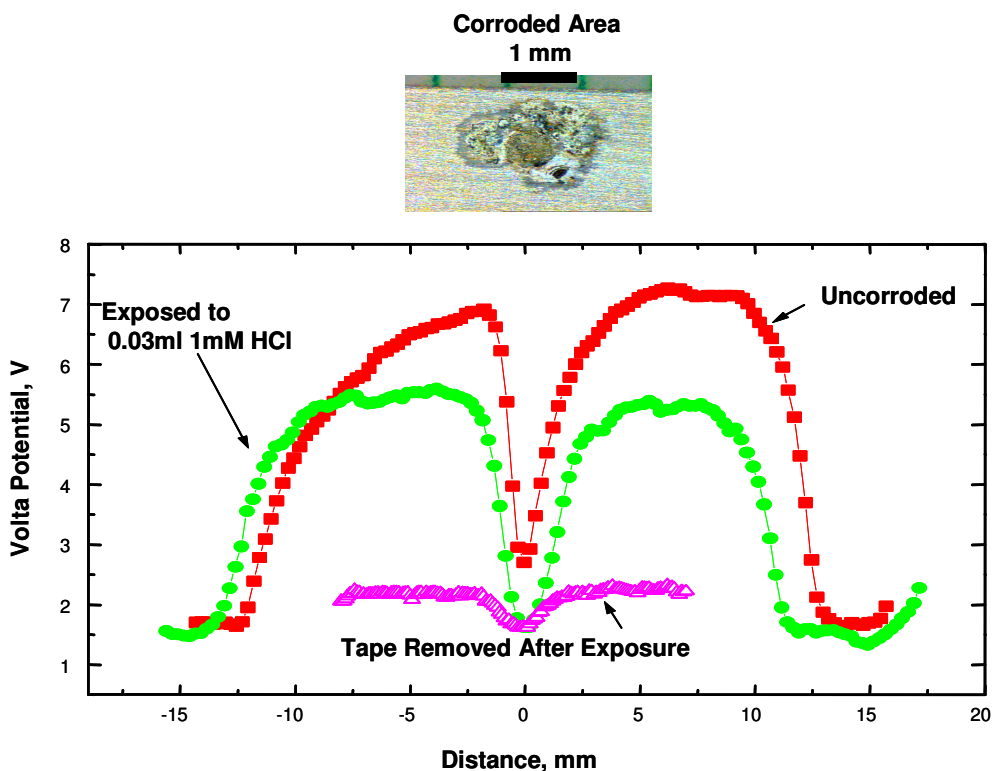


Figure 120 Volta potential measurements in ionized air for a simulated coating defect.

The measured potentials for the as prepared sample showed potential variations of more than 5 V. These large voltages cannot be attributed to any chemical effects that may produce voltages up to 1.5V. The high voltages were caused by the build-up of charge on the tape. Large decreases in potential were seen when the scan was over the defect in the coating demonstrating that the technique would be extremely sensitive as a method for detecting coating defects. Further work will be carried out to determine if the properties of the polyester played a part in the charging and what effects will be seen with painted surfaces. Humidity may also be important and the charging could be reduced by increased humidity.

The taped sample was then corroded by placing a drop of 0.03 M HCl over the defect in the coating. The apparent size of the defect, as indicated by the width of the potential decrease during the scan, increased and the magnitude of the potential showed a small decrease. The effect of the acid on the coating and the subsequent deposition of corrosion products from the defect was to increase the surface conductivity of the tape. This allowed charge to dissipate into the defect and produced the observed changes after corrosion. Finally the tape was removed from the sample and the surface was again scanned over the corroded area. The corroded region was detected by the Volta potential measurements demonstrating that the technique was sensitive to the presence of corroded areas Al7075.

Electrochemical Project Accomplishments BHL 2000

Summary – The research effort during the last year was focused on the detection of corrosion under an intact coating. Aluminum samples prepared were first corroded and then painted. Three techniques were used in these measurements: localized impedance spectroscopy, conventional Volta potential measurements with a Kelvin probe and Volta potential measurements in ionized air. The results obtained have shown that corroded localized area under 3.4 mils of paint can be detected by using Kelvin probe and impedance techniques. Further work is needed to demonstrate the possibilities of these measurements in humidified ionized air.

Sample Preparation – Aluminum coupons obtained from Northrop Grumman Corporation were used as samples. An unprotected part of each coupon was exposed to 40 μl of 1 mM HCl in a humidified atmosphere from two weeks to 3.5 months. After exposure approximately 3.4 mils of paint was applied over the whole area of each coupon.

Localized Impedance Spectroscopy – Direct impedance measurements, without electrolyte, were made on painted surfaces with a copper disk (3.14cm^2) as a probe. This new technique replaced a standard wet method that was also investigated. The impedance obtained with a wet method had shown a distinct time dependence, which may be caused by wetting or electrolyte penetration of the coating surface. The delay in establishing a constant impedance value would affect measurements to detect corrosion under painted surfaces.

The initial measurements were performed with a Solartron Dielectric Interface 1296 and a Solartron Impedance/ Gain Analyzer 1260. This equipment is specially designed for impedance measurements up to $10^{14} \Omega$ over 12 decades of frequencies (10 μHz - 10MHz) and it is used in testing dielectric materials. Measurements were also carried out with standard impedance equipment (Solartron Electrochemical Interface SI 12587 and Solartron Frequency Response Analyzer 1250).

Figure 121 illustrates the time dependence of the impedance of painted Al sample measured using the wet technique and compares the results with a dry impedance measurement. The sample (EAG-BF-14, #161 prime 2.4mils, #655 ghost gray 36375) was not previously exposed to corrosion. Bode plots and a complex-plane plot are given for 5 consecutive measurements on the same spot of the sample in 0.1M Na_2SO_4 . For comparison, the data obtained using the dry impedance measurement are also included. The results with this and other samples using the dry method gave reproducible results.

The Bode plots of a dry impedance measurement of a painted sample shows a phase angle close to 90 over the whole frequency range indicative of a capacitor behavior. Impedance values for a wet measurement show a dramatic change after the first measurement and then a gradual change with time up to 120 minutes. The initial measurement made from high to low frequency shows a drop in the impedance at the low frequencies. These measurements are slow and required extended periods. Water penetration or wetting of the paint occurred during

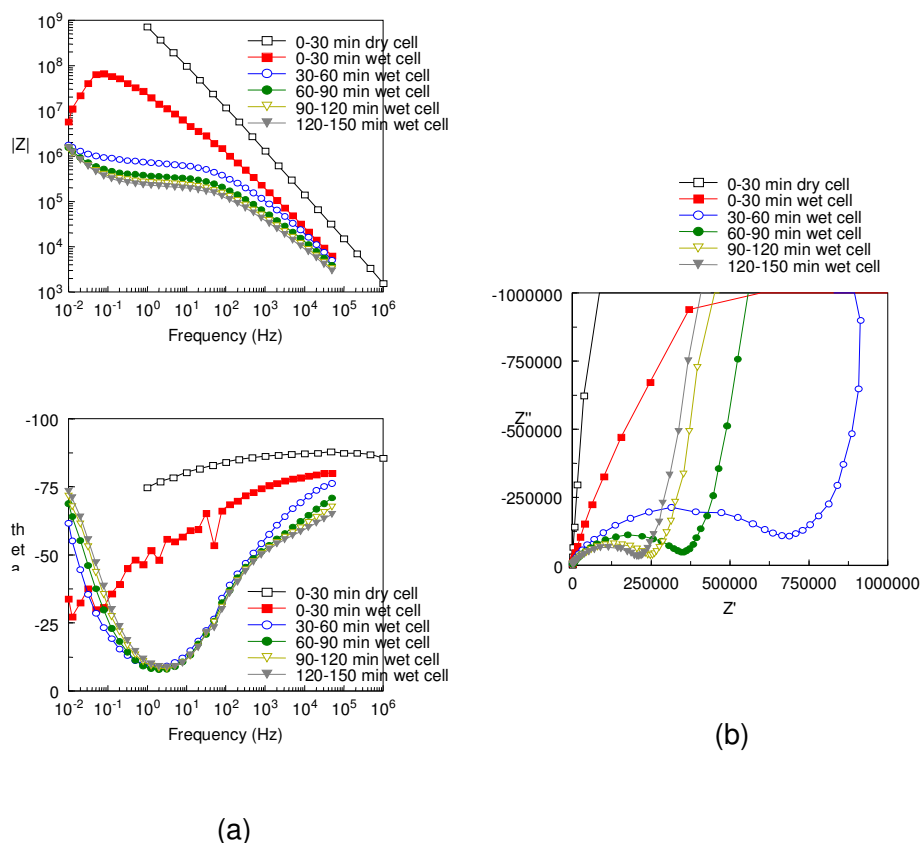


Figure 121 Wet (0.1M Na₂SO₄) and dry impedance measurements of painted Al (#6 prime 2.4 mil #655 ghost gray 36375); (a) Bode plot; (b) Nyquist plot.

this time and was reflected in all the following measurements. The subsequent measurements then showed a gradual change below about 100 Hz. The Nyquist plot of the result clearly show two major components of the impedance of the painted surface. The decreasing arc with each subsequent measurement was attributable to the decreasing resistance of the paint. The vertical line is indicative of a capacitor. The capacitor is consistent with an interfacial or faradaic impedance with a very high resistance.

In order to obtain numerical values of the relevant variables, a standard equivalent circuit for coated metals is considered (Fig. 122a). In this circuit, R_s represents the solution resistance of the cell, R_{coat} is resistance of the coating, R_{corr} is faradaic resistance of an interface. Constant phase elements CPE1 and CPE2 are introduced instead of a pure capacitance of the coating (C_{coat}) or an interfacial capacitance (C_{corr}). The sum of R_{coat} and R_{corr} is usually taken as the “paint resistance”. On the basis of this model, the values for R_{cot} , C_{coat} , R_{corr} and C_{corr} are calculated and plotted as functions of time in Figure 122b and c. It is seen that the capacitance of coating, C_{coat} , increases as the resistance of coating, R_{cot} , decreases with time of exposure to the electrolyte. The faradaic resistance, R_{corr} , has a constant high value, and faradaic interfacial capacitance, C_{corr} , increases slowly with time. This behavior is to be expected for the coating penetrated by water or electrolyte. Penetration of water and ions

through the coating depends strongly on the type of coating. The possibility of the use of poor coatings and the time dependence of the measurements creates difficulties in employing wet electrochemical methods to detect corrosion under coatings.

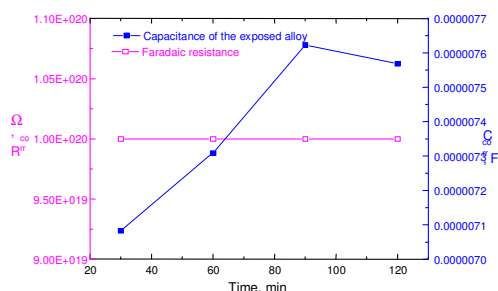
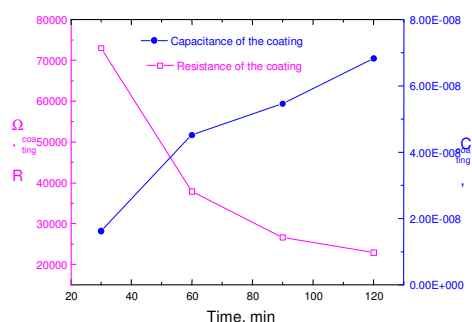
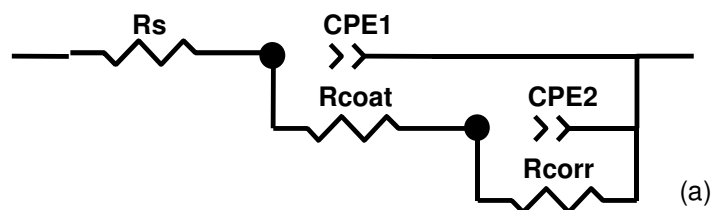
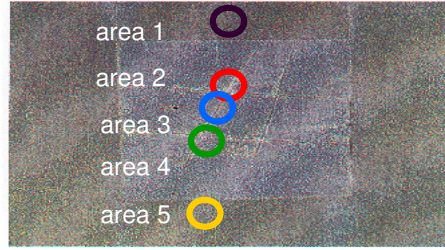
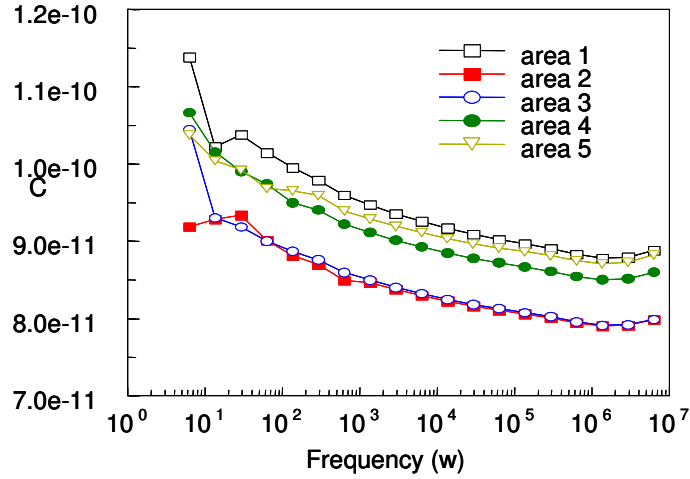


Figure 122 Changes in wet impedance measurements with time
(a) Equivalent circuit (constant phase elements CPE1 and CPE2 are in place of capacitors);
(b) changes of resistance and capacitance of the paint with time;
(c) changes of faradaic resistance and interfacial faradaic capacitance with time.

A comparison of results using the dry method on the corroded and painted clad AA2024 are presented in Figure 123. The sample was scribed, corroded and then painted. The circles on the photograph in Figure 123a, show areas where impedance measurements were performed. Figure 123b presents the results in the form of capacitance(C_{coat}) vs. frequency for each area. It is seen that the capacitance over the entire range of frequencies is higher for the uncorroded areas 1 and 5 than for the areas corroded 2, 3 and 4. Although some changes of the capacitance may be caused by differences in the thickness of a paint layer, the results clearly indicate that the largest change in capacitance occurs at areas where corrosion exists.



(a)



(b)

Figure 123 Dry impedance measurements of scratched, clad AA2024 painted after corrosion; (a) photograph of corroded surface before painting, circles 1-5 show areas of measurements; (b) capacitance as a function of frequency for areas shown in (a).

Figures 124 and 125 show variations of the capacitance with frequency over a wedge shaped corroded area on an Al sample. The AA 2024 sample originally had a conversion coating and was scribed and exposed to humidity for 14 days. After this exposure a wedge shaped area was masked off and the sample was corroded again for two weeks in the 1 mM HCl. After exposure, approximately 3.4 mils of paint were applied. Figure 124b and 125b, clearly show a decrease in capacitance over the heavily corroded (424, 425, 426, 428, 429, 430) compared to the masked (421, 431) areas. The results indicate that the capacitance is lower for the corroded areas.

The physical model of the system can be represented as a layer of paint over a passive surface oxide or over a corroded layer. This model corresponds to the equivalent circuit of three capacitors $C_{\text{surface oxide}}$, $C_{\text{corrosion product}}$ and C_{paint} . The measured capacitance, C , for the capacitors in series is determined by the relation,

$$1/C = 1/C_{\text{paint}} + 1/C_{\text{surface oxide}} \quad (1)$$

or

$$1/C = 1/C_{\text{paint}} + 1/C_{\text{corrosion product}} \quad (2)$$

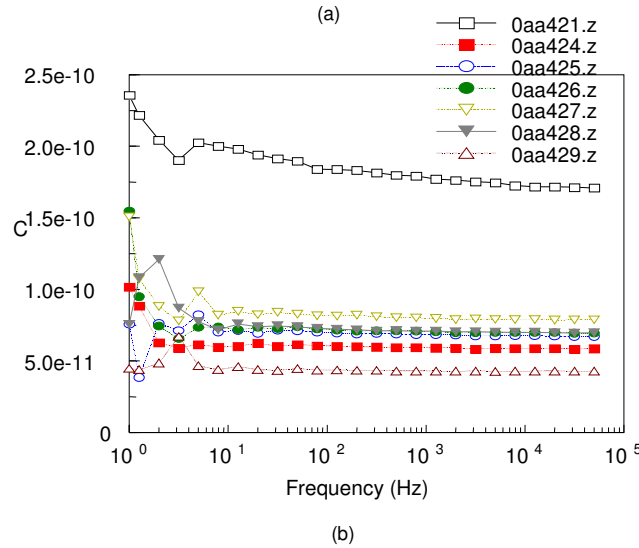
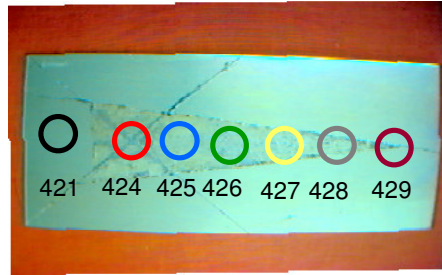


Figure 124 Dry impedance measurements of AA2024 painted after corrosion;
(a) photograph of the corroded sample before painting, circles show areas of measurements;
(b) capacitance as a function of frequency for areas in (a).

As a consequence of the relation in (1) and (2) the value of C always approaches the smaller capacitance. When there is a significant amount of corrosion product under the paint, the capacitance $C_{\text{corrosion product}}$ is much smaller than either C_{paint} or $C_{\text{surface oxide}}$, and the overall capacitance C is then close to that value. The results in Figures 123, 124, and 125 show a much smaller capacitance values for the heavily corroded parts of the samples. In the cases where the very small amount of corrosion is present under the paint, other model should be applied. Detailed analysis of the data is still in progress to determine the most sensitive frequencies for conducting these measurements in field tests.

Kelvin Probe Measurements

Conventional Volta potential measurements were carried out using an EG&G Scanning Kelvin Probe System. Platinum or stainless steel Kelvin probes, with diameters up to 1mm and with different insulating supports, were

used in these tests. All the measurements were performed in a humidified atmosphere to reduce the effects of static charge. The best results were obtained with a probe consisting of a 0.5 mm diameter Pt disk embedded in glass.

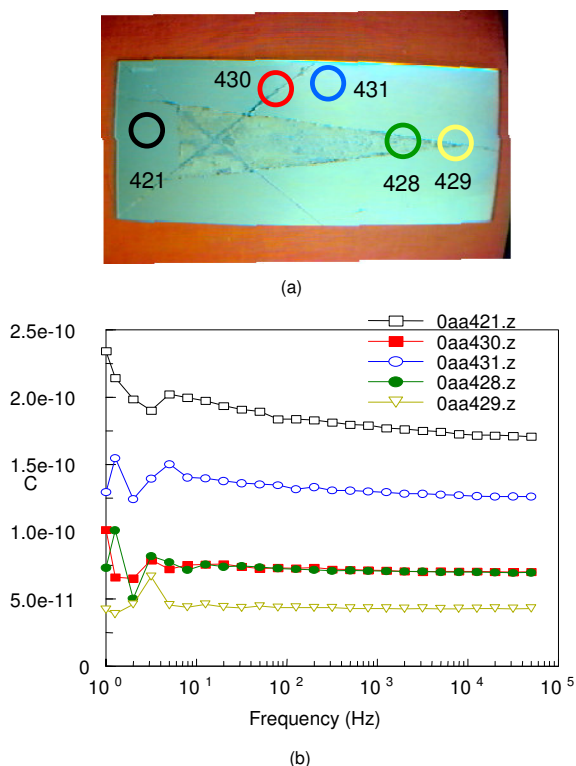


Figure 125 Dry impedance measurements of AA2024 painted after corrosion;
(a) photograph of the corroded sample before painting, circles show areas of measurements;
(b) capacitance as a function of frequency for areas shown in (a).

Figure 126a shows a photograph of the sample before painting. The area scanned by the Kelvin probe is marked with white lines. The sample was the same as in Figure 123a. Figures 126b and 126c show 2D and 3D images obtained from work function measurements on this sample. Different colors of these images correspond to varying values of the work function. The area that had been scribed and corroded showed the highest potential, while the area that has not been damaged were low. This clearly indicates a difference between the work function values of corroded and uncorroded metal surfaces. Similar results were obtained with the Al alloy 2024, which has been anodized in sulfuric acid.

Figure 127 shows a photograph of a sample taken before painting and the Volta potential scan over the same area after painting. The sample was originally a conversion coated AA 2024. The wedge shaped area was masked off and exposed to corrosion for two weeks. After exposure, approximately 3.4 mils of paint were applied on the sample. The results presented as a 3D image in Figure 127b delineate the corroded and uncorroded surfaces. These results demonstrate the possible use of this technique for detecting corrosion under coatings.

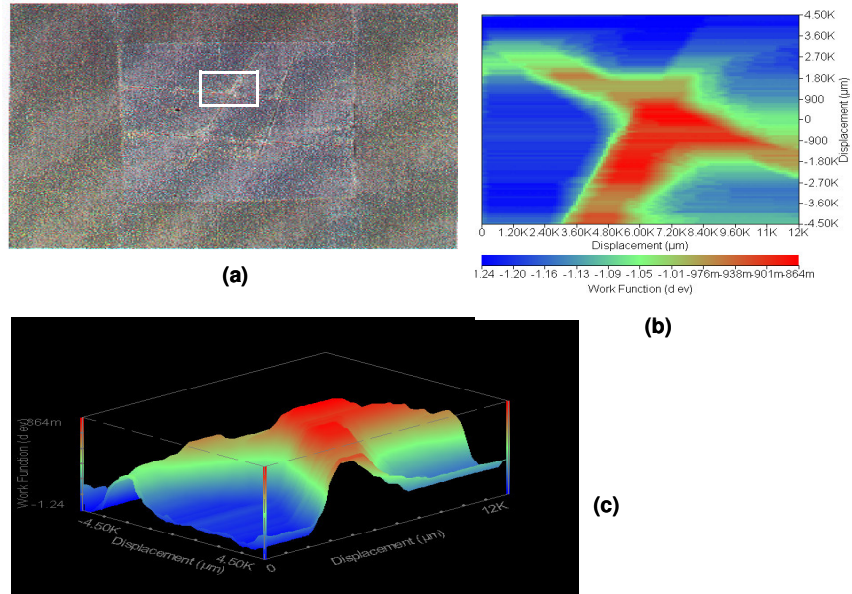
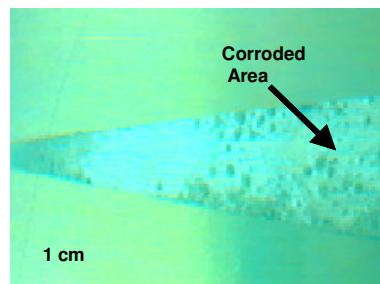
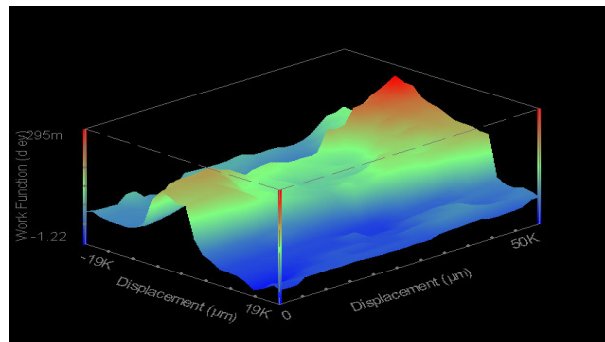


Figure 126 Volta potential measurements over corroded and painted AA2024; (a) photograph of the scanned area before painting; (b) 2D image of the Volta scan of the area; (c) 3D image of the Volta scan of the area showing the location of corroded regions.



(a)



(b)

Figure 127 Volta potential measurements over corroded and painted AA2024; (a) photograph of the scanned area before painting. (b) 3D image of the Volta scan of the area showing location of corrosion region.

Volta Potential Measurements in Ionized Air

Volta potential measurements in ionized air were performed at the National Synchrotron Light Source, at the beam line 18B. The measurements were carried out at a fixed energy of x-ray beam of 6090 eV. A reference electrode was placed at a distance of about 0.2 mm from the surface of the samples. The measurements were performed on multi-metal sample that served as a reference and on clad Al alloy 2024. Figure 128 gives a photograph of the area scanned during Volta potential measurements. The sample was originally sulfuric-acid-anodized clad Al alloy 2024 with scratches down to the underlying alloy. The wedge shaped area was taped off and corroded. The chloride solution that was used to corrode the exposed area has also penetrated and corroded the areas under the tape and along the scratches. Figure 128 shows the direct correspondence between the equipotential contour map and the corrosion in the photograph. A limited study on painted coupons showed that surface charging occurred on the painted samples. The use of humidified atmosphere, that successfully resolved difficulties with conventional Kelvin probe scanning, have still to be tested in ionized gas Volta measurements.

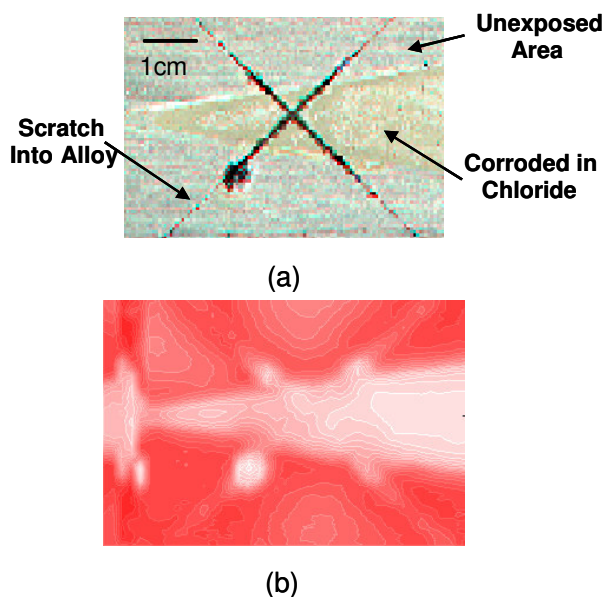


Figure 128 Volta potential measurements in ionized air over a scratched and partly corroded clad AA2024 sample; (a) photograph of the scanned area; (b) 2D image of Volta scan of the area.

Electrochemical Plans for 2001

Electrical and electrochemical measurements will be continued with the goal to demonstrate that all three above techniques can be used to detect corrosion under the paint. Future work will involve different samples and coating thickness with the application of these three techniques.

A new effort will be started to support Northrop Grumman's work in the area of spectral imaging. BNL will conduct the studies using IR microscopy. A recently acquired IR microscope will be used to evaluate both the spectra of corrosion products and also changes in the paint as a result of pH changes induced by the corrosion process.

BNL PROGRESS SUMMARY FOR YEAR 2001

The detection of corroded Al areas beneath the paint coatings has been demonstrated using three surface imaging techniques: During this reporting period we have emphasized the applications of Volta potential measurements and infrared microspectroscopy (IMS). Volta potential measurements were made with a conventional Kelvin probe and in ionized air. Comparison of the results shows that both methods can be used for detecting corrosion on both painted and unpainted samples. It was demonstrated that well-defined images of the corroded Al surface could be obtained under 6 mil thick film of paint.

Corrosion of two different Al alloys AA2024 and AA7075 was studied by using IMS, x-ray diffraction (XRD) and energy dispersive x-ray spectroscopy (EDX) techniques to characterize structures that must be detected under paint. It was found that IMS technique can detect corrosion below paint coating, and that it can identify species like sulfates, hydroxides and carbonates in the corrosion products. The IMS technique was also used to investigate the pH effect on films of paint applied on glass slides to determine the effects of the changes induced by the corrosion process on the paint.

Volta Potential Measurements Year 2001

Experimental – Volta potential or work function measurements were made using a PerkinElmer Instruments scanning Kelvin probe system (SKP100). It utilizes a vibrating, shielded 0.25 mm diameter Pt probe tip at a working distance of 0.08 mm from the sample surface. This system also derives the surface topography of a sample, from the capacitance between the probe and the sample. This is necessary as the probe tip must be at a constant height above the sample during SKP measurements.

Volta potential were also made directly in an ionized atmosphere. A high intensity x-ray beam from Beamline X18B at the National Synchrotron Light Source was used to produce ionization above the sample surface adjacent to a scanning probe. The probe was a platinum/iridium wire generally positioned 0.2 mm from the sample. The potential difference between the probe and the sample was recorded with an electrometer.

All Volta potential measurements on painted samples were made under a humidified air introduced over the painted surface to reduce static charge during the measurements. The total of four sets of samples (Table1) analyzed using ionized air, SKP or both to demonstrate the use of Volta potential method in detecting corrosion.

TABLE 1

Figure # and Alloy	Surface Condition	Corrosion Method	Paint	Measuring Technique
1. AA2024	Clad and sulfuric acid anodized	Scribed, salt fog 7 days; masked, 0.1M HCl 12 weeks	none	SKP100 and dc ionized air
2. AA2024	Abraded	none	Multi-layer nitrocellulose	SKP100 and dc ionized air
3. AA2024	Clad and CCC (Alodine 1200)	Scribed, masked, salt fog	Primer and gloss coat 5.6 mils	SKP100
4. AA2024	CCC (Alodine 1200)	Masked, 0.1M HCl 2 weeks	Primer and gloss coat 3.6 mils	SKP100, dc ionized air and IMS

Results – Figure 129 shows Volta potential measurements using both the ionized air and the scanning Kelvin probe (SKP) technique, for an un-painted sample. The sample was clad AA 2024 and sulfuric-acid-anodized and scratched exposing the underlying alloy. A wedge shaped area was left exposed after masking (3Ms Tape # 5) and then corroded. The 0.1 M HCl was used to cover the exposed area which was then held in water saturated air for 12 weeks. During this exposure the solution also penetrated along the scratches under the masking tape and led to crevice corrosion. After exposure the tape was remove and the sample was washed in Milipore water and dried. Figure 1a is a photograph of the scanned surface. Figure 129b is a 2-dimensional (2D) map of the Volta potentials in ionized air. Distinct differences in the Volta potentials were observed between the corroded versus the non-corroded areas. Particularly noticeable are the potential differences between the masked area and the scribe marks, where the electrolyte penetrated and corroded along the scribe under the masking tape. This behavior simulates what can take place under paint. Figure 129c is a SKP scan of the same area as shown in Figure 1b. The corroded areas are again readily visible. The sites along the scribe marks showed that crevice corrosion was developing underneath the masked area. This produced distinctly different corrosion products from the freely exposed area, probably as a result of the copper in the corrosion product. The difference in Volta potential on this sample was 652 mV, compared to 800 mV for the ionized air measurements. The discrepancy between the measured voltages for the two methods can be attributed to a number of factors, including the measurement technique (ionization of the air above the sample) as well as the proximity of the probe to the surface.

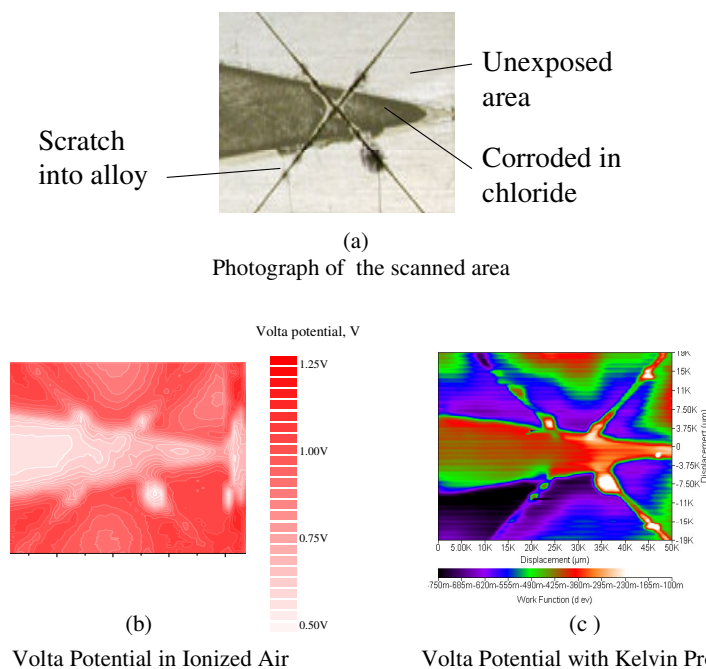


Figure 129 Volta potential measurements of corroded clad Al alloy AA2024. (a) Photograph of the scanned area. Measurements using the ionized air method (b) and SKP method (c).

Figure 130 shows the effect of paint thickness on the Volta potential, for a AA 2024 specimen. Four different thicknesses of nitrocellulose paint were applied in strips over an abraded sample. The thickness of paint was nominally 0, 1, 2, 3, and 4 mil. The topography of the painted surface, leveled parallel with the scanning head, is shown in Figure 130a. The topography scan indicated a difference in the paint layers of about 15 μm or about 0.6 mil. Volta potential changes are shown in Figure 130b where five distinct steps were observed with increased thickness of paint. The total potential difference was approximately 360 mV or about 80 mV/mil. A Volta potential scans over an area of about 20 x 20 mm is shown in Figure 130c. Each line scan again showed the difference in Volta potential between bare metal and each of the four layers of pant but the background potential varied. Causes of this change in background potential are being investigated. It may be due to instrumental causes, or variations in potential of the reference probe. The results nevertheless demonstrated that the Volta potential measurements respond to the differences in the thickness of the paint. However, the magnitude of the changes, due to paint thickness is smaller than the change of over 0.6 V between corroded and non-corroded areas.

Figure 131 shows SKP measurements of the corroded clad chromate conversion coated AA2024 covered with several layers of paint. The sample was masked leaving a square section exposed. The unmasked area was scribed, and the sample was then exposed to salt fog for an extended period of time. After corrosion the masking was removed and the entire sample was coated with PRF 23377 primer and a Hentzen gloss white topcoat so that

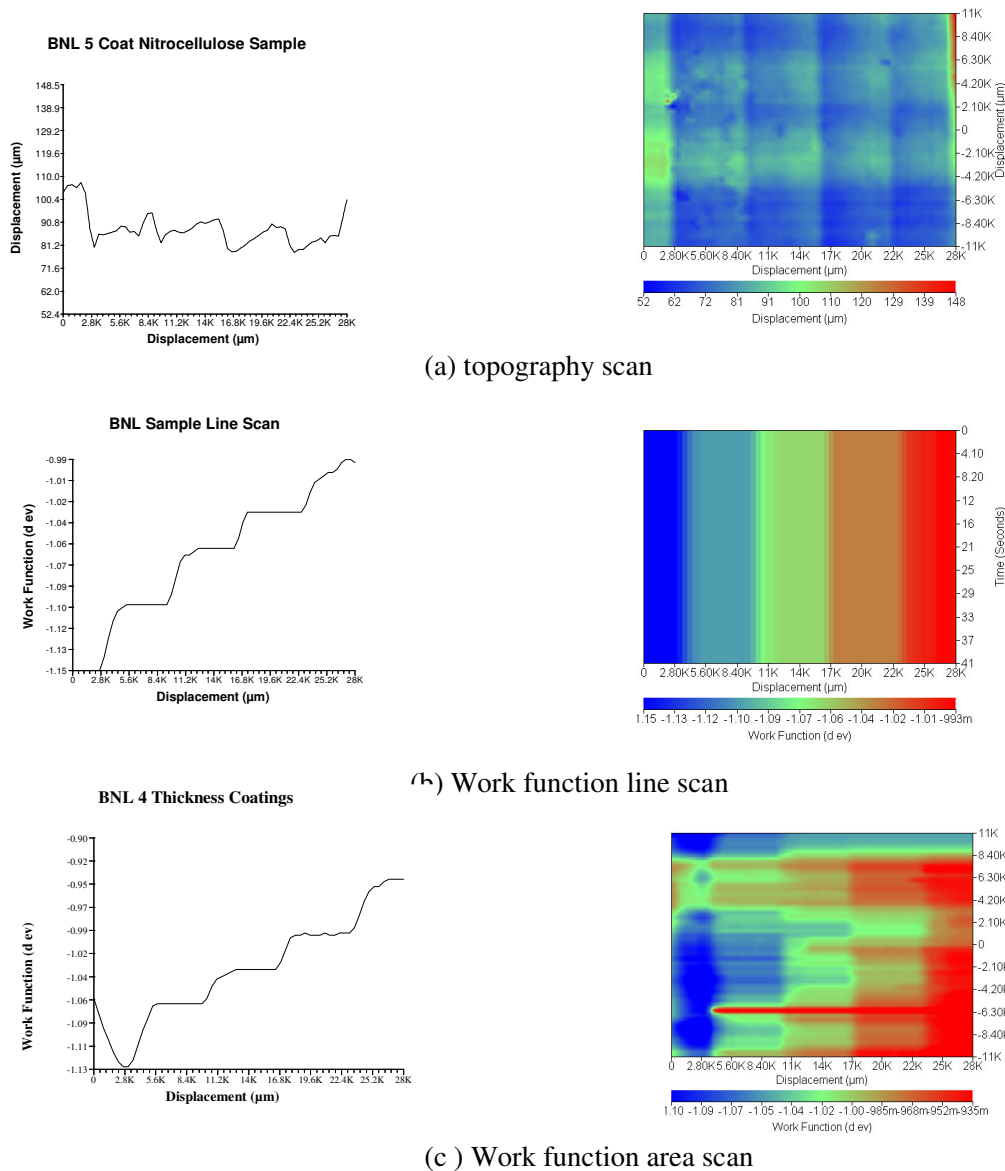


Fig. 130 Volta potential measurements of Al alloy AA2024 covered with four different thickness of nitrocellulose paint.

the overall thickness of paint was 5.6 mil. In Figure 131 the Volta potential scanned area is presented in the form of 2D and 3D maps. The exposed area and the scribe marks were also detected by the SKP. The difference in Volta potentials, between the corroded scribe and surrounding area was approximately 580 mV. Differences in the potential between the exposed and unexposed areas were much smaller, about 20mV. While it is recognized that there are differences in the chemistry of the coatings involved, the observed difference in Volta potential for the scribe marks is primarily due to the presence of corrosion products within the scribe mark and not due to the

“filling in” of the scribe marks with coating resulting in a thicker coating layer immediately above the scribe marks.

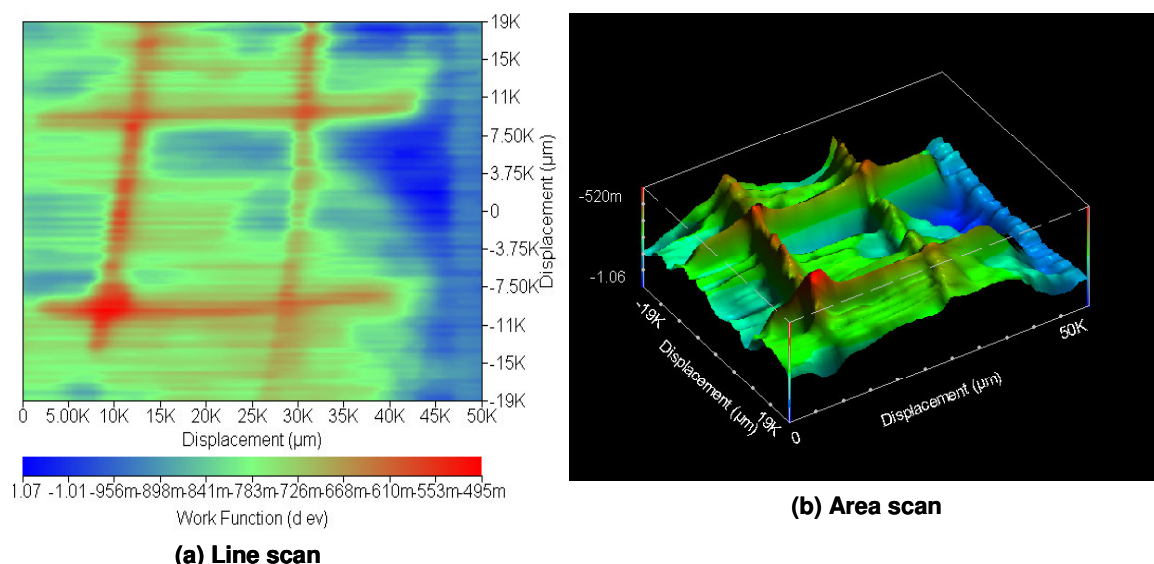


Figure 131 SKP Volta potential measurements of corroded clad Al alloy AA2024 covered with several layers of paint. The overall thickness of the paint is 5.6 mil.

A comparison of the two Volta potential methods and the infrared microspectroscopy (IMS) method for detection of corrosion under a film of a defect-free paint is given in Figure 132. The first image shows a photograph of an AA 2024 sample with a visible corroded area, prior to being painted. The sample had been chromate conversion coated. The sample was masked leaving a wedge shaped area exposed. The sample was first covering with 0.1 M HCl and then placed in a humid atmosphere for two weeks. The masking was then removed, the sample washed and dried, and the surface painted. The photograph of the sample Figure 132a, shows the area that was scanned using the three different techniques.

The SKP results are shown in Figure 132b. The map of the scanned surface obtained by Volta potential measurements in ionized air is shown in Figure 132c. The 3D map of Volta potential shows the difference between the corroded and non-corroded areas. The last image in Figure 4d represents the results obtained by infrared microscopy. The intensities of the peaks at 1042 and 2086 cm^{-1} were used to generate the 2D plot. It exhibits the same locations of corrosion, as the two Volta potential techniques. All three techniques can therefore be used to detect of corrosion under paint.

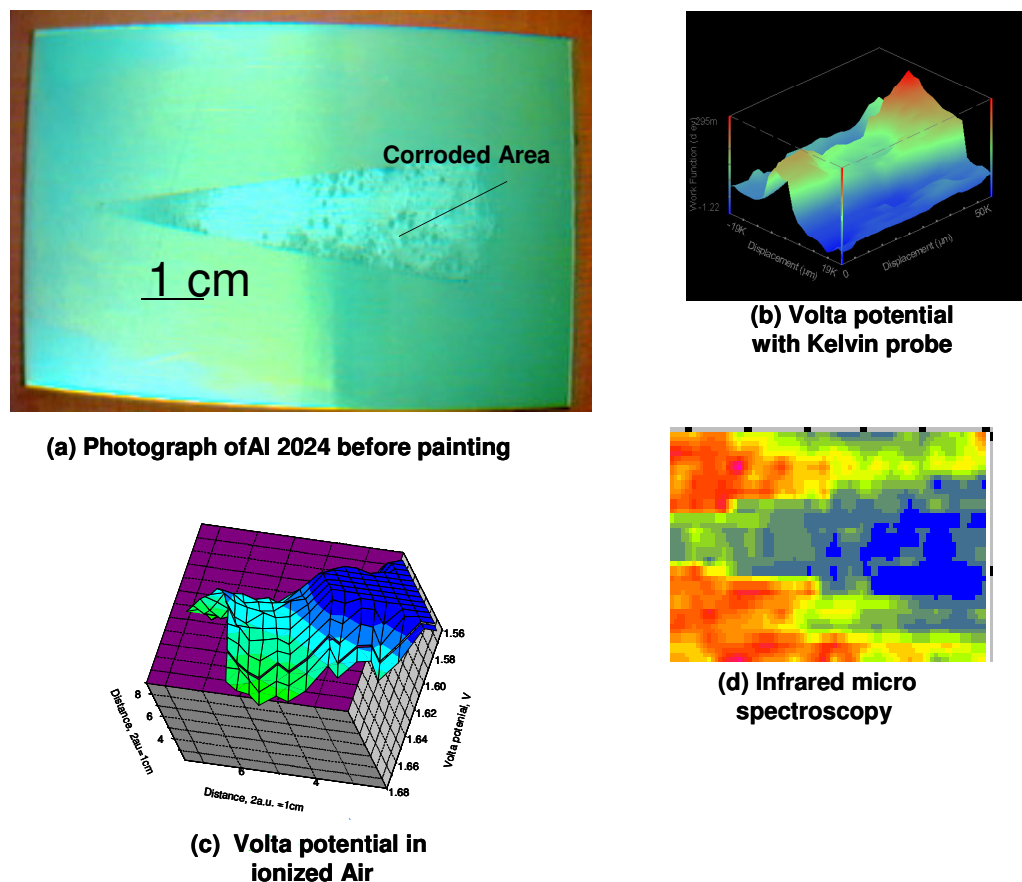


Fig. 132 Detection of corrosion under 3.6 mil paint layer using three different scanning techniques.

Identification Of Corrosion By Infrared Microspectroscopy (IMS) For Year 2001

Experimental – A Nicolet Nexus 470 FTIR equipped with a Spectro Tech Continuum Microscope was used for IMS measurements to locate areas of corrosion on Al alloys with different treatments and coatings. Additional techniques were also used to study corrosion of Al alloys AA2024 and AA7075 and their corrosion products. X-ray diffraction (XRD) data were collected at Philips Automated Powder Diffractometer with a $\text{Cu}_{\alpha 1}$ radiation. Energy dispersive x-ray spectroscopy (EDS) measurements were performed on a Jeol JSM-6400 scanning electron microscope. Visualization of corrosion process using a video camera and gel technique [1] was used for comparing the corrosion behavior of AA2024 and AA7075.

Results

IMS Investigation of AA 2024 – IMS mapping of an unpainted corroded AA 2024 surfaces identified a species similar to sulfate or bisulfate as can be seen in Figure 133 along scribes after corrosion. The sample was originally sulfuric acid anodized, scribed, exposed to salt fog for 1 week, masked, covering with 0.1 M HCl,

exposed for 12 weeks to a humid atmosphere, washed, and dried. Figure 133a shows a photograph of the scanned area that correlated with generated 2D map in Figure 133b showing the variations in intensity a peak at 1149 cm^{-1} . This data was generated with an aperture size of $100 \times 100\text{ }\mu\text{m}$, and a step size of 0.1 mm . The presence of this peak is shown in the spectrum in Figure 133c. The presence of this peak was observed close to the edge of the scribes as it can be seen for spectra (shown in Figure 133d) taken along the line B in Figure 133d.

An example of the detection of corrosion under a paint layer using IMS is given in Figure 134. The sample was a scribed, chromate conversion coated AA2024, which was then exposed 3 days to humidity, masked, exposed two weeks in a humid atmosphere after covering with 0.1 M HCl , washed, dried, and finally painted with a 3.5 mil thick paint layer. The spectrum for a corroded area showed a typical window between 1850 and 2850 cm^{-1} which makes it possible to see through the paint (Figure 134b). The 2D map (Figure 134a) was derived from the overall intensities of the absorbance. This mode of plotting clearly identified the areas of corrosion. The differences were greatest at heavily corroded sites that can be seen in Figure 134b for the 5th and 6th and the 22nd and 23rd spectra which were recorded over the scribes taken along the line in Figure 134a

Figure 135 shows the photograph of crevice corrosion under tape at the crossing of scribes for AA 7075. The sample was previously anodized in sulfuric acid, scribed, exposed to salt fog for 1 week, partially taped covering where the scribes intersected, corroded in 0.1 M HCl for 12 weeks, washed, and dried. IMS was used for mapping the image shown in Figure 135a. The 2D plot and corresponding line spectra are shown in the same figure. The first 6 spectral lines, over non-corroded parts of the surface, were typical for anodized coating. The following three spectral lines were over corroded areas.

IMS Investigation of Different Alloys

Investigations were started to determine any differences in infrared characteristics of different alloys after corrosion. The alloys AA2024 and AA7075 were compared.

A gel technique [3] was used to visualize corrosion process on two different alloys. Surfaces were covered with an agar gel containing NaCl and a wide range pH indicator. Figure 136 demonstrates the differences in behavior of the two alloys in 1M NaCl Agar gel. Both samples had been abraded. AA7075 was additionally scribed to verify the spreading of corrosion laterally along the grooves as it was found that corrosion appeared to spread along scratches. The samples were masked with tape and then covered with gel. The red color due to a low pH marks the spots where corrosion of the alloy takes place. A blue color indicates a high pH due to the oxygen

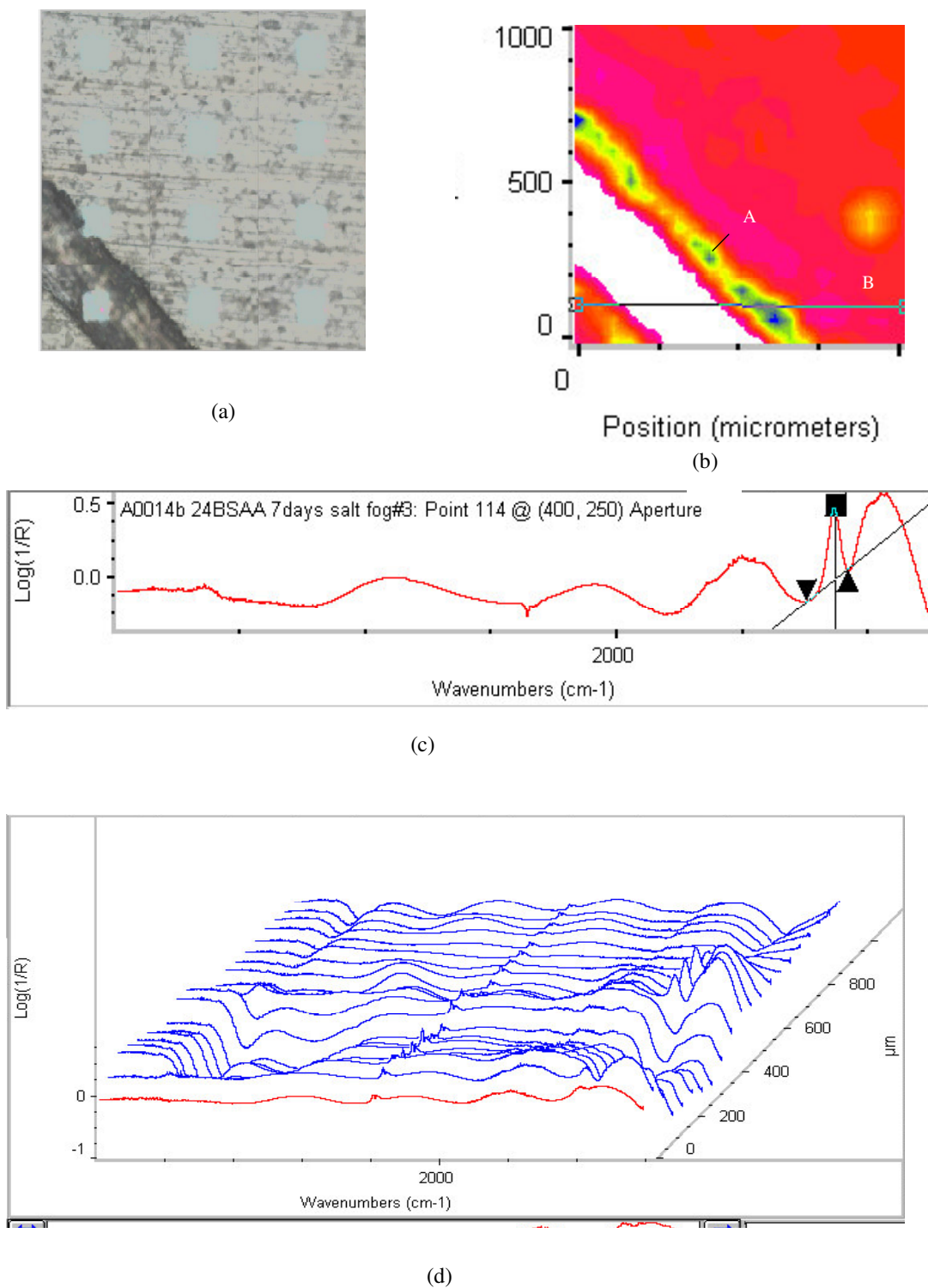


Figure 133 IMS of corroded sulfuric acid anodized AA 2024: (a) photograph of the scanned area; (b) map for the variation of the peak height at 1149cm⁻¹; (c) spectrum in point A shown in (b); (d) spectra along the line B shown in (b).

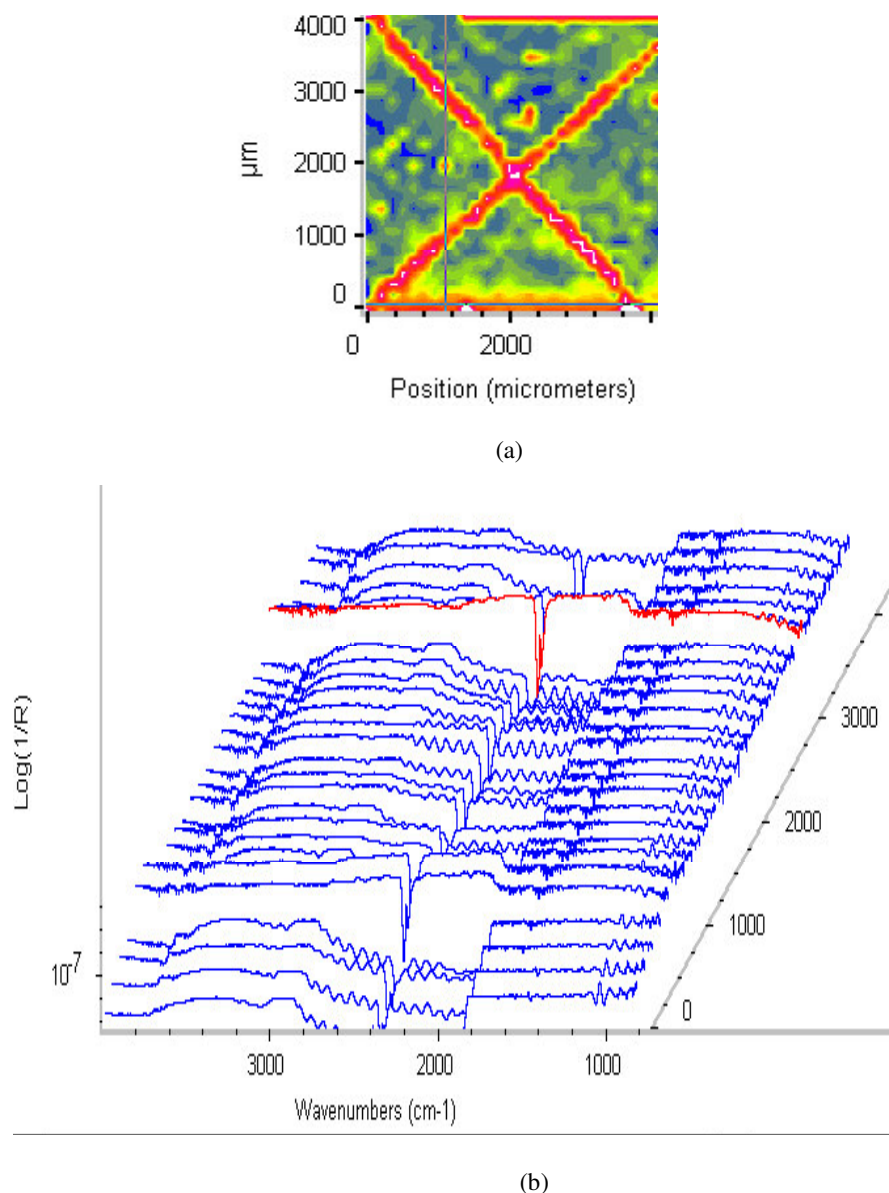


Fig. 134 IMS of painted AA2024 scribed before corrosion. (a) Map for the overall intensities of absorbance spectra; (b) absorbance spectra along the line shown in (a).

reduction reaction. Corrosion of AA2024 occurs mainly by a pitting mechanism. Some pits repassivate, others continue to corrode as may be seen from Figure 136a. The early stage of corrosion of AA7075 does take place mainly along the scribes but eventually general corrosion takes place.

The appearances of the samples after removal of the gel are shown in Figure 137a and b, respectively after 12 weeks of corrosion in a humid environment covered with gel. The appearance was quite different for the two alloys. In both cases the pH indicator disappeared. The alloy AA7075 produces a cloudy white corrosion product.

The gel over AA2024 was clear. Heavy pitting occurred on Al 2024 with red spots in the pits that blackened with

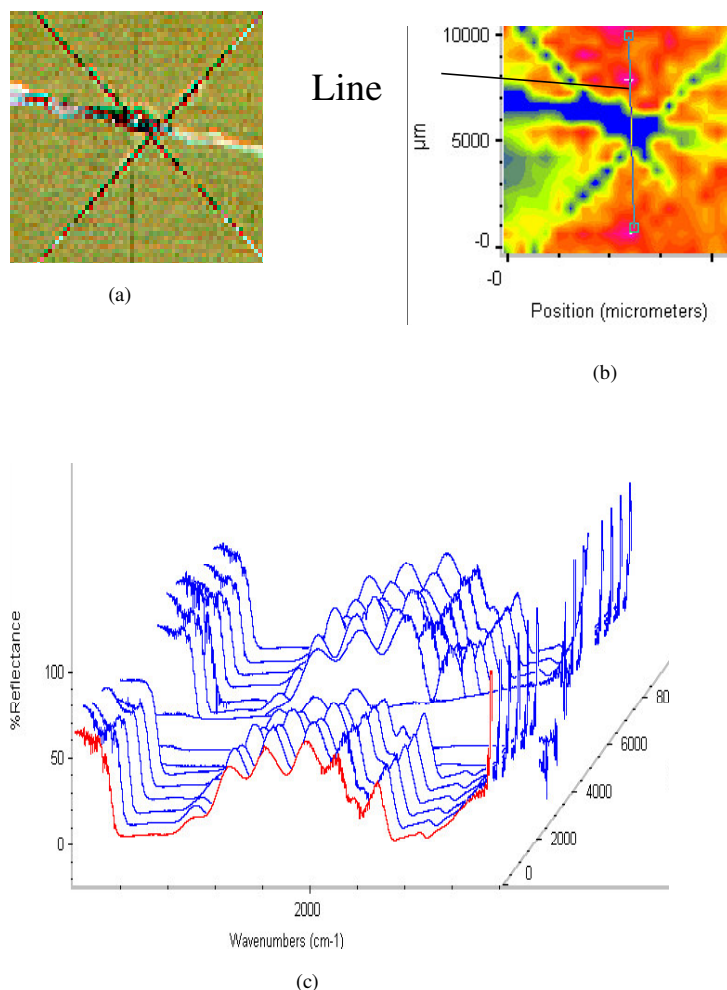


Figure 135 IMS of AA 7075 anodized in sulfuric acid after crevice corrosion under masking. (a) Photograph of the scanned area; (b) variations of the reflectance intensities for the region 1560 – 1670 cm⁻¹; (c) reflectance IR spectra along the line shown in (b).

time when exposed to air. The AA7075 had quite a different appearance, showing white and black areas on the surface. Corrosion had also spread into crevices under the tape, and had a similar red coloration seen in the AA2024 pits and also turned black with time.

Figure 137c shows IMS spectra taken over different spots on the corroded alloys. There is a marked difference in the spectra between the black and the white spots for the alloy AA7075, while for the AA2024 the difference is due to intensity variations of the reflectance spectra. Preliminary analysis of AA70 75 ascribes the peaks at 1400 to 600 cm⁻¹ to a zinc aluminum carbonate [2]. A broad absorption region at 3400 cm⁻¹ corresponds to an OH⁻ starching group that can be seen in all the spectra.

IMS mapping of the corroded AA7075 surface is shown in Figure 138a. The map was generated from the variations in intensity of the absorbance peak highlighted in the spectrum shown in Figure 138b. The spectrum was taken from the center of the area shown in Figure 138a. It can be seen that the black and with areas of the corroded sample in Figure 137b corresponds to the differences in the corrosion products

Figure 139 shows XRD data for corroded and uncorroded alloys AA2024 and AA7075. All patterns show strong peaks for Al, and smaller peaks for intermetallics. Distinct peaks for 2θ of 18.429° and 20.523° were observed when the corrosion product on AA7075 was present. The product can be ascribed to aluminum hydroxide (Gibbsite) $\text{Al}(\text{OH})_3$. However, the carbonate that was indicated from the IMS data and has been observed [3] with Zn-Al alloys could not be seen probably because of the small quantities present.

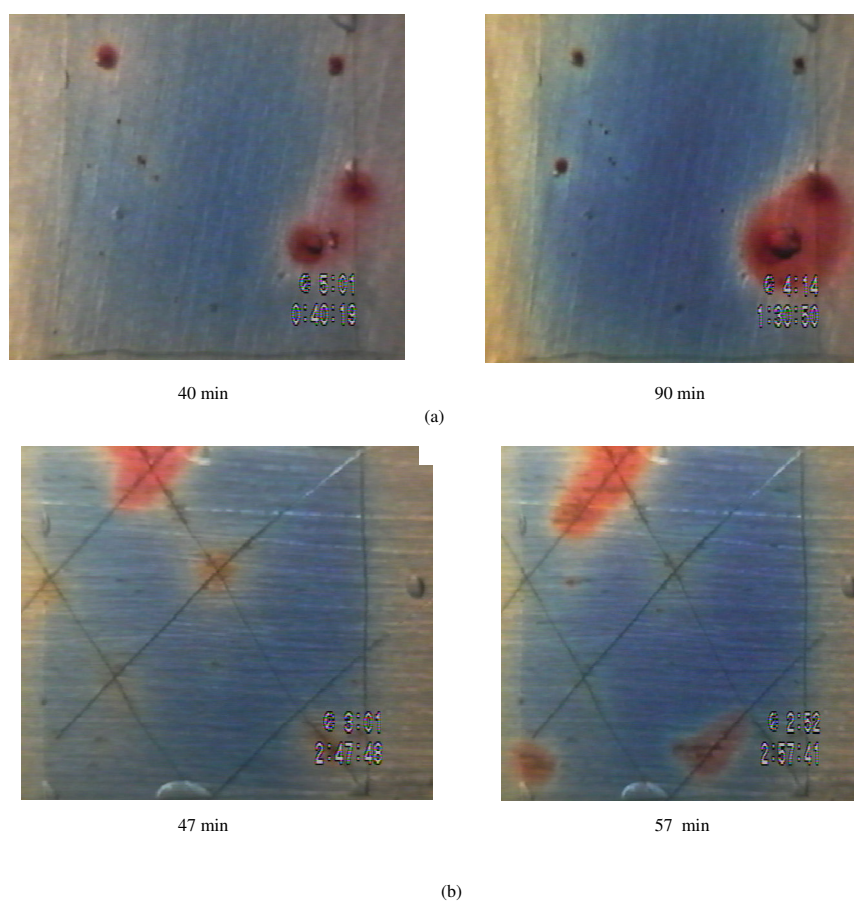


Figure 136 Video images of the corrosion in 1M NaCl Agar gel: (a) Al alloy AA2024; (b) Al alloy AA7075.

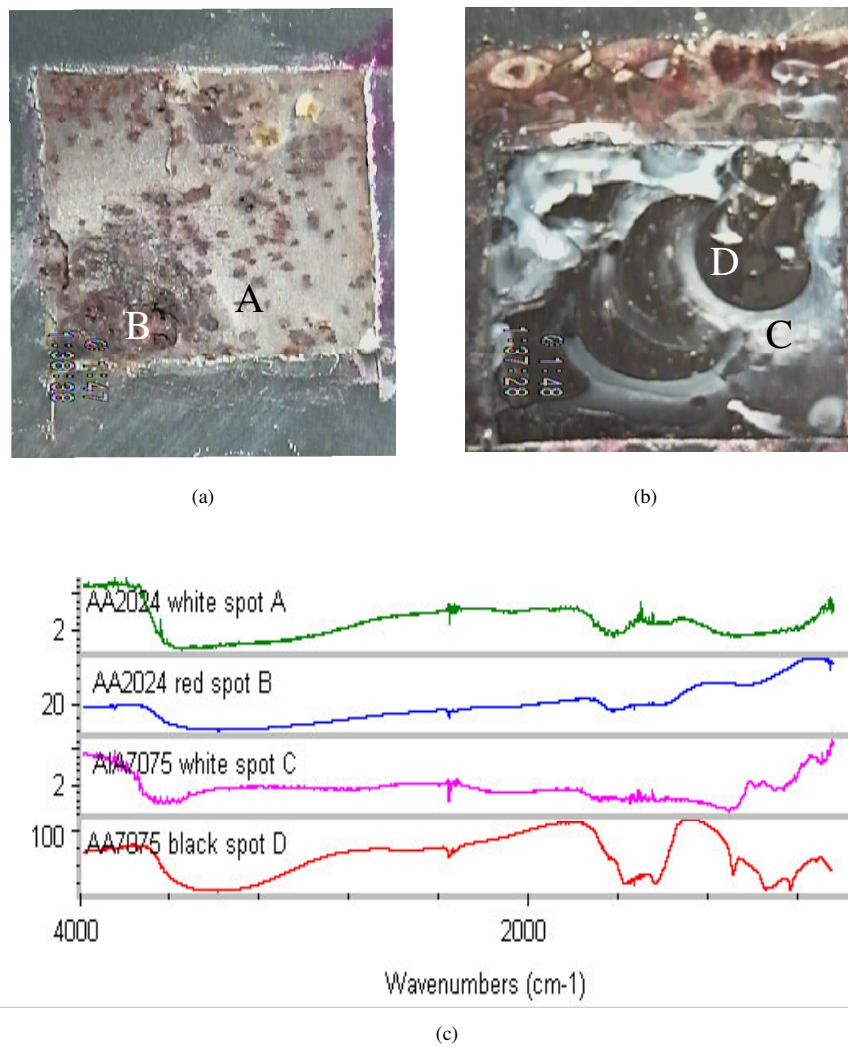


Figure 137 IMS on the corroded Al alloys AA2024 and AA7075. Video images of the samples after 12 weeks corrosion in gel: (a) AA2024; (b) AA7075 and corresponding reflectance spectra (c).

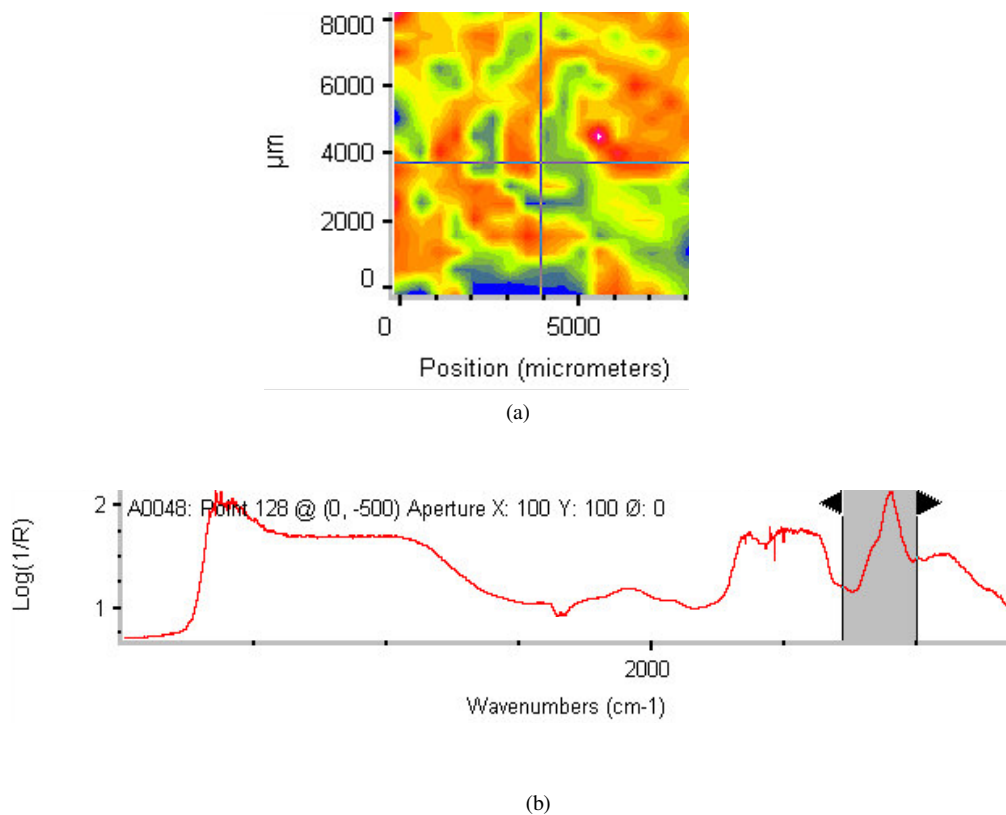


Figure 138 IMS on Al alloy AA7075 (shown in Fig. 9b) after 12 weeks of corrosion in gel: (a) Map of the surface for the variation of the highlighted peak; (b) absorbance spectrum at the cross point shown in (a).

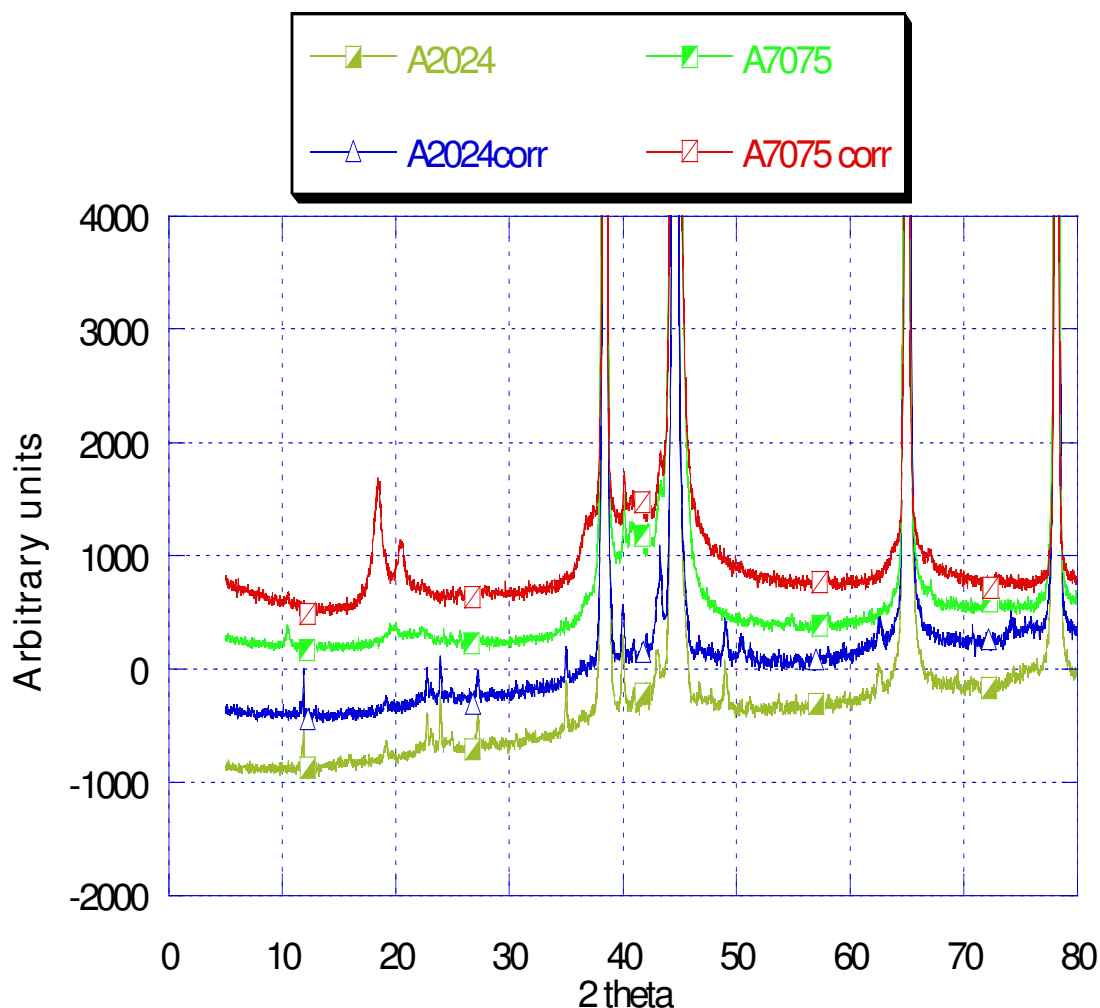


Figure 139 XRD patterns for AL alloys AA2024 and AA7075 corroded in 1M NaCl gel and for the corresponding non corroded alloys.

Conclusions

Volta potential measurements with SKP and in ionized air can be used to detect corrosion on painted and unpainted surfaces. Changes were also observed due to differences in the thickness of the paint, but the effects on thickness were smaller. However, with very uneven paint layers difficulties may arise in separating out the presence of corrosion.

Investigation of the different types of custom corroded samples as studied by IMS, XRD, EDX shows that there is a difference in the elemental composition of the samples between the corrosion in air and the corrosion in the crevices. There is also a difference in the corrosion products between the two examined alloys AA 2024 and AA7075. Characterizations of the corrosion process and identification of the different products of corrosion by these techniques could be an important part of the overall detection of corrosion.

BNL PROGRESS SUMMARY YEAR 2002

Detection of corrosion under paint has been investigated by infrared micro-spectroscopy (IMS) and impedance spectroscopy. Precorroded and coated aluminum alloy 2024-T3 corrosion standards were prepared with different aircraft paint systems. Three types of paint systems were investigated. A spectral database of substrate reflectance was generated with IMS for both corroded and uncorroded samples. Spectral ratio analysis was used to determine changes in reflectance due to corrosion in the wave number range of 1800 to 2700 cm^{-1} . The results for the procedures adopted showed that corrosion was detected through paint thicknesses up to 6 mil for Insignia White, 4.39 mil for Dark Camouflage gray and 1.76 mil for Dark Camouflage Type II Low IR paints. For the thicker coatings differences due to corrosion were not detected.

Impedance measurements on all painted samples were performed with both dry and wet contacts in the frequency range 1 to 65000 Hz and. The complex behavior of impedance measuring on painted samples has been investigated using known thicknesses of films to substitute for paint layers. Work is also being carried out to develop a probe for scanning the surface using impedance spectroscopy. First results are very encouraging, obtaining images show a distinct difference between corroded and non-corroded areas. It was found that capacitance changes in the frequency range of 100 to 1500 Hz were sensitive to the presence of corrosion. Corrosion was detected for paint thicknesses up to 4mil. For thicker layers of paint a clear indication of corrosion has not as yet been obtained.

Sample Standards Year 2002

Painted AA 2024-T3 panels were prepared at Northrop Grumman as corrosion standards for SERDP 1137 Lab Work Order. All panels, 3"x6" coupons of 2024-T3 aluminum, were solvent wiped with MPK plus 5 vol% Z-6040 prior to finishing (Patent No's 6,248,403 and 6,096,700). A primer, MIL-PRF-23377TY1CLC and three types of top coatings (MIL-PRF-85285TY1 Insignia White 17925, Dark Camouflage and Dark Camouflage Type II Low IR) were used in these configurations. Corroded samples had been exposed to two-week salt fog in accordance with ASTM B117. Ten different organic finish configurations were applied on both corroded and non-corroded panels. Eight of them had a layer of primer and layers of top coating. The thickness of the primer was approximately 0.7mil.

Infrared Microspectroscopy (IMS)

Experimental Year 2002 – A Nicolet Nexus 470 FTIR equipped with a Spectro Tech Continuum Microscope was used for IMS measurements. The aperture of the incident beam for this technique corresponds to the size of 100x100 microns. A total of 200 scan in the range of 650 to 4000 cm^{-1} wavenumbers were averaged for each site measured. Then the reflectance of 6 sites was averaged for each panel of both corroded and non-corroded samples. The spectral database of the averages substrate reflectance was obtained for both corroded and non-corroded samples. Spectral ratio analysis was used to determine changes in reflectance for the transparent window of the paints as a result of corrosion, in the wavenumber range of 1800 to 2700 cm^{-1} .

Results Year 2002 – Figure 140 represents the effect of paint thickness on the reflectance of non-corroded samples. Each spectrum shows an IR transparent window from 1800 to 2700 cm^{-1} giving a maximum around 2000 cm^{-1} ranging. This peak is obtained for all types of paint studied. Comparison of different types of paint for the same substrate shows that the spectral reflection decreases in the order, Insignia White, Dark Camouflage and is the lowest for Dark Camouflage Type II Low IR. There are also less pronounced reflectance peaks at 3100 and 3800 cm^{-1} observed for the thinner top coating. The spectra for three paints are very similar except that Dark Camouflage and Low IR paints have the higher intensity reflectance peaks for thicker coatings at the lower frequencies (1050 and 800 Hz). The intensity of the peak decreases with the paint thickness.

Corrosion produced changes in reflectance. The changes were determined by applying a data analyses technique to calculate the ratio of the average reflectance of uncorroded panels relative to corroded panels. The reflectance spectra were baseline corrected at 1250 cm^{-1} within a spectral region where the paint is opaque. Figure 141 represents the calculated spectral ratio for three different paint systems. The ratio spectra show peaks higher than 1.0 in transparent regions. When the intensity is close to 1.0 the thick coating are opaque. However below 1800 cm^{-1} there are definite indications of reflectance which differ with corroded and uncorroded surfaces.

The intensity for the prominent peak at the 2200 cm^{-1} is plotted against the thicknesses for the three paint system in Figure 142. The signal decreases with a thickness of the paint. The highest signal is obtained for the Insignia White topcoat. A lower one is found for Dark Camouflage and the lowest for Dark Camouflage Type II Low IR. Using the measuring procedure adopted reflection from the metal was detected for 6 mil Insignia White, 4.39 mil Dark Camouflage gray and 1.76 mil for Dark Camouflage Type II Low IR.

The analysis shows that very small signal, spectral ratio close to 1.0, is obtained for 8.82 mil Insignia White, 7.47 mil Dark Camouflage, and for only 3.87 mil thick Low IR paint at the frequency region around the reflectance peak of 2200 cm^{-1} . A more detailed spectral analysis is needed for Low IR paint below 1800 cm^{-1} (Figures 140 and 141) to characterize the behavior at the lower frequencies.

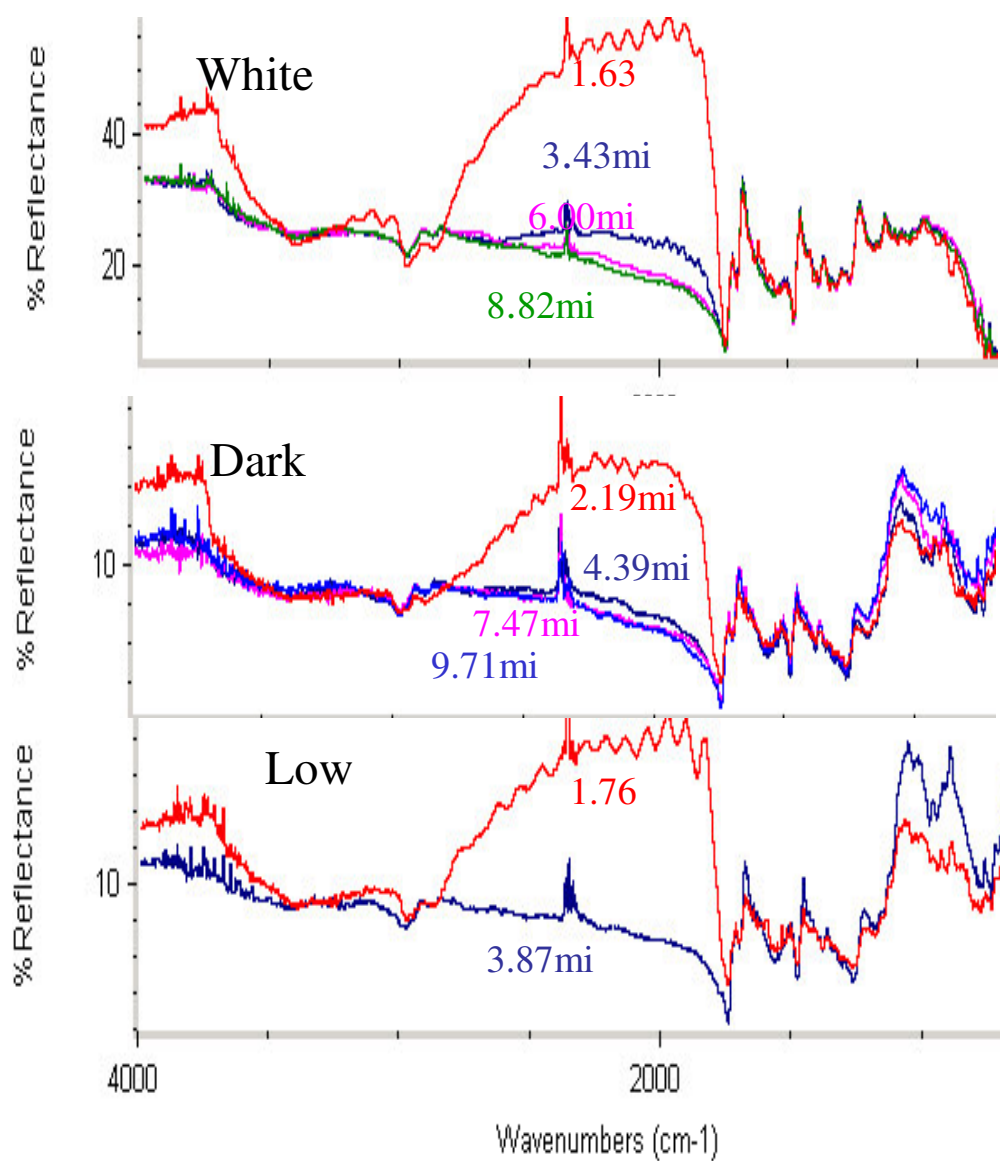


Figure 140 Effect of paint thickness on reflectance of painted non-corroded Al alloys 2024-T3.

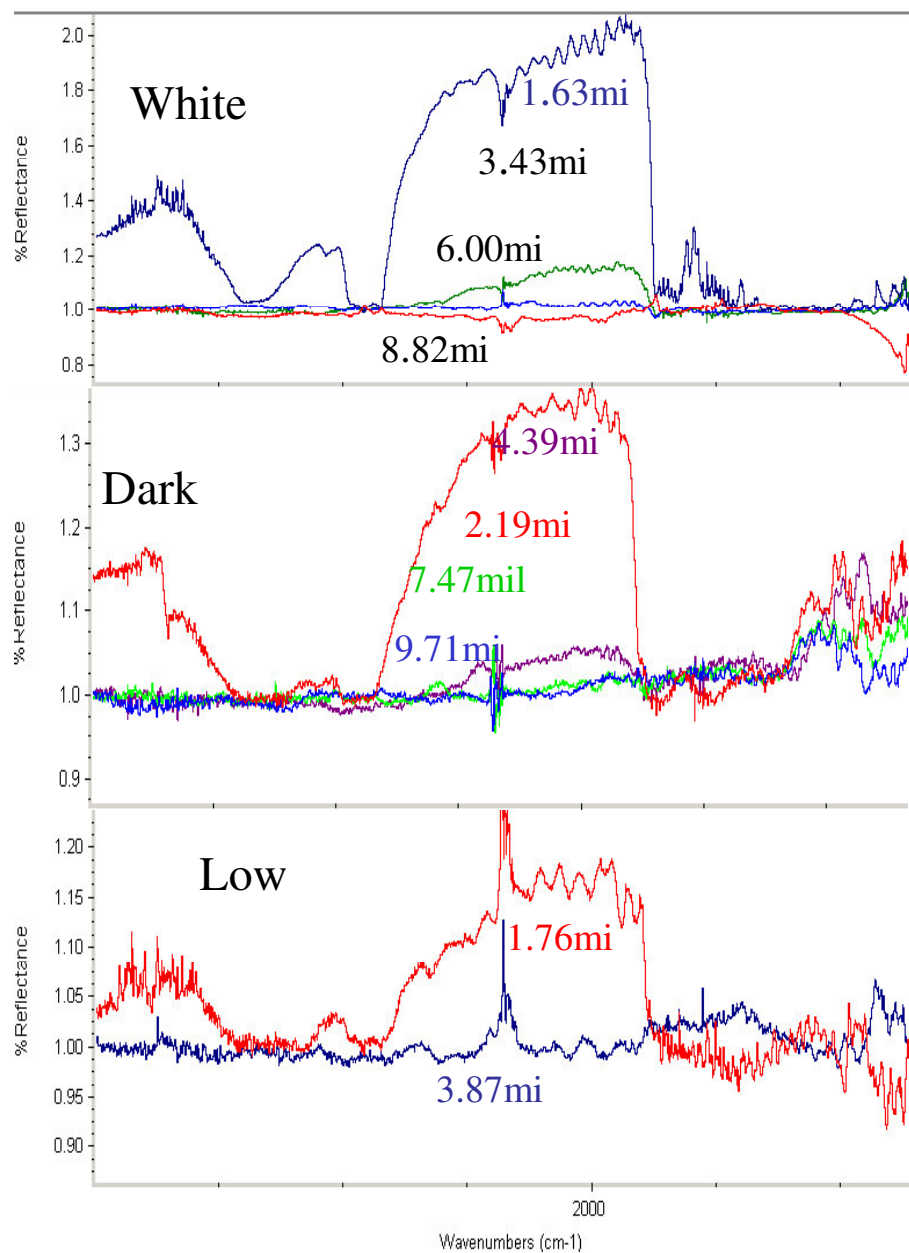


Figure 141 Reflectance spectral ratio of painted non-corroded/corroded Al 2024- T3 samples.

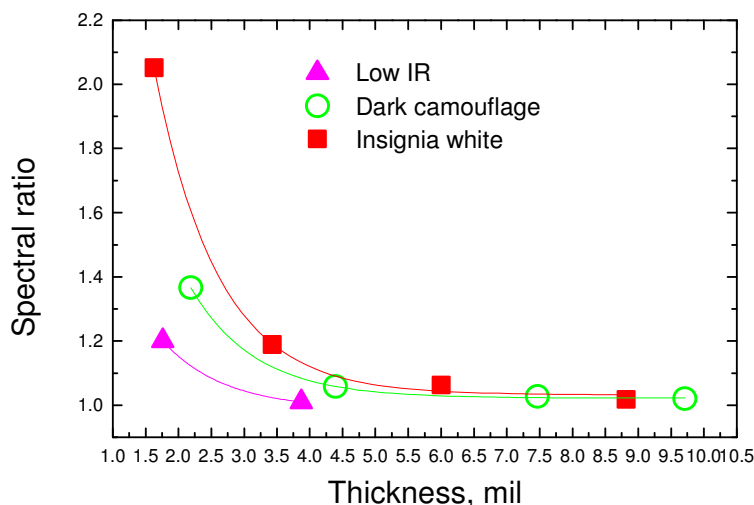


Figure 142 Reflectance spectral ratio vs. paint thickness for different paint systems.

Impedance Spectroscopy

Experimental Year 2002 – Localized impedance measurements were carried out with conventional electrochemical impedance equipment (Solartron Electrochemical Interface SI 12587 and Solartron Frequency Response Analyzer 1250). The equipment was tested with a series of capacitors in the range of 100 to 1 pF. It was found necessary to applying different voltage amplitudes to obtain the correct values of capacitance because of amplifier limitations. Hence, a 100mV was used for the high frequencies (6500 to 100Hz) and 10000mV for the low frequencies (1 to 100 Hz). The same procedure was applied to measure the capacitance of the painted samples. All measurements are performed at three or more sites on each sample and average values of capacitance were compared for corroded and non-corroded samples.

Several probes with different wet and dry contact areas were tested. The largest area was a copper disk with a cross sectional area of 3.14cm². A copper rod with a line contact, a hemisphere, and a point contact were also used. Wet contacts were introduced to eliminate the air gap between the probe and rough sample coatings which were most pronounced because of rough corrosion product layers on corroded samples having thinner layers of paint. A fast-wetting, conducting (~550mS/cm) ultrasound gel (Ultrage 2 supplied by Diagnostic Sonar Ltd) was placed between the probe and the coating¹.

Previously we found that the wet method had shown a distinct time dependence, which may have been caused by wetting or water penetration of the coating surface. The previous measurements down to very low frequencies (0.01 Hz) were made over long periods of time (30 min). The present measurements were made within 4 min as the lowest frequency was 1Hz.

Results Year 2002 – In order to determine any limitations with the impedance equipment, a series of measurements were made with multiple plastic foils sandwiched between the metal and a probe to simulate

different thicknesses of paint. Three plastic foils have been used: Saran (PVDC) (0.5mil), Mylar® (polyester) (3mil and 6micron) and aluminized Mylar® (1mil).

Figure 143a shows the capacitance in the frequency range 2000 to 100Hz for multiple layers of Mylar foil (3mil thick). Measurements were performed in a dry mode with the copper disk as a probe. The applied voltage amplitude was 10V for all layer thicknesses. Capacitance for very thin Mylar foil (6micron) obtained with 10V and 100mV amplitudes is given in the same figure. The 100mV curve is a flat line, while the 10 V curve has a sloping part in the high frequency region. The same behavior could be seen for the group of curves of the 3mil thick Mylar foil, where the thinnest layers have the slope. The comparison of the capacitance for multiple layers would be incorrect for the frequencies in the sloping region. A flat frequency response was therefore chosen for all comparisons.

The plot in Figure 143b shows capacitance at 100Hz vs. the number of reciprocal Mylar layers. A straight line is expected when the capacitance is plotted against reciprocal of layer thickness or number of layers. The expected straight line was not obtained. Reasons for the deviations could be due to the capacity loss because of the wiring or to the limitation of the instruments.

The copper disk probe in a dry mode was used for impedance measurements on painted panels. The results for White Insignia paint are given in Figure 144. Measurements were performed with two amplitudes, 100mV and 10V, in the frequency region from 6500 to 1Hz. Measurements at 60 Hz are always in error because of noise. Capacitance for non-corroded samples (Figure 144a) is decreasing with a thickness of the paint, while for non-corroded samples (Figure 144b) the thinnest paint has the lowest capacitance. A plot of the capacitance vs. reciprocal paint thickness (Figure 144c), gave the expected linear dependence for non-corroded samples, but non-linear curve with a maximum was obtained for the corroded samples. The obtained smaller than expected capacitance for thin paint layers on corroded samples, was probably due to the roughness of the corroded surface. The protruding corrosion product increased the gap between the probe and the aluminum reducing the measured capacitance. A similar behavior was observed for the Gray Camouflage and the Low IR paint.

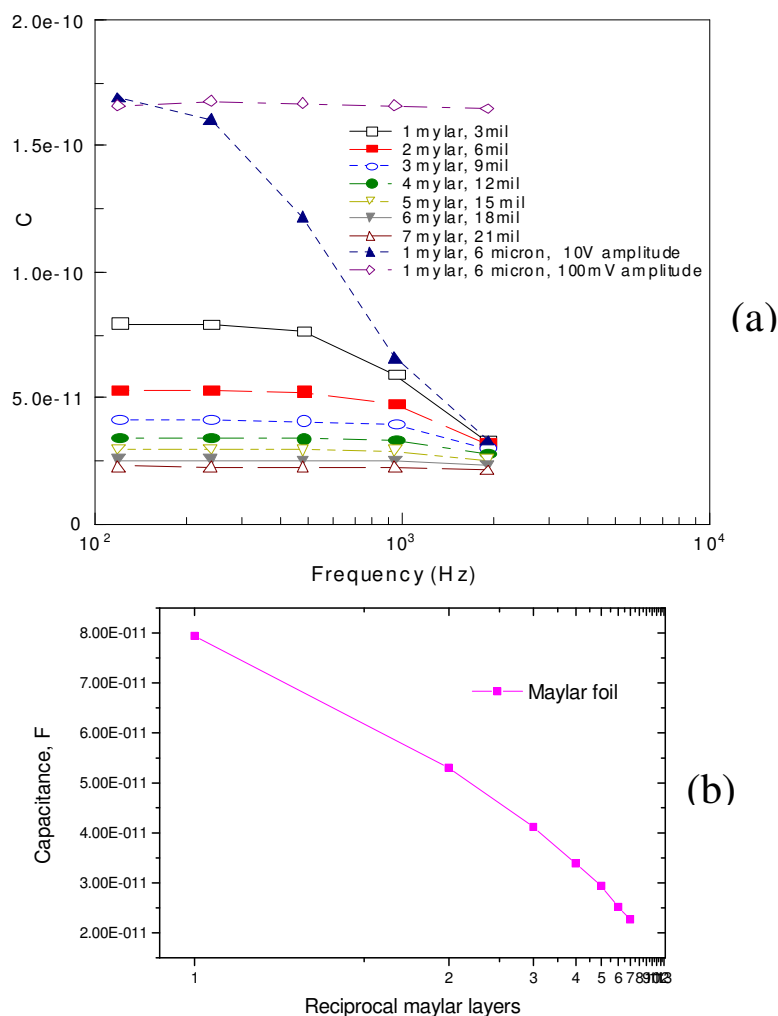


Figure 143 Impedance measurement of Mylar layers with a dry copper disk (3.14cm^2): (a) capacitance vs. frequency; (b) capacitance at 100Hz vs. reciprocal of the number of layers.

Using the gel as a wetting agent reduces this effect but does not overcome the non-uniformity of the painted surface. White paint with a gel and a stainless steel hemisphere as a probe having a contact area of 0.2 cm^2 , are given in Figure 145. Measurements were made at frequencies from 2000 to 1Hz with a voltage amplitude of 10V. It is seen that capacitance of both corroded and non-corroded samples (Figure 145a) decreases with the paint thickness. Capacitance at 1500 Hz for the corroded and non-corroded samples is plotted vs. reciprocal paint thickness (Figure 145b). Significant differences for the corroded and uncorroded samples was again observed up to 4mil indicating that the thinner films were not changing in a predicted manner and was not only due to surface roughness producing an air gap between the sample and the probe.

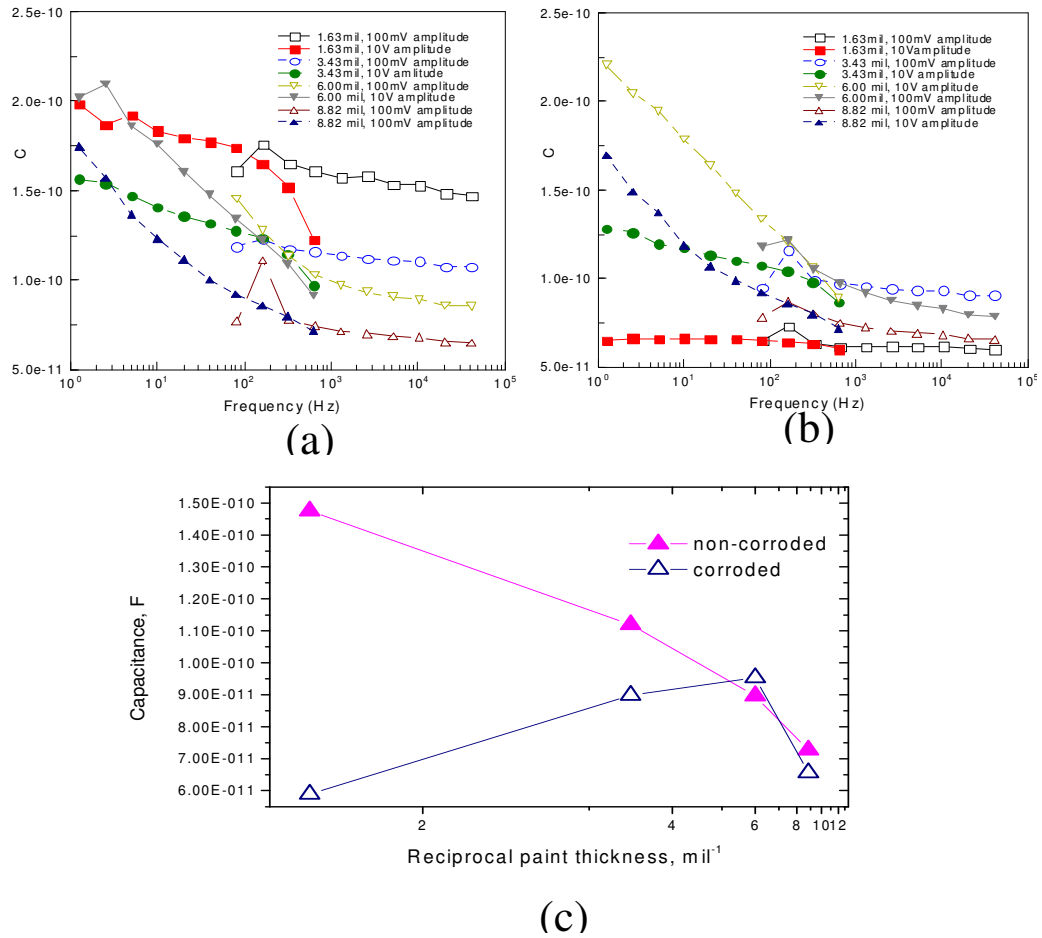


Figure 144 Impedance measurements of Insignia White paint on Al alloys 2024-T3 with dry copper disk (3.14cm^2): (a) Non-corroded; (b) Corroded; (c) Capacitance at 650 Hz vs. reciprocal paint thickness.

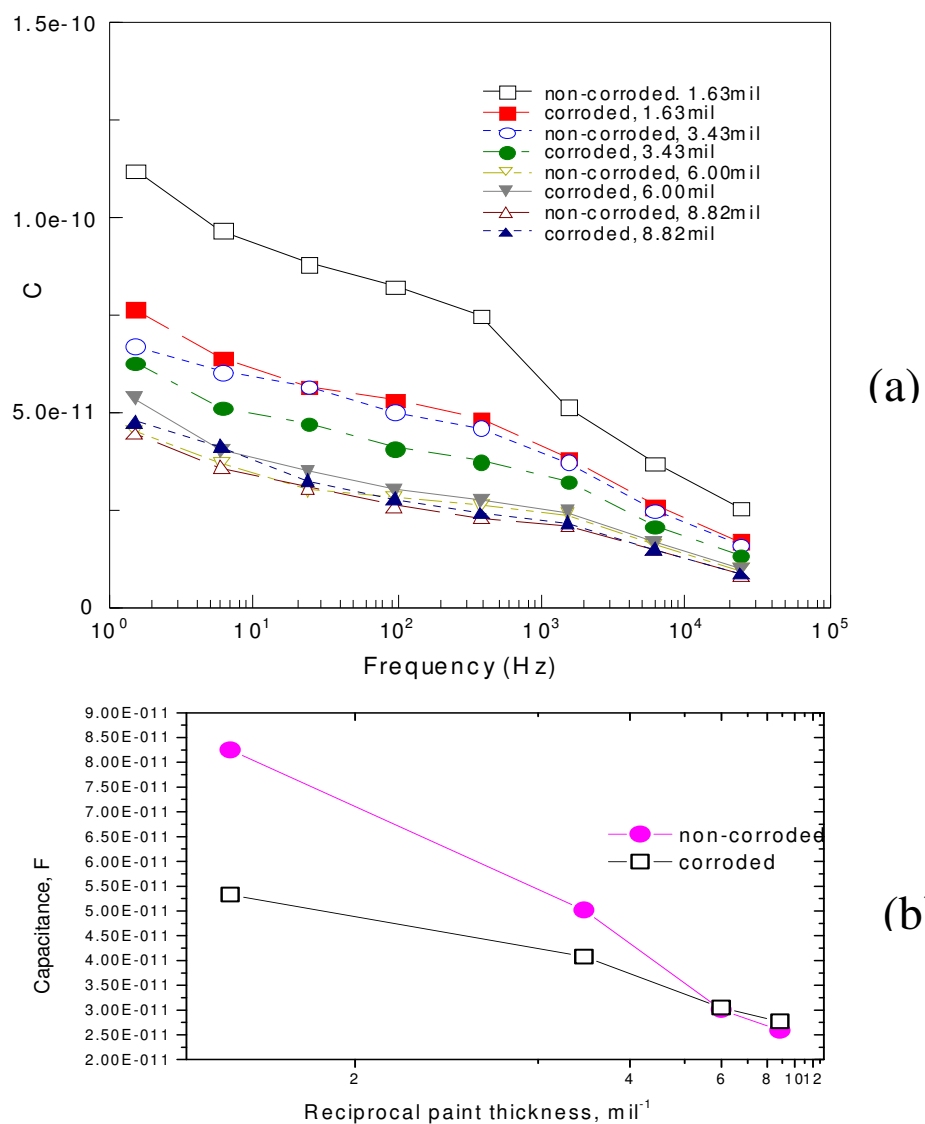
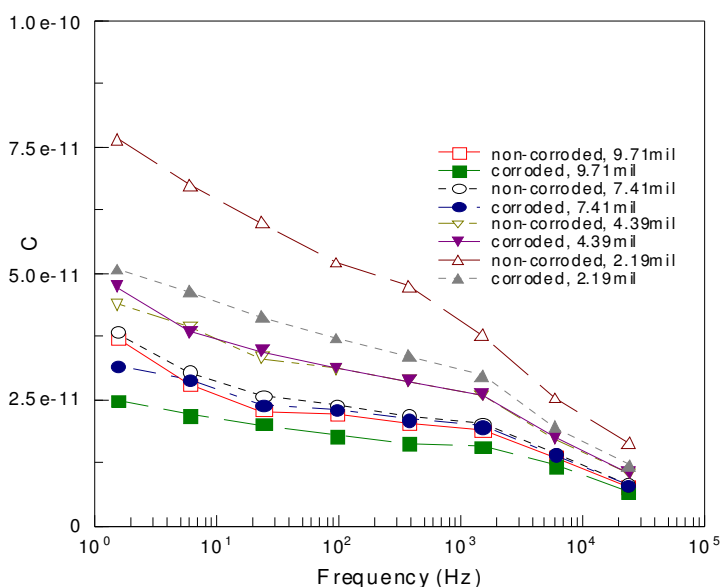


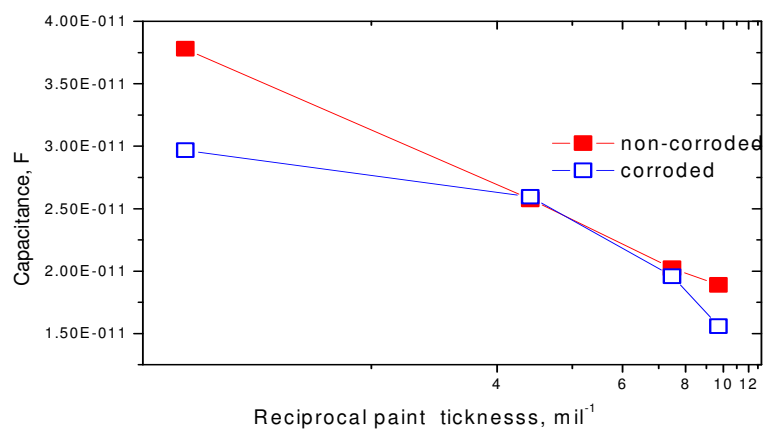
Figure 145 Impedance measurements of Insignia White paint on corroded and non-corroded Al alloys 2024-T3 with wet stainless steel hemisphere probe (0.2cm²): (a) Capacitance vs. frequency; (b) Capacitance at 1500 Hz vs. reciprocal paint thickness

Similar results are obtained with Dark Camouflage and Low IR paint system shown in Figures 146 and 147, respectively. The capacitance difference for corroded and uncorroded samples was again seen up to 4mil (Figure 146b and Figure 147b).

More research is needed to develop this technique to measure the small changes due to corrosion for the thicker coatings. There are several possibilities for improving the impedance measurements to locate corrosion under the thicker paint coatings with the higher impedances. These include the design of a fully protected shielded probe and connections to reduce stray capacitance.



(a)



(b)

Figure 146 Impedance measurements of Dark Camouflage paint on corroded and non-corroded Al alloys 2024-T3 with wet stainless steel hemisphere probe (0.2cm²): (a) Capacitance vs. frequency; (b) Capacitance at 1500 Hz vs.

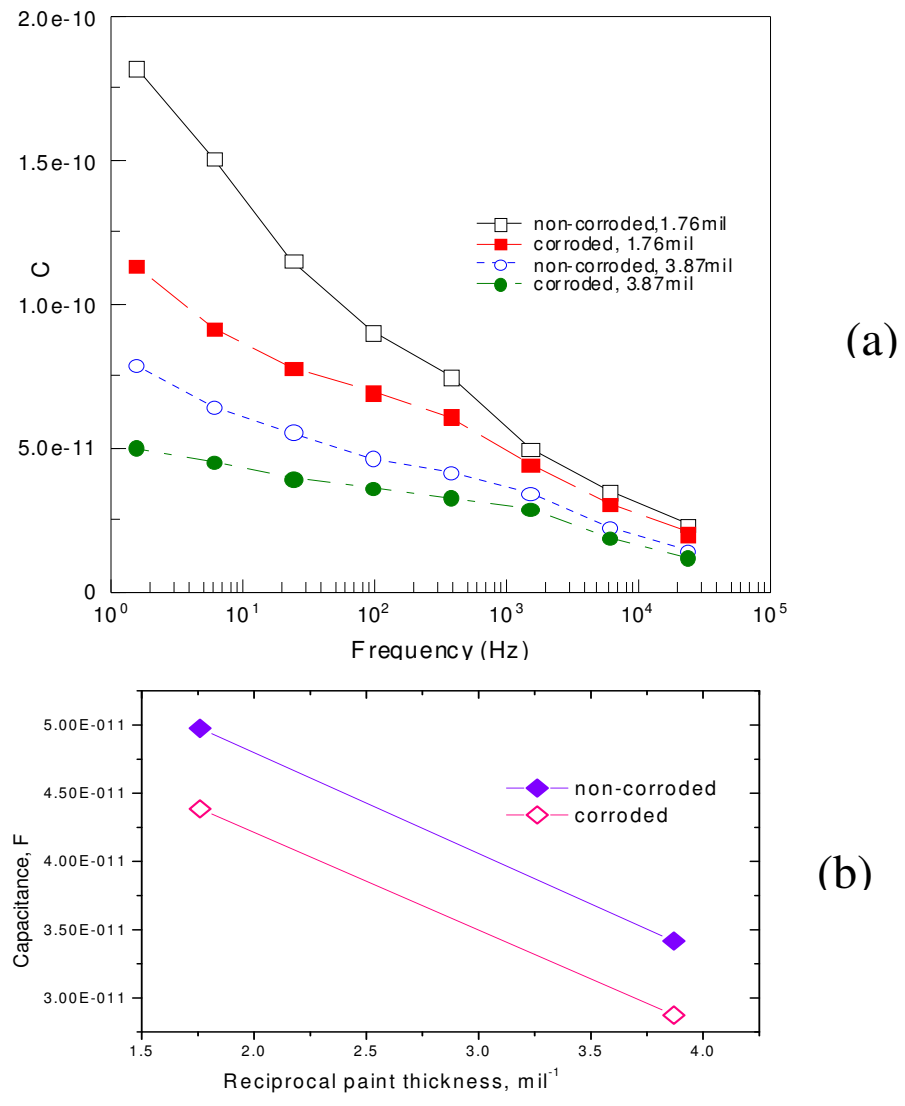


Figure 147 Impedance measurements of Low IR paint on corroded and non-corroded Al alloys 2024-T3 with wet stainless steel hemisphere probe (0.2cm²): (a) Capacitance vs. frequency; (b) Capacitance at 1500 Hz vs. reciprocal paint thickness.

Scanning Impedance Probes Year 2002

Experimental – A number of scanning probes for field studies of impedance measurements are being tested. Flat, round or rotating areas in contact with painted surfaces have been used. A disk probe had the largest contact area of 3.14cm². A rotating probe was a cylinder 2cm in diameter and 5 cm long. A stainless steel ball probe had a 1cm diameter. Each probe has advantages and disadvantages. The ball gave the best solution regarding the ease of movement over the surface. It should also offer the best resolution to detect small areas of corrosion. On the

other hand its smaller contact area reduces the signal making small differences, due to corrosion, difficult to measure. Scanning equipment was modified for Impedance Scanning Probe measurements. Measurements were made at 100 and 1000 Hz with amplitude of 50mV.

Results – Figure 148 shows the impedance scanning probe measurements over partially corroded painted Al alloy 2024. The sample was originally conversion coated A wedge shaped area was masked off and corroded, and then the sample was coated with 3.6mil thick White military paint. Figure 148a shows the photo of the sample before painting, indicating the scanned area. The generated images of the scanned surface are obtained by plotting the change in impedance. Measurements at 1000 Hz are shown in different three-dimensional projections (Figures 148b-d). The spikes on the edge between corroded and non-corroded area are probably due to the particles in the paint. The areas with the heaviest corrosion were apparent in the 3D plots.

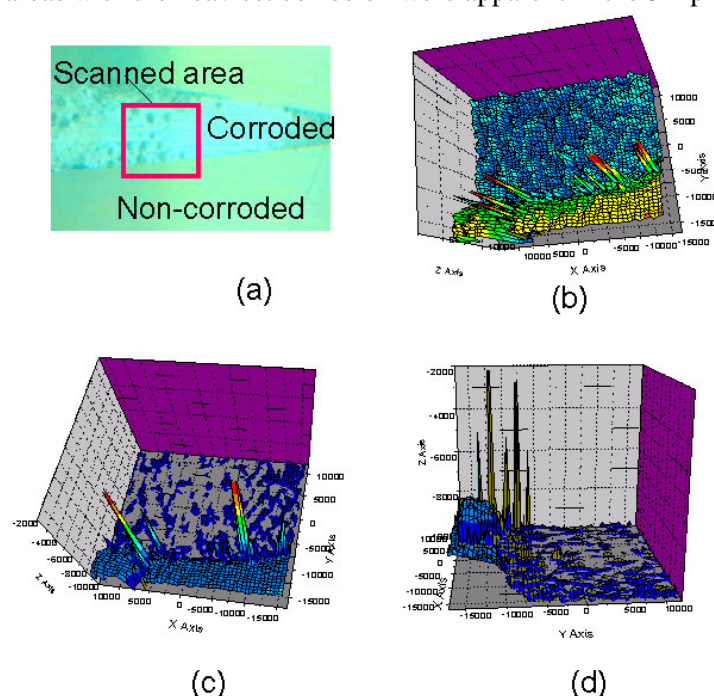


Figure 148 Scanning impedance probe measurements on painted Al alloy 2024:
(a) Photo of the sample; (b), (c), (d) Three-dimensional plot of impedance change over the scanned area.

IMS Conclusions Year 2002

IMS measurement showed limitation associated with the type of paint. In particular transparency for a low IR paint was limited to 2 mil. Impedance measurements on corroded Aluminum alloy 2024 standards, covered with multiple layers of paint, have shown a complex behavior for the thicker films of paint. The presence of corrosion could be detected for all types of paint up to 4 mil. However, results for thicker layers of paint were not sensitive to changes in coating thickness or to the presence of corrosion. The impedance scanning probe technique was developed and the first results show corrosion through 3.6 mil paint.

CONCLUSIONS AND FUTURE WORK

SNDE

Northrop Grumman has made substantial progress in the implementation of the SNDE concept. Specifically, we have developed a database of spectral reflectances of a variety of coatings and coated substrates. In addition, we have modeled the reflectance of corroded aluminum. A data analysis technique was developed to permit the detection of moderate amounts of corrosion at thickness up to 10 mil of topcoat.

While work continues on the completion of the DHR database and SNDE data analysis techniques, we will begin the development of a simple shop based application of the DHR SNDE technique. This will include investigation of the use of fiber optic cable to connect a reflectance head to a spectrometer. Using a limited number of spectral bands as determined by the database, a simple system using an IR source and few selected filters may all that is need to complete this system.

Work will also begin on the wide Area spectral Imaging (WASI) system. This will begin with a thermal IR imaging coupled to a number of IR band pass filters. Images in various spectral regions (transmissive and opaque) will be ratioed to reveal contrast formed by corrosion products and the metal/paint interface.

Impedance Measurements

Probes for the measurement of impedance on coated surfaces have been developed. The results obtained have shown that the impedance methods can clearly detect changes on a range of alloys with different surface preparations with and without scribing to accelerate corrosion. This approach with samples, exposed to standard salt fog and to humidity testing, will be extended. More accelerated corrosion methods will be used to establish the appropriate solutions for use with heavily corroded samples to identify the corrosion sites. Measurements will be made with painted samples where the paint has been undermined by the corrosion process and where corrosion is present and the coating is intact or the surface has been re-coated burying the corrosion.

The impedance measurements to detect the sites of corrosion under intact coatings will emphasize high frequency measurements that respond to capacitance changes due to thickness increases and changes in dielectric constants due to the growth of corrosion products.

Scanning Volta Potentials Measurements

Volta potential measurements using conventional Kelvin probe methods and conducting gases have been investigated. The conducting gas technique is significantly more easy to use because of less stringent height restrictions and expected simpler instrumentation.

The conducting gas technique has been found to give high potential measurements because of charging of the simulated painted surface. The high voltages make the method highly sensitive to the detection of defects in coating. However, the effect of the degree of charging of painted surfaces and its effect on the detection of corrosion under painted surfaces must still be investigated in the future.

The conducting gas technique, has used x-rays to create the ionize gas. This approach is not applicable for application to aircraft. Alternative methods will be tested. One approach will be to use a spark source in a confined volume and flow the ionized gas from this source to between the coated surface and scanning reference electrode.

Environmental and Business Case

See Appendix 7 for actual calculations.

An analysis for the implementation of the newly developed Infrared Reflectance Technology used to detect defects under coatings has been conducted and estimates for pollution reduction and the cost avoidance have been made for the aircraft industry. The figures calculated below are based on deployed aircraft and exterior coating material usage per aircraft. Additionally, these figures are based on the use of long-life topcoats systems that are currently being applied to both military and commercial aircraft. The infrared inspection technology, as configured and developed by the SERDP 1137 Project enables inspect under these long-life coatings for corrosion, cracks and other potential structural defects. Hence, the long-life coatings do not have to be stripped every five years just for inspection purposes. This improved inspection method results in both a significant reduction in pollution and cost avoidance.

Investment for Military and Commercial Aircraft

\$7 Million over two Years as follows:

- \$ 2 Million for Transition related Development Work
- \$ 5 Million for Equipment/Standards/Procedures/Manuals

Aircraft Industry Cost Savings

- Commercial Aircraft \$160 Million per year
- Military Aircraft \$40 Million per year

Aircraft Industry Environmental Benefit/Savings

Volatile Organic Compounds (VOC) from Paint Formulations

- Commercial Aircraft 279,982 lb per year (Saving)
- Military Aircraft 48,418 lb per year (Saving)

Volatile Organic Compounds from Paint Strippers (Estimated)

- Commercial aircraft 1,572,827 lb per year (Saving)
- Military Aircraft 330,152 lb per year (Saving)

Chromates (Carcinogenic Compound)

- Commercial Aircraft 21,282 lb per year (Saving)
- Military Aircraft 7,907 lb per year (Saving)

The full implementation of the Infrared Inspection System developed under the SERDP 1137 Pollution Prevention Project when used in conjunction with an extended life topcoat will have a net environmental impact of reducing pollution generated by the application and removal of aircraft paints by 2,231,379 lb of volatile organic compounds (VOC) and 29,189 lb of carcinogenic chromates per year. Additionally, the implementation of this “under the coating inspection system” in both the commercial and military aircraft industries will have the potential of generating an estimated cost avoidance of \$200M per year which can easily justify an initial one time global investment of \$7 million for the cost of implementation over a two year period. Individual aircraft programs and other vehicles or structural items requiring inspection by removal of paints may take advantage of this novel inspection tool along with the reduction in pollution and associated cost benefits.

REFERENCES

- Almond, D., and Patel, P., Photothermal Sciences and Techniques, Chapman and Hill, London (1996)
- Elachi, C. Introduction to Physics and Techniques of Remote Sensing, John Wiley and Sons, New York (1987)
- Hilgeman, T. *The Agile Bandpass Tunable Filter in Target Recognition*, proceedings of the IRIS Specialty Group on Passive Sensors (1996)
- Pistorius, P.C., “Electromechanical testing of intact organic coating,” ICC International Corrosion Council, 14th International Corrosion Congress, Co-operation in Corrosion Control, 26 September-1 October 1999, Cape Town, South Africa
- Conway, B. E., “Electrochemical Supercapacitors”, p.467, Kluwer Academic Publishers, New York, 1999

APPENDIX A1

Success Story

The following success story and informational sheets were handed out at the SERDP/ESTCP Partners Conference held in Washington, December 2002.

The function or purpose of the success story was to give a quick over view of the IR camera system's capability and to show the potential environmental and economic savings with the application of this system to aircraft maintenance. See handout below:

SUCCESS STORY

SERDP Pollution Prevention Program 1137 Nondestructive Testing of Corrosion Under Coatings

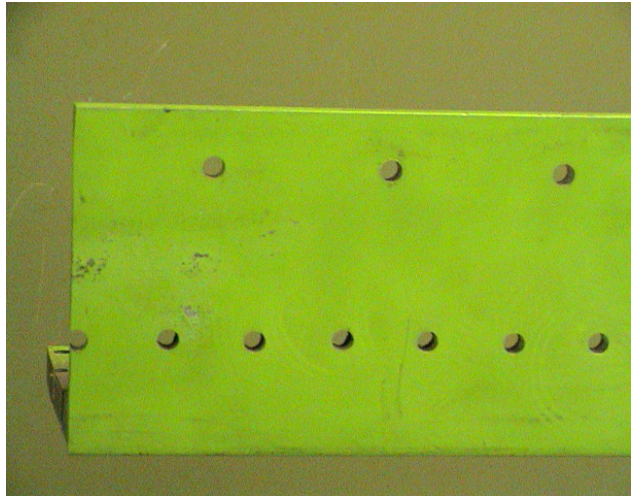
Invents and pioneers method to “see” under organic coatings to eliminate the requirement for stripping of organic coatings when required for structural inspection purposes. This newly developed technology enables aircraft maintenance facilities to minimizing environmental wastes and emissions associated with coating removal techniques and required finishing.

Demonstrating the concept of being able to visually see under organic coatings with IR vision in real time has previously eluded scientists and engineers. The

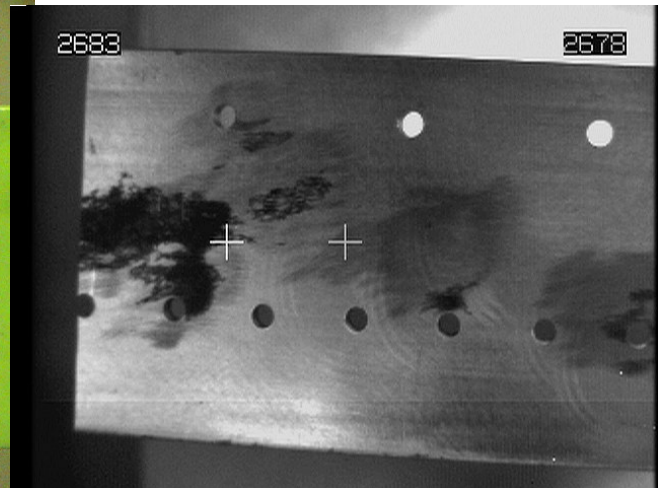
inspection under aircraft coatings for corrosion and other structural defects such as cracks, pitting, and gouges has been desired in order to eliminate the need to strip organic coatings from aircraft solely for inspection purposes. However, the means of accomplishing this task has not been technically available until just recently. The real technical issues involved producing images with high enough fidelity to see critical-size defects, which can adversely affect the structural integrity of aircraft. Once the fidelity issues were resolved by the use of this novel method of producing IR images, intelligent decisions about structural integrity such as in the case of aircraft can now be made. Essentially, understanding of the physics of IR transmission through organic coatings and pigments in conjunction with the application of commercially available, but modified, equipment established this patent-pending breakthrough.

It is anticipated that implementation of this technology, as developed under the SERDP Pollution Prevention Program, will significantly reduce pollution in terms of RCRA waste and hazardous air emissions for aircraft maintenance facilities. This IR advanced inspection technology makes possible the practical use of extended-life fluoro-polyurethane topcoat systems, which have the potential to protect aircraft structures for a period of up to ten years. Since aircraft coating removal is generally scheduled every five years due to coating degradation and the need to do structural inspections, the potential to save a significant amount of pollution is apparent, if a ten-year stripping and refinishing cycle is used in lieu of a five-year cycle. Associated cost savings from the elimination of one stripping cycle over the ten-year period makes the business case an economical option. Once the equipment is capitalized, a net positive cash flow will result with rapid payback. For a quick example, a Joint Stars aircraft (707 type) costs approximately \$250K to strip and refinish. Saving stripping this model aircraft on a one-time basis will result in a savings of at least \$150K, as the IR camera and associated equipment can be commercially purchased for well under 100K. In the above case, the payback period relates only to the lead times of ordering the camera and using it the first time.

Special Note: A video was created of the corrosion survey and played at the 2002 IPR. Corrosion was clearly seen around pasteworks and splice plates on the E-8 wing.



*J-STARS Part Showing
Green Primer Surface*



*Same J-STARS Part Showing
Corrosion Under Primer Surface Using
IR Reflectance Technology*

Example paint taken from E-8 aircraft above shows clear evidence of corrosion under the primer coating (BMS 10-11).

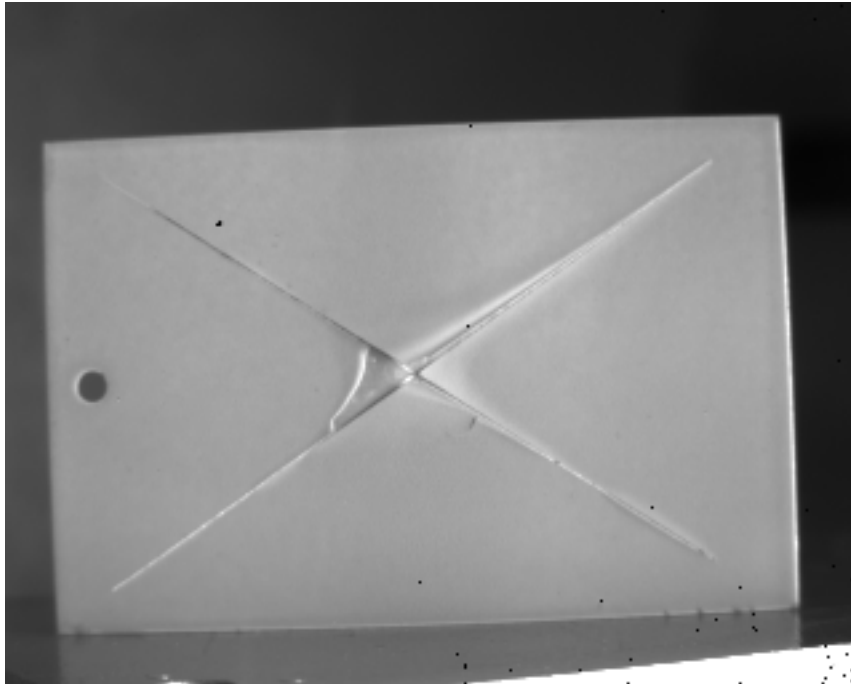
APPENDIX A2

Northrop Grumman
Laboratory Summary Report of a Corrosion Survey to Detect Corrosion
Under Chemical Agent Resistant Coatings (CARC)

The photographs attached to this summary report were made from bitmap files of the IR images digitally captured from the 320x256 pixel IR Merlin camera using an Infra Red reflectance technique. Each sample was imaged in its entirety. Some samples labeled “close” are images using the 25.4mm lens with the sample brought closer to the camera. For greater detail, a 1x magnification lens was attached to the IR Merlin camera. Those image files have a “1xmag” added to the sample name. The following is a description and/or interpretation of observations, as seen from the IR photographs taken during the visit by Steve Cargill. It should be understood that this is the first time CARC coatings were actually observed using IR Reflectance, as a method of detecting corrosion under coatings and that the process may have to be optimized to more fully understand the benefits and limits of the method for use to detect corrosion under CARC on steel panels. Each Numbered IR photograph is shown along with an interpretation of observations. As the actual surfaces on each panel under the coatings were unknown to the observers (Steve Chu and John Weir), the interpretations are solely based on the IR photographs.

Prepared by:

John Weir (516-575-5422) and Steven Chu (516-346-9285)
Northrop Grumman Corporation
South Oyster Bay Road
Mail Stop A01-26
Bethpage, NY 11714



21 C4

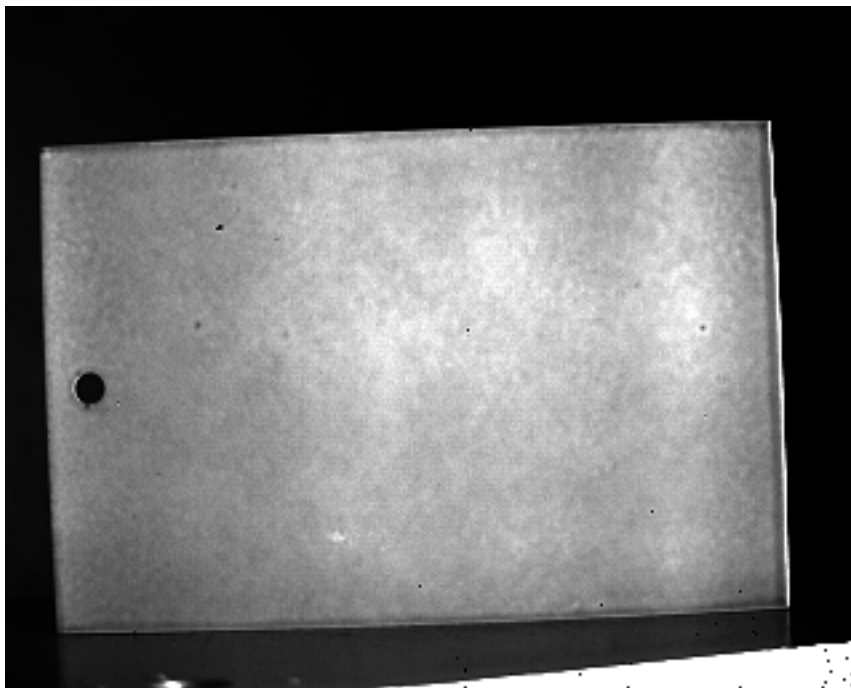
IR Photograph

Indicates Paint Peeling away from the substrate and corrosion in the scribe zone.



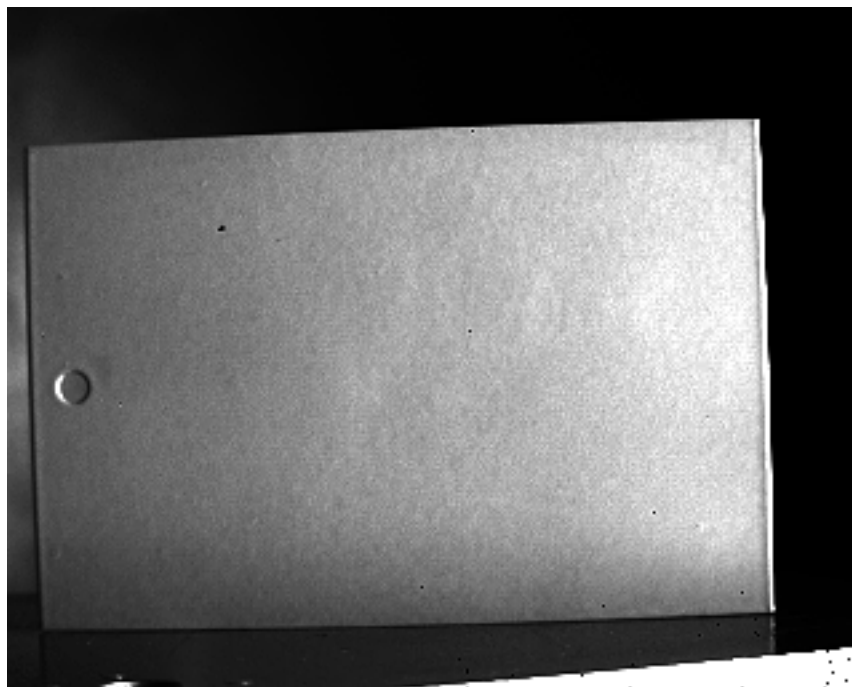
21 C4

Standard Illumination Photograph



21 j5

IR Photograph does not indicate the presence of corrosion.



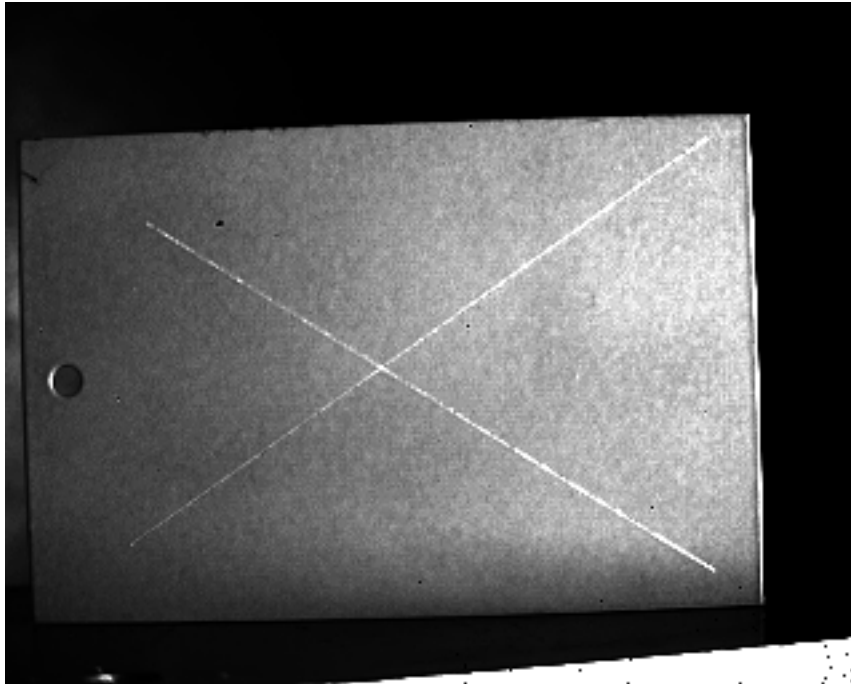
31 C2

IR Photograph does not indicate the presence of corrosion.



31 C2

Standard Illumination Photograph



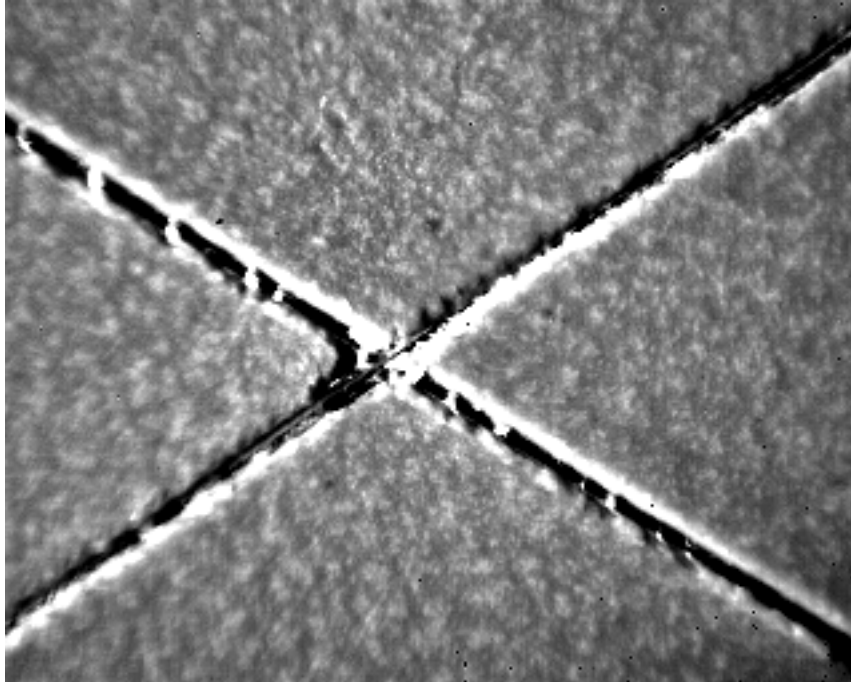
31 C4

IR Photograph indicates minor corrosion in scribed zone.



31 C4

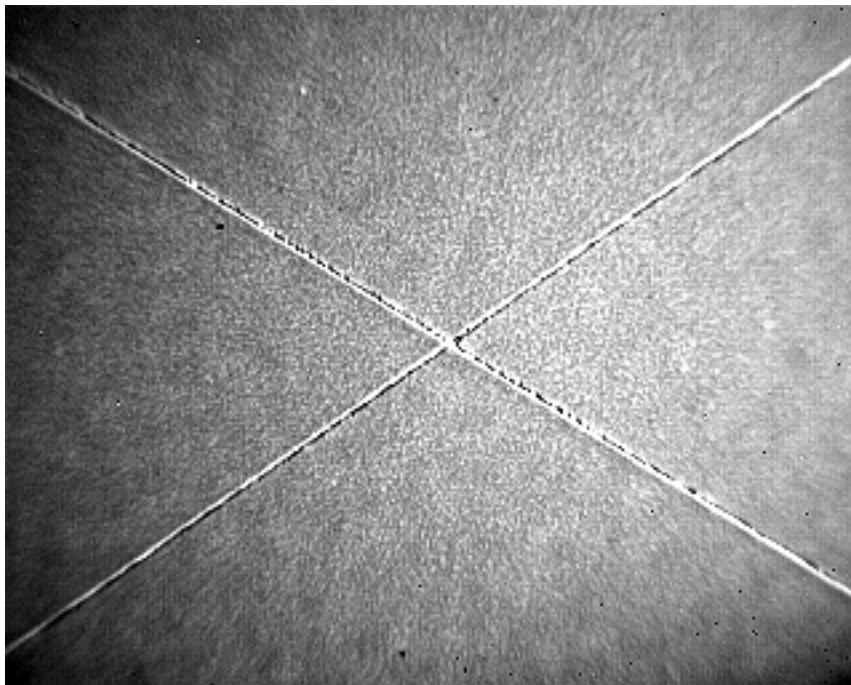
Standard Illumination Photograph



31 C4 (1XMAG.)

IR Photograph

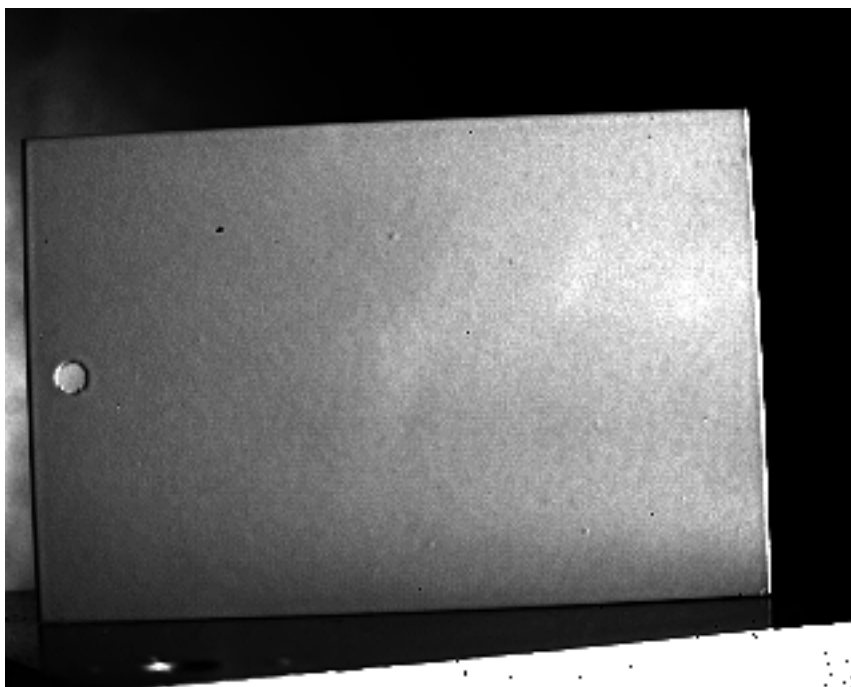
Corrosion present in scribed area and possible corrosion under coating to be confirmed after coating removal.



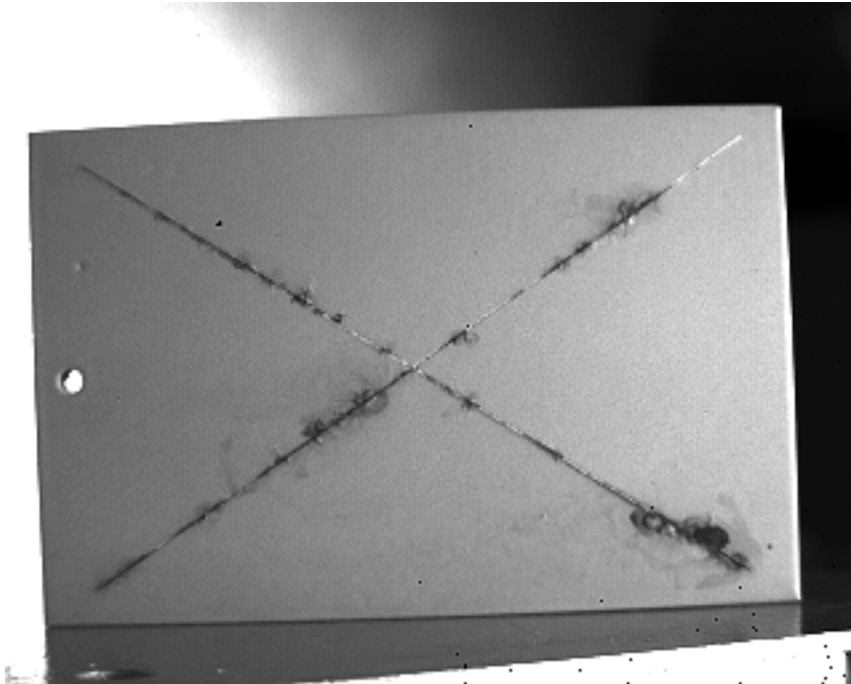
31 C4 (CLOSE)

IR Photograph

Observations same as 31 C 4.



31 j1
IR Photograph
No corrosion observed



47 C4

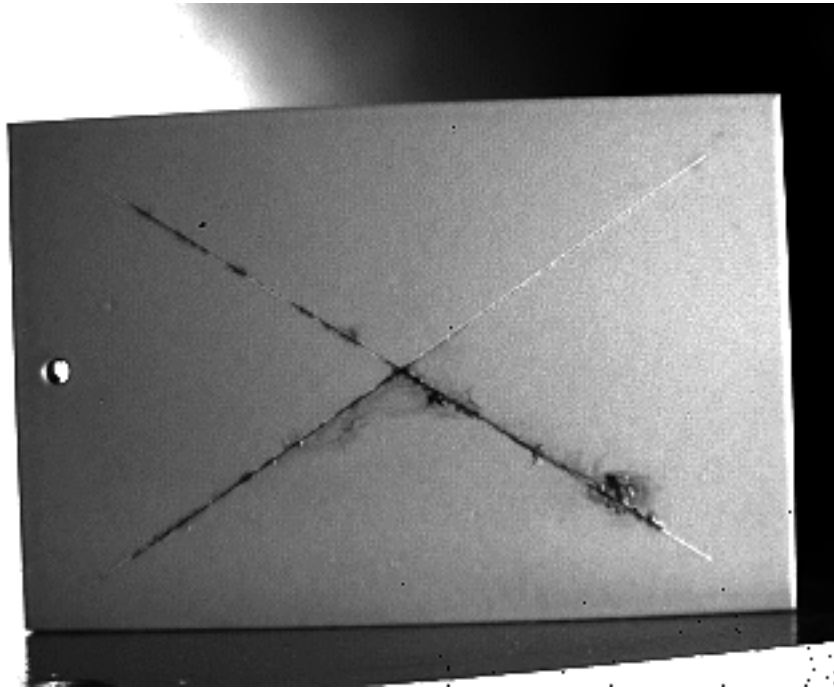
IR Photograph

Extensive corrosion in scribed area with corrosion under coatings extending from scribed area. Additionally there are indications of corrosion under the coating in areas that are not yet peeling.



47 C4

Standard Illumination Photograph



47 c5

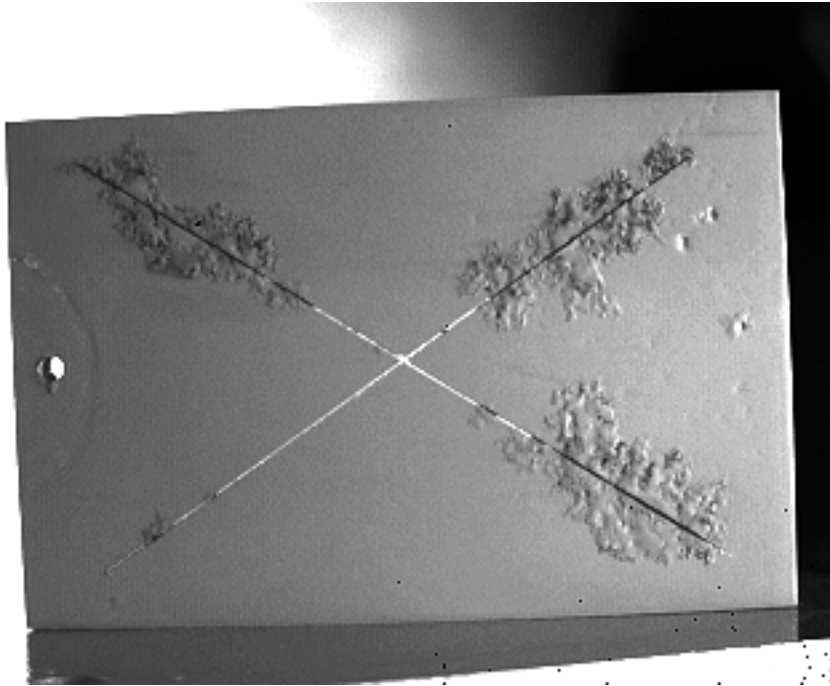
IR Photograph

Extensive corrosion under coatings in some areas adjacent to scribed areas.



47 c5

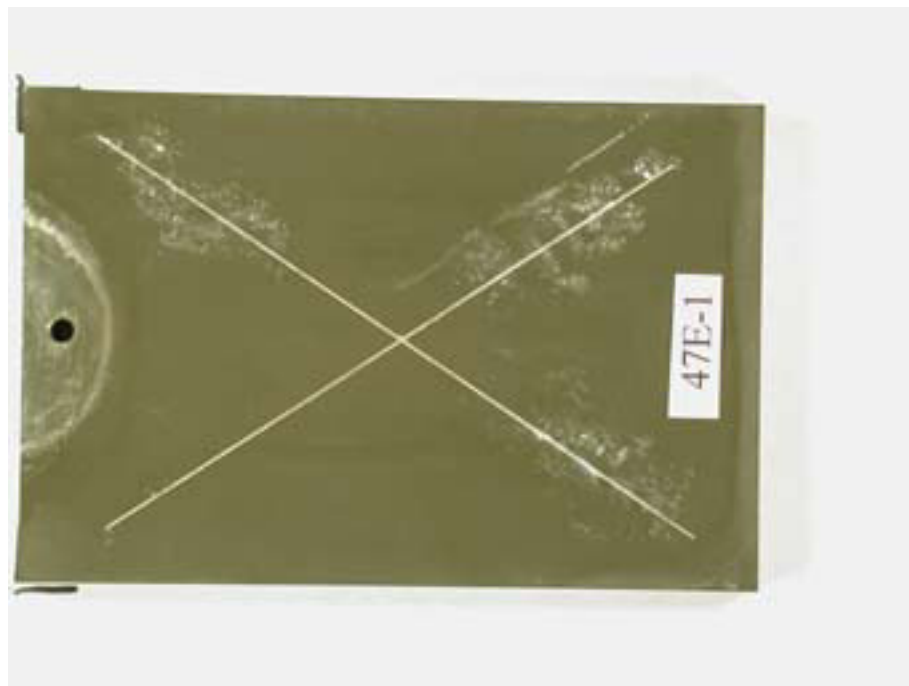
Standard Illumination Photograph



47 e1

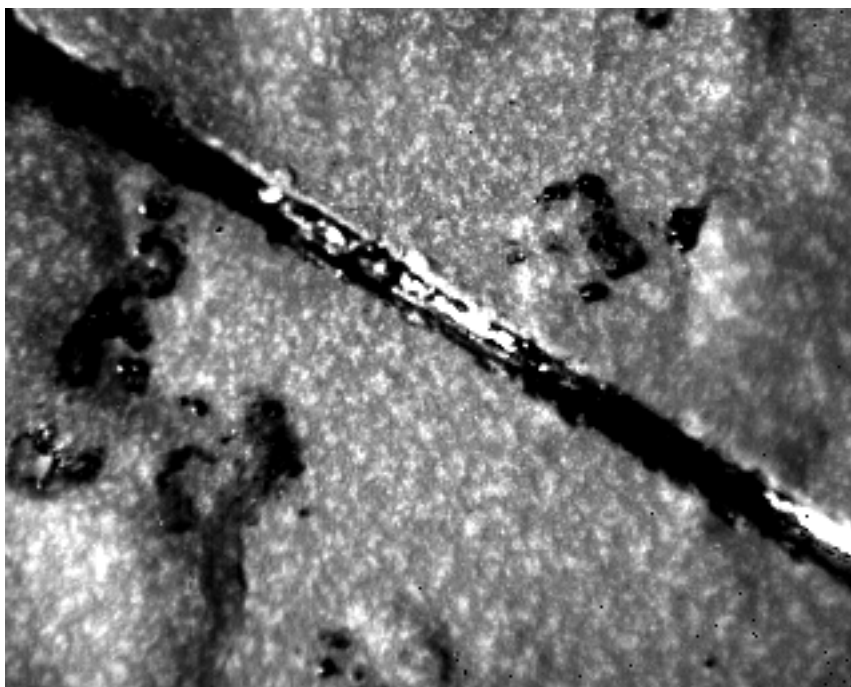
IR Photograph

Extensive corrosion observed under the coating in the local areas around the scribe.



47 e1

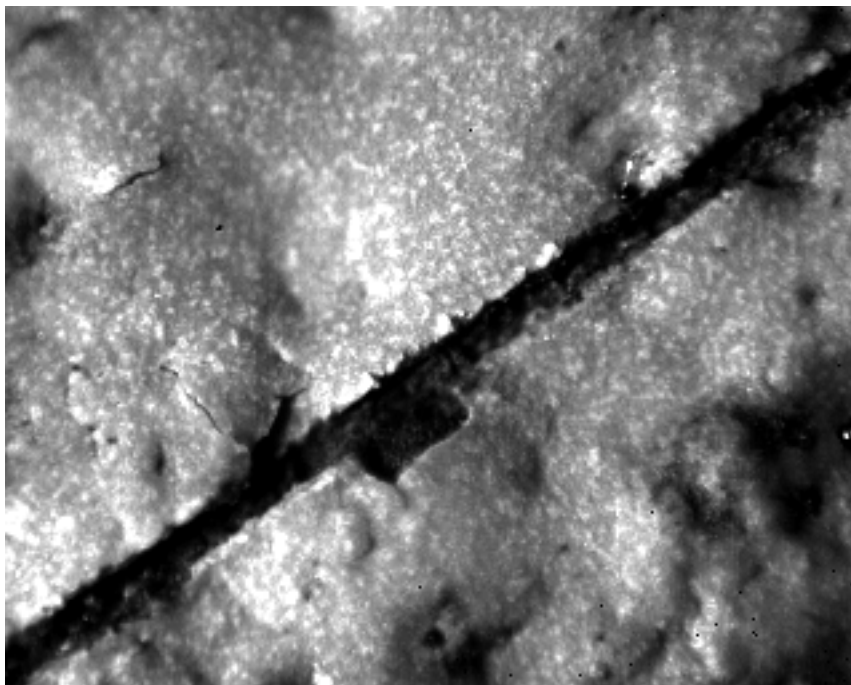
Standard Illumination Photograph



47 e1 (1XMag)

IR Photograph

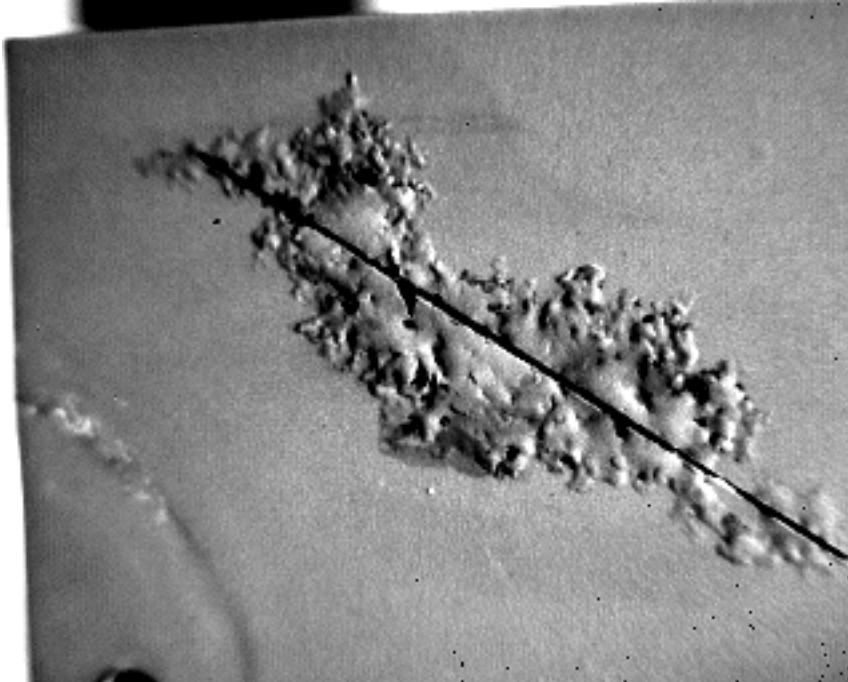
Photo indicates corrosion in scribe as well as some corrosion away from scribe.



47 e1 (1X Mag)2

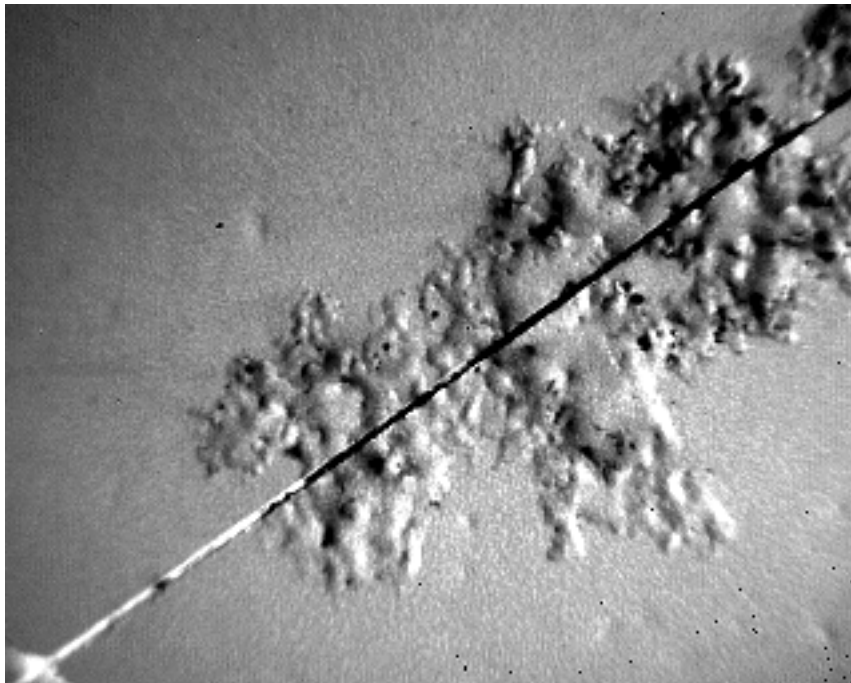
IR Photograph

Same as 47 e1, except indications of cracks in coating around scribed area.



47 e1 Close 1

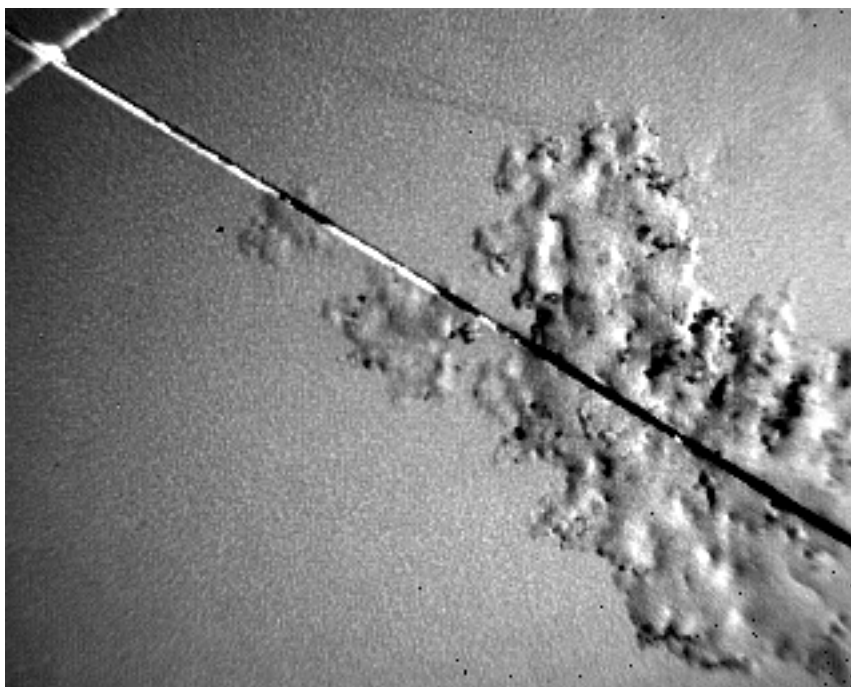
IR Photograph indicates extensive corrosion seen under coating, as well as corrosion in scribe.



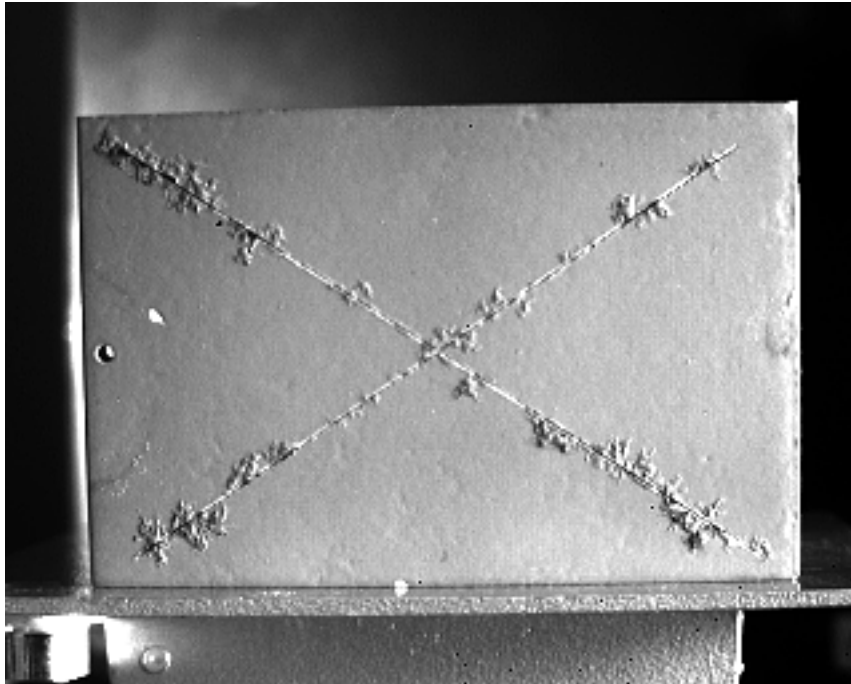
47 e 1 Close 2

IR Photograph

Comments same as 47 e1 close 1 above. Note: Corrosion under coating by corroded scribe. The non-corroded scribe area did not show indications of corrosion under the coating.



47 e1 Close 3
IR Photograph
Comments same as close 2 above.



47 e3

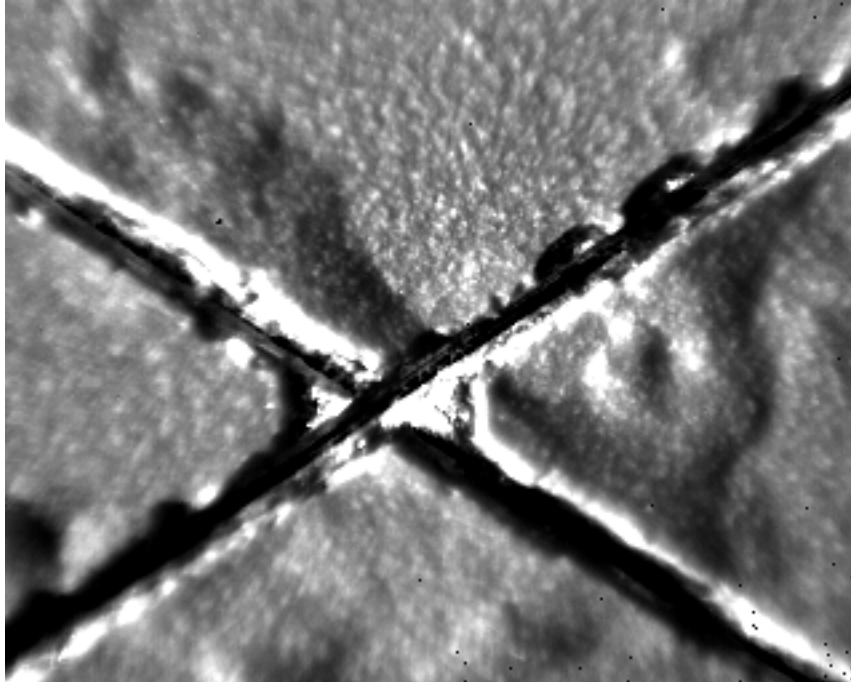
IR Photograph

Indicates corrosion under coating adjacent to scribed area that is corroded



47 e3

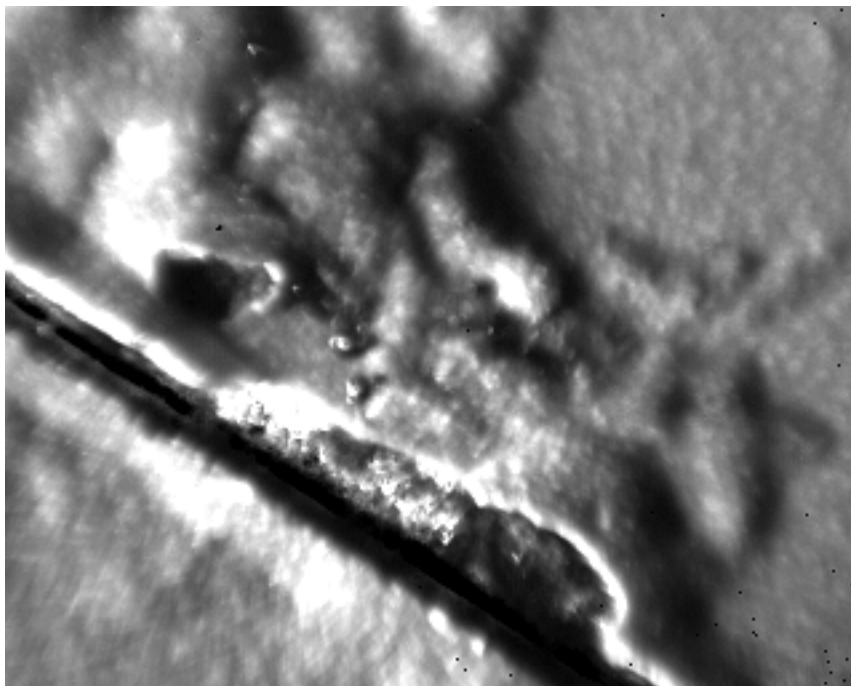
Standard Illumination Photograph



47 e3 (1 x Mag.)

IR Photograph

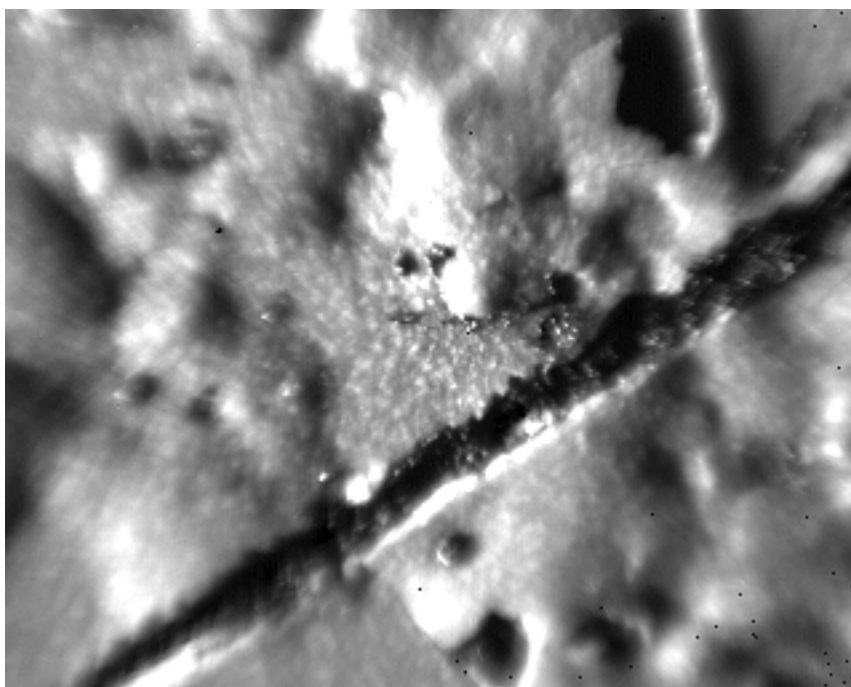
Indicates corrosion in scribe as well as corrosion under coating.



47 e3 (1 X Mag.2)

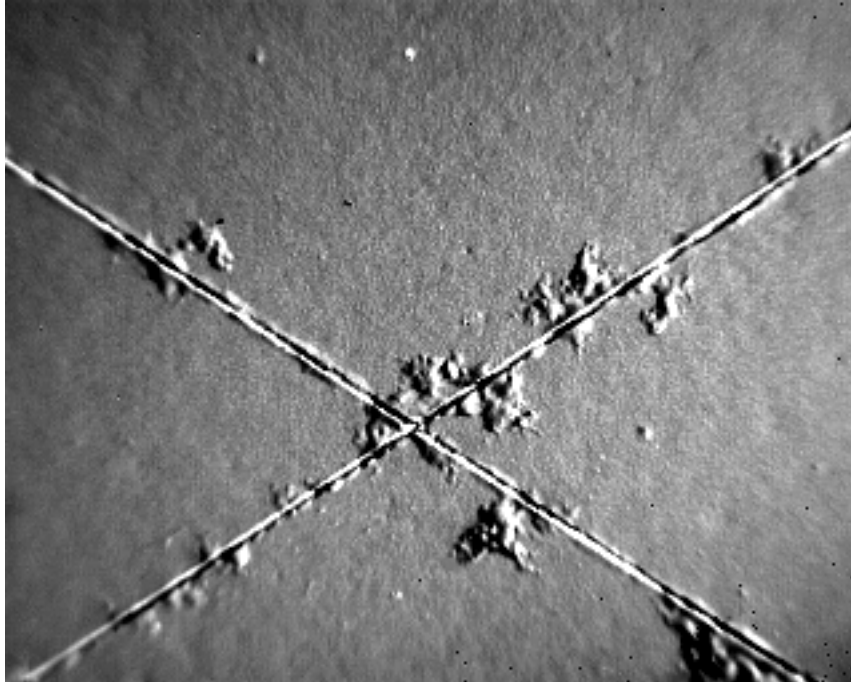
IR Photograph

Comments same as 47 e3 (1XMag.)



47 e3 (1 X Mag.3)
IR Photograph

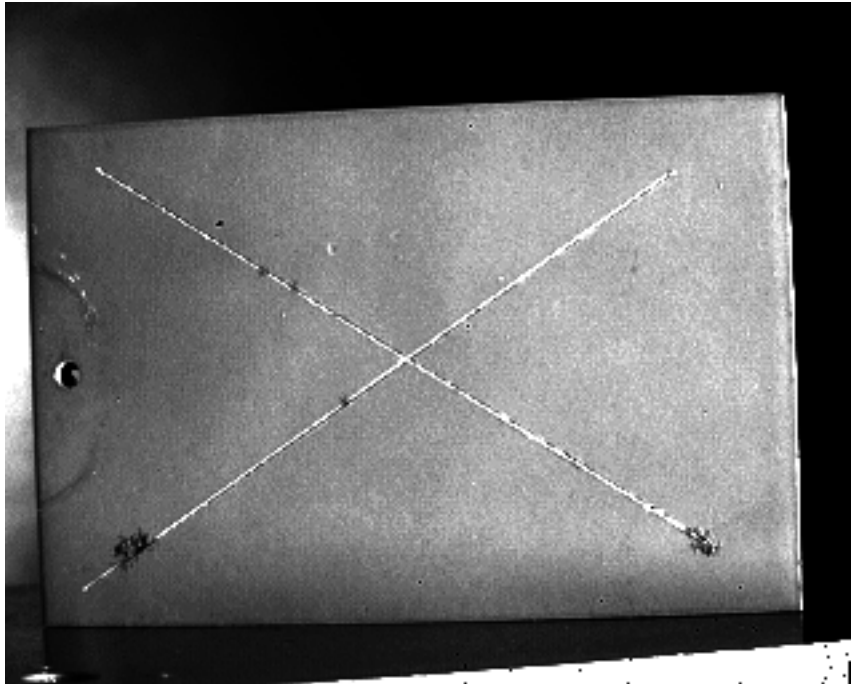
Comments same as 47 e3 (1XMag.2)



47 e3 Close

IR Photograph

Filiform like corrosion under coatings as seen on Photograph



47 e4

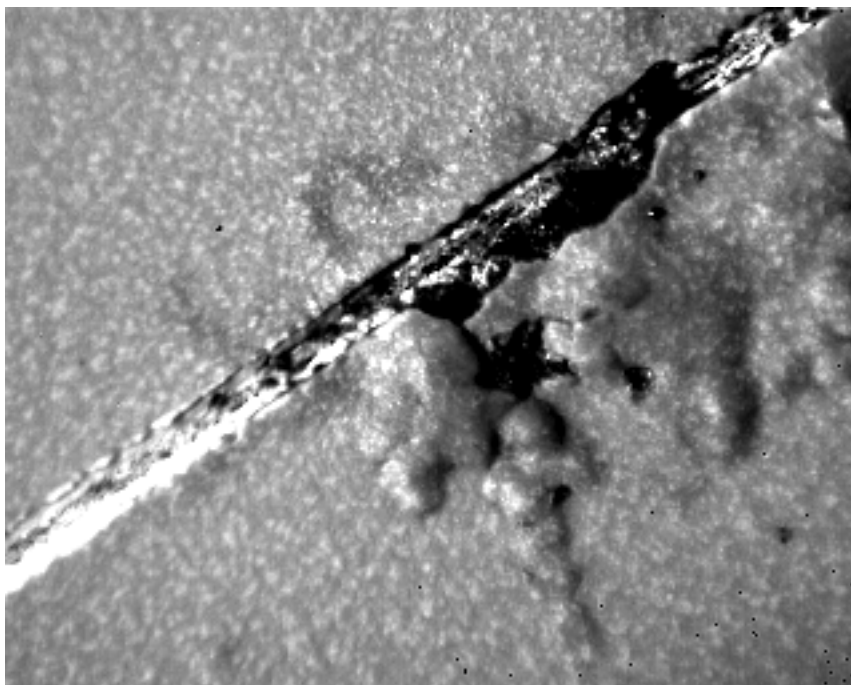
IR Photograph

Minor corrosion seen at end of each scribe is observable. Corrosion under coating is apparent at the end of each scribe.



47 e4

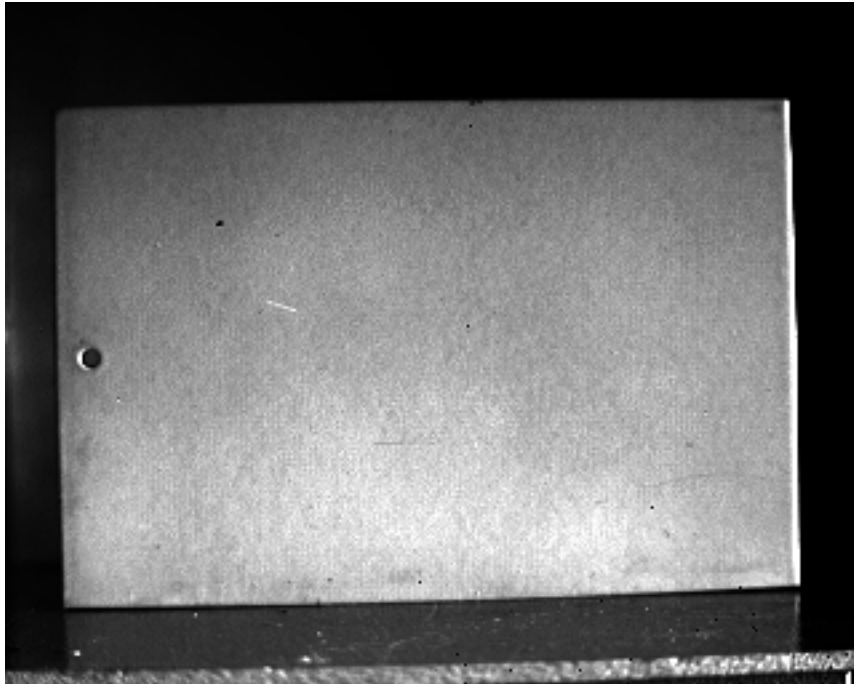
Standard Illumination Photograph



47 e4 (1X Mag.)

IR Photograph

Corrosion clearly visible under coating adjacent to corroded scribe area.



47 j1

IR Photograph

No corrosion apparent or detectable under the coating.



55 c3

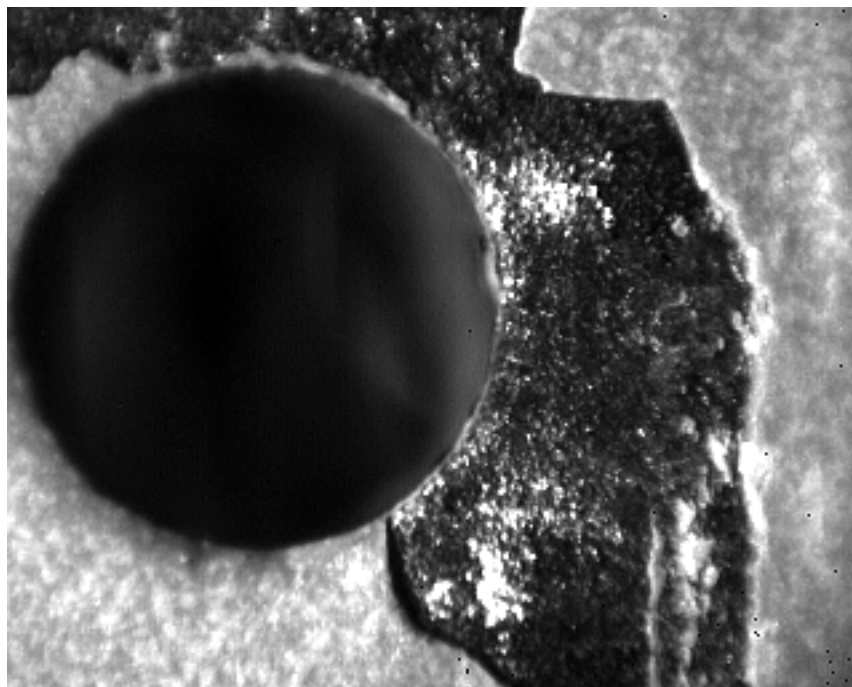
IR Photograph

Corrosion under coating is detectable by the hole in the panel.



55 c3

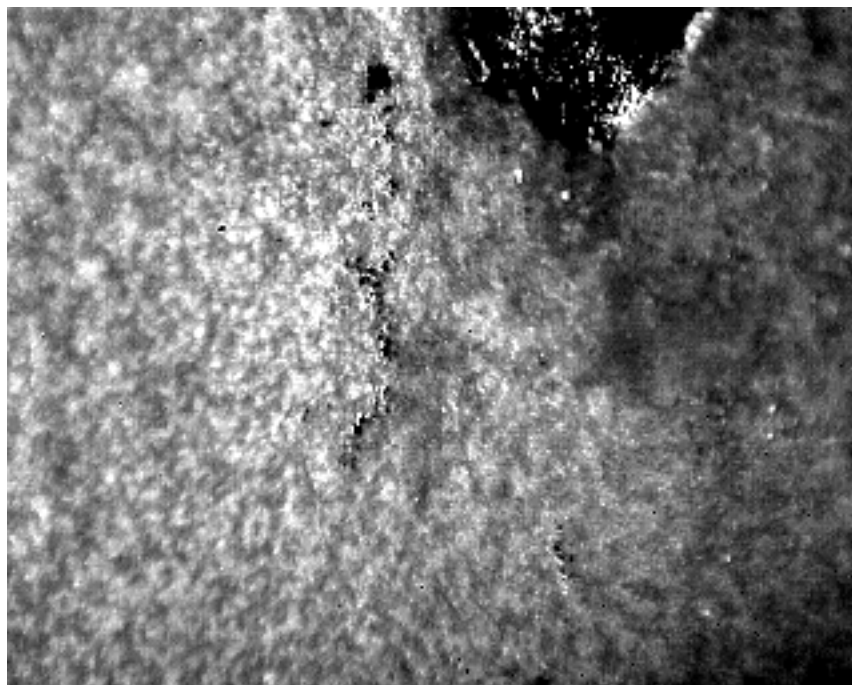
Standard Illumination Photograph



55 c3 (1XMag.)

IR Photograph

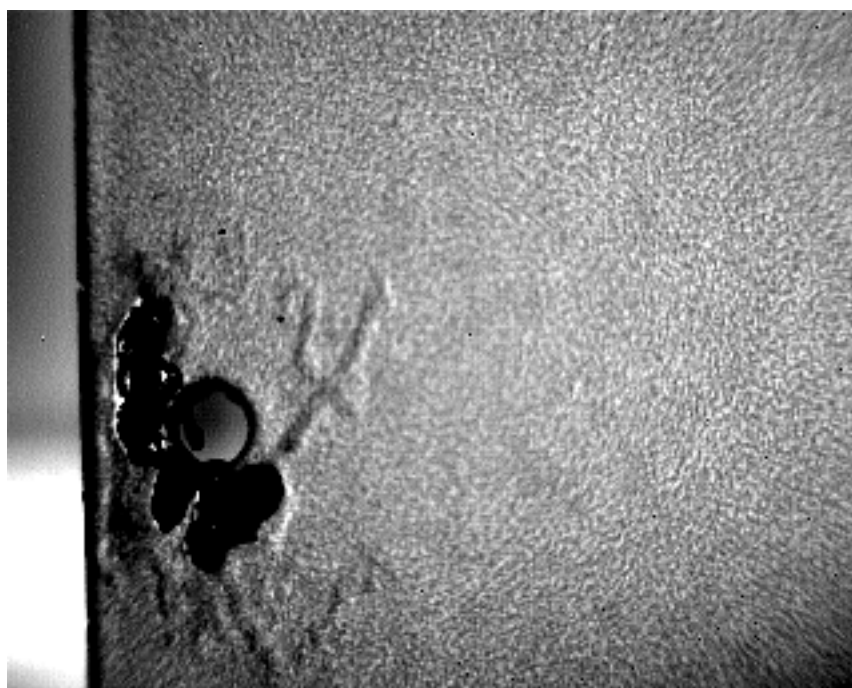
Corrosion quite apparent under coating next to hole in panel.



55 c3 (1Xmag.2)

IR Photograph

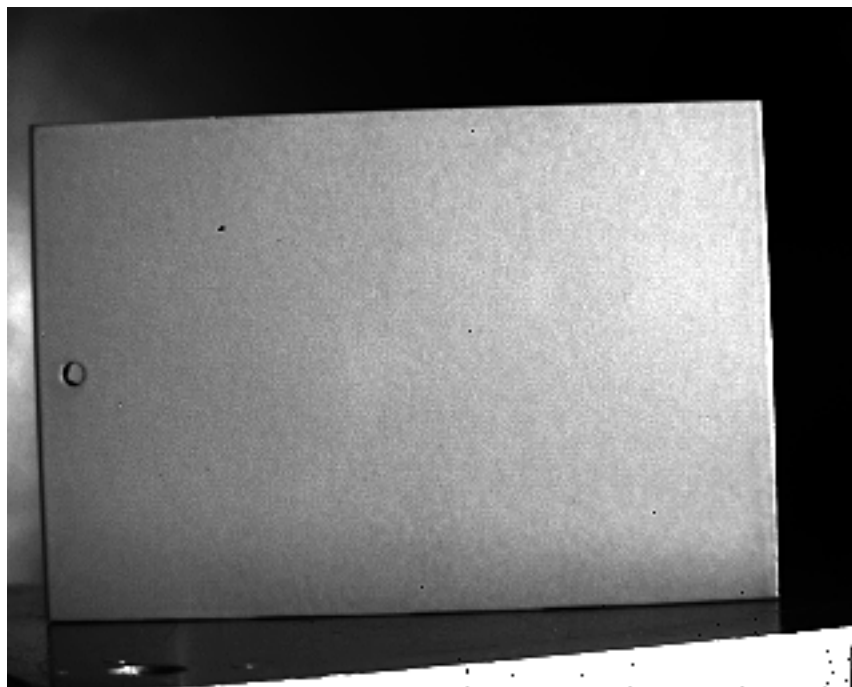
Corrosion under coating detectable next to hole in panel.



55 c 3 Close

IR Photograph

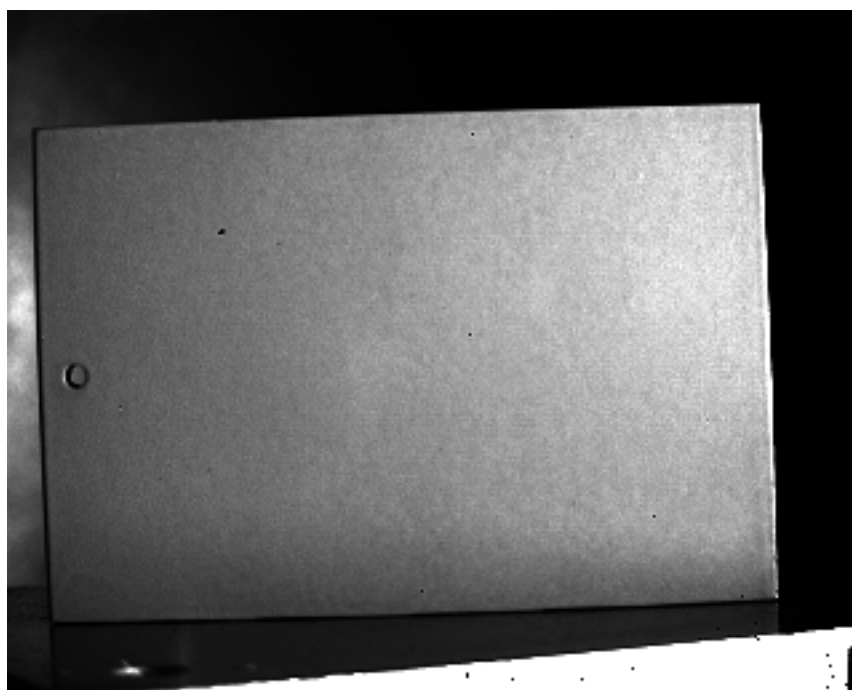
Corrosion detected near hole, as well as under coating.



55 j1

IR Photograph

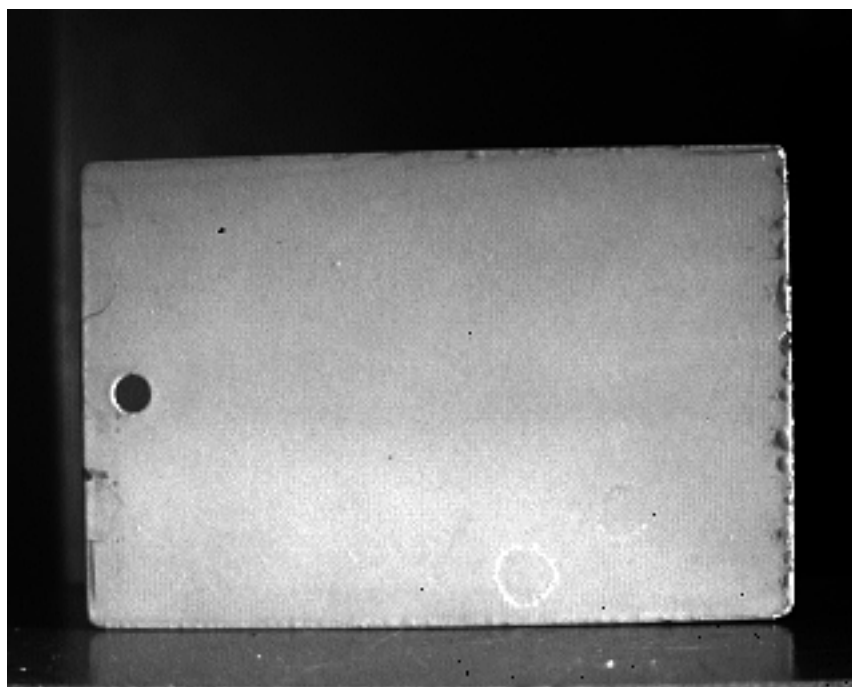
No corrosion apparent or detectable under coating.



55 j1b

IR Photograph

No corrosion apparent or detectable under coating.



7 c2a (Front Side)

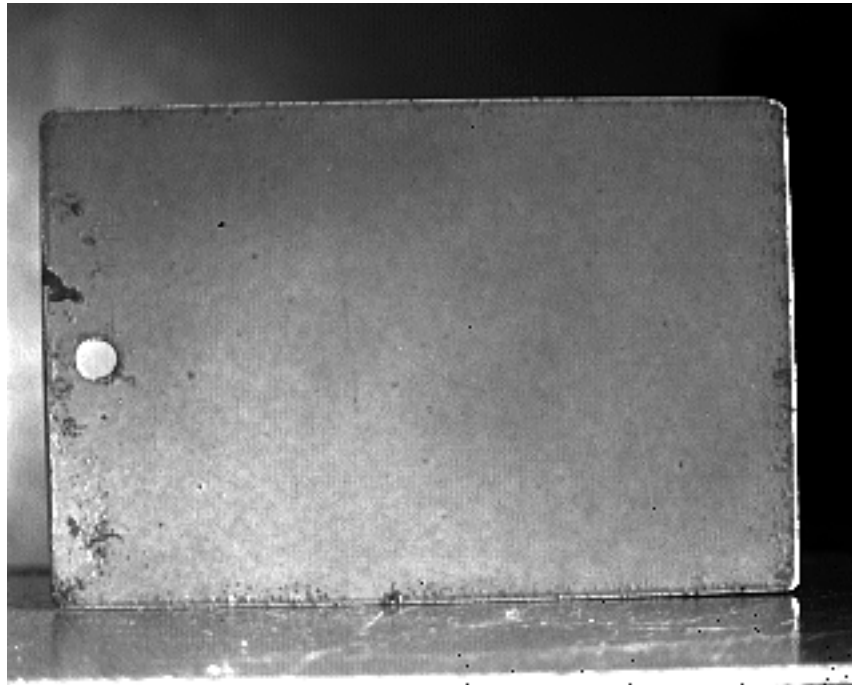
IR Photograph

Corrosion Detected on Edge of panel Right Side.



7 c2a (Front Side)

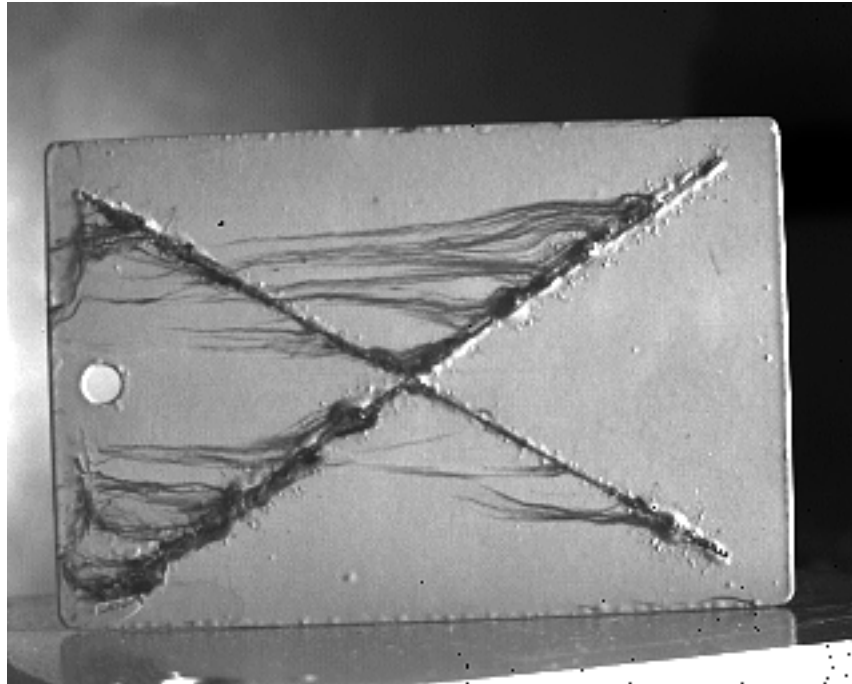
Standard Illumination Photograph



7 c2b (Back Side)

IR Photograph

Panel appears to have a contamination or indication of corrosion near edge by hole.



7 c 5

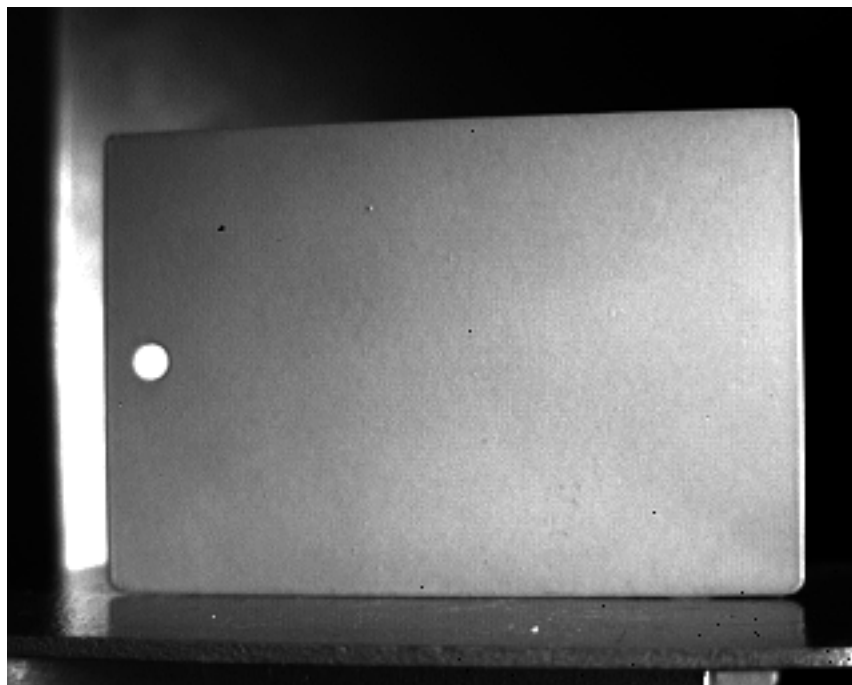
IR Photograph

Photograph indicates corrosion in scribe area and under coating.
Corrosion Product on top of coating.

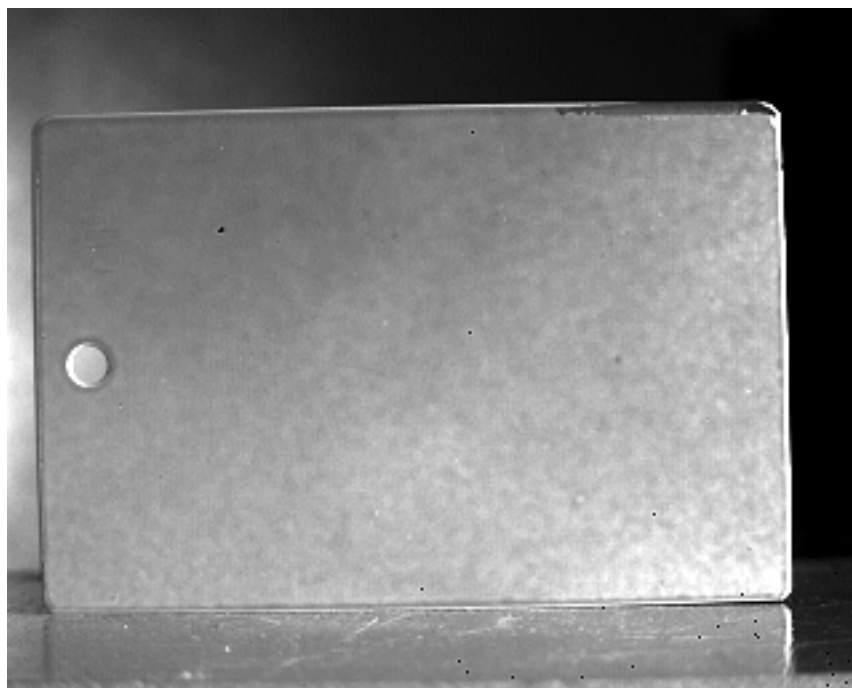


7 c 5

Standard Illumination Photograph



7i 1
IR Photograph
Indicates no corrosion present.

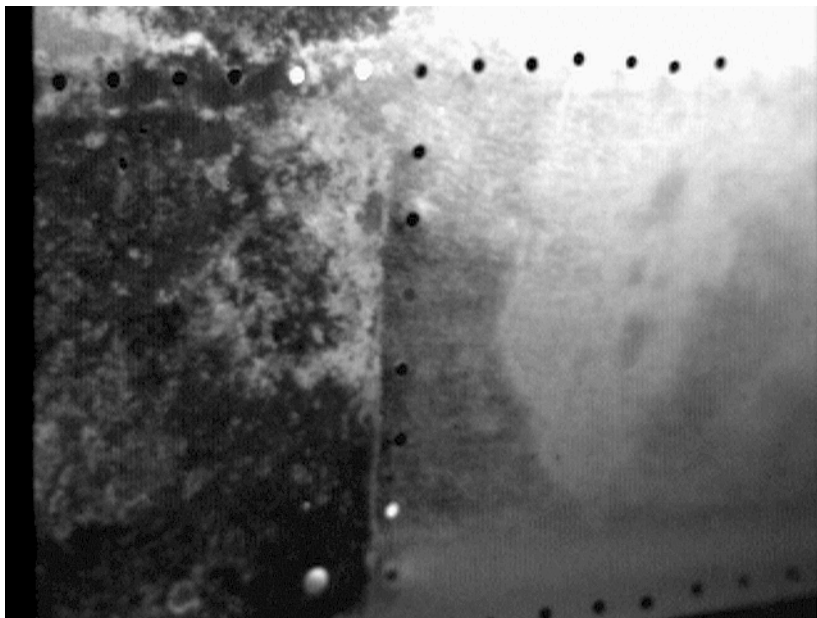
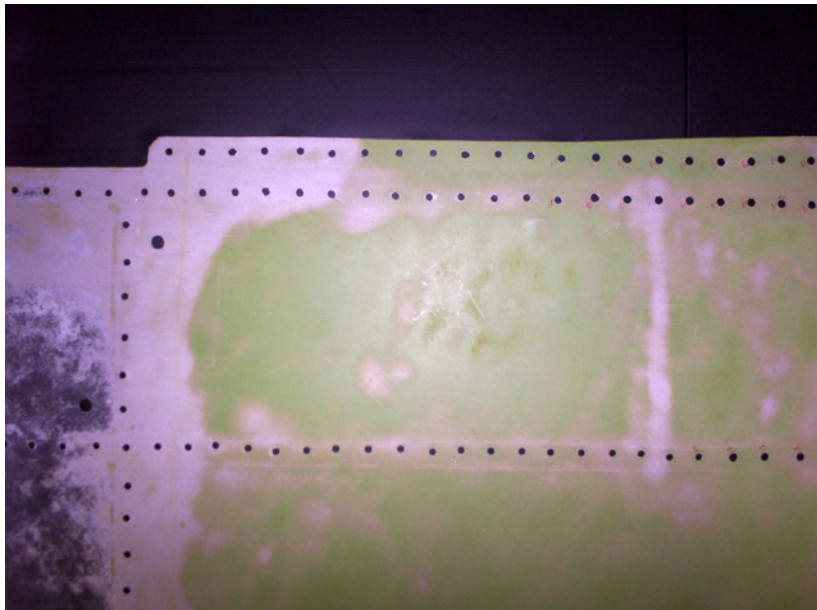


7i b
IR Photograph
Indicate potential for corrosion under coating or possible surface roughness.

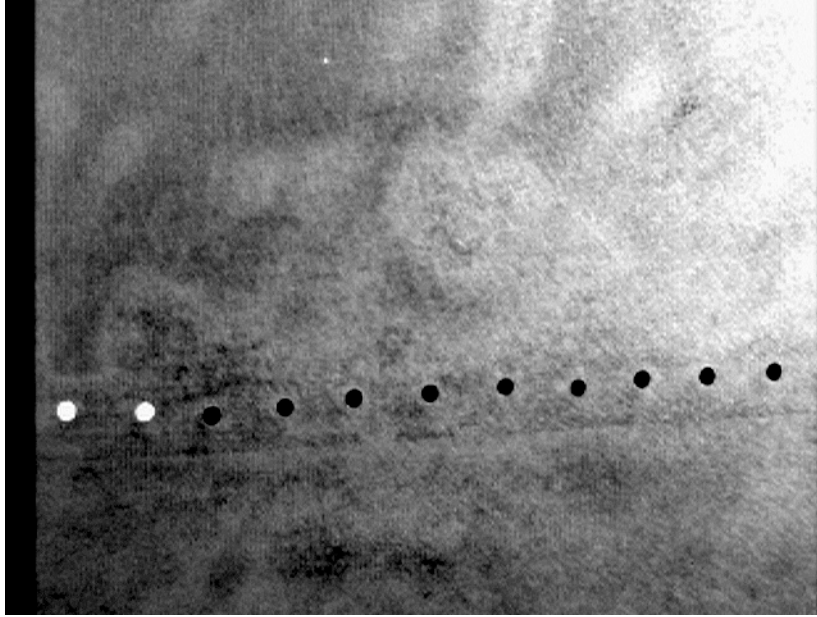
APPENDIX A3

NOT ITAR APPROVED

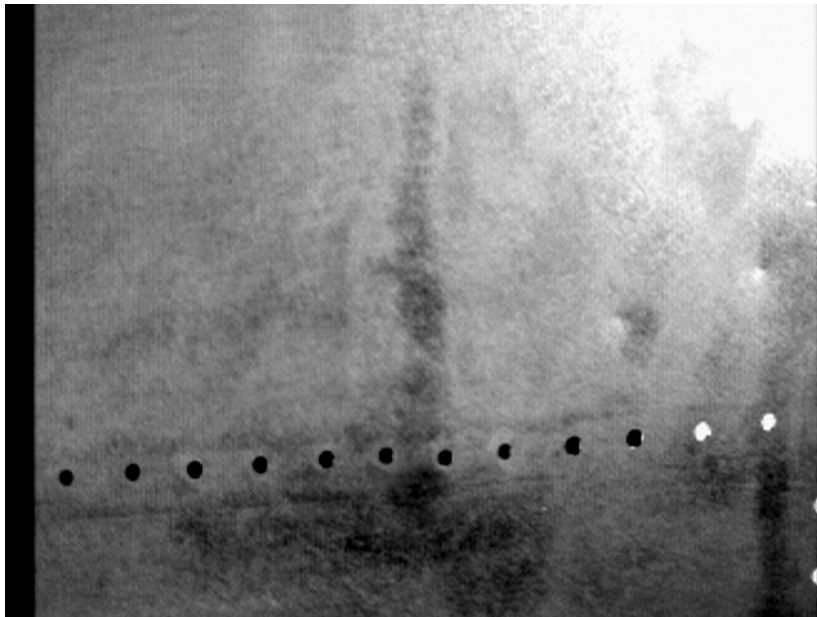
Redstone Arsenal IR Demonstration 07/09/2003



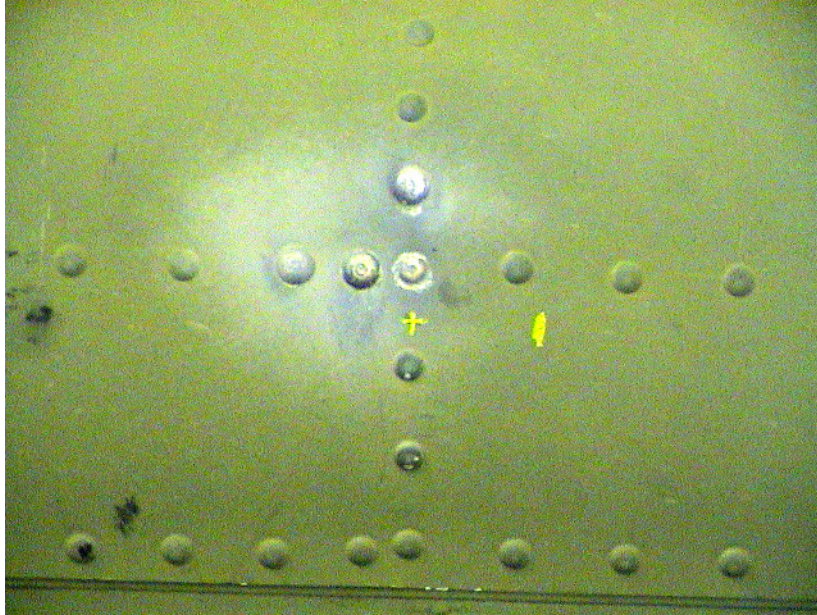
Visible and IR images of belly skin. One side is corroded, the other side has primer on surface.



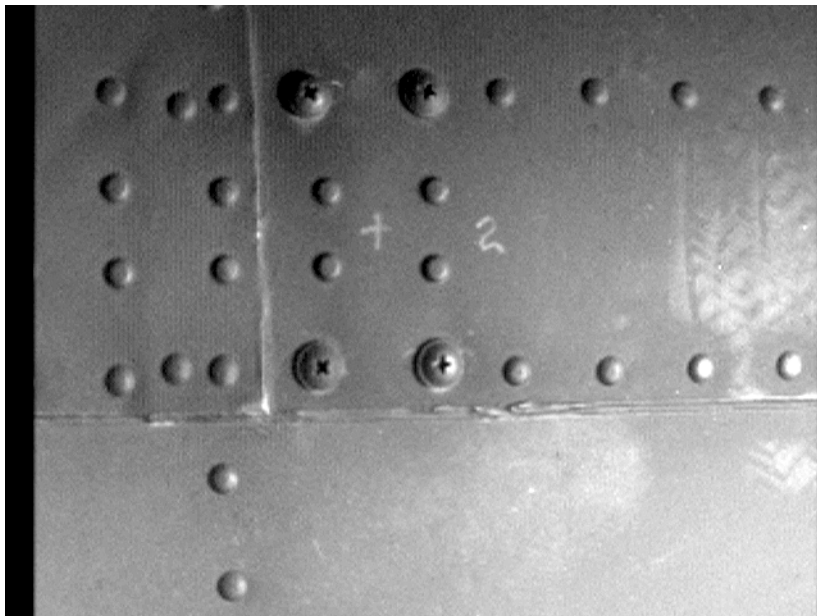
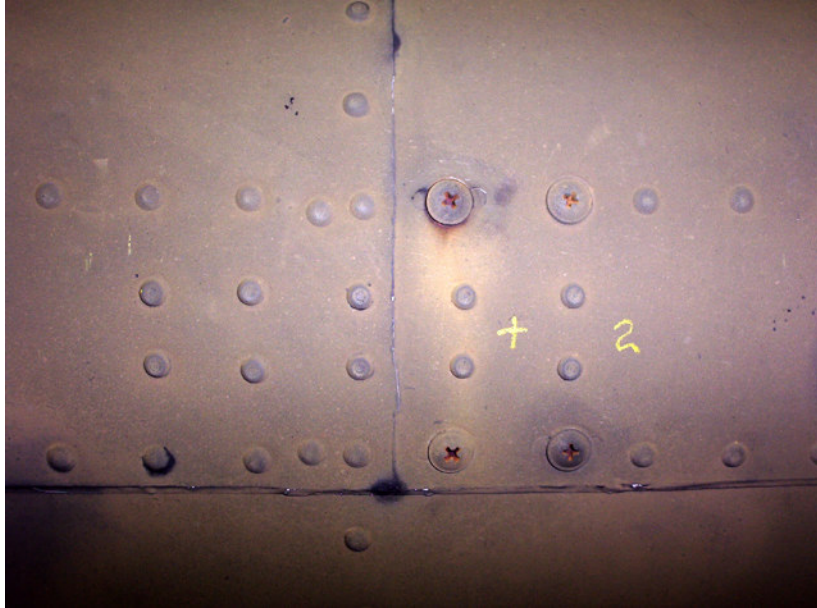
IR image of belly skin part.



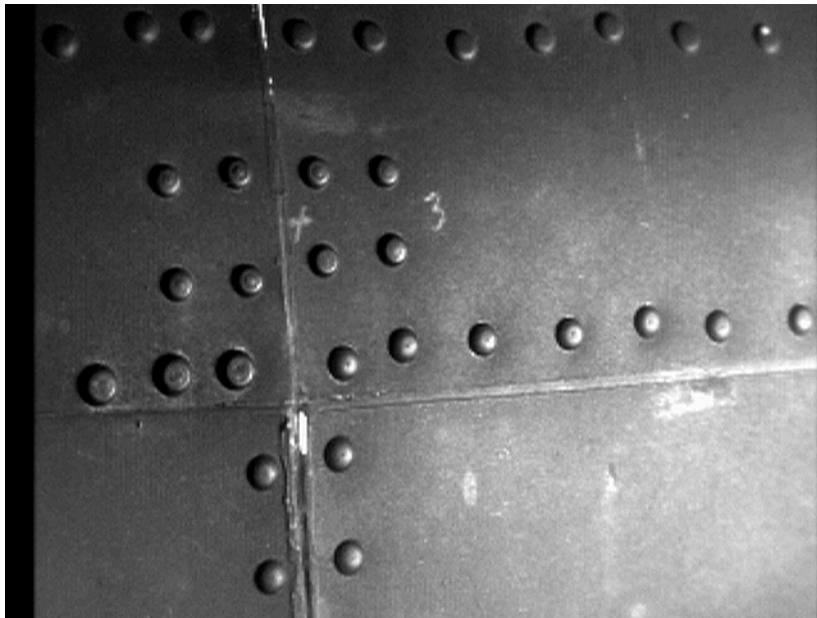
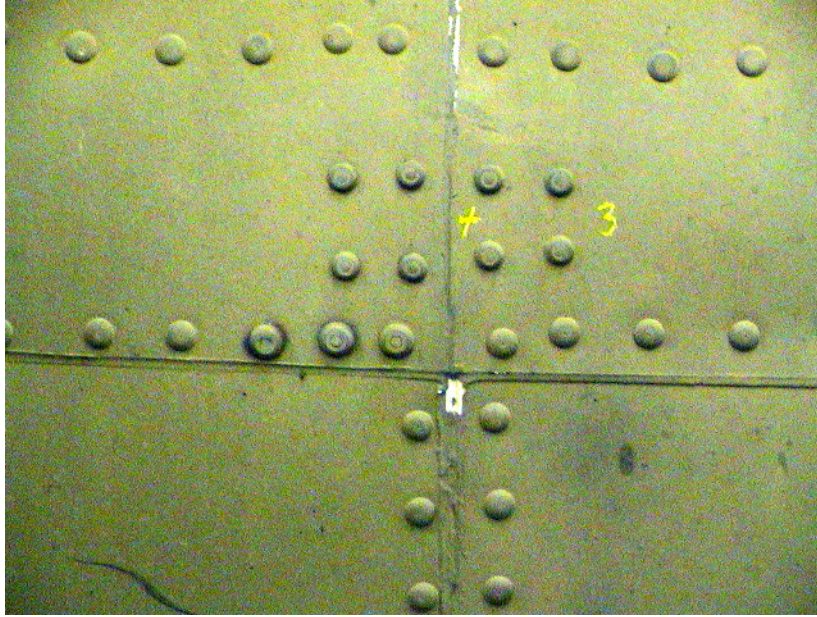
IR image of belly skin with 2 dimples on right hand side.



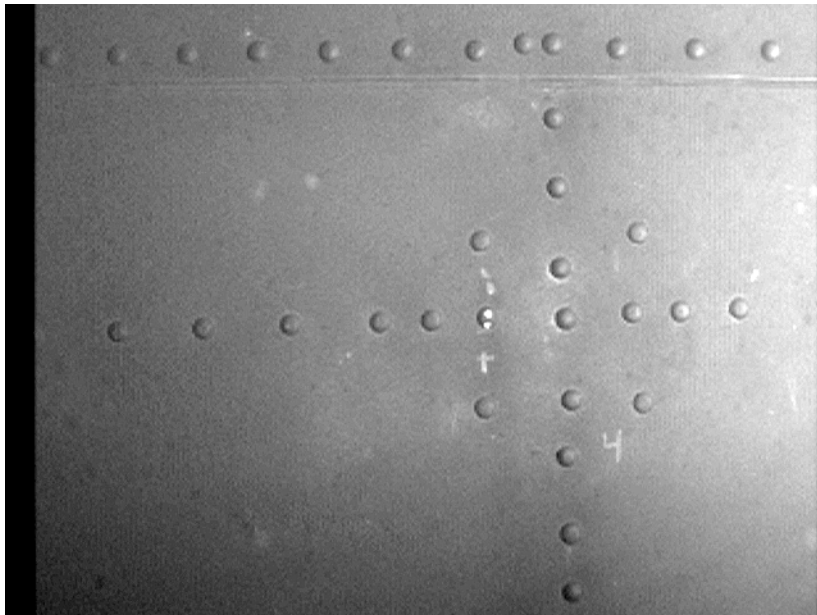
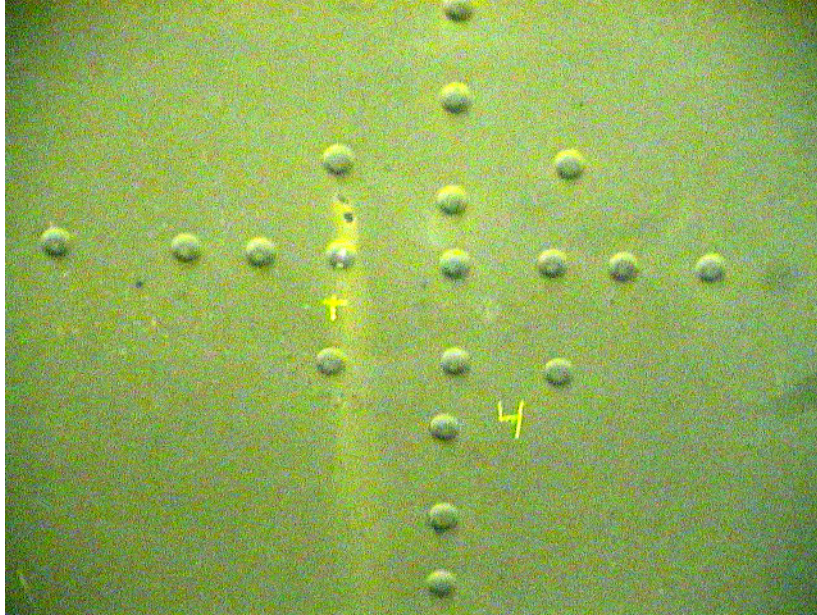
Visible and IR images of Boom Position 1.



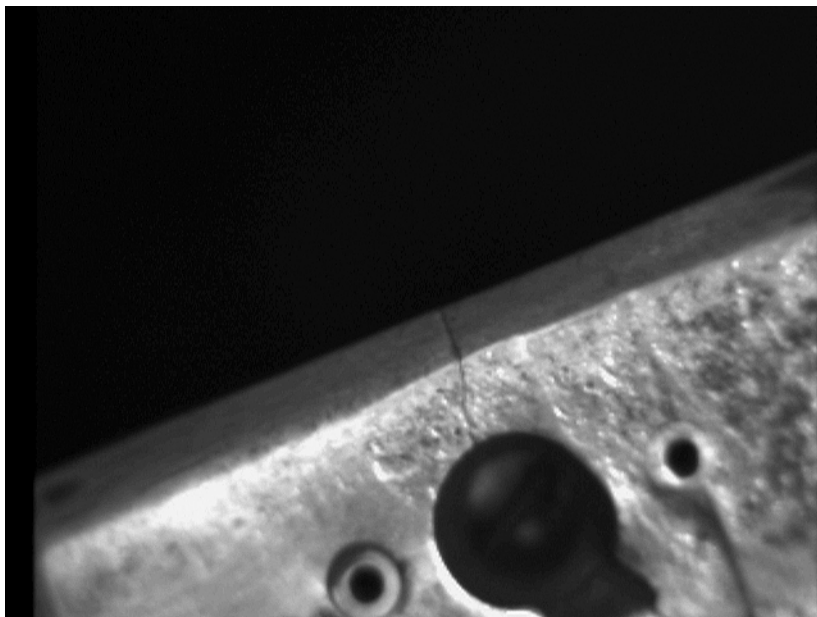
Visible and IR images of Boom Position 2. Note the “footprint” in the IR image.



Visible and IR images of Boom Position 3.



Visible and IR images of Boom Position 4.



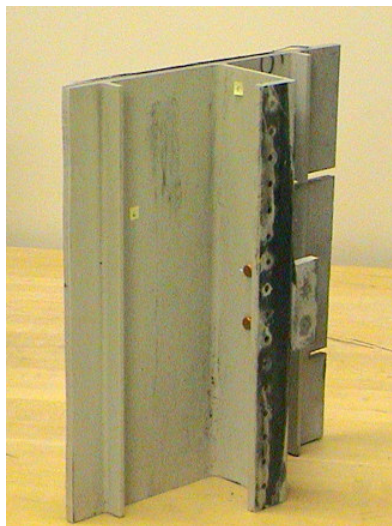
Visible and IR images of crack.



Visible and IR images of Dog Bone part

APPENDIX A4

B-52 Fuel Tank Coating

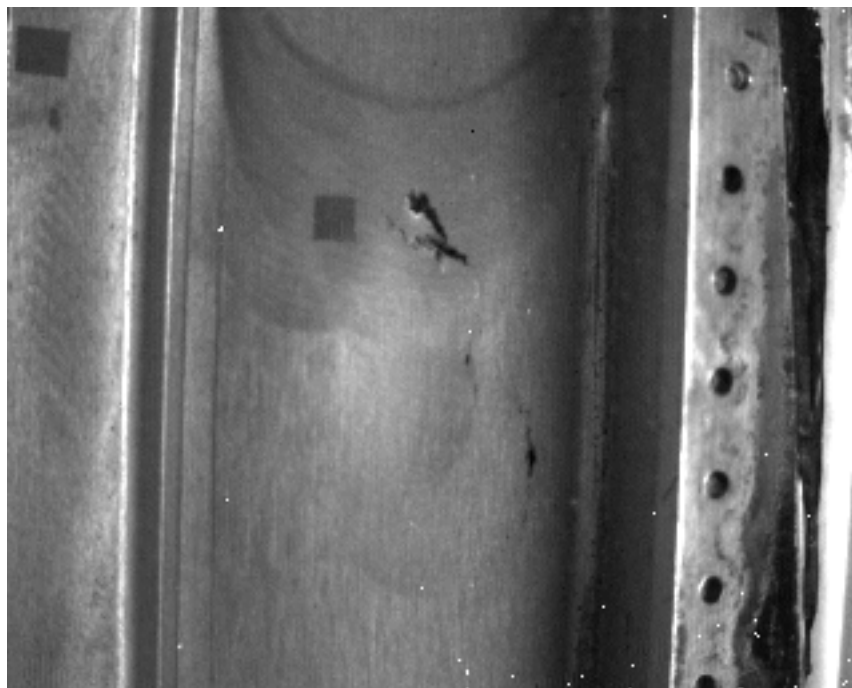


Visible image of B-52 parts.

B-52 Fuel Tank Coating



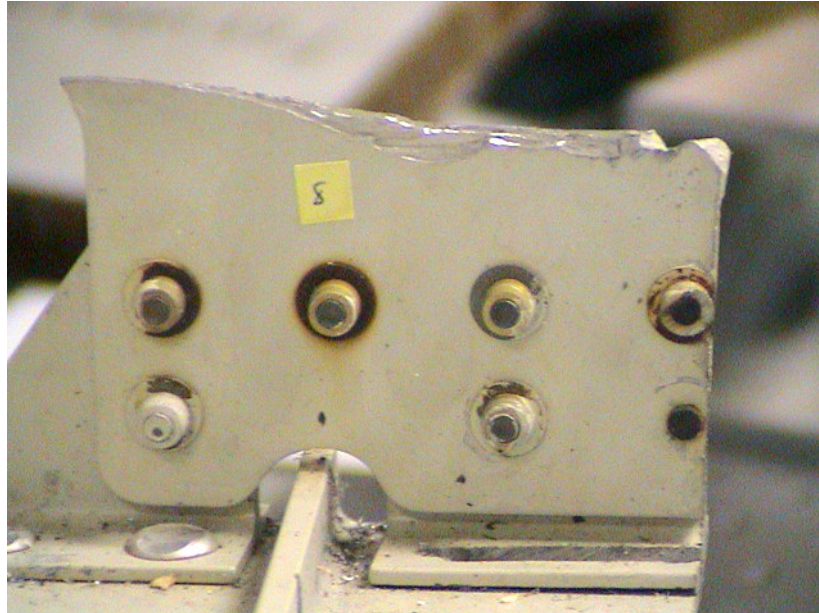
Visible



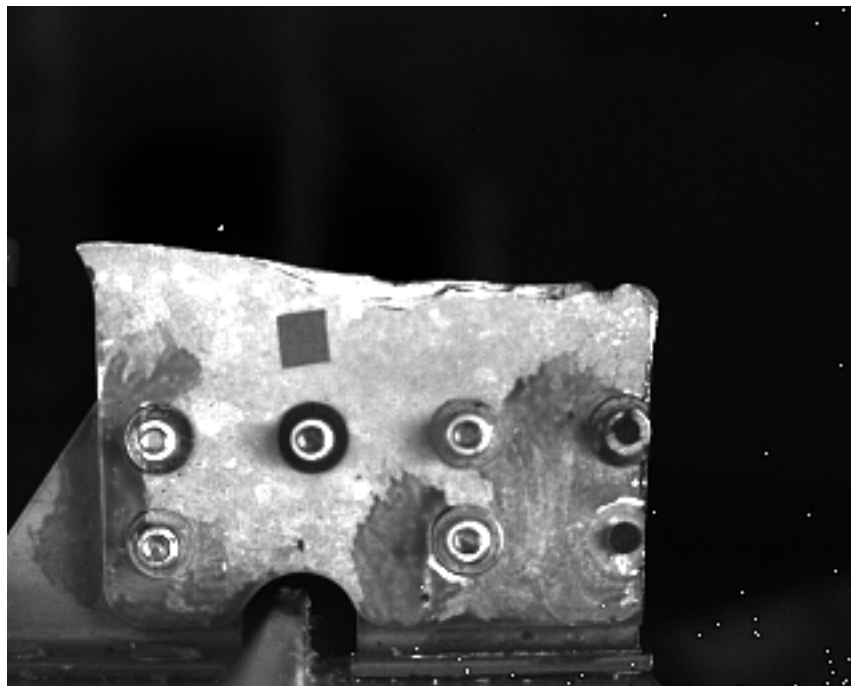
IR

Visible and IR reflectance images of spot 1 and 2. The IR image shows the metal grain structure underneath the paint. Rework and corrosion can be seen in the IR.

B-52 Fuel Tank Coating



Visible



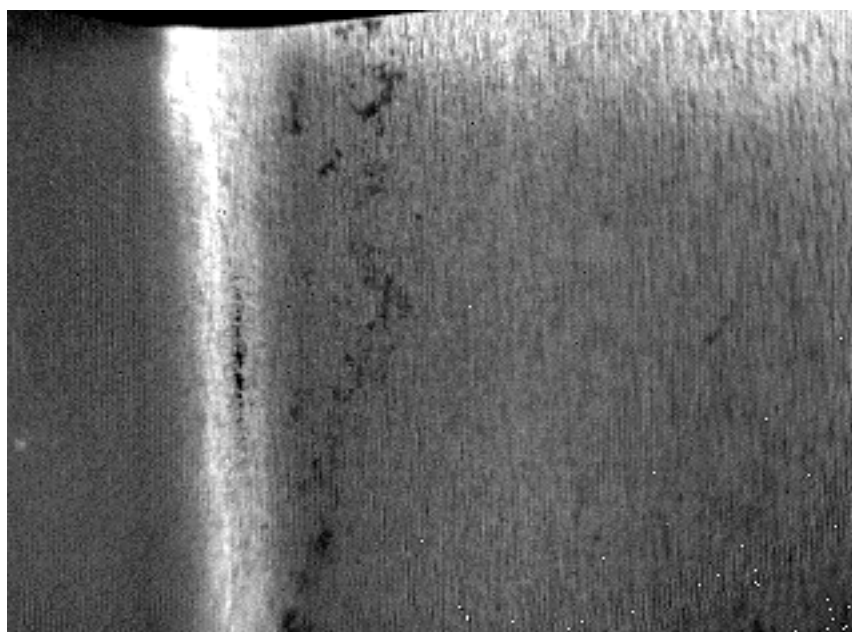
IR

Visible and IR reflectance images of spot 8. The IR image shows the possible rework underneath the paint. The IR image reveals features not seen in the visible image.

B-52 Fuel Tank Coating



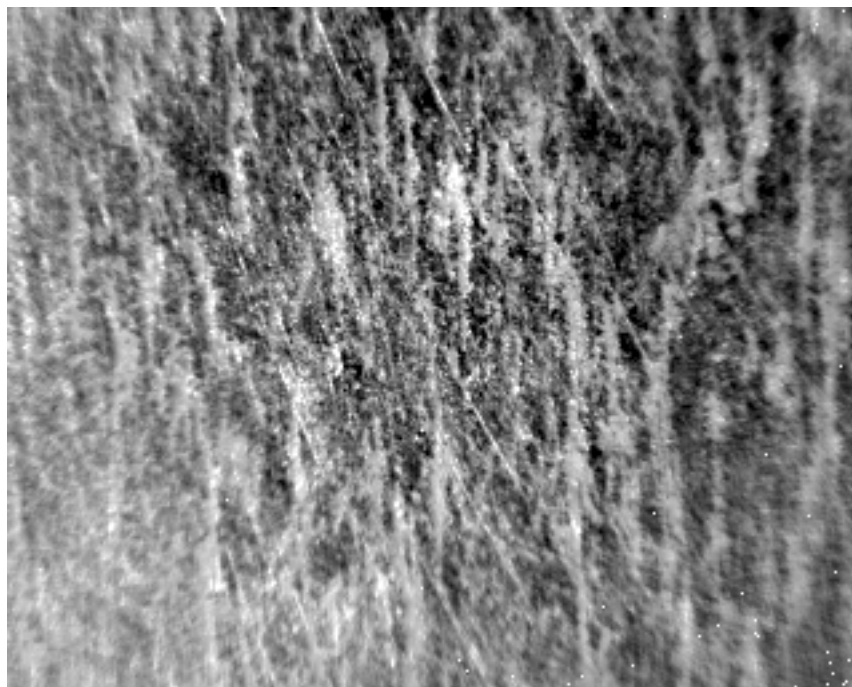
Visible



IR

Visible and IR reflectance images of spot 5. After cleaning area with Naphtha, corrosion is clearly seen underneath the paint in the IR mode.

B-52 Fuel Tank Coating



IR

IR reflectance image of spot 1. This is a 1x mag. IR image. The metal surface is clearly seen. Dark areas may be sites of corrosion.

APPENDIX A5

1. **Title:** Environmentally Friendly NDI for Corrosion Inspection Through Coatings (IR²NDI)

2. **ESTCP Thrust Area:** Area 3b. Pollution Prevention – Alternative Maintenance

3. **Lead Organization:**

Air Force Research Laboratory Materials and Manufacturing Directorate W-PAFB, OH; Mr. Paul Ret;
COMM: 937.656.9154; DSN: 986.9154; FAX: 937.656.4600

email: paul.ret@wpafb.af.mil

4. **Problem Statement:** The DoD, including the Coast Guard, is being required to maintain aging fleets of aircraft (A/C) and ground vehicles. For example, the average age of the naval aviation fleet is in excess of 18 years. These A/C must be inspected not only during regular depot phase inspections, which occurs approximately every five years, but on an increasing basis in the field, as corrosion is very often monitored in high corrosion areas sooner than the standard five-year cycle. And ground vehicles have similar constraints and cycles.

Since paint stripping and refinishing costs of A/C have been increasing due to new but slower acting environmental paint strippers and disposal costs associated with RCRA waste, an improved technology is needed to detect corrosion under coatings to eliminate potential for stripping organic coatings. Also, newer extended life topcoats such as the Advanced Performance Coating (APC) currently used on A/C like the C-17 and F-15 have been implemented to economically reduce the need to repaint these A/C and minimize pollution. Further, new coatings such as low VOC formulations including non-chrome primers, as well as non-chrome surface preparations will put increasing pressure/requirements on improving NDI techniques for detecting corrosion under coatings.

If a validated NDI inspection system existed that could inspect for corrosion under existing coatings, significant amounts of VOCs and hazardous waste could be avoided. For example, removing the coating system from a fleet of 180 cargo type A/C using a five year cycle with complete coating system strip and repaint results in 252,000 lbs of VOCs per year and 3,600 lbs of hazardous chromate waste per year. If an advanced NDI method could make it possible to extend the average life of this fleet of aircraft coating systems by just one-year, then approx. 50,400 pounds of VOC emissions per year and 720 lbs of chromate waste per year could be eliminated for just one weapon system (See Attachment pg. 2, Ex. A.)

A new and easy to use technique is needed to assess and reduce the risk of corrosion effects, not only in depot operations, but between normal inspection phases in the field, to reduce costs and environmental burdens.

In fact the use an improved NDI system to detect corrosion under coatings will aid in accepting and monitoring newer environmental formulations to assure a high confidence level of substrate viability, prior to stripping organic coatings solely for corrosion inspection.

The proposed IR Reflectance NDI technique (**IR² NDI**), once demonstrated and validated, would be used as an inspection tool that will enable extending the life of topcoats, should the logistics/operational commands decide not to remove the paint between the normal five-year inspection period, and during a normal depot PDM cycle.

Many of the existing NDI technologies for detecting corrosion under coatings are not easy to use and sometimes interpreting their results can be a problem even for the most skilled NDI experts with years of experience. Table 1 of the attachment summarizes test data showing many of these technologies and how they compare with each other for detecting corrosion under coatings.

5. Project Description:

a. Technical description justification, and innovation: IR radiation from A/C hanger lights, the sun, or a low-wattage IR heater illuminates the area to be observed. The IR radiation, being in the long wavelength, passes directly though the coating and then reflects off the metallic substrate back though the coating and into the IR Camera. Since the corroded areas do not reflect the IR energy as well as the non-corroded areas, a picture or image is generated by the IR camera much the same as observing the corrosion under standard visual techniques. Figure 1 in the attachment illustrates how this new technology functions. Examples of images of corrosion under coatings can be seen in Figures 2 and 3.

The project will address reducing pollution from actual and realistic field data validated by field demonstrations showing the capability to detect corrosion under coatings with the IR Reflectance NDI researched under a previous SERDP project 1137 led by Northrop-Grumman as prime contractor. After successfully demonstrating and validating this new technology, field maintenance operations will have the choice of being able to inspect for corrosion without having to remove the coatings. This technology will significantly reduce pollution and dollars by eliminating needless paint stripping operations.

b. Evidence the technology is mature enough for demonstration: The IR²NDI was down-selected from a number of innovative technologies that were investigated during the SERDP Project, as it was able to produce visual images of high fidelity most similar to corrosion as seen either with or without magnification by the eye. This new technology is capable of producing a real-time image, as well as an electronic copy of the corrosion subject to little interpretation.

It was found was that laboratory corrosion could be detected easily though 5- 6 mils (.005" to 006") of standard A/C primer, MIL-PRF-23377TYICLC, and urethane topcoat, MIL-PRF-85285 TYI. In some cases

corrosion could be successfully observed though 12 mils of total paint thickness. The following table is a summary of locations and weapon systems that can potentially use this new corrosion detection technology.

Note: Items in bold include those systems/sites directly supporting and participating in this proposal.

Service/OEM/Org.	Locations	Weapon Systems
Air Force	OC-ALC, Tinker AFB	KC-135, E-3, B-52, & B-1,
Air Force	OO-ALC, Hill AFB	C-130, F-16, & A-10 ⁽¹⁾
Air Force	WR-ALC, Warner-Robins AFB	C-5, C-130, C-141, F-15 & E-8
Air Force	Boeing contractor depot support	C-17, KC-10
Navy	NADEP Jacksonville, FL	P-3 , F-14 ⁽¹⁾ & F-18 ⁽¹⁾
Navy	North Island, CA	E-2C
Army	Corpus Christi Army Depot (CCAD) Tx	CH-47, UH-60, Humvee, Med Tact Veh, Heavy Tact Truck
Coast Guard	Elizabeth City NC	H-65, H-60, H-25, C-130
Northrop Grumman	Melbourne, FL	E-8 refurbishment (JSTARS)
Northrop Grumman	St. Augustine, FL	E-2C Rework & EA-6B ⁽¹⁾
Commercial Org	TBD	TBD

(1) Inner Mold Line (IML) or Landing Gear Applications only, due to IR primer or other specialty coatings

c. Relationship to other similar projects: In addition to the SERDP 1137 Project, Northrop Grumman Bethpage is currently under a \$1.7M contract with the ONR to develop a Thermography system that is able to detect deep corrosion in A/C structural parts. Although this system is quite different in capabilities, the same IR camera could possibly be used in both systems, hence saving the need to procure two cameras.

d. Potential issues of concern and technical risks in taking the technology from the lab to field-testing: Some limits do exist. For example, it is more difficult to see through coatings when low IR primer, MIL-PRF-23377TYIICLC, is used. This is due to the IR absorbing characteristics of the primer. Test work did, however, demonstrate that corrosion on aluminum test panels could be observed underneath 2.5 mils of IR primer and polyurethane topcoat. However, most coatings, if applied to military specification requirements, do not exceed 3.0 mils. In some cases, but certainly not all cases, the Outer Mold Line (OML) is coated up to 20 mils of conventional primer/topcoat in the field. This problem can occur when multiple scuff sanding and repainting/touch up operations happen prior to their five-year stripping cycle. Most A/C inner mold lines (IMLs) generally do not experience this type of build up and hence original OEM/Military thickness requirements are generally maintained on the IML. Regarding Air Force inventory, very little MIL-PRF-23377TYIICLC, Low IR Primer, is used with the only exception being the A-10.

However, to address this concern, a new camera developed by Indigo known as the Phoenix camera may be able to see deeper into extremely thick conventional coatings. This camera will be investigated during the first phase of the program to establish if an up grade to the baseline IR camera is warranted.

e. Approach for determining performance and expected operational costs of the technology: Will be a four-task approach over 3 years, with multiple Team partners as described below.

Task I - Preliminary Field Surveys, Lab Support Testing & JTP/Dem/Val Plan – Since Task I is the foundation of the project, a major A Kick-Off meeting with the Team, program offices, and expert consultants will be organized to establish detailed requirements, logistics needs and schedules for preliminary site surveys. The Team will establish which weapons systems and what specific locations on those systems can best use the IR²NDI. Participants will be briefed on the IR system operation, equipment configurations and current capabilities. Proposed sites will be discussed to establish specific engineering needs, camera ergonomics and other requirements. Historical high corrosion areas will be determined. Potential areas requiring corrosion inspections include: not only the OML of weapons systems, but landing gear, A/C/ground vehicles, wheels, fuselage/ground vehicle interior & exterior structures, and A/C wing skins (interior and exterior).

To lower project risk, samples of candidate coatings/substrates will be prepared and tested in the laboratory to assure the system is sensitive enough to determine the degree of corrosion required by the specific site/program requirements. Preliminary IR camera system capability performance will be investigated in both the laboratory and on actual fielded weapons systems/components. A sensitivity study will be conducted in the laboratory to demonstrate that the system is first capable of handling the selected weapons systems finish configurations including field-reported total coating thickness. Standard finishes using laboratory prepared panels with the identical alloys, surface preparations and coating systems used in the field will be tested. This approach will minimize risk, prior to conducting field-testing. The laboratory sensitivity analysis will involve corrosion of panels in accordance with ASTM B117 for one, three, and seven-day exposures.

These specimens will be used to make a Go/No-Go decision concerning coating types and thickness limits. Special coatings such as F-15/C-130 barrier, CARC, appliqué, Intermediate coatings, LO and Low-IR coatings may also be investigated at this time depending on user and program offices requirements. Moreover, an improved and more sensitive Phoenix™ Camera manufactured by Indigo will be investigated over the baseline Merlin™ Camera manufactured by Indigo.

To support the above, and to assess cost-related parameters, preliminary fact-finding surveys will take place at potential user sites. The purpose is to introduce site NDI and maintenance personnel and other associated A/C program disciplines to this technology and also to assess special corrosion inspection needs and applications of each site. The information gained during these surveys will be shared and coordinated with the cognizant personnel to assure the IR²NDI has distinct advantages over the more convention technologies used to inspect corrosion under coatings. Data will then be analyzed to assure the project is on track, or if adjustments need to

be made regarding scope, techniques/methods, and IR camera equipment. After completing the preliminary surveys, a Preliminary Cost Benefit Analysis (PCBA) will be conducted for the sites visited. Environmental benefits, as well as cost advantages will be analyzed for specific weapons systems and sites maintaining those weapons systems. Pertinent documentation used to inspect these selected weapons systems will be reviewed to help establish costs and methods, as well as to provide baseline information for comparison purposes.

The knowledge gained from the fact-finding surveys/initial demonstrations will be used to prepare the Demonstration/Validation Plan, which will be used to guide the actual Dem/Vals, and to prove the system is ready for implementing into field operations. Additionally, the Joint Test Protocol (JTP) will include participants' inputs from NDI personnel, corrosion engineers, program offices, and user site maintenance personnel. The dem/vals will not occur until full Team coordination and ESTCP has approved the JTP and Dem/Val Plan.

Task II – Optimize IR Camera System – Task II run almost in parallel with Task I, and will optimize the equipment used with task I. The parameters or special techniques investigated during Task I, along with the images produced from the laboratory specimens in Task II, will be documented for future field use (Task III) and evaluation, as well as incorporation into the JTP. Applicable software development and image processing techniques will be assessed during this task.

Task III – Perform Demonstration and Validations – Sites for Dem/Val will be selected based on the highest projected return and environmental benefit. After final ESTCP approval demonstrations and validations will be conducted. The Optimized IR camera system from Task II will be used. The demonstrations will be conducted on a non-interference basis with complete coordination and approval of the site coordinators. Northrop-Grumman will be the lead for conducting the Dem/Vals, with active participation by the site coordinators and the AFRL Project Manager.

Task IV – Assessment & Documentation – Data will be validated with selected sites, corrosion control experts, program offices, maintenance and NDI experts. Briefings will be conducted for all parties. The briefings will include the results of the final CBA and an environmental benefit analysis for each site/weapon system, as well as overall technical results. Recommendations/documentation for procedure changes for corrosion inspections will be made. The final report and cost & performance report will be prepared covering all work accomplished on the program, projected environmental benefits, and projected cost savings, including final recommendations for implementation.

6. Expected DOD Benefit: The expected DOD benefits would include lowering of air emissions, reducing hazardous RCRA waste and lowering maintenance costs including NDI inspection costs. **Environmental benefits** can be realized by either extending coating life and/or scuff sanding and repainting in the depot or in the field without stripping the full coating system by using the IR² NDI. The results of deploying the IR² NDI for a

fleet of 180 A/C with 30,000 sq. ft of OML surface area (similar to the size of a C-17) will save approximately 115,650 lbs of VOCs every year or 1,156,000 lbs of VOC saved over a ten year period. (See Attachment pg.2, Ex B). The table below summarizes estimated VOC reductions and cost benefits and/or avoidance at the A/C depot sites listed below. These are estimated savings and must be validated in the ESTCP CBA and environmental benefits analysis.

Depot	Weapon System	# VOC Reductions/Year	\$Cost Avoidance/Year
OC-ALC, Tinker AFB	KC-135, E-3, B-52, & B-1	150,000	5M
OO-ALC, Hill AFB	C-130, F16, & A-10	90,000	2M
WR-ALC, Tinker AFB	C-5, C-130, C-141, F-15, E-8	300,000	7M
NADEP/Jacksonville	P-3, EA-6B	20,000	.5M
Boeing Contract Support	C-17, KC-135	150,000	5M
Totals		710,000 # of VOC/Year	19.5M

Cost benefits are derived from the labor savings, procured chemicals, and material RCRA waste disposal costs assuming either a minor touch-up and/or a scuff sand and paint was accomplished on the A/C, once the surface to be inspected indicated that corrosion was not present. Since the cost of a typical IR² NDI system is \$70K, it is anticipated that the sites listed above will be able to pay or have a Return on Investment (ROI) for the unit in less than 2-months (NADEP/Jax Ex.) using the above cost figures. In many cases the cost avoidance from stripping just one A/C (such a C-17, which costs approx. \$375K) would pay for the system, if just one of these A/C would not have to be stripped, after IR² NDI inspection. Note: Cost based on interviews with cognizant maintenance personnel during the prior SERDP project.

The life-cycle costs of maintaining each weapon system would be expected to be lower with IR² NDI than any of the other NDI systems for inspection of corrosion under coatings. This is because the IR² NDI system is capable of inspecting corrosion under coatings at least 2 times faster than other techniques, and will produce superior and easier to interpret images relative to the other NDI techniques. (See Attachment)

Environmental savings from recurring non-depot field inspections of local high corrosion areas would have additional benefits/savings. Down times and operational readiness of A/C weapon systems would be greatly enhanced by eliminating the time to remove coatings, refinishing, and curing, prior to flight. Hence, IR²NDI would minimize environmental issues, reduce overall inspection costs, and improve flight safety.

7. Program Schedule: Milestones

Task/Activity	2004				2005				2006			
	Q1	Q2	Q3	Q4	Q1	Q2	Q3	Q4	Q1	Q2	Q3	Q4
Execution Plan	▲											
Project Team Meetings	▲	▲	▲	▲	▲	▲	▲	▲	▲	▲	▲	▲
Task I – Field Survey, Lab Support & JTP Dem/Val Plan	▲			▲	ESTCP APPROVAL							
Task II – Optimize IRCamera System		▲		▲								
Task III – Perform Dem/Val's					▲				▲			
Task IV Assessment/ Documentation							▲				DRAFT	▲
Cost Benefit Analysis	▲		PRELIM CBA			▲				CBA DRAFT		FINAL CBA
Draft & Final Transition Plan									▲	▲	DRAFT	FINAL
ESTCP In-Progress Reviews (IPRs)		NEW START			▲					▲		
Quarterly Reports		▲										▲
Monthly Financial Reports	▲											▲
Annual Reports				▲				▲				
Final Report & Cost/Performance Report									▲		DRAFT	FINAL

8. Transition Plan: We have established a solid team listed in the Attachment to assist in transitioning to the field/depot. First, we have active participation by a number of users who are sponsoring the Dem/Val's, and in some cases will provide test coupons/components to the program and/or perform testing. We have viable letters of endorsement (attached) or informal confirmation from AF, Army, Navy, and Coast Guard participants representing multiple weapons systems. These organizations are not only supporting the program, they ARE the key participants/users, and in some cases, such as noted in the W-RALC letter, their mission is to actively transfer technology into maintenance processes. We are working to secure active participation by applicable program offices, and industry participants will, of course, need to attend quarterly and JTP Planning Meetings and coordinate on the JTP/Dem/Val Plan. The program offices will have the final decision on incorporating NDI techniques into the -36 series of TOs for the applicable weapons systems. Additionally, although not recognized team participants, we have a number of coatings suppliers and commercial industry interests who serve as informal advisors for the program.

Second, we have the right balance of DoD experts actively involved the program, consisting of NDI, corrosion, aging A/C, former maintainers, coatings, and other experts, also listed in the Attachment. We will employ this Technical Advisory Board (TAB) to continually assess our progress and serve as advisors for making program technical recommendations to ESTCP via the Project Manager. For example, the TAB will address the up front requirements for the dem/vals along with the users. And, these folks are uniquely situated, based on

years of extensive experience in their respective fields, and have the right inter-related contacts throughout government and industry to champion the program. For example, the NDI experts are active in service and DoD NDI Working Groups, which sponsor annual forums for NDI related activities. The corrosion representative is in an office that is actively involved in major corrosion conferences, and sponsors the Air Force Worldwide Corrosion Program Conference. These venues will provide a means to present this program to wide audiences to gain acceptance. Additionally, these TAB members are participants with ASTM and SAE committees who assess new testing techniques. And, the NDI members control TO 33B-1-1, which is the general NDI field guide. Further the corrosion experts manage the corrosion TO 1-1-691, which will be affected by the new IR² NDI technique, once implemented.

Thirdly, the prime contractor of the SERDP IR²NDI technique, Northrop-Grumman will be the prime on this program. And, Mr. Kovalski, a TAB member, and the contracting officer representative for the SERDP program, will also play a key role as advisor. This will help to ensure that the lessons learned under the previous program are incorporated into this program. And, since Northrop Grumman is a prime weapons systems OEM supplier, N-G is uniquely positioned to bring an integrated approach to the various technical disciplines required to assure a successful transition.

Lastly, we believe in solid coordination and keeping all the responsible offices informed of program progress. Hence, as noted in the schedule, we are establishing quarterly face-to-face- meetings or major telecoms to help produce the desired results.

Following successful demonstration, each of the applicable weapons systems will have already been long on-board as well as the constituent NDI/corrosion/coating communities, to stimulate and achieve a rapid introduction into the field.

9. Funding: Requested funding is divided by organization. Detailed \$ breakouts and substantiation available. *(IN WORK)*

	2004	2005	2006	<i>TOTAL</i>
AIR FORCE	TBD			
NAVY	TBD			
ARMY	TBD			
COAST GUARD	TBD			
TOTAL				TBD

10. Performers: See Attachment – Note: contracting will be accomplished via in-place deliver order-type contracts.

10. Performers: Project Mgrs and Demonstration/Validation Site Coordinators

POC	Org	Location	Phone/Fax	Role
Paul Ret	AF Mtls & Mfg Directorate	Wright-Patterson AFB, OH (W-PAFB)	937.656.9154 937.656.4600	ESTCP Project Mgr.
John Weir, P.E.	Northrop-Grumman	Bethpage, NY	516.575.5422 516.575.6672	Project Mgr. for Northrop Grumman
Dr. Don DiMarzio	Northrop-Grumman	Bethpage, NY	516.575.6452	PI Scientist for Northrop Grumman
Bill Pember	Northrop Grumman	Melbourne, FL	321.951.6166 XXXXXXXXXX	Joint Stars NDI Manager Dem/Val Site Coordinator
MSgt John Birhanze	445 th Airlift Wing	W-PAFB	937.257.4667 XXXXXXXXXX	A/C Maintenance Supervisor Dem/Val Site Coordinator
MSgt Leroy Carpenter	445 th Airlift Wing	W-PAFB	937.257.7781 XXXXXXXXXXXX	NDI Manager
Richard Slife	Environmental Compliance Branch/W-RALC	Robins AFB, GA	478.926.1197x139 478.926.9642	Dem/Val Site Coordinator
Jack Benfer	NADEP/Air Vehicles Engrg/Mtls	Jacksonville, FL	904.542.4516 x153 904.542.4523	Dem/Val Site Coordinator
CWO Paul Cassere Rusty Waldrop	Coast Guard Depot	Elizabeth City, NC	252.335.6953 XXXXXXXXXX	Dem/Val Site Coordinator NDI Manager
Don Skelton	Industrial Ecology Center	Picatinny Arsenal, NJ	973.724.4071 973.724.6759	Army Corrosion Measurement/Control Program PI
Larry Gintert Steve Cargill	Concurrent Technologies Corp	Clearwater, FL	727.549.7092 (772.546.7718) 727.549.7230	CTC Corrosion Measurement and Control Prog. Mgr. and Dem/Val Site Coordinator

Technology Advisory Board (TAB)

POC	Org	Location	Phone/Fax	Role/Representing
Dr Deborah Peeler	Aging A/C SPO	W-PAFB	937.255.7210 x3739 XXXXXXXXXXXX	Aging A/C Program Office and Structures
Dr Tom Moran	XXXXXXXXXXXX XX	W-PAFB	937.255.9800 937.255.9804	NDI advanced research techniques
John Brausch	AF Materials Directorate NDI	W-PAFB	937.656.9151 937.656.4600	NDI Supervisor for AF Field Support DoD NDI Wkg Group
Robert Lewis	AF NDI Program Office	Tinker AFB, OK	405.739.2884 405.339.4822	Mgt of AF NDI advanced programs and field implementation DoD NDI Wkg Group
Dave Kessen	Coatings Tech Integration Office	W-PAFB	937.656.9265 937.255.0954	Coatings technology and A/C maintenance practices
Dick Kinzie	AF Corrosion Prevention & Control Office	Robins AFB, GA	478.926.3284 478.926.6619	Corrosion chemistry & effects
Kevin Kovaleski	Organic Coatings Team Leader	Patuxent River NAS, MD	301.342.8049 301.342.8119	Coatings development and SERDP PI for predecessor program

Attachment Page 2 of 3 **Table 1 NDI System Comparisons**

NDI Method	Speed of Survey for 10 Ft ² Per hour	Skill Level	Initial System Cost	Near Surface Detection Sensitivity Level	Comments
Ultrasonic	4	High	Medium 30K to 100K	Low to very poor on surfaces	Interpretation Issues
Eddy Current, Conventional	1	High	Medium 45K to 100K	High, but problems with fasteners/joints	Interpretation Issues/problems
MOI (Eddy Current)	0.5	Med.	Low 25K	Poor-Low	Interpretation Issues
Thermography	1	High/ Med.	High 150K+	High	Images require Interpretation
X-Ray	4	High	High/Medium 50K to 125K	Medium	Health Issues Work Stopped during use
Microwave	1	Low	Low 5K to 10K	Medium, but issues with Fasteners / joints	Edge Effects, Interpretation Problems
IR Reflectance (IR ² NDI)	0.25* Quickest NDI Technique	<u>Low</u>	Medium 70K	<u>Very High</u>	<u>Real Images.</u> <u>Easy to Interpret*</u> Real Time Fast

*Unique to IR² NDI: Lowest projected labor times and rates needed for cost effective corrosion surveys. Easiest technique to interpret because of real time images with highest fidelity of all systems compared.

ENVIRONMENTAL/COST ADVANTAGES CALCULATIONS:

Cargo Type A/C (30,000 SQ. Feet OML), Example VOC and Chromate Calculations:

Full PDM Cycle for Coating System Strip and Paint

USAGE DATA FOR OML OF CARGO A/C PER A/C: 1375 gallons of Stripper, 40 Gallons of Primer & 130 Gallons of Topcoat

Environmental Data: (2.9#/Gal. of VOC for primer, Deft), (3.5#/Gal. of VOC for topcoat, Deft), (2.5#/Gal. Of Chromate in Primer, Deft) and (4.67#/ Gal. of VOC In Paint Stripper, Calculated From MSDS for Turco 6813ED Paint Stripper)

VOC AND CHROMATE CALCULATIONS:

STRIPPER: $(1,375)(4.67) = 6425\#$ of VOC per A/C

PRIMER: $(2.9)(40) = 116\#$ of VOC per A/C;

PRIMER: $(2.5)(40) = 100\#$ of chromate per A/C.

Total VOC from stripping and repainting $(6425+116+455) = 7000\#$ VOC per A/C.

Total chromate 100# per A/C

1. CURRENT PDM VOC & CHROMATE POLLUTION RATES: Assuming 36 A/C Processed per Year with a fleet of 180 A/C on five-year full coating system strip and paint cycle.

$(7000)(36) = 252,000\#$ of VOC generated each year from stripper and paint

$(100)(36) = 3,600\#$ of Chromate generated each year from primer

2. AFTER IR² NDI UTILIZATION TWO EXAMPLES: (A. Coating Life-Extension and Scuff Sand; B. Painting Skipping one Coating System Stripping Cycle)

EXAMPLE A. If Coating Life Extension of one year or 20% (six-year cycle) savings of VOC's and Chromate:

$(252,000)(.20) = 50,400\#$ of VOC saved per year for fleet of 180 A/C

$(3,600)(.20) = 720\#$ of chromate saved per year for fleet of 180 A/C

EXAMPLE B. If Scuff Sanding and Painting at the Five Year Point, Paint stripper VOC Savings:

The processing of 18 A/C (180 on ten-year cycle for coating system stripping) per year will save $(18A/C)(6425\#) = 115,650\#$ of stripper VOC per year.

Financial Calculations: (Cost of coating system stripping) – (Cost of Scuff Sanding and Recoat) or $(\$375K - \$250K) = \$125K$ savings per A/C

$(\$125K)(36) = \4.5 M saved, if scuff sanding is selected, after NDI inspection for corrosion. If repainting is not required at the five-year cycle, $(\$375K)(36)$ or \$13.5M saved, prior to the ten-year cycle. Note; minor low cost touch up may be required with APC.

APPENDIX A6

JSF (F-35) PRIMER AND TOPCOAT FEASIBILITY EVALUATION FOR THE DETECTION OF CORROSION UNDER COATINGS

Candidate for Non-Chromated Primer for F-35 Program

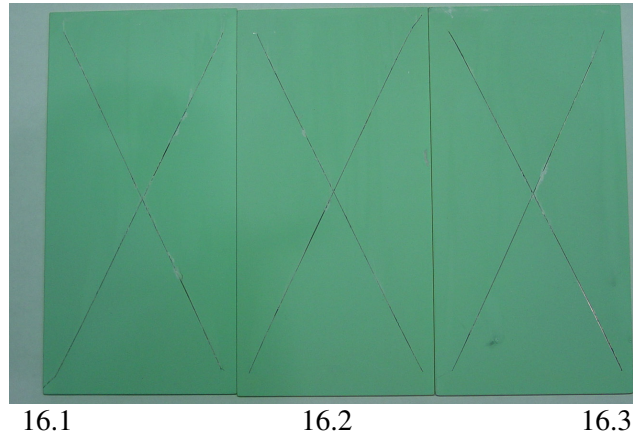
Item or Panel	Type of Primer	Type of Topcoat	Test
16.1, 16.2, 16.3	Deft 44-GN-098 (Candidate for specification MIL-PRF-85582D Type 1, Class N)	None	2000 Hours Salt Fog Exposure per ASTM B117
17.1, 17.2, 17.3	Deft 44-GN-098 (Candidate for specification MIL-PRF-85582D Type 1, Class N)	MIL-PRF-85285 Type I, Gloss Color No. 17925 ELT	2000 Hours Salt Fog Exposure per ASTM B117
18.1, 18.2, 18.3	Deft 44-GN-098 (Candidate for specification MIL-PRF-85582D Type 1, Class N)	MIL-PRF-85285 Type I, Camouflage 36375 ELT	2000 Hours Salt Fog Exposure per ASTM B117
19.1	Deft 44-GN-098 (Candidate for specification MIL-PRF-85582D Type 1, Class N)	MIL-PRF-85285 Type I, Color No. Gloss 17925 ELT	2000 Hours Filiform Exposure per MIL-PRF-85582
20.1	Deft 44-GN-098 (Candidate for specification MIL-PRF-85582D Type 1, Class N)	MIL-PRF-85285 Type I, Camouflage Color No. 36375 ELT	2000 Hours Filiform Exposure per MIL-PRF-85582
42.1	Deft 44-GN-098 (Candidate for specification MIL-PRF-85582D Type 1, Class N)	None	None

The above table describes the paint scheme of the panels that are shown on the following pages A6-3, A6-4, A6-5, A6-8, and A6-9.

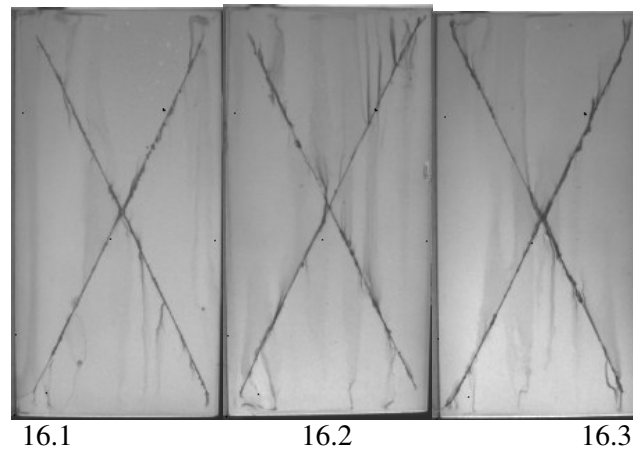
Deft Chemical Part No. 44-GN-098 is the leading candidate primer for use on the JSF (F-35) Program and other aircraft programs. Class N indicates non-chromated primer. The extended life to topcoat (ELT) qualified to MIL-PRF-85285TYI would allow coating life to be extended beyond the normal 5-year schedule for coating removal on military aircraft and hence, it was selected as the topcoat of choice to save or minimize pollution, once the IR detection of corrosion under coatings system has been demonstrated/validated for depot/field operations.

Candidate for Non-Chromated Primer for F-35 Program

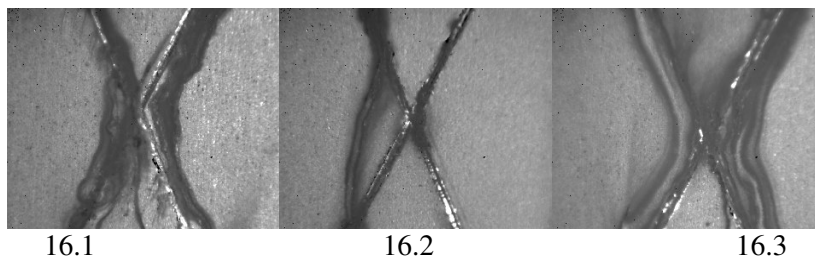
Visible Image



IR Image with 25mm Lens



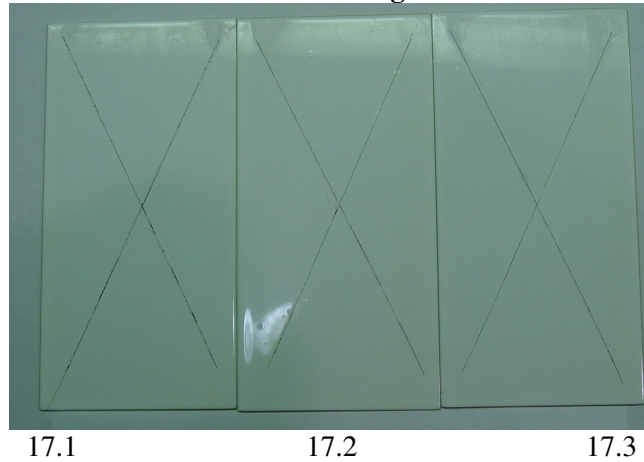
IR Image with 1X Magnification Lens



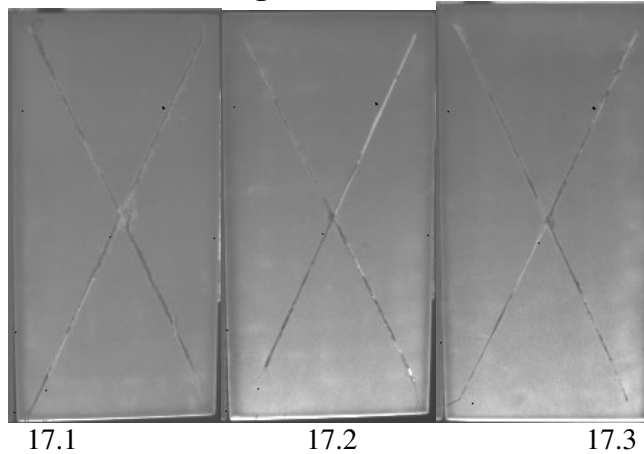
Visible and IR reflectance images of panels 16.1, 16.2, and 16.3. Panels 16.1, 16.2, and 16.3 all consist of the same paint scheme. These panels all have a Deft 44-GN-098 non-chromated primer (candidate for specification MIL-PRF-85582D Type 1, Class N). The panels were exposed to ASTM B117 Salt Fog for 2000 Hours. Note: Aluminum grain structure on IR Images (16.1, 16.2, and 16.3) indicates candidate primer is compatible with IR Detection System.

Candidate for Non-Chromated Primer for F-35 Program

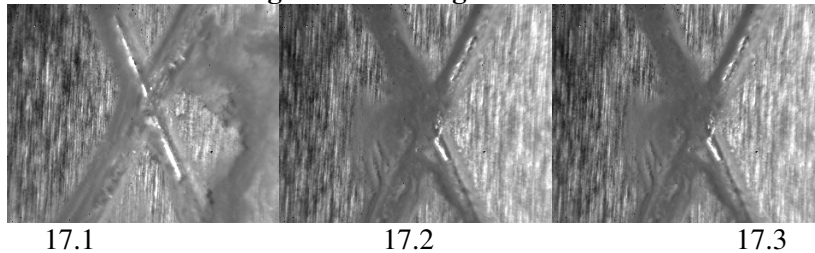
Visible Image



IR Image with 25mm Lens



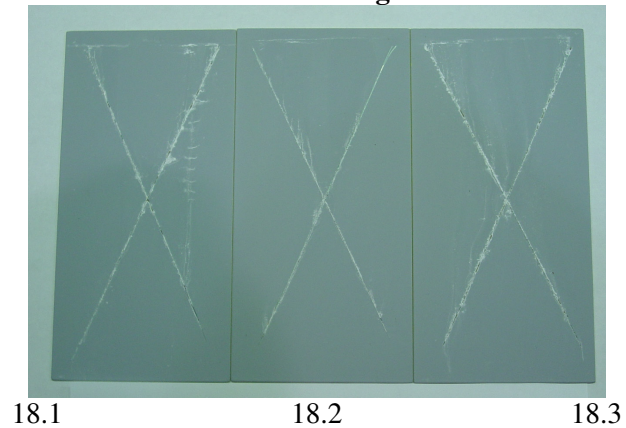
IR Image with 1X Magnification Lens



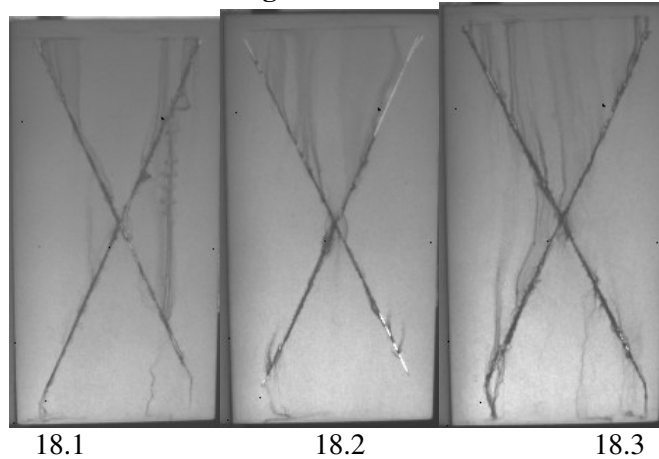
Visible and IR reflectance images of panels 17.1, 17.2, and 17.3. Panels 17.1, 17.2, and 17.3 all consist of the same paint scheme. These panels all have a Deft 44-GN-098, non-chromated primer (candidate for specification MIL-PRF-85582D Type 1, Class N), and topcoat MIL-PRF-85285 Type 1, Gloss 17925 ELT). The panels were exposed to ASTM B117 Salt Fog for 2000 Hours. Note: Aluminum grain structure on IR images (17.1, 17.2, and 17.3) indicates the candidate primer and gloss topcoat system are compatible with the IR Detection System.

Candidate for Non-Chromated Primer for F-35 Program

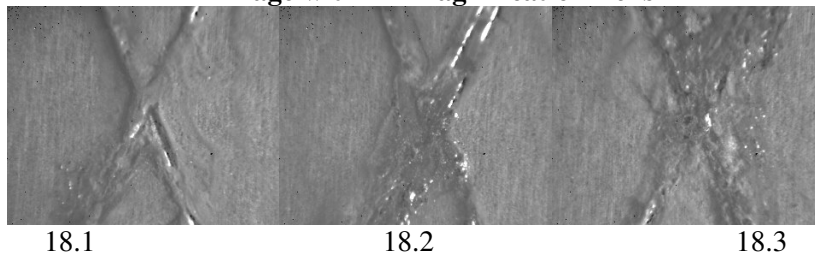
Visible Image



IR Image with 25mm Lens

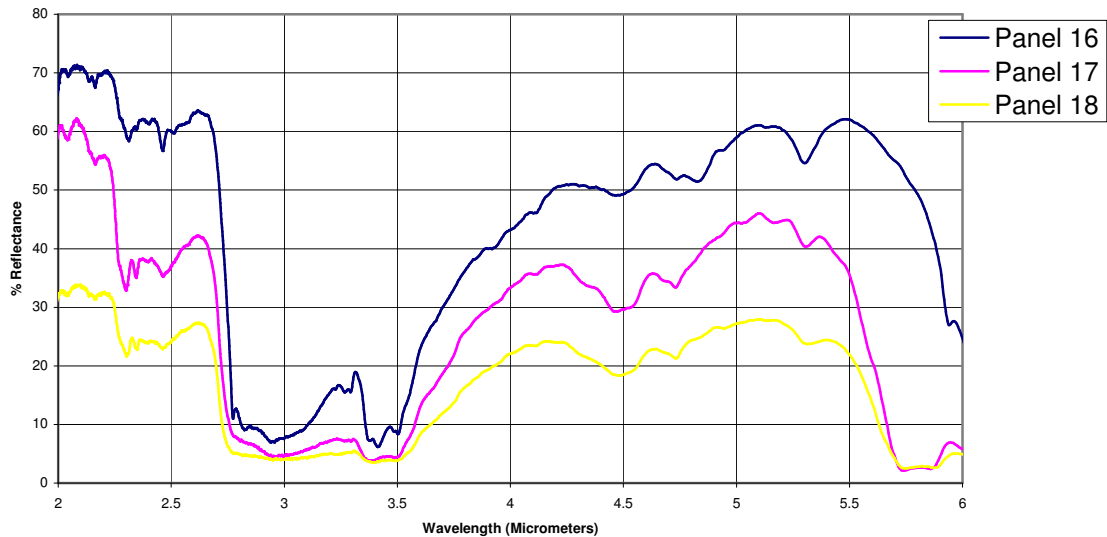


IR Image with 1X Magnification Lens



Visible and IR reflectance images of panels 18.1, 18.2, and 18.3. Panels 18.1, 18.2, and 18.3 all consist of the same paint scheme. These panels all have a Deft 44-GN-098, non-chromated primer (candidate for specification MIL-PRF-85582D Type 1, Class N), and topcoat MIL-PRF-85285 Type 1, Camouflage 36375 ELT). The panels were exposed to ASTM B117 Salt Fog for 2000 Hours. Note: Aluminum grain structure on IR Images (18.1, 18.2, and 18.3) indicate primer and camouflage topcoat system are compatible with IR Detection System.

Candidate for Non-Chromated Primer for F-35 Program

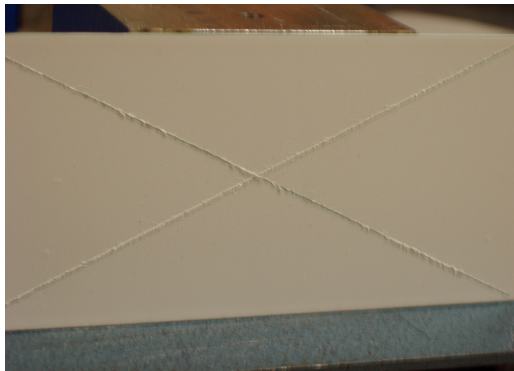


The above chart is the IR Reflectance spectra of panels 16, 17, and 18. Panels 16, 17, and 18 each consisted of 3 panels, the spectra was then averaged. The panels were exposed to ASTM B117 Salt Fog for 2000 Hours. The IR Reflectance measurements were not taken on the scribe line, where corrosion and salt residue appear most often.

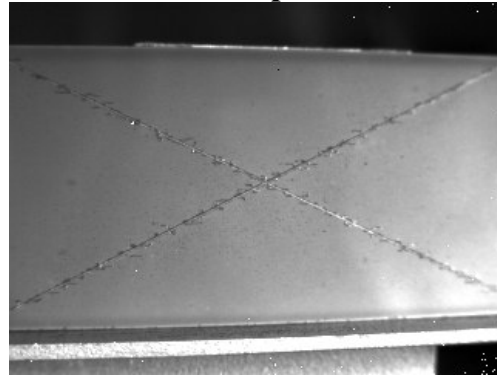
The above chart indicates coating/substrate reflectance in the 2 to 6 micron wavelength range. The current production Merlin™ Camera has a 3 to 5 micron window. However, the chart also indicates that if the filter was moved to the 3.5 to 5.5 window, an enhanced IR flux intensity may improve contrast of the corroded areas vs the non-corroded areas.

Candidate for Non-Chromated Primer for F-35 Program

Panel 19.1 Gloss Topcoat: 2000 Hours Filiform Exposure



Visible Image



IR Image

Panel 19.1 Gloss Topcoat (With 1x Magnification Lens)

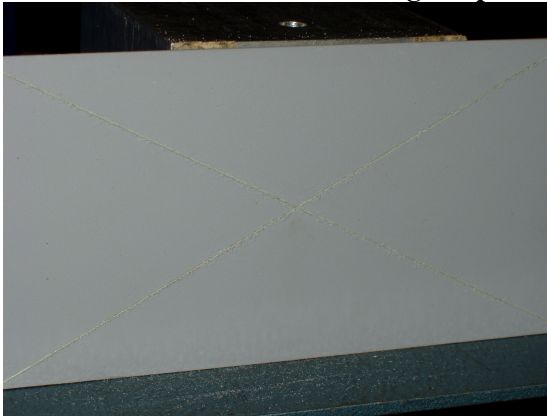


IR Image

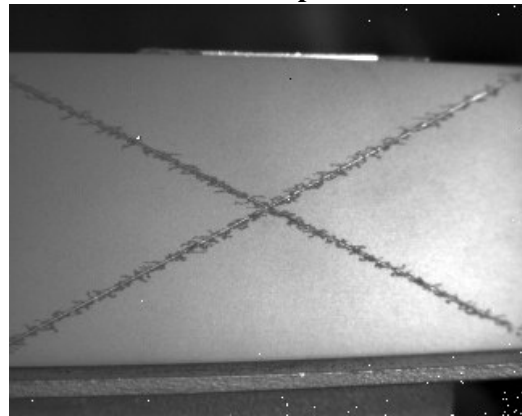
**IR Images enhance the ability to see filiform corrosion through gloss topcoat. Note:
Filiform corrosion exposure protocol was conducted in accordance with MIL-PRF-85582.**

Candidate for Non-Chromated Primer for F-35 Program

Panel 20.1 Camouflage Topcoat: 2000 Hours Filiform Exposure

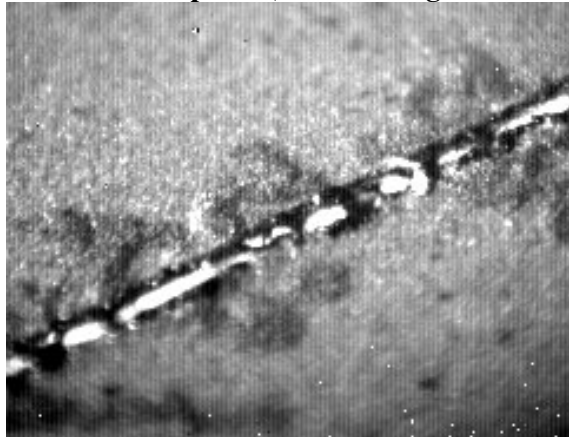


Visible Image



IR Image

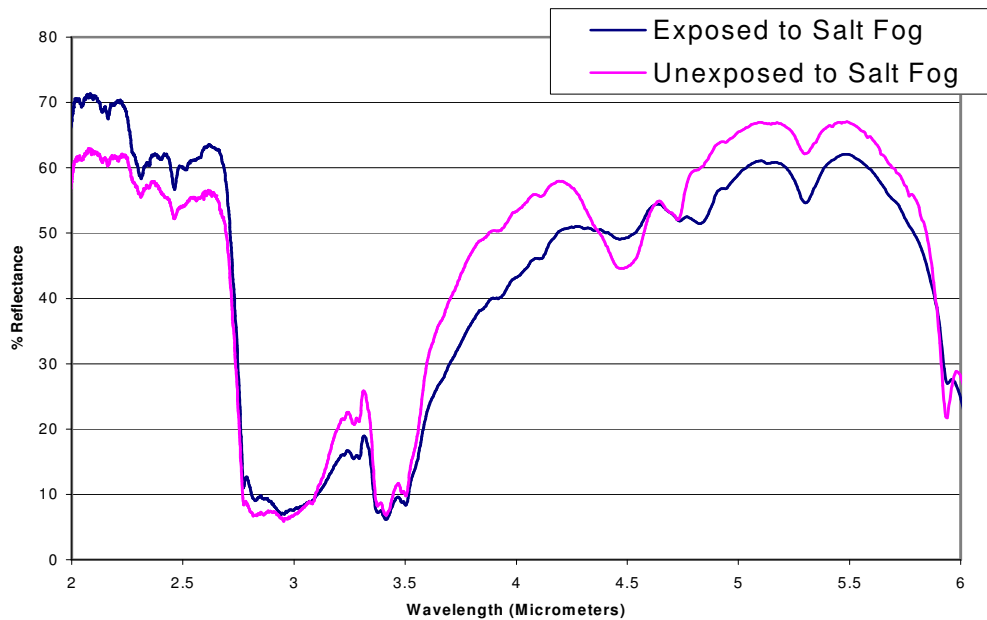
Panel 20.1 Gloss Topcoat (with 1X Magnification Lens)



IR Image

Candidate for Non-Chromated Primer for F-35 Program

Deft 44-GN-098: Degradation of Coating w/Exposure to Salt Fog



The above chart is the IR Reflectance spectra of panels that were painted with a Deft 44-GN-098 non-chromated primer (candidate for specification MIL-PRF-85582TYCLN). The line marked “Exposed to Salt Fog” represents a panel with non-chromated primer that was exposed to ASTM B117 Salt Fog for 2000 Hours (panel 16.1). The line marked “Unexposed to Salt Fog” represents a panel with non-chromated primer that was not exposed and tested as new (panel 42.1). This chart shows the potential degradation of the non-chromated primer with the addition of increased salt fog exposure. Both the exposed and the unexposed panels with this non-chromated primer prove to transmit in the 3-5 micrometer wavelength region, this is evident in the above spectra. It is also apparent that an improved IR signal may be obtained in the 3.5 to 5.5 micron range.

APPENDIX 7

POLLUTION SAVINGS CALCULATIONS & BUSINESS CASE

MILITARY AIRCRAFT PROGRAMS

Col 1	Col 2	Col 3	Col 4	Col 5	Col 6	Col 7	Col 8	Col 9
Aircraft Program	Est. Active A/C Req. Maintenance	Gallons of Primer Outer Mold Line	Gallons of Top Coat Outer Mold Line	Aircraft/YR Requiring Finishing (5-Year Cycle)	Estimated Stripping Cost per A/C (\$K)	Total Cost per A/C Program (\$M)	Total Gallons Used per Aircraft	Total Gallons Used per year per Aircraft Program
Military								
A-10	325	8	19	65	75	4.875	27	1755
B-1B est	84	25	50	16.8	150	2.520	75	1260
B-2 est	20	25	50	4	200	0.800	75	300
B-52 est	5	40	130	1	250	0.250	170	170
C-130 est	140	20	40	28	150	4.200	60	1680
C-141 est	41	30	60	8.2	125	1.025	90	738
C-2	39	10	18	7.8	85	0.663	28	218
C-5A est	81	60	220	16.2	750	12.150	280	4536
C-17 est	16	40	130	3.2	375	1.200	170	544
E-8 J-Stars	2	40	130	0.4	233	0.093	170	68
E2C	135	10	18	27	85	2.295	28	756
EA-6B	128	26	20	25.6	85	2.176	46	1178
F-117 est	57	8	19	11.4	120	1.368	27	308
F-15 est	628	6	26	125.6	75	9.420	32	4019
F-16 est	1316	6	12	263.2	60	15.792	18	4738
F-18 est	797	7	14	159.4	60	9.564	21	3347
F-14	400	6	26	80	75	6.000	32	2560
T/AT-38	471	3	6	94.2	50	4.710	9	848
Totals	4685	370	988	937	N/A	79.101	N/A	29023

Data on active aircraft taken from Aviation Week for year 2000 (Col 1, Col 2)

Primer VOC = 2.9 lbs/gallon

Top Coat VOC = 3.5 lbs/gallon

COMMERCIAL AIRCRAFT PROGRAMS

Col 1	Col 2	Col 3	Col 4	Col 5	Col 6	Col 7	Col 8	Col 9
Aircraft Program	Est. Active A/C Req. Maintenance	Gallons of Primer Outer Mold Line	Gallons of Top Coat Outer Mold Line	Aircraft/YR Requiring Finishing (5-Year Cycle)	Estimate Stripping Cost per A/C (\$K)	Total Cost per A/C Program (\$M)	Total Gallons Used per Aircraft	Total Gallons Used per year per Aircraft Program
Commercial								
Airbus A-310E	222	20	39	44.4	100	4.400	59	2619.6
Airbus A-320E	405	25	55	81	100	8.100	80	6480
Airbus A-340E	379	10	20	75.8	75	5.685	30	2274
L1329E	3	45	120	0.6	100	0.060	165	72
DC-10E	351	45	120	70.2	375	26.325	165	11583
DC-9E	785	16	28	157	120	18.840	44	4396
DC-8E	263	15	25	52.6	100	5.260	40	2104
L1011E	190	50	200	38	375	14.250	250	9500
MD-11E	159	40	160	31.8	375	11.925	80	2544
MD-80E	1120	20	40	224	90	20.160	60	13440
747	996	50	200	199.2	375	74.700	250	49800
757	815	20	39	163	120	19.560	59	9617
767E	628	30	60	125.6	125	15.700	90	11304
737	3134	16	28	626.8	100	62.680	44	27579.2
727E	1363	16	28	272.6	100	27.260	44	11994.4
777E	45	40	180	9	375	3.375	220	1980
Totals	10858	458	1342	2171.6	N/A	318.280	N/A	167287.2

Primer VOC = 2.9 lbs/gallon
Top Coat VOC = 3.5 lbs/gallon

Military Aircraft Programs

VOC and chromate calculations for released pollution (see page A7-2 and appropriate column).

Calculation of Ratio of Primer to Total Paint (primer + topcoat)

$$\frac{\text{Gallons of Primer (Col 3)}}{\text{Total Gallons of Primer (Col 3) + Topcoat (Col 4)}} = \frac{370 \text{ (Col 3)}}{370 \text{ (Col 3) + 988 (Col 4)}} = \frac{370}{1358} = 0.272459$$

29,023 (Col 9) X 0.272459 = 7,907 Gallons of Primer

(29,023 – 7,907) = 21,116 Gallons of Top Coat

VOC and Chromate Calculations

- Top Coat – 21,116 X 3.5 lb/gal. Topcoat = 73,906 lb of VOC
- Primer – 7,907 X 2.9 lb/gal. Primer = 22,930 lb of VOC
- Chromates for military primer: 2 lbs/gallon (Ref., Deft Chemical)

(73,906 + 22,930) = 96,836 lb VOC per year

$$7,907 \text{ X } \frac{2 \text{ lb chromate}}{\text{gallon}} = 15,814 \text{ lb of chromate per year}$$

If military aircraft could be stripped every 10 years, rather than every 5 years, a 50% savings of VOC and chromates would be realized.

Therefore,

48,418 lb of VOC could be saved per year

7,907 lb of toxic chromate could be saved per year

on military aircraft provided a long-life coating was qualified for a 10 year life and a means of inspection was demonstrated for detection of corrosion under the long-life coating system.

Business Case – Military Aircraft

Because the total cost for stripping aircraft for a 5-year cycle is approximately \$80M per year (see Col 7), total savings would be approximately \$40M per year going to a 10-year cycle.

Commercial Aircraft Program

VOC and chromate calculations for released pollution (see page A7-3 and appropriate column).

Calculation of Ratio of Primer to Total Paint (primer + topcoat)

$$\frac{\text{Gallons of Primer (Col 3)}}{\text{Total Gallons of Primer (Col 3) + Topcoat (Col 4)}} = \frac{458 \text{ (Col 3)}}{458 \text{ (Col 3)} + 1,342 \text{ (Col 4)}} = \frac{458}{1,800} = 0.2544$$

$167,287.2 \times 0.2544 = 42,565$ Gallons of Primer

$(167,287 - 42,565) = 124,722$ Gallons of Top Coat

VOC and Chromate Calculations

- Top Coat – $124,722 \times 3.5 \text{ lb/gal. Topcoat} = 436,527 \text{ lb of VOC}$
- Primer – $42,565 \times 2.9 \text{ lb/gal. Primer} = 123,438 \text{ lb of VOC}$

Total = 559,965 lb of VOC per year

- Chromates for commercial primer: 1 lb of chromate/gallon (Ref Deft Chemical)

$$42,565 \times \frac{1 \text{ lb chromate}}{\text{gallon}} = 42,565 \text{ lb of chromate per year}$$

If commercial aircraft could be stripped every 10 years rather than every 5 years, a 50% savings of VOC and chromates would be realized.

Therefore,

279,982 lb of VOC could be saved per year

21,282 lb of toxic chromate could be saved per year

on commercial aircraft provided a long-life coating was qualified for a 10 year life and a means of inspection was demonstrated for corrosion under the long-life coating system.

Business Case – Commercial Aircraft

Since the total cost for stripping aircraft for a 5-year cycle is approximately \$318M per year (see Col 7), total savings would be approximately \$159M per year for a 10-year cycle vs a 5-year cycle.